December 2018

Chimera Ligand for Pili and Lectin A Protein Controls Antibiotic-Promoted Biofilm Formation, Swarming Motility, Tolerance and Persister Formation by Pseudomonas aeruginosa

Hewen Zheng
Syracuse University

Abstract

Throughout the human history, the fight against bacterial infections had never stopped but the remedies for bacterial infections were often insufficient and for many infectious diseases, there was no treatment available. The revolution in antimicrobial infection therapy began with the discovery of penicillin by Alexander Fleming in 1928. However, since the first introduction of antibiotics, bacteria over time have evolved sophisticated resistant strains against almost all the available antibiotics which cause selection pressure on the bacteria to evolve their genetic makeup and develop resistance against such agents. Furthermore, bacteria can form surface attached multicellular communities known as biofilms. Bacteria residing within biofilms are protected by biofilms which renders the bacteria more difficult to eliminate because of the low permeability of antibiotics through outer membranes. Combating such resistant bacteria is an extremely difficult task if using antibiotics alone. Hence scientific community continuously seeks new strategies to overpower these resistant bacteria.

The focus of the research work presented here is to develop a class of chimera ligands that can bind to both pili and LecA protein of *Pseudomonas aeruginosa* to inhibit both swarming motility and biofilm formation. The potential adjuvant agents of these chimera ligands that can increase the effectiveness of antibiotics were demonstrated. In addition, the ability of our adjuvant molecules to eliminate drug-tolerant bacteria and to reduce persisters, in combination with antibiotics was demonstrated.

The binding property of chimera ligands was demonstrated by competitive fluorescence polarization assay (LecA) and by adding a functional group to a ligand that can covalently attach to the receptor protein only when the physical ligand-receptor binding takes place (Pili). In addition, the effect of externally added pili on the swarming motility of *Pseudomonas*

aeruginosa was tested to support the mechanistic study of the pili as the receptor (or one of the receptors) that will bind to rhamnolipids and our synthetic agents, and upon binding, causing the bacterial activities.

For quantification of polysaccharides, two efficient detection and quantification methods that make use of the negative charges of the alginate polymer and do not involve degradation of the targeted polysaccharide were described. Both approaches provide efficient methods for monitoring alginate production by mucoid *Pseudomonas aeruginosa*.

The effect of a class of synthetic analogs of rhamnolipids at controlling (promoting and inhibiting) the biofilm formation activities of a non-rhamnolipid-producing strain – rhlA – of Pseudomonas aeruginosa was demonstrated. The bioactive synthetic analogs of rhamnolipids promote biofilm formation by rhlA mutant at low concentrations but inhibit the biofilm formation at high concentrations. To explore the internal structures formed by the biofilms, the wild-type biofilms formed with substantial topography (hills and valleys) when the sample is under shaking conditions were observed by confocal microscope. Using this observation as a comparison, the effect of synthetic analogs of rhamnolipids on promoting structured (porous) biofilm of *rhlA* mutant, at intermediate concentrations between the low ones that promoted biofilm formation and the high ones that inhibited biofilm formation was demonstrated. This study suggests a potential chemical signaling approach to control multiple bacterial activities.

Chimera Ligand for Pili and Lectin A Protein Controls Antibiotic-Promoted Biofilm Formation, Swarming Motility, Tolerance and Persister Formation by *Pseudomonas aeruginosa*

by

Hewen Zheng

M. Phil., Syracuse University, 2015

B.Sc., Dalian University of Technology, China, 2013

Dissertation

Submitted in partial fulfillment of the requirements for the degree of

Doctor of Philosophy in *Chemistry*

Syracuse University

December 2018

Acknowledgment

I would like to thank all the people who contributed in some way to the work described in this thesis. First and foremost, I would like to thank my academic advisor, Professor Yan-Yeung Luk, for accepting me into his group. During my Ph.D. career, he contributed to a rewarding graduate school experience by giving me intellectual freedom in my work, supporting my attendance at the high-quality conference, engaging me in new ideas, and demanding a high quality of work in all my endeavors. Under Dr. Luk's guidance, I have developed my academic skills in a variety of ways. I deem myself fortunate to work under his guidance and for providing me conductive atmosphere for my research work.

I am grateful to Professors, Anthony Garza, Ivan Korendovych, Michael Sponsler, John D Chisholm and Weiwei Zheng for finding time from their busy schedules to be on my defense committee. I thank all of you for critically reviewing my Ph.D. thesis. Your comments and suggestions have helped improve the scientific quality of this thesis.

My sincere thanks also go to Dr. Weiwei Zheng and Dr. Zhijun Li who graciously allowed me to utilize the Edinburgh FLS9801 Spectrometer, and they fully supported our efforts with their time and their extensive knowledge of fluorescent polarization. Dr. Zhijun Li also help me tremendously with the interpretation of the data.

Throughout my five years in graduate school I have received help from colleagues and great friends; Arriza, Felicia, Yuchen, Pankaj, Tongyin. I would like to thank visiting scholar, Changqing Jia for his help and patience during my 1st year in the group. I wish

also to thank my departmental colleagues and classmates for ideas shared and for making my stay in SU comfortable and enjoyable.

I would like to acknowledge the Department of Chemistry at SU. My graduate experience benefitted greatly from the courses I took, the opportunities I had to serve as a teaching assistant, and the high-quality seminars that the department organized.

Finally, I would like to acknowledge friends and family who supported me during my time here. First and foremost, I would like to thank my parents and my grandparents for their constant love and support. My time at SU was made enjoyable in large part due to the many friends that became a part of my life. An extra-special thank you is reserved for my girlfriend Yijie Zhi, your encouragement and determination was very gratefully appreciated during the write-up phase, and I am grateful that you have been at my side through thick and thin and a constant source of motivation and support.

Hewen Zheng

Table of Contents

List of Figures **Page**

Chapter 1 Introduction: The Need of Controlling Pathogen Activities of Bacteria

1.1 Bacteria activities – Biofilm, swarming, alginate production, and twitching motilities – impact infectious diseases

1.1.1. Pseudomonas aeruginosa is related to multiple diseases

Pseudomonas aeruginosa (*P. aeruginosa*) is a gram-negative, rod-shaped opportunistic pathogen associated with a wide range of diseases.[1] Common victims of *P. aeruginosa* infections are the patients with weakened immune systems and patients with wounds from surgery or burn.[2] The *P. aeruginosa* infection is especially prevalent among the victims of cystic fibrosis (CF), which is a genetic disorder that disrupts the normal function of epithelial cells where *P. aeruginosa* colonizes the lung and mutates to an alginate overproducing mucoid phenotype.[3-4] The alginate-containing matrix of the mucoid strain is thought to allow the formation of protected microcolonies and provide increased resistance to opsonization, phagocytosis, and destruction by antibiotics.[5-6] In addition, outer membrane permeability of *P. aeruginosa* is lower than that of *Escherichia coli* (*E. coli*).[7] *P. aeruginosa* is intrinsically resistant to many structurally unrelated antimicrobial agents because of the low permeability of its outer membrane, the constitutive expression of various efflux pumps with wide substrate specificity, and the naturally occurring chromosomal AmpC beta-lactamase.[8]

1.1.2. The clinically relevant mucoid strain of P. aeruginosa

Over time *P. aeruginosa* in the lungs of Cystic Fibrosis (CF) patients converts into a mucoid strain which is known to overproduce and secrete the exopolysaccharide alginate.[3] Alginate production by CF strains is the major source of morbidity for CF patients. This is mainly due to the ability of the bacteria to undergo genotypic and phenotypic changes from the typical nonmucoid form to a mucoid phenotype.[9] The relationship between conversion to mucoidy and the establishment of chronic infection is still not fully understood. Ever since its discovery in the 70s, the exact causes for this conversion to mucoid has been elusive.[10] Conflicting opinions have been on the contribution from ligands on the airway cells of the patients.[11-12] Kharazmi reported that exposure of a *P. aeruginosa* to hydrogen peroxide will cause nonmucoid to mucoid conversion.[13] Yu and coworkers found that truncation of type IV pilin induces mucoidy in certain nonmucoid strain.[14] In vitro studies have also indicated that alginate reduces *P. aeruginosa* uptake by rabbit neutrophils, guinea-pig alveolar macrophages, and murine peritoneal macrophages, as well as reducing human neutrophil function.[15-18] The most common mutations responsible for the mucoid conversion are found in mucA, which encodes an inner-membrane-associated anti-σ-factor.[19-20] MucA normally limits the expression of the algD operon, which encodes the enzymes required for alginate synthesis.[21-23] σ22, which is encoded by algU, regulates stress response and virulence-associated genes and is involved, directly and indirectly, in the regulation of virulence and motility in P. aeruginosa.[24-26] This suggests the primary selective advantage of the mucA mutations might be activation of the cellular envelope stress response, and the overproduction of alginate might be a secondary consequence of the mutations. The known or proposed pathogenic roles of alginate can be classified as the following

categories: 1) a direct physical barrier against phagocytic cells, 2) alginate production may play a role in biofilm-related phenomena, including contribution to adhesion and antibiotic resistance owing to the increased impermeability for antibiotics.[3, 27-28] Parsek and co-workers showed that the biofilm formed by mucoid strain was a thousand-fold more resistant than the non-mucoid strain to the action of antibiotic Tobramycin.[29] Hengzhuang and coworkers demonstrated that the treatment of biofilms formed by mucoid strains required higher doses and longer treatment times with two antibiotics, Colistin and Imipenem, as compared to the biofilms of nonmucoid strain.[30] Singh and coworkers did explore the use of Esomeprazole molecules to control the biofilms formed by mucoid strain.[31] In chapter 2, we will introduce a novel alginate quantification method that offers better chemoselectivity and easier operations over a conventionally used carbazole assay. We also focused on discovering synthetic molecules on inhibiting alginate produced by a pathogenic strain of *P. aeruginosa* (mucoid phenotype) extracted from cystic fibrosis patients.

1.1.3. Bacterial biofilms are a major source of infectious diseases and persistent pathogens

Biofilm is any group of microorganisms in which cells stick to each other on a surface.[32] *P. aeruginosa* biofilms are difficult to eliminate because of the low permeability of antibiotics through outer membranes of *P. aeruginosa*.[33-34] Parsek and his co-workers found that the biofilm formed by mucoid strain was 1000 times more resistant than the non-mucoid strain to the action of antibiotics.[7] About 80 % of bacterial infections in humans are associated with biofilms.[35] Bacteria residing inside the biofilms are phenotypically different from those within the culture.[36] Biofilm formation is

commonly considered to occur in the following main stages.(See Figure 1.1) The first step of biofilm formation is the reversible attachment of bacteria on the biotic or abiotic surfaces which is governed by Van der Waals forces and at this stage bacteria can be easily removed from the surface.[37] In the second step, bacteria adhere irreversibly onto the surface through its pili and flagella.[8] In the third step, bacteria start communicating with each other through quorum sensing. When a quorum is achieved, bacteria start secreting polysaccharides to create a three-dimensional matrix. The fourth step in the process is the formation of mature biofilms. Mature biofilm is usually a mushroom-shaped structure consisting of different phenotypes as we move from cap to root of the mushroom. The last step of biofilm formation is a dispersion of mature biofilm. Dispersion is an important stage of the biofilm cycle as it allows bacteria to spread and colonize new surfaces.[38]

The stimulation of biofilm production induced by sub-inhibitory concentrations of antibiotics was observed in numerous human pathogens, such as Staphylococcus or Pseudomonas species.[39] Biofilms can directly challenge the treatment of infectious diseases by greatly reducing the antibacterial efficacy of antibiotics.[40-41] Within a biofilm, bacteria face gradients of physical and chemical parameters, such as nutrients, oxygen, pH.[40] Thus, those bacteria living within biofilms are in distinct physiological states, which increased their capacity to tolerate antibiotics. In addition, the physical barrier created by the biofilm structure can hinder the diffusion of antibiotics.[29, 33] Biofilm formation, induced by sub-inhibitory concentrations of antibiotics targeting ribosomes, such as aminoglycosides, phenicols or tetracyclines, was shown to involve cyclic-di-GMP signaling both in *P. aeruginosa* and *E. coli*.[42] In *P. aeruginosa*, biofilm induction

requires the presence of an inner membrane protein, coded by the arr gene, containing an EAL domain, which is commonly present in enzymes involved in the degradation of the cyclic-di-GMP, thus aminoglycosides may modulate the level of this second messenger by acting on the inner membrane protein.[42]

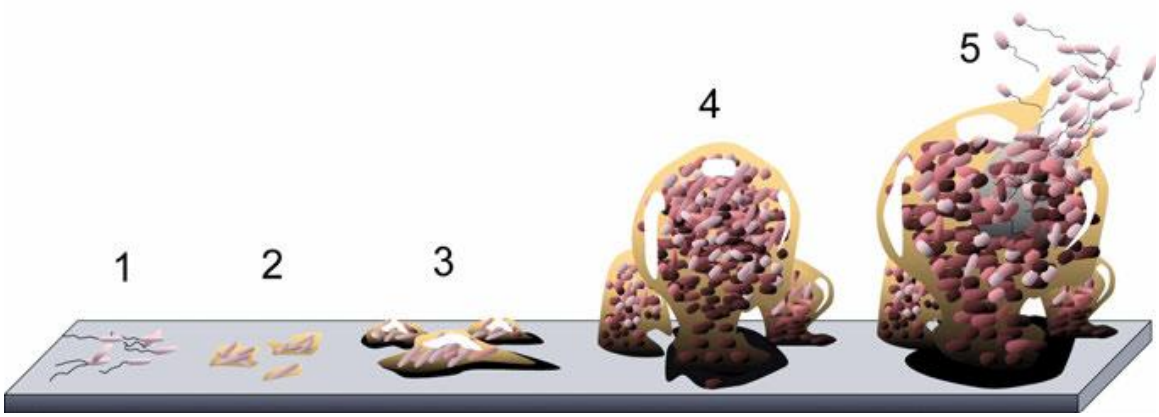

Figure 1.1 The five stages of biofilm development. Stage 1: Planktonic (free-floating) bacteria adhere to the biomaterial surface. Stage 2: Cells aggregate, form microcolonies and excrete extracellular polymeric substances (EPS), i.e. slime. The attachment becomes irreversible. Stage 3: A biofilm is formed. It matures and cells form multi-layered clusters. Stage 4: Three-dimensional growth and further maturation of the biofilm, providing protection against host defense mechanisms and antibiotics. Stage 5: The biofilm reaches a critical mass and disperses planktonic bacteria, ready to colonize other surfaces [Citation: Monroe D (2007) Looking for Chinks in the Armor of Bacterial Biofilms. PloS Biol 5 (11):e308. Doi: 10.1371/journal.pbio.0050307; Image Credit: D. Davies; Copyright: © 2007 Don Monroe. This is an open-access article distributed under the terms of the Creative Commons Attribution License, which permits unrestricted use, distribution and reproduction in any medium, provided the original author and source are credited.]

1.1.4. Swarming and twitching motilities are multicellular behaviors

P. aeruginosa exhibits a large variety of translocation movements, including swarming, swimming, twitching, gliding, sliding and darting.[43] Among those different translocation movements, swarming is regarded as a multicellular behavior. Swarming bacteria move in multicellular groups and exhibit adaptive resistance to multiple antibiotics.[44-46] Both biofilm formation and swarming are surface-associated multicellular bacterial activities that are inversely regulated.[47-48] Swarming is a flagella mediated rapid movement of bacteria on a semisolid surface.[49-50] Some bacterial species like *Vibrio parahaemolyticus* and *Proteus mirabilis* swarm on 1.5 to 3% of agar gel while other bacteria like *E. coli*, *P. aeruginosa* and *Bacillus subtilis* swarm on 0.5 to 0.8 % agar gel.[44] Previous studies have suggested that quorum sensing, rhamnolipid production, type IV pili, and the flagellum all contribute to swarming.[46, 51] Quorum sensing control of swarming is thought to be mediated by RhlR, which activates expression of the *rhlAB* genes and these genes encode enzymes required for production of the surfactant, rhamnolipid.[52-53] While, some strains of *P. aeruginosa* when inoculated at the center of a semisolid surface, grow outward from the point of inoculation to form complexly branched tendrils, others simply grow outward from the point of inoculation without forming any pattern.[54] Figure 1.2 has shown the different type of swarming pattern under similar swarming conditions. However, the formation of complex patterns on the swarm gels is still being poorly understood.

Figure 1.2 Swarm patterns of different P. aeruginosa strains on the semisolid surface (0.5% agar).

Henrichsen and coworkers established that the mode of surface-associated movement termed “twitching motility” is related to the presence of thin pili on various bacterial species.[55-56] They also found that strains exhibiting twitching motility form “spreading and corroding colonies”.[57] It has been shown that type IV pili are required for twitching motility.[58] Twitching motility is regarded as a result of the extension and retraction of pili, which propels the bacteria across a surface.[59-60]

1.2. A brief history of antibiotic discovery and their classification

Throughout the human history, the fight against bacterial infections had never stopped but the remedies for bacterial infections were often insufficient and for many infectious diseases, there was no treatment available.[61] Bacterial infections frequently led to serious illnesses and caused high mortality rates. The revolution in antimicrobial infection therapy began with the discovery of penicillin by Alexander Fleming in 1928.[62]

The development of penicillin for medical use, and its enormously successful application during the World War II led to a great interest in searching for other natural antibiotics. Use of the whole cell antibacterial activity screening platform developed by Waksman directed at a wide variety of fungi and bacteria led to the "golden age" of antibiotic discovery.[63]

There are different ways to classify antibiotics, but the most common classification methods are based on their molecular structures and spectrum of activity.[64] Some common classes of antibiotics based on chemical or molecular structures include Beta-lactams, Tetracyclines, Quinolones, Aminoglycosides, Macrolides, Sulphonamides, Glycopeptides, and Oxazolidinones.[65-67] Most of the antibiotics are targeting at a certain unique feature of the bacterial structure or their metabolic processes completely different or even not presented in mammalian cells.[68-70] The common targets of antibiotics are presented in Figure 1.3.[71]

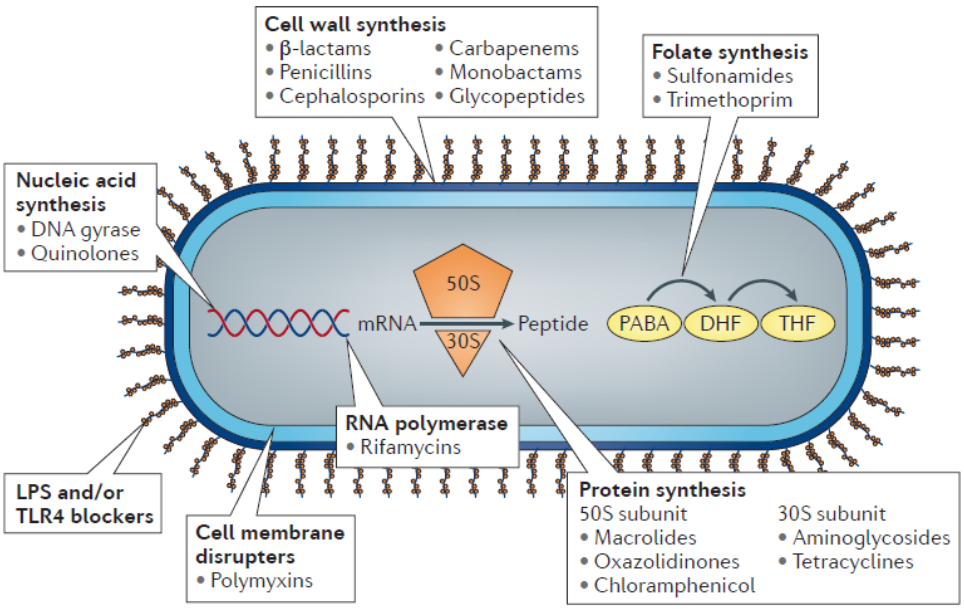

Figure 1.3 Sites of antibacterial action and mechanisms of resistance. Antibiotics can be classified by their mechanism of action. DHF, dihydrofolic acid; LPS, lipopolysaccharide; PABA, para-aminobenzoic acid; THF, tetrahydrofolic acid; TLR4, Toll-like receptor 4. [Citation: Brown, D., Antibiotic resistance breakers: can repurposed drugs fill the antibiotic discovery void? Nature Reviews Drug Discovery 2015, 14 (12), 821. doi: 10.1038/nrd4675. Epub 2015 Oct 23. This is an open-access article distributed under the terms of the Creative Commons Attribution License, which permits unrestricted use, distribution and reproduction in any medium, provided the original author and source are credited.]

1.3. Antibiotic resistance is a big problem

The origin of antibiotics is ancient and antibiotic biosynthetic genes and resistance-conferring genes date back to the ancient period.[72] Thus, many microorganisms have naturally been exposed to these antibiotics over evolutionary timescales. It has been proposed that antibiotics have evolved to be global regulators within microbial communities, contributing to quorum sensing and microbial communication in the natural environment.[73-74] At the low concentrations, antibiotics can act as signaling molecules that trigger transcription responses important for environmental survival.[75-76] While the growth of surrounding microorganisms could be inhibited at high concentrations of antibiotics are present.[77] Since the first introduction of antibiotics, bacteria over time have evolved sophisticated resistant strains against almost all the available antibiotics which cause selection pressure on the bacteria to evolve their genetic makeup and develop resistance against such agents.[78-80] Combating such resistant bacteria is an extremely difficult task if using antibiotics alone. Hence scientific community continuously seeks new strategies to overpower these resistant bacteria.

1.4. Antibiotic adjuvants do not seem to eradicate the problem

An alternative strategy to combat bacterial infections is through using antibiotic adjuvants, compounds that enhance the activity of current drugs and can minimize resistance.[81-83] In general, adjuvants are delivered together with antibiotics and therefore are combination drugs which have been used to achieve synergy, cover the microbial spectrum, and suppress resistance to enhance and preserve the activity of existing drugs.[84-87] Such synergistic effects are implying the greater efficacy of the combinations

than the sum of the individual components. Antibiotic adjuvants can be divided into two general classes based on target profile: Class I adjuvants that work with antibiotics on bacterial targets (inactivating enzymes, efflux pump systems, or alternate targets), and Class II adjuvants that enhance antibiotic activity in the host.[88] The example of beta-lactamase inhibitors in the clinic over the past decades is proof that the antibiotic adjuvants are powerful and important.[89]

The molecular basis of antibiotic synergy is poorly understood. However, without mechanistic data, machine-learning strategies were applied to predict the efficacy of combinations in the antifungal realm and to offer an opportunity to identify new antibacterial combinations as well.[90] Although there are adjuvant molecules that are believed to have a reduced potential to elicit resistance from bacteria, so far do not seem to eradicate the problem.

1.5. Our hypothesis: Controlling bacterial activities leads to eliminating antibiotic tolerance and new persister formation

It is recognized that antibiotics that kill bacteria can also cause responses that, over time, lead to bacterial drug resistance, making the treatment of infectious diseases more challenging.[8, 91] At sub-lethal concentrations, antibiotics can readily increase the population of tolerant bacteria; these tolerant populations require a higher antibiotic dosage to kill than typical susceptible bacteria.[92] Studies also suggest that drug-tolerant bacteria have a higher propensity to evolve into drug-resistant bacteria making antibiotics

ineffective, even at a high dosage.[93-94] Antibiotics can also enhance a pre-existing population of bacteria, called persisters, which are non-growing and thus extremely difficult to eradicate using current antibiotics.[95-97]

Luk lab has developed a class of molecules that inhibit both swarming motility and biofilm formation by *P. aeruginosa*.[98-99] In contrast, at low concentrations, the antibiotic tobramycin, a front-line treatment for chronic infections associated with cystic fibrosis (CF), increases swarming motility and biofilm formation by *P. aeruginosa*.[100] This result prompted us to assess our molecules as a potential adjuvant agent to increase the effectiveness of tobramycin. Preliminary results show our molecules enable tobramycin to kill both planktonic bacteria and tolerant bacteria in a preformed biofilm that was promoted by the sub-lethal concentration of tobramycin. Our molecules, in combination with antibiotics, also eliminated newly formed persisters in a biofilm that are induced upon exposure to antibiotic treatment. This finding is significant, as our novel adjuvants will drastically improve the performance of existing antibiotics. Treating antibiotic-resistant infections is a major medical concern; which this project can address. In the following chapters, we will evaluate the ability of our adjuvant molecules to eliminate drug-tolerant bacteria and to reduce persisters, in combination with antibiotics. We have established growth conditions that generate tobramycin-tolerant bacteria and tobramycin-induced persisters. Using these assays, our preliminary result shows that our molecules enable tobramycin to kill tobramycin-tolerant bacteria, as well as to prevent the formation of persisters.

1.6. A brief introduction of the following chapters

In Chapter 2, two efficient detection and quantification methods that make use of the negative charges of the alginate polymer and do not involve degradation of the targeted polysaccharide were described. Both approaches provide efficient methods for monitoring alginate production by mucoid *Pseudomonas aeruginosa*.

In Chapter 3, the effect of a class of synthetic analogs of rhamnolipids at controlling (promoting and inhibiting) the biofilm formation activities of a non-rhamnolipid-producing strain – *rhlA* – of *Pseudomonas aeruginosa* was described.

In Chapter 4, a class of disaccharide derivatives that can inhibit both swarming motility and biofilm formation of *Pseudomonas aeruginosa* were described. Those potential adjuvant agents can increase the effectiveness of antibiotics. In addition, the ability of our adjuvant molecules to eliminate drug-tolerant bacteria and to reduce persisters, in combination with antibiotics was demonstrated.

In Chapter 5, the binding property of a fluorophore-derivatized disaccharide to LecA protein was demonstrated by fluorescent polarization assay. In addition, the binding properties of synthetic molecules to LecA protein were demonstrated by competitive fluorescent polarization assay.

In Chapter 6, the binding property of synthetic ligands to pili protein was demonstrated by adding a functional group to a ligand that can covalently attach to the receptor protein. In addition, the effect of externally added pili on the swarming motility of *Pseudomonas aeruginosa* was tested to support the mechanistic study of the pili as the receptor (or one of the receptors) that will bind to rhamnolipids and our synthetic agents,

and upon binding, causing the bacterial activities. Together these results in chapter 5 suggest that SFβM is a chimeric ligand that binds to two different targets, $LecA^{101\text{-}102}$ and pili, and also explains why two distinct processes (biofilm formation and swarming) are inhibited by the same molecule.

Chapter 2 Quantification of alginate by aggregation induced by calcium ions and fluorescent polycations

2.1. Introduction

2.1.1. Development of alginate quantification methods and its importance

Quantification of polysaccharides bearing negative charges, such as various heparins and alginate, is important for understanding cell signaling for both mammalian cells and bacteria.[103-105] Various approaches such as colorimetric assays coupled with covalent reactions, salt complex forming induced staining, aggregation,[106] as well as high-performance liquid chromatography-diode array detector methods[107] have been developed to achieve this goal. Recently, Correa and coworkers have demonstrated the successful use of FT-IR spectroscopy to quantify alginate production by several *Pseudomonas fluorescens* strains.[108] The most commonly used carbazole assays involve heating the polysaccharides with concentrated sulfuric acid followed by an addition of an aromatic amine – carbazole. Carbazole-sulfuric acid method was first described by Dische[108] and further developed by Gurin and Hood[109] for the identification and estimation of hexoses and pentoses. Later, Bitter described a modification of the carbazole method for the analysis of uronic acids, which is the major component of alginate.[110] Reactivity of several uronic acids and uronic acid-containing mucopolysaccharides (MPS) was studied systematically at various temperatures and for various heating periods.[111] The study revealed that different uronic acids and MPS upon heating with sulfuric acid produce products with different absorbance in the carbazole assay.[111] The acid treatment generates a range of chemical species starting with breaking

the glycoside bonds, generating the aldehyde that can react with the amine to form a colored imine. Other chemical species from further decomposition such as furic acid were reported, giving a chemically poorly defined mixture. A modification of the carbazole reaction was obtained, in which the intensity of the color depends not only on the structure of individual hexuronic acids but also on specific linkages in polyuronides.[112] Because of the harsh conditions, and dependence of the reaction on the nature of the polysaccharide, carbazole-based assays have been reported to produce false positives and inconsistent results for various polysaccharide structures.[113] More detrimental to the selectivity, both mono- and disaccharides react with the carbazole, producing a high level of background noise that requires the purification of targeted polysaccharides.

We are interested in the detection of alginates, polysaccharides with 1-4 linked D-mannuronic (M) and L-guluronic (G) acid residues that are produced by the opportunistic bacterium *Pseudomonas aeruginosa*. This bacterium often resides in the lungs of patients with cystic fibrosis who have mutations in cystic fibrosis transmembrane conductance regulator (CFTR) protein, which can cause impaired ion transport.[114] In the lungs of patients with cystic fibrosis, *P. aeruginosa* rapidly converts to mucoid *P. aeruginosa*, a phenotype that overproduces alginate. Thus, development of a direct method for the detection of alginate without purification from the culture of mucoid phenotype is greatly desired for the screening of chemical agents that can inhibit the production of alginate by the pathogenic strain of *P. aeruginosa*.

2.1.2. The aim of the chapter

In this chapter, we report two new approaches to detect the production of alginate. In the first method, calcium ion is used to aggregate the alginate *in situ* without purifying the alginate from the culture medium; the aggregates were hydrogel-like and quantified by using the conventional crystal violet dye assay. In the second method, alginate aggregation was induced by multivalent binding between a fluorescently-labeled polycation and alginate. This approach (labeling the polycation) provides a sensitivity comparable to that of the carbazole assay, but without the need for chemical reactions and multiple steps of operations. we will describe two efficient detection and quantification methods that make use of the negative charges of the alginate polymer and do not involve degradation of the targeted polysaccharide. The first method utilizes calcium ions to induce hydrogel-like aggregate with alginate polymer; the aggregates can be readily quantified by staining with a crystal violet dye. This method does not require the purification of alginate from the culture medium and can measure a large amount of alginate that is produced by a mucoid *Pseudomonas aeruginosa* culture. The second method employs polycations tethering a fluorescent dye to form suspension aggregates with the alginate polyanion. Encasing the fluorescent dye in the aggregates provide an increased scattering intensity with a sensitivity comparable to the conventional carbazole assay. Both approaches provide efficient methods for monitoring the alginate production by mucoid.

2.2. Results and discussion

2.2.1. Design of alginate quantification methods by aggregation induced by calcium ions and fluorescent polycations

P. aeruginosa is an opportunistic Gram-negative bacterium that can undergo phenotypic changes to convert from the wild-type to a mucoid phenotype in the lungs of immunocompromised individuals (e.g. with fibrosis patients).[9, 115-116] This mucoid strain is characterized by the overproduction of alginate polysaccharides, which are copolymers of 1-4 linked D-mannuronic and L-guluronic acid residues.[117] The adhesion of mucoid alginate to the lung of a patient is a major virulence factor that causes a series of problems including hosting dormant bacteria, reducing the effectiveness of antibiotics, and difficulty in breathing.[118] We are interested in developing methods for efficient detection of alginate production by mucoid P. aeruginosa. Such methods are useful for evaluating chemical agents that can inhibit alginate production by the mucoid strain.

The conventional carbazole assay does not take advantages or make use of the existence of negative charges on the alginate polymer. Here, we explore the multiple carboxylate groups in the alginate to enable aggregation and detection by using two different approaches. First, we use calcium ion to form aggregates with alginates, followed by crystal violet staining of the aggregate as a quantification means. Second, we explore the aggregation induced by the multivalent binding between a polycation, polyallylamine (PAA), and alginate in aqueous solutions (Figure 2.1). To increase the sensitivity of this method, we also covalently modified PAA with fluorescein isothiocyanate (FITC), a fluorescent fluorophore. Polyallylamine (PAA) tethered with FITC has been used in many applications, including the photophysical study of

fluorescent core nanoparticles fabricated by the layer-by-layer assembly,[119] probes for TNT detection based on FRET[120] and colloidal DNA carriers.[121]

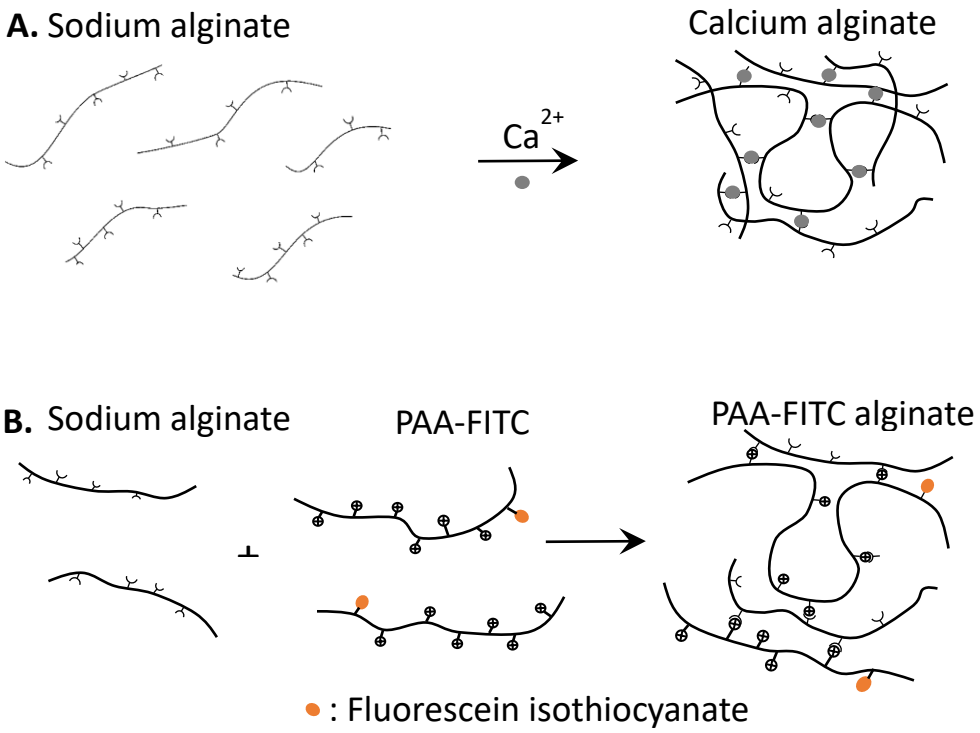

Figure 2.1 Schematic representation of aggregate formation between (A). Alginate and calcium ions, (B). Polyallylamine (PAA)-FITC and alginate.

Calcium and other divalent metal ions have long been recognized to form an aggregate with alginate polymers due to the chelation of the carboxylate groups of the polymer with calcium.[122] The direct detection of these aggregates, however, has not been explored. Here, we first examine the effect of calcium ion present in growth medium alone for bacterial culture to evaluate the background noise, if any, from calcium ion in the LB broth. Figure 3 shows that, after treatments with Ca^{2+}, sodium alginate and mucoid *P. aeruginosa* grown in LB broth media form aggregates, while LB broth media

itself and wild-type *P. aeruginosa* PAO1 grown in LB broth media do not show any aggregate after Ca^{2+} treatment (Figure 2.2). This result suggests that calcium ion does not cause any aggregation in LB broth alone but causes aggregation for both purchased sodium alginate and the alginate produced by mucoid *P. aeruginosa*.

Upon adding calcium chloride, the mucoid *P. aeruginosa* culture exhibits the formation of large aggregates. After centrifugation of this culture solution, we observed cell pellets at the bottom of the falcon tube. In the solution above the cell pellets, large hydrogel-like calcium alginates are observed. The calcium alginate was recollected by pouring out the supernatant along with the hydrogel-like aggregate; the cell pellet was left behind and discarded.

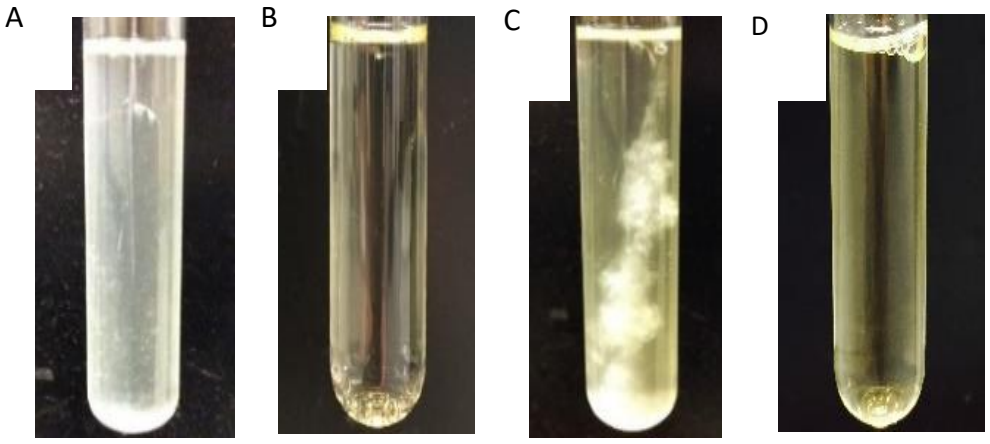

Figure 2.2 Pictures of (A) 2 mL of 6 mM $CaCl_2$ mixed with 200 µL of 5 mg/mL of sodium alginate; (B) 500 µL of 60 mM $CaCl_2$ mixed with 5 mL of LB broth media; (C) 500 µL of 60 mM $CaCl_2$ mixed with 5 mL mucoid *P. aeruginosa* (OD=0.7) grown in LB broth media; and (D) 500 µL of 60 mM $CaCl_2$ mixed with 5 mL wild-type *P. aeruginosa* PAO1 (OD=0.7) grown in LB broth media. Before adding $CaCl_2$, the solution was centrifuged; and the bacteria pellets were removed.

We quantified the resulting aggregates by staining them with a crystal violet dye – a common staining agent.[123] To establish the concentration dependence, we studied the optical density of aggregates formed between calcium and commercially available sodium alginate with a series of concentrations from 0.1 mg/mL to 2 mg/mL. A linear correlation between 0.2 mg/mL to 2 mg/mL are readily obtained (Figure 2.3). However, the signal is rather weak when the concentration of alginate is lower than 0.2 mg/mL (corresponding to an OD value of 0.04 for 0.2 mg/mL of alginate).

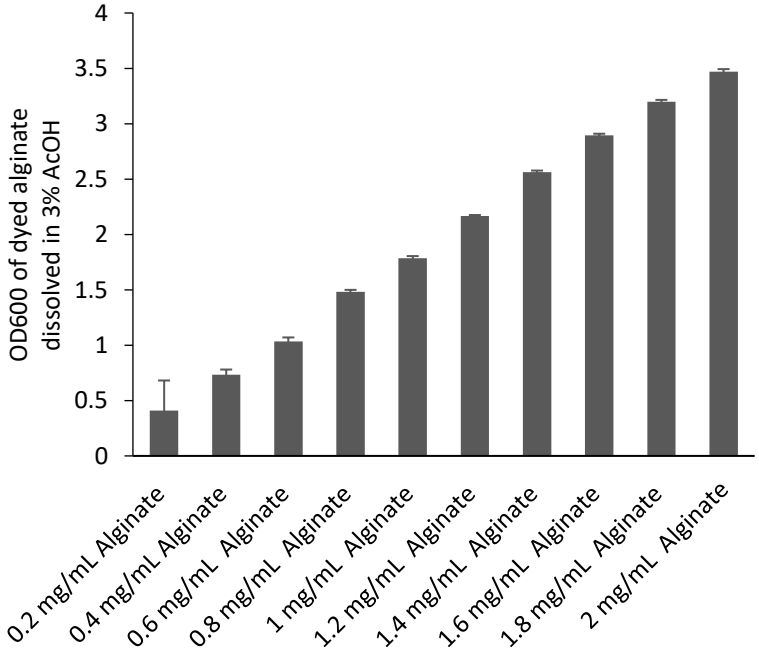

Figure 2.3 Optical density at 600 nm of calcium alginate by crystal violet dye staining assay

2.2.2. Quantification of by alginate produced by mucoid P. aeruginosa

Next, using this linear relationship, we quantified alginate produced by mucoid *P. aeruginosa* over the span of 24 h culture. In this study, we used a mucoid phenotype (PA2192) isolated from CF patients. Goldberg and coworkers revealed the differences between proteins expressed by CF isolates of *P. aeruginosa* that have phenotypes associated with the initial versus chronic infection process.[124] Figure 2.4.A shows the growth curve of mucoid *P. aeruginosa* in 24 h, Figure 2.4.B shows the corresponding alginate production in mg/mL determined by using crystal violates dye staining assay. Our result showed that mucoid *P. aeruginosa* did not produce any noticeable amount of alginate in the first 2 hours, but measurable amount of alginate was observed after 3 hours. This result is consistent with the notion that significant alginate production by mucoid *P. aeruginosa* starts in the exponential growth period and reaches a plateau after 7 hours when the bacterial growth slows down.

A.

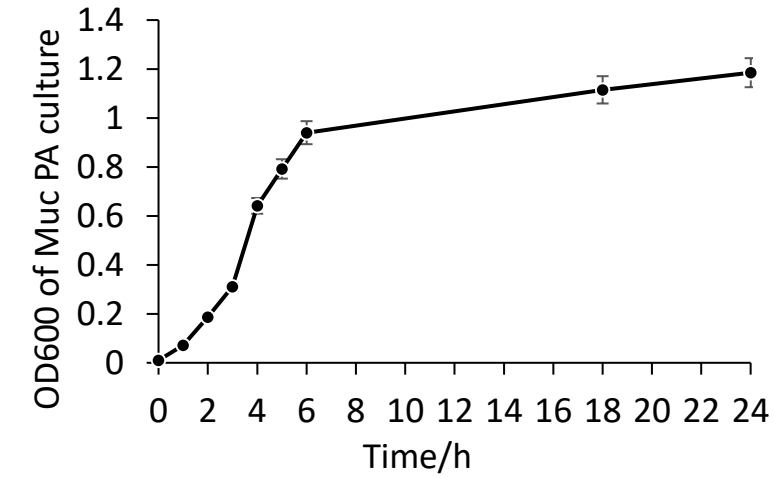

B.

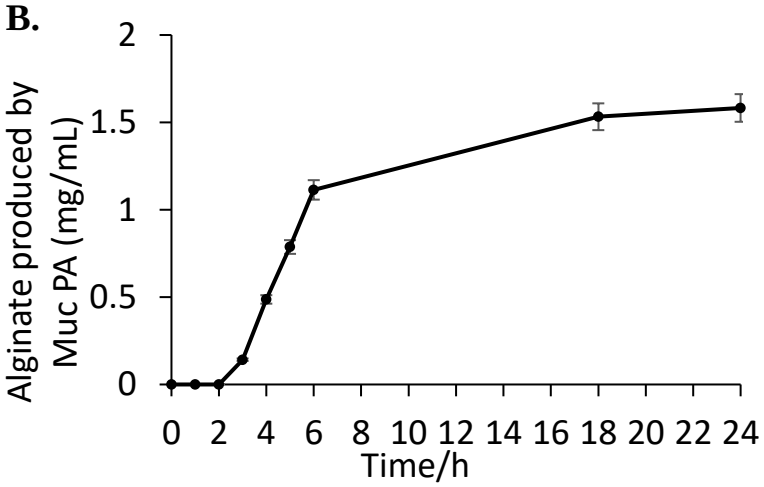

Figure 2.4 Plot of (A) the mucoid *P. aeruginosa* growth curve, and (B) the optical density of Ca^{2+} induced aggregation of mucoid alginate by using crystal violate dye staining assay, versus time of culture. The bacterial culture was grown in LB broth media shook at 250 rpm.

2.2.3. Comparison of different alginate quantification methods

Comparing to the carbazole assay, the calcium aggregation-CV staining method can directly measure 0.05 mg/mL (or more) alginates without dilution and without purification, which is well-suited for monitoring the alginate production by mucoid *P. aeruginosa*. More importantly, the calcium aggregation method does not have a background signal for pure LB broth medium, for carbazole assays, however, a background signal of the optical density of ~0.12 for pure LB broth was observed. This value is comparable to the signal from 0.04 mg/mL of sodium alginate in water (Figure 2.5 and Figure 2.6). However, the sensitivity of measuring the optical density of calcium-alginate aggregation (not staining method) is limited to about 0.2 mg/mL of alginate in solution.

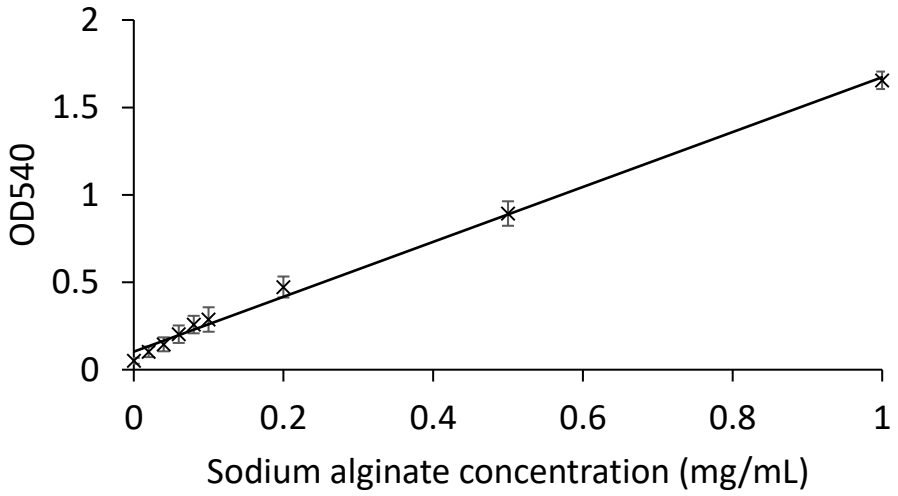

Figure 2.5 Optical density at 540 nm of sodium alginate aqueous solution (0~1.0 mg/mL) by carbazole assay

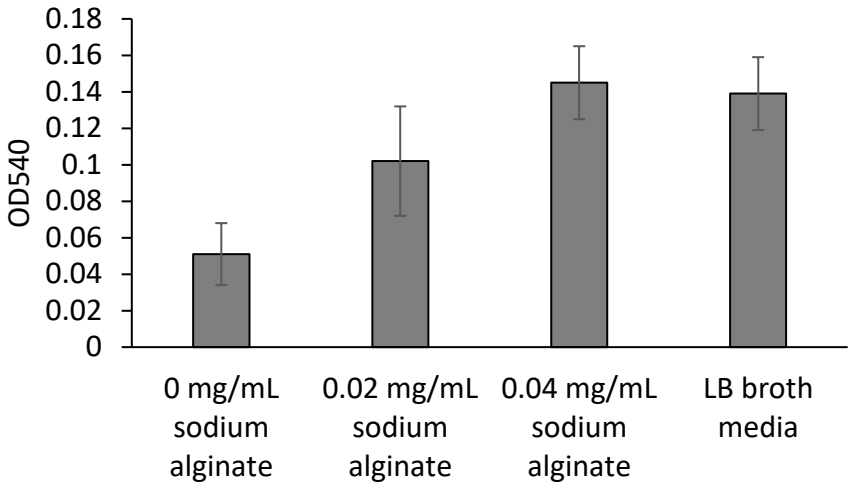

Figure 2.6 Optical density at 540 nm of 0 mg/mL, 0.02 mg/mL, 0.04 mg/mL sodium alginate aqueous solution and LB broth media by carbazole assay

Considering this low sensitivity, we explored the use of a polycation to aggregate alginate. Polycations readily form aggregates with polyanions through multivalent binding. This aggregation effect is used in various applications, including layer-by-layer deposition of polyelectrolytes[125] and medical and pharmaceutical applications like self-assembled shells for drug delivery.[126] By mixing 2 mL of poly allylamine (0.5 mg/mL) and 200 µL of sodium alginate (0.5 mg/mL), a cloudy and stable suspension solution was obtained (Figure 2.7), rather than a hydrogel-like aggregate. Because the suspension is stable, we measured the optical density directly to correlate to the amount of alginate present in the solution. Sodium alginate in solution forms aggregates by mixing with a $CaCl_2$ or PAA solution. However, our method shows that using a solution of $CaCl_2$ or PAA, the optical density value was less than 0.16 when the sodium alginate concentration

is 0.50 mg/mL (Figure 2.5), whereas, for carbazole assay, the optical density is around 1.0 for the same sodium alginate concentration. Thus, the sensitivity of these two methods is still low, and not comparable to carbazole assay.

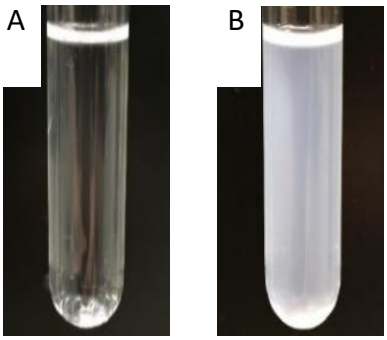

Figure 2.7 Pictures of the solution of 2 mL of 0.5 mg/mL of PAA (A) mixed with 200 µL of 5 mg/mL of sodium alginate to form aggregates (B).

To improve the sensitivity of an aggregation assay, we grafted a fluorophore onto the polycation to explore an increase in the optical density signal. As the intensity of the light scattering depends on the induced dipoles in the particles – a phenomenon less explored for applications, we believe that introducing polarizable groups into the aggregates will increase the polarizability of the particle, and thus may increase the signal intensity. Furthermore, as the fluorophores are confined in the aggregates, a coherent scattering is possible, which further increases the scattering. Mixing alginate with fluorescent polycations resulted in a similarly stable suspension of aggregates (inset of Figure 2.8). Measuring the UV-Vis spectra of different concentrations of sodium alginate in the presence of 0.5 mg/mL PAA-FITC showed a band at 495 nm, which decreased as the concentrations of added sodium alginate were increased. Interestingly, the baseline of

the UV intensity from 250 to about 850 nm increased significantly with the concentration of added sodium alginate. This result is consistent with increased light scattering due to the fluorescent aggregates. To measure the light scattering, we plotted the optical density at 405 nm (OD_{405}) of the solution mixtures with different sodium alginate concentrations (0.01~0.50 mg/mL). A linear relation between the optical density and the alginate concentration was obtained (Figure 2.9). Comparing to the optical density obtained from polyallylamine (without fluorescent labeling) and alginate, this result indicates that fluorescent aggregates increase the intensity of optical density measurement. Thus, this fluorescent polycation enables a more sensitive method for detecting targeted molecules through aggregation.

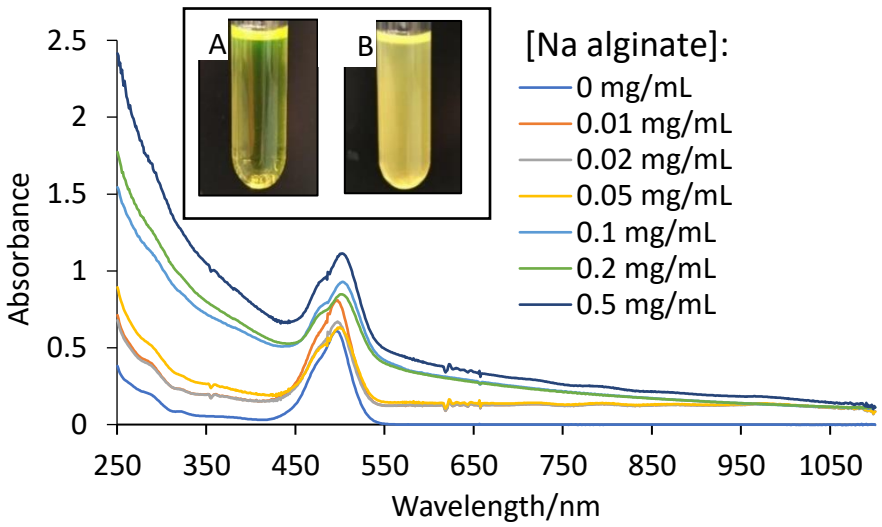

Figure 2.8 UV-Vis Spectra of different concentrations of sodium alginate in the presence of 0.05 mg/mL PAA-FITC. The pictures of the solution of 2 mL 0.5 mg/mL of PAA-FITC (A) and the solution of 2 mL 0.5 mg/mL of PAA-FITC mixed with 200 µL of 5 mg/mL of sodium alginate to form aggregates (B) are also shown.

Figure 2.9 includes the signals for optical absorption of the carbazole dye reacted with the decomposed alginate, optical density of aggregation with PAA-FITC, PAA, and calcium chloride as a function of the concentration of sodium alginate. At relatively high concentration, 0.5 mg/mL, aggregation with $CaCl_2$ and PAA showed an optical signal less than 0.2, whereas aggregation with PAA-FITC and carbazole assay showed optical signals above 0.8. These results indicate that aggregation with PAA-FITC and carbazole assay offer a larger signal range than aggregation with $CaCl_2$ or PAA. This result also indicated that aggregation using PAA-FITC has a comparable sensitivity to the carbazole assay, the conventional method for detecting alginate. However, aggregation with PAA-FITC does not require multiple steps of covalent reactions. This simplification increases the ease of the operation and the reliability of the results, as the reaction yields of the covalent reactions become irrelevant.

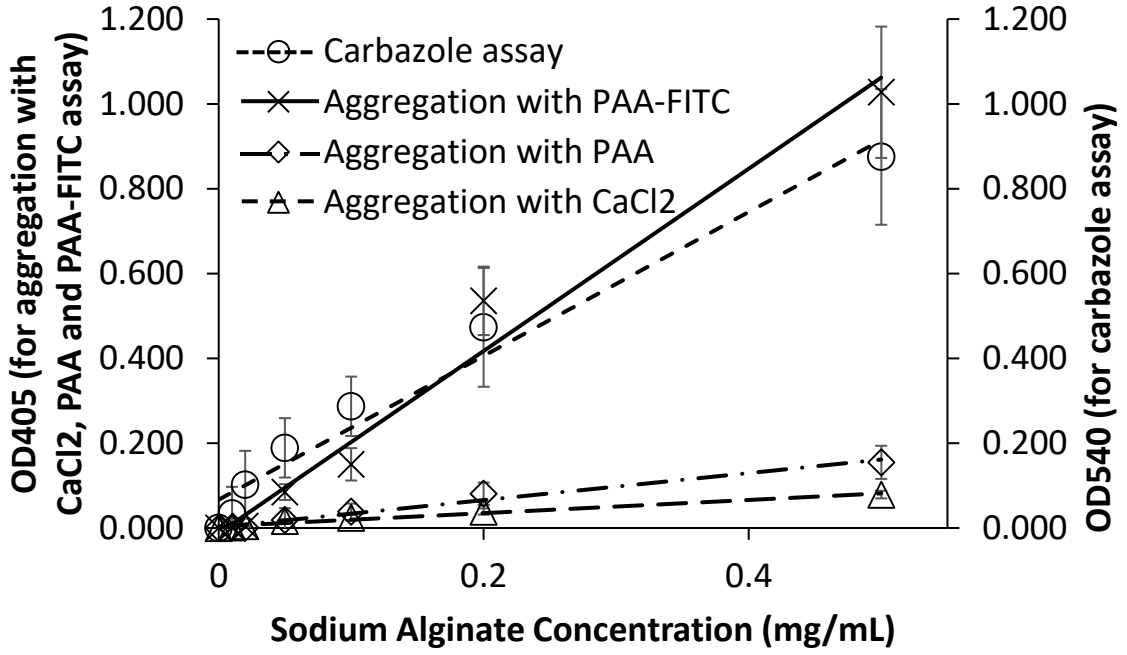

Figure 2.9 Plot of optical density (OD_{405}) of sodium alginate aqueous solution treated with 6 mM of $CaCl_2$, 0.5 mg/mL of PAA, or 0.5 mg/mL of PAA-FITC solution; and the optical absorption (at 540 nm) of carbazole dye reacted with decomposed alginate.

2.3. Conclusion

To conclude, we demonstrated two efficient methods for detecting and quantifying alginate polymer in a solution. The calcium aggregation-staining assay stains directly the calcium-alginate aggregates formed in a bacterial culture without purification and provides a one-step detection/quantification method. This assay has a dynamic range (0.05 mg/mL and up) that is suitable for monitoring and quantifying the alginate production by mucoid *P. aeruginosa* directly from an LB broth culture over 24 h. Using polycations tethered with fluorescent dyes, we obtained the sensitivity that is similar to

carbazole assay. To conclude, the calcium aggregation-staining method does not require the purification and can be used directly for detecting the alginate produced by a mucoid *P. aeruginosa* culture, whereas aggregation by fluorescently labeled polycations provides similar sensitivity to conventional carbazole assays; and both methods do not require covalent reactions and multiple steps of operations.

2.4. Materials and methods

2.4.1. Bacterial strains and growth media

Wild-type *P. aeruginosa*, PAO1 were obtained from Dr. Guirong Wang (Upstate Medical University). Mucoid *P. aeruginosa* strain PA2192 was isolated from CF patients by Dr. Goldberg at Emory University.[27, 28] All the bacterial strains were grown in Luria-Bertani (LB) medium containing 10 g/L tryptone, 5 g/L yeast extract, and 10 g/L NaCl at 37 °C.

2.4.2. Synthesis of PAA-FITC[29]

Fluorescein isothiocyanate (FITC) was dissolved in dimethyl sulfoxide (final concentration of 1 mg/mL) and protected from light by wrapping the tube in aluminum foil. The FITC solution (40 μL) was then added to each milliliter of a 2 mg/mL polyallylamine (PAA, average Mw ~17,500) solution of pH ≈ 10 so that the FITC to -

NH_2 monomer ratio was 1:50. The mixture was gently stirred and allowed to react at 4 °C overnight. The PAA-FITC product was purified by adding acetone to the reaction mixture resulting in the precipitation of the product forming a cloudy solution. After centrifuged at 8.5 x 10^3 rpm for 10 min, a reddish-brown precipitate was observed, and the solution was discarded. The precipitates were further washed with acetone and dried overnight by vacuum. By comparing the neat UV absorption of FITC in 1:1 MeOH/H_2O solution and PAA-FITC product in 1:1 MeOH/H_2O solution, we have confirmed there is no observable unreacted FITC in either the precipitate product or in the solution, or in the reaction mixture before precipitation. The reaction is quantitative, and the ratio of FITC to the monomers of PAA is 1 to 50. Thus, the degree of labeling (DOA) is 3.76 FITC per polymer of PAA, which contains an average of 188 monomers.

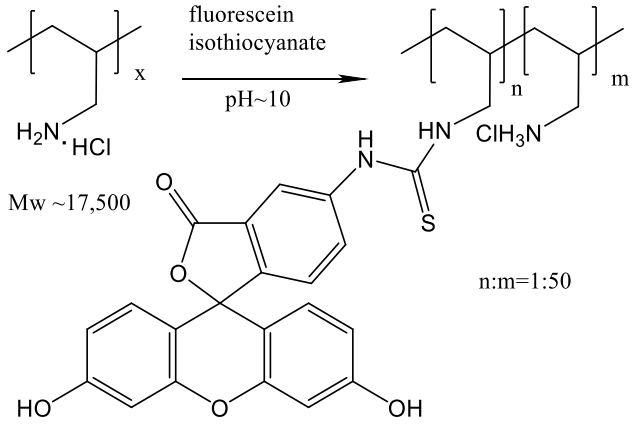

Figure 2.10 Synthesis of PAA-FITC

2.4.3. Quantification of alginate by crystal violet dyed glycolipid assay

A solution of 500 µL $CaCl_2$ (60 mM) was added to 5 mL of neutral (pH 7.0) aqueous solution containing known concentrations of sodium alginate. A hydrogel-like suspending aggregate was observed. The mixture was centrifuged at 5600 rpm for 5 min. The supernatant was removed by discarding the solution while using a glass rod to prevent alginate aggregate from falling out. The alginate aggregate was then rinsed 3 times with deionized water (18 mΩ) to obtain a wet alginate. The alginate aggregate was soaked in 500 µL of 0.3 % crystal violet (CV) dye aqueous solution for 20 min. The CV dye solution was discarded, and the alginate was rinsed 3 times with deionized water. The absorbed CV dye was then extracted from the aggregate by 5 mL acetic acid and gently shaking. The optical density of the dye solution is measured by using 100 µL with a 96-well plate on a Biotek ELx800 Absorbance Microplate Reader at a wavelength of 600 nm.

2.4.4. Quantification of alginate by direct optical density measurement assay

Stock solutions of 60 mM $CaCl_2$, 0.5 mg/mL PAA and 0.5 mg/mL PAA-FITC solution are prepared. Stock solutions (100 µL of $CaCl_2$, PAA or PAA-FITC) were mixed with 1 mL of sodium alginate aqueous solution with known concentrations by using a vortex mixer. The optical density of the solutions was measured by using 100 µL in a 96-

well plate on a Biotek ELx800 Absorbance Microplate Reader at a wavelength of 600 nm.

2.4.5. Carbazole assay

Carbazole assay was performed as described by A. M. Chakrabarty and coworkers, with slight modifications.[25] Briefly, a borate stock solution was prepared by diluting 24.7 g of H_3BO_3 in 45 mL of 4 M KOH to a total of 100 mL using sterile water. Before every use, a borate working solution was prepared by mixing 1 part of the borate stock solution with 40 parts of 98% H_2SO_4, and a 0.1 wt % carbazole solution was prepared in ethanol. Before doing the assay, the borate working solution was put in an ice-water bath for 10 min. A 70 µL of sodium alginate sample with known concentrations (0.01 to 1.00 mg/mL) was added onto the ice-cold borate working solution. Two layers of the solution were observed; the solution (sample mixture) was for about 4 sec by using a vortex and put back to the ice-water bath. A carbazole solution (20 µL) was added onto the sample mixture and warmed at 55 °C for 30 min. The absorbance at 530nm was measured. The standard curve was derived by plotting absorbance against the concentration of sodium alginate ranging from 0.01 to 1.00 mg/mL.

Chapter 3 Synthetic Analogs of Rhamnolipids Modulate Structured Biofilms Formed by Rhamnolipid-nonproducing Mutant of *Pseudomonas aeruginosa*

3.1. Introduction

3.1.1. The importance of rhamnolipids and its analogs on biofilm structure

Bacterial biofilm is the source of infectious diseases in many contexts, including in human hosts with compromised immune systems, and on a wide variety of surfaces in contact with aqueous solutions.[127-130] These bacterial biofilms consist of sophisticated internal structures including pore and channels, mushroom and pillar-like structures,[131-132] heterogeneous distribution of secreted chemicals and bacteria strains.[133] The biology of forming such structured biofilms is complex, and not well understood for a wide range of microbes. For *Pseudomonas aeruginosa*, a class of molecules called rhamnolipids are secreted; the presence of these secreted molecules are critical for forming structured biofilms with pore and channels.[134-137] When the biofilms age, rhamnolipids are also needed for dispersion of bacteria from the biofilm.[138-140] In addition, this class of molecules, rhamnolipids, is also required for the swarming motility of *P. aeruginosa* on an aqueous soft gel surface.[46, 141-142] Interestingly, while biologists have established how rhamnolipids are produced [143-145] and regulated[146-147] in the bacteria and have identified many, if not all, of the bio-functions of rhamnolipids, we still do not know the mechanism of how rhamnolipids build such structured biofilm or enable and facilitate the swarming motility of the bacteria. One of the challenges is that rhamnolipids are surfactants, and thus, it is not clear if the mechanism of their functions is just physical – by reducing the surface tension; or is biological – by having one or more specific

receptors, the binding of which triggers a series of chemical signaling events that control these activities; or whether both physical and biological mechanisms are involved.[141-142]

Recently, we have demonstrated that some synthetic molecules with a polar head group and an aliphatic chain can reinitiate and promote the swarming activities of *rhlA* – a mutant of *P. aeruginosa* that does not produce rhamnolipids, and thus does not swarm.[148-149] While these synthetic molecules are also surfactants, the potent members inhibit the swarming motility of the wild-type *Pseudomonas aeruginosa* (PAO1). This result, along with other findings, suggests that the mechanism of rhamnolipids and these synthetic analogs are unlikely to be physical or a surfactant effect because our molecules can also reduce the surface tension, and would offer the same physical mechanism argument. The activities of swarming modulation (promotion and inhibition) are extremely sensitive to the molecular details while all molecules resemble surfactant structure and show surface activities. In addition, synthetic molecules with intermediate potency exhibited oscillation in their bioactivities (promoting and inhibiting swarming motility) as a function of concentration in the soft gel. This oscillation of bioactivities is a strong indication of cell signaling events responding to an external stimulus.[150-151] Furthermore, novel biological phenomena were observed. Synthetic molecules with intermediate potency at controlling swarming motility induce tendril formation in the swarming pattern[152] suggesting the formation of two opposite phenotypes – hyperswarming and lazy-swarming – while abandoning the original phenotype.[148] Thus, this class of synthetic molecules represents a class of chemical signals.[148-149] While these findings have focused on the influences on swarming motilities, in this work, we demonstrate that synthetic analogs of rhamnolipids, at different concentrations, promote

biofilm formation, help build structured biofilm, as well as inhibit the biofilm formation by a mutant of *Pseudomonas aeruginosa* – *rhlA* – that does not produce rhamnolipids and forms non-structured and thin biofilms.

3.1.2. The aim of the chapter

In this chapter, we explore the effect of a class of synthetic analogs of rhamnolipids at controlling (promoting and inhibiting) the biofilm formation activities of a non-rhamnolipid-producing strain – *rhlA* – of *P. aeruginosa*. This class of rhamnolipid analogs is known to modulate the swarming motilities of wild-type PAO1 and *rhlA* mutant, but its effect on biofilm formation of the *rhlA* mutant is unknown. We show that small structural details of these molecules are important for the bioactivities, but do not affect the general physical properties of the molecules. The bioactive synthetic analogs of rhamnolipids promote biofilm formation by *rhlA* mutant at low concentrations but inhibit the biofilm formation at high concentrations. To explore the internal structures formed by the biofilms, we first demonstrate that wild-type biofilms are formed with substantial topography (hills and valleys) when the sample is under shaking conditions. Using this observation as a comparison, we found that synthetic analogs of rhamnolipids promoted structured (porous) biofilm of *rhlA* mutant, at intermediate concentrations between the low ones that promoted biofilm formation and the high ones that inhibited biofilm formation. This study suggests a potential chemical signaling approach to control multiple bacterial activities.

3.2. Results and discussion

3.2.1. Structural considerations for rhamnolipids analogs

We choose six disaccharide-hydrocarbons to explore their activities in controlling the biofilm formation by *rhlA* mutant (Figure 3.1). These synthetic molecules consist of a disaccharide moiety tethered with various single aliphatic chains. We note that while these small molecules do not bear significant structural similarity to rhamnolipids, depending on the specific structures, they can mimic or dominate the activities of rhamnolipids at controlling swarming motilities.[148-149] Two of these molecules, saturated farnesyl-β-maltoside (SFβM) and saturated farnesyl-β-cellobioside (SFβC), are strong inhibitors of the swarming motility of PAO1 strain; and do not initiate swarming by *rhlA* mutant, and are strong inhibitors of biofilm formation by PAO1 strain.[148] Two of them, dodecyl-β-maltoside (DβM) and benzophenonedecyl-β-maltoside (BPDeβM), promote swarming of *rhlA* mutant and can cause tendril formation at specific concentrations in the soft gel; they are also an intermediate inhibitor of biofilm formation relative to the saturated farnesol derivatives.[149] Here, we explore two more new structures, with the introduction of an ether linkage in the two different positions in eleven-carbon aliphatic chains that are tethered with a cellobioside, $C_6OC_5\beta C$, and $C_3OC_8\beta C$. These two structures allow us to explore the effect of other functional groups (ether) rather than just hydrocarbons at controlling the activities of *P. aeruginosa*.

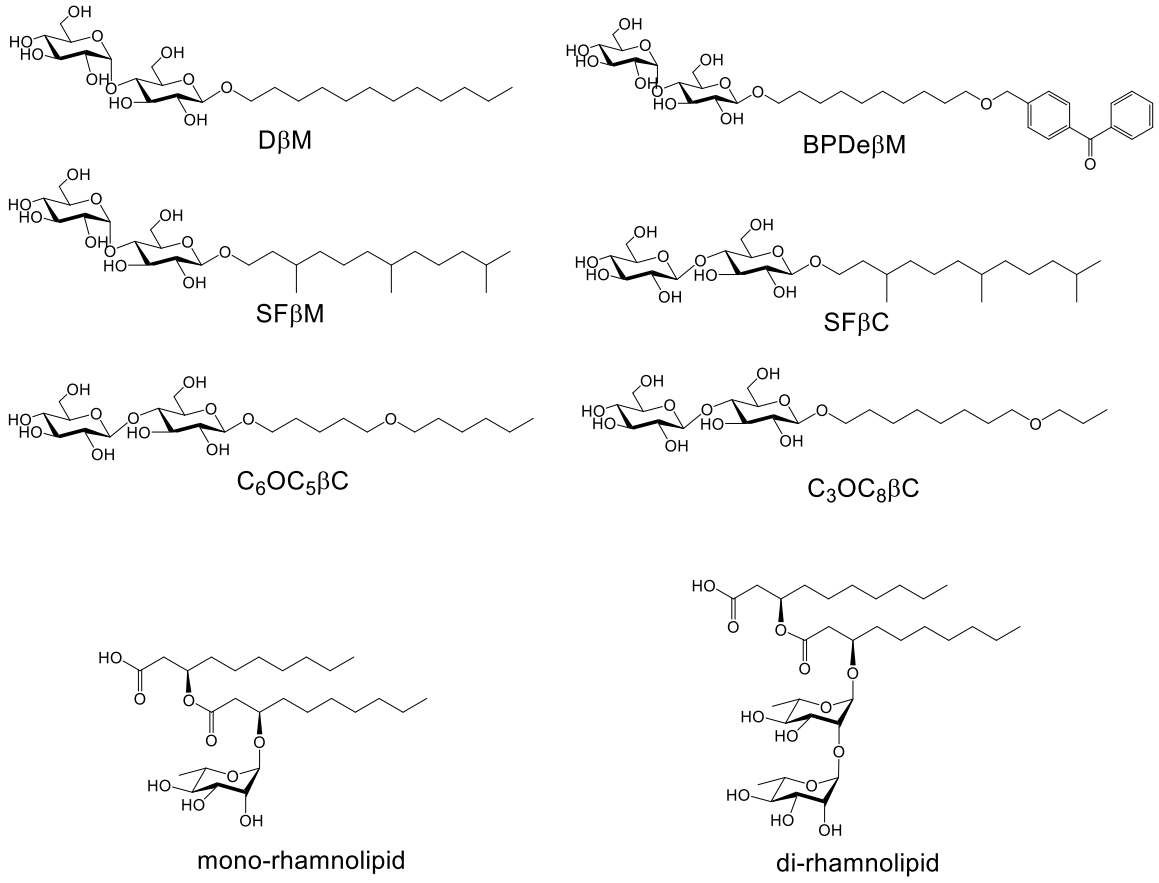

Figure 3.1 Structures of rhamnolipids and their analogs with disaccharide maltose (M) or cellobiose (C) tethered with different aliphatic chains.

3.2.2. Active synthetic analogs of rhamnolipids stimulate and then inhibit biofilm formation by rhlA mutants

We first use the traditional crystal violet staining assay to characterize the total amount of biofilm formed by the *rhlA* mutant in the presence of different concentrations of the six disaccharide hydrocarbons. Interestingly, for DβM, BPDeβM, SFβM, and SFβC, promotion of the biofilm formed by *rhlA* mutants is observed as the concentration is increased from 20 μM to 170 μM, in 24 h under non-shaking condition. The inhibition of

biofilm formation is observed, most noticeably for SFβM and SFβC, when the concentration is further increased to 340 μM (Figure 3.2A). For C_6OC_5βC and C_3OC_8βC, there is no noticeable change in the amount of biofilm formed over the entire range of concentrations studied, in comparison to the control, to which there are no agents added.

To examine the effect of our rhamnolipids-analogs at reducing the count of bacteria from the biofilm as a consequence of biofilm inhibition, we dried the 24-h old biofilm of rhlA mutant, and reintroduced fresh media, and measured the optical density of the media that contained bacteria from the biofilm. At relatively low concentrations (20 μM and 40 μM), DβM, BPDeβM, SFβM, and SFβC have no significant effect on the bacteria in the biofilm, while at 340 μM, the number of bacteria from the biofilm is reduced almost by half. For C_6OC_5βC and C_3OC_8βC, there is no noticeable change in the number of bacteria that remained in the biofilm (Figure 3.2B). These results are consistent with the corresponding amount of biofilm inhibited (Figure 3.2A).

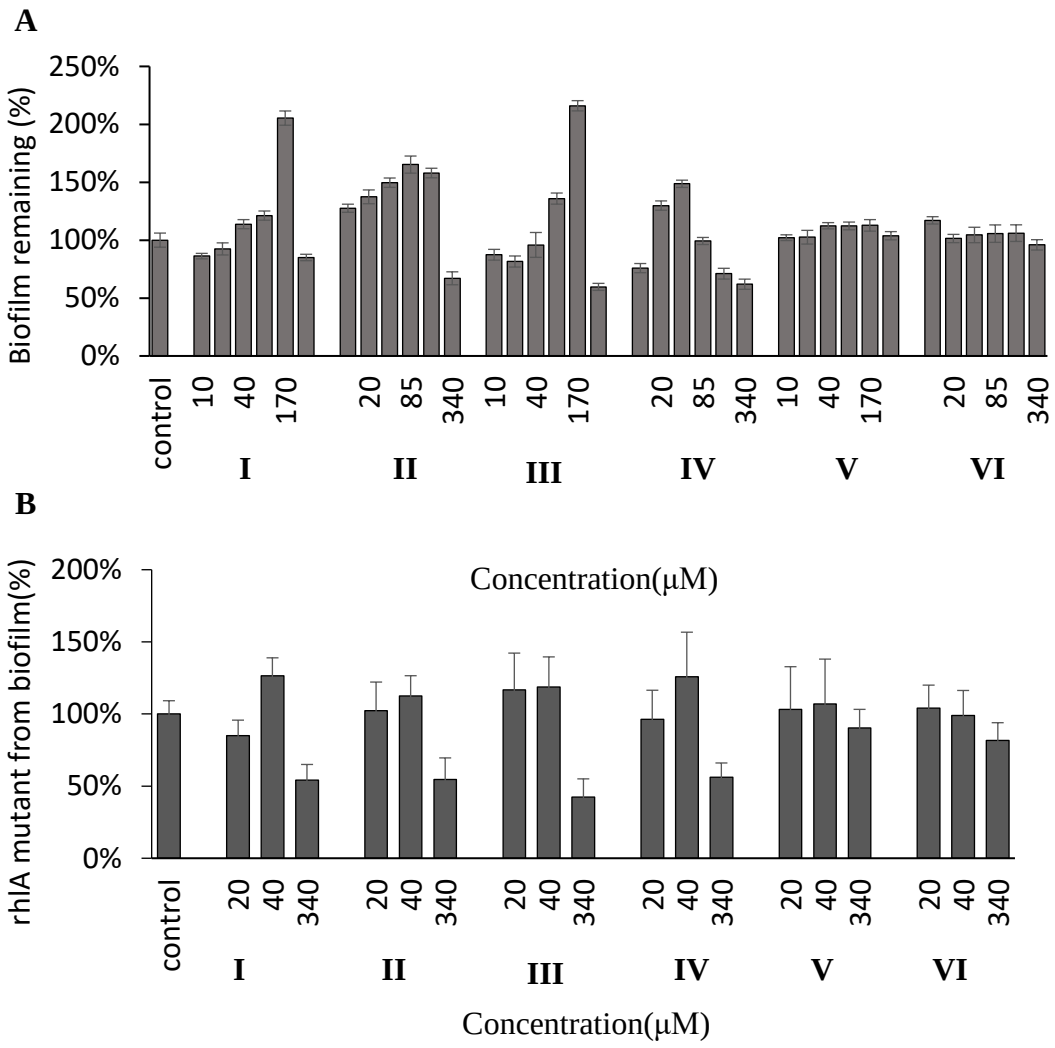

Figure 3.2 The percentages of biofilm that remained (A) were obtained by comparing biofilm content treated with an agent to the control (without agents). The percentages of bacteria from a 24-h old rhlA mutant biofilm (B) were obtained by comparing the OD600 of LB media in contact with rhlA biofilm without our agents (control) to that with our agents under identical conditions. Added agents from left to right are I. DβM, II. SFβM, III. SFβC, IV. BPDeβM, V. C6OC5Bc, VI. C3OC8βC. Error bar is the standard error of the mean from six replicates.

For inhibiting the biofilm formation, the effective concentrations for the *rhlA* mutant (340 µM), are considerably higher than for wild-type PAO1. Considering this high concentration, we examined the growth of the *rhlA* mutant in the presence of the six molecules. At both 20 µM and 340 µM (Figure 3.3), these agents did not exhibit any significant influence on the growth of *rhlA* mutant of *P. aeruginosa* in shaking culture media. This result indicates that the mechanism of biofilm inhibition is not due to any bactericidal effect, but rather likely due to the interference of a ligand-receptor binding that triggers signaling events.

A.

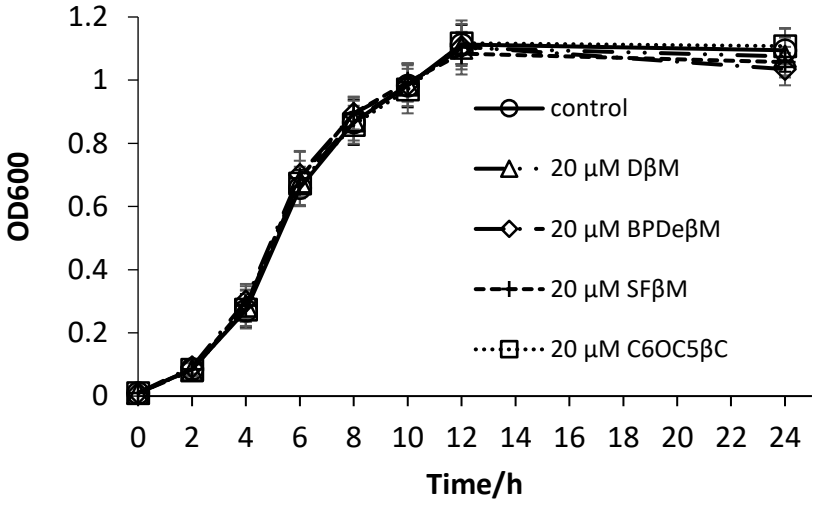

B.

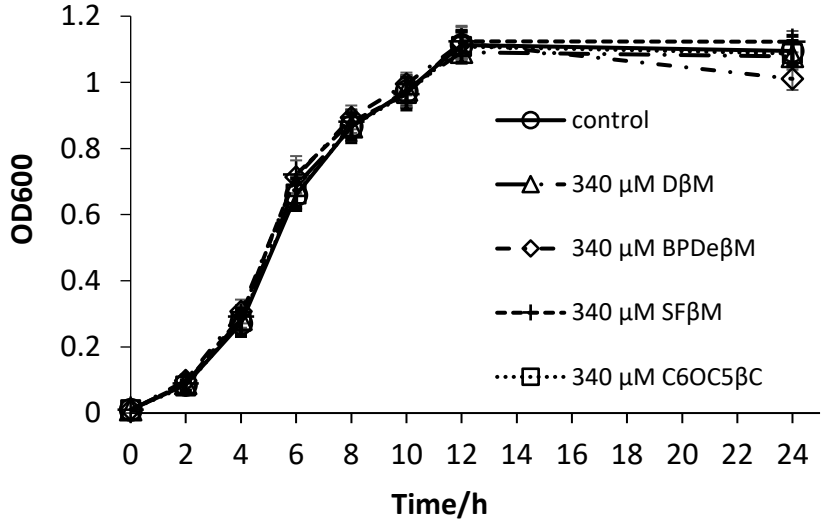

Figure 3.3 *rhlA* mutant of P. aeruginosa growth–response curve with and without 20 µM(A) or 340 µM(B) rhamnolipids analogs. Error bar is the standard error of the mean from six replicates.

Because *rhlA* mutant, which does not produce rhamnolipids, forms a nonporous biofilm, rhamnolipids are implicated in the formation of porous biofilm.[134] However, the exact mechanism of how rhamnolipids help create such a porous biofilm is not clear yet. We have previously shown that externally added rhamnolipids had only a mild effect on inhibiting biofilm formation of PAO1 strain.[149] Together with the fact that *rhlA* mutant form biofilms slower and form thinner biofilms than a PAO1 strain, rhamnolipids are required for efficient formation of full biofilms. Thus, we believe that, in a biofilm growth experiment, a significant amount of synthetic analogs of rhamnolipids are first used to facilitate efficient formation of biofilm; only when the full biofilm is formed, additionally added rhamnolipids-analogs may then start to inhibit the formation of biofilm. Thus, this strong requirement of rhamnolipids or rhamnolipid-analogs for biofilm formation caused a high concentration requirement for the rhamnolipid-analogs to exhibit biofilm inhibition activities for *rhlA* mutants. The mechanism of how rhamnolipids or its analogs are facilitating the biofilm formation is still not clear. As these molecules are likely causing cell signaling events, we believe that the presence of these ligands is changing the expression level of their receptors.

We have previously demonstrated that synthetic agents that are active for controlling swarming motility may or may not be active for inhibiting biofilm formation. For example, saturated farnesol tethered with tetra(ethylene glycol) inhibits swarming but not biofilm formation, whereas saturated farnesol tethered with disaccharides strongly inhibits both swarming and biofilm formation.[149] Furthermore, swarming motilities is sensitive to the agents' concentrations, in that oscillation in swarming activities is exhibited as the concentration increases. For these reasons, we carried out a detailed

concentration study on the effect of ether-linked disaccharides ($C_6OC_5\beta C$ and $C_3OC_8\beta C$) on the swarming motility of PAO1 and *rhlA* mutants. For controls, we used DβM with more expanded concentration ranges than that previously studied.[148-149] Figure 4 shows that while DβM activated swarming of *rhlA* and further caused tendril formation in the swarming pattern, $C_6OC_5\beta C$ did not show a noticeable effect for influencing the swarming motilities of *rhlA* mutant. For PAO1, $C_6OC_5\beta C$ also did not show any noticeable effect on swarming, but expanded concentrations of DβM indicated slight promotion of swarming at about 50 μM and caused tendril formation at 85 μM or higher (Figure 3.4). Wild-type *P. aeruginosa*, PAO1, does not form tendrils on its own. Together with the sensitivity to the chemical agents' structural details, this chemically induced tendril formation suggests a ligand-receptor binding event for DβM. We note that $C_3OC_8\beta C$ is also not active (Figure 3.5). Thus, ether-linked disaccharides are not active for controlling either swarming or biofilm formation. These results suggest that the structures of the aliphatic chains play a critical role in controlling the bioactivities of the molecules.

A

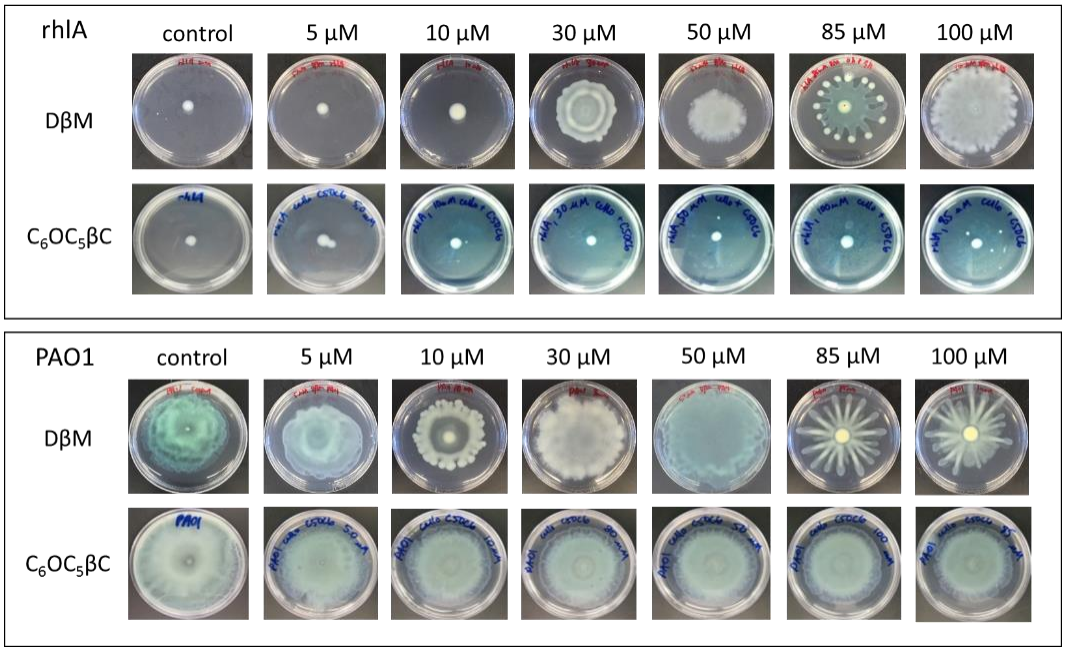

B

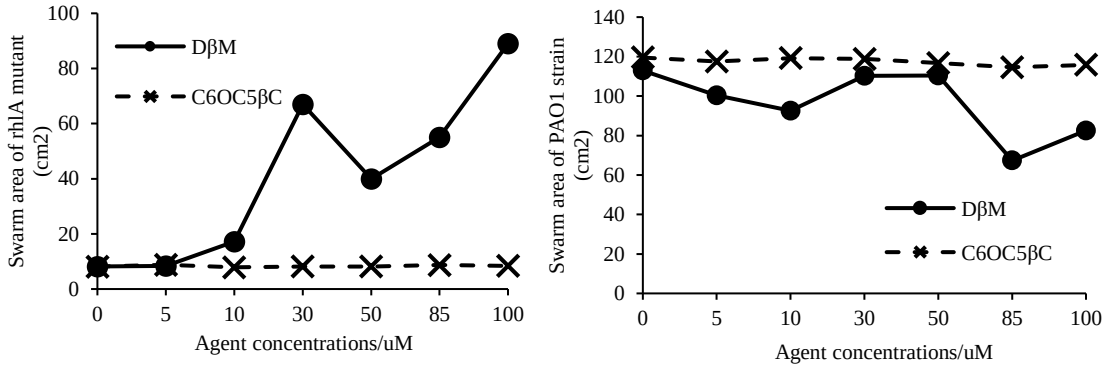

Figure 3.4 Swarming patterns (A) and the plots of swarming areas of *rhlA* and PAO1 strains on the soft gel (0.5 wt% agar) containing different concentrations of DβM and C_6OC_5βC. Controls contain no added synthetic agents. The concentrations are shown above the swarming images. Images were taken 24 h after inoculation of bacteria at the center of the plate.

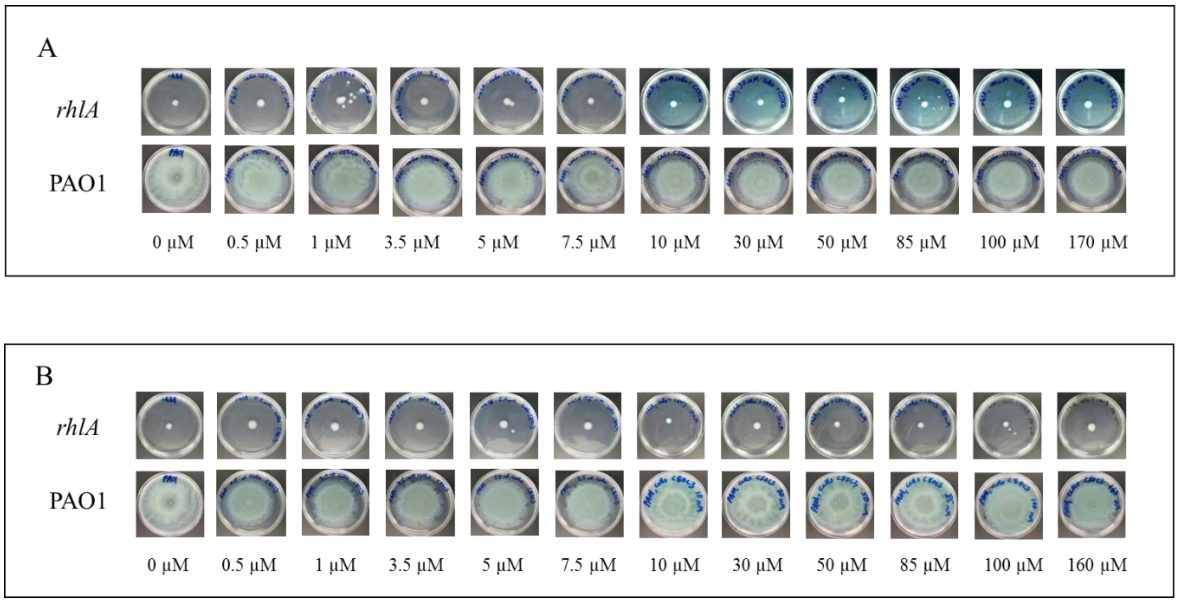

Figure 3.5 Swarming of PAO1 and *rhlA* on the soft gel (0.5% agar) with the presence of different concentrations of (A) $C_6OC_5\beta C$ and (B) $C_3OC_8\beta C$. Compounds do not promote swarming of *rhlA* or promote tendril formation in PAO1. Bacteria were inoculated at the center of the semisolid gels (~0.5 % agar). Pictures were taken 24 h after inoculation with bacteria.

3.2.3. Shaking produces structured biofilms by PAO1 strain

To explore whether our synthetic analogs can produce structured biofilms, in addition to promoting biofilm formation, we first explore conditions that will give structured and less-structured biofilms. It is known that flow of media can enhance the production of structured biofilms with channels, pores, and in general, with a high degree of topography.[131, 133, 137] Tolker-Nielsen and coworkers have reported that in under flow conditions, biofilms were formed with channels and pores.[131, 133] Unfortunately, for

synthetic analogs, the number of agents we obtain from organic synthesis is quite limited in comparison to the amount needed for continuous flowing of agent-contained media that last for hours to days. For this reason, we seek a different and new condition that would allow us to explore the effect of our agents on the structure of the biofilm formed by the rhlA mutant. To create a dynamic condition of the media, but without flow, we explored shaking of the 96-well plate, in which biofilm is formed, to examine the structures (pores and channels) of biofilm with and without such shaking agitation.

We first tagged PAO1 and *rhlA* strains with plasmid pSMC2 that constitutively expresses the green fluorescent protein,[153] and then examined the biofilms formed by these bacteria with and without shaking. Figure 3.6 shows that PAO1 formed a flat and thick bed of biofilm in the non-shaking condition. Shaking the plates with 100 rpm, PAO1 biofilm exhibited distinct features that resembled structured biofilm, including topography of hill and valley-like structures in the confocal fluorescent signals, instead of a plain flat biofilm. However, *rhlA* mutant formed flat and thinner biofilm with and without shaking. This result indicates that shaking at 100 rpm produce a highly structured biofilm by PAO1. For the *rhlA* mutant, this strain produced significantly less biofilm than PAO1 strains, and the biomass with and without shaking is at a similar level. The mechanism, whether physical or biological in nature, is unknown for how shaking induces the formation of such structured biofilm of *P. aeruginosa*. Considering the drastic structural difference in the PAO1 biofilm produced with and without shaking, we used these two kinds of biofilm as standards to compare and evaluate the degree of structural features of biofilms formed by the *rhlA* mutant that is stimulated by the presence of our synthetic analogs.

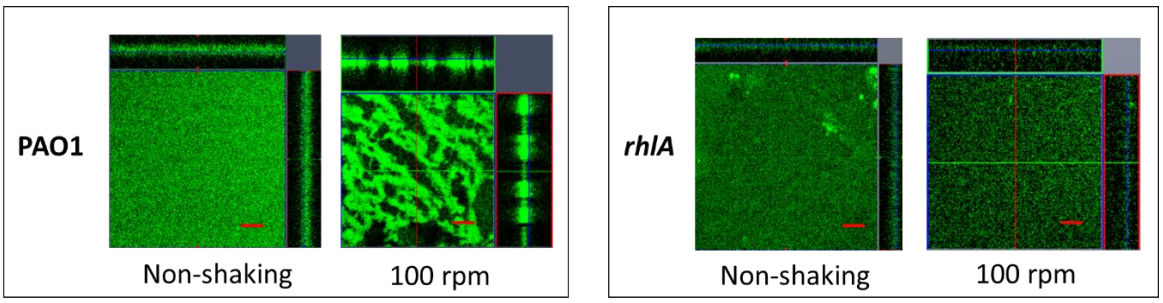

Figure 3.6 The effect of shaking (non-shaking and 100 rpm) on biofilm formation by the *rhlA* mutant of *P. aeruginosa* in 24h. Representative confocal laser scan microscopy (CLSM) images (A) of biofilm formed by *rhlA*- EGFP mutant (plasmid pSMC2 that expresses green fluorescent protein). Scale bar = 76 µm.

3.2.4. Synthetic analogs of rhamnolipids induce structured biofilm formed by rhlA mutant

Next, we examined the influence of synthetic analogs of rhamnolipids on biofilm structures of *rhlA*-EGFP strain formed under non-shaking conditions by using confocal fluorescence. At 24 h, there is visibly more fluorescence signal for biofilm formed by the *rhlA*-EGFP strain which was treated with 20 µM of all four agents, DβM, BPDeβM, SFβM, and SFβC, than biofilm formed without any added agents. Among these agent-treated biofilms, BPDeβM caused the most biofilms. When we examined the same biofilms but treated with 340 µM instead of 20 µM of the four agents, each biofilm sample formed by *rhlA*-EGFP strain showed less fluorescent signal than the control biofilm that had no added agents (Figure 3.7). These results suggest that at 340 µM, all four agents, DβM, BPDeβM, SFβM, and SFβC, are inhibiting the biofilm formation. To confirm these results – promotion at 20 µM and inhibition at 340 µM – we examined the biofilm formed by the *rhlA*-EGFP strain with the same agent treatments (20 and 340 µM)

after 48 hours of culture. Overall, more biofilm was observed for all samples. For BPDeβM, SFβM, and SFβC, more biofilms were observed for samples containing 20 µM of agents than the control sample without agent treatment; however, significantly less biofilm was observed for samples containing 340 µM of agent than the control. These results suggest that BPDeβM, SFβM, and SFβC inhibited biofilm at 340 µM. The agent DβM did show a slight promotion of biofilm at 20 µM, but a comparable amount of biofilms were observed at 340 µM. To quantify the amount of biomass of the biofilm, software COMSTAT was used. According to the COMSTAT-based quantification of biomass, 10 % ~ 60 % biofilm promotion was observed for the biofilm samples containing relatively low concentrations of agents (20 µM and 40 µM). While at 340 µM, around 80 % of the biofilms were inhibited by DβM, BPDeβM, SFβM, and SFβC.

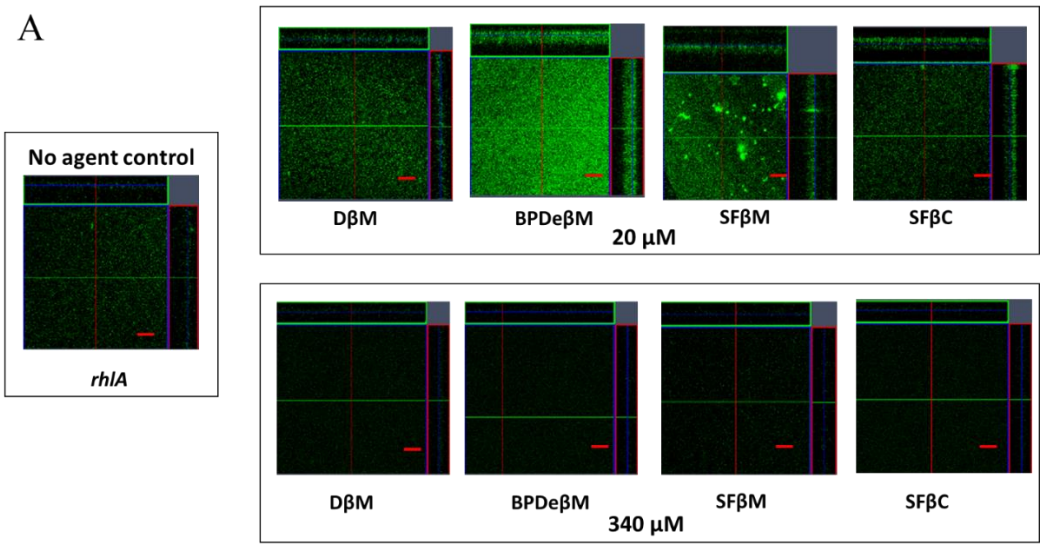

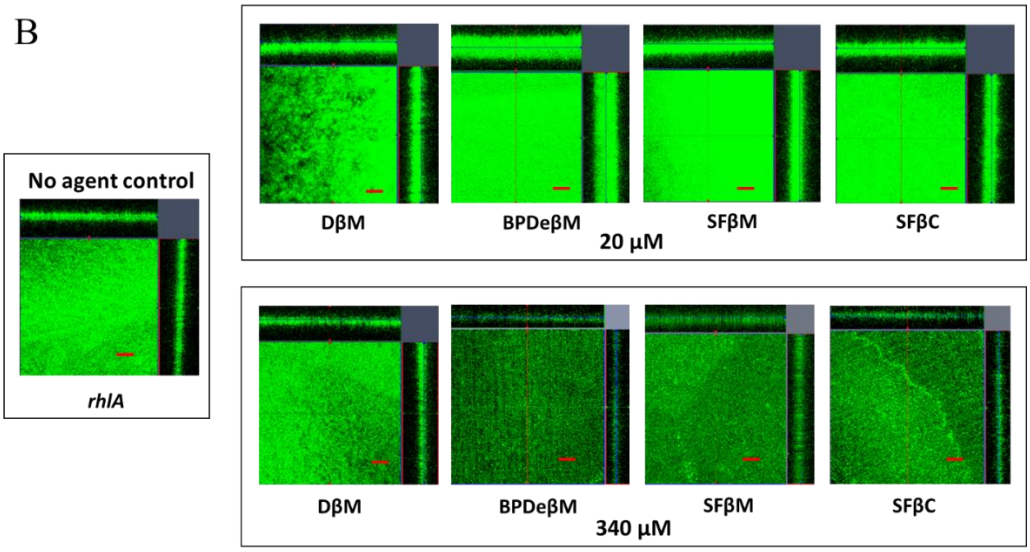

Figure 3.7 The effect of rhamnolipid analogs on biofilm formation by the *rhlA* mutant of *P. aeruginosa* (A) in 24 h, and (B) in 48 h under 100 rpm shaking condition. Representative confocal laser scan microscopy (CLSM) images of biofilm formed by *rhlA*-EGFP strain (plasmid pSMC2 that expresses green fluorescence). Scale bar = 76 µm.

We note that in a 24 well-Plate under shaking conditions, the biofilm formed by the *rhlA* mutant in the presence of saturated farnesol agents exhibited a conspicuously different appearance than the biofilm formed without added agents. Without added agents, the biofilms formed by *rhlA* mutant appeared to have more exopolymers covering the bottom of the wells, whereas, with SFβM at both low (20 µM) and high (85 µM) concentrations, there were fewer exopolymers covering the bottom of the wells (Figure 3.8). For $C_6OC_5\beta C$ and $C_3OC_8\beta C$, there is no significant change in the number of

fluorescent signals in the biofilm formed by *rhlA*-EGFP strain as compared to the control that has no added agents (Figure 3.9).

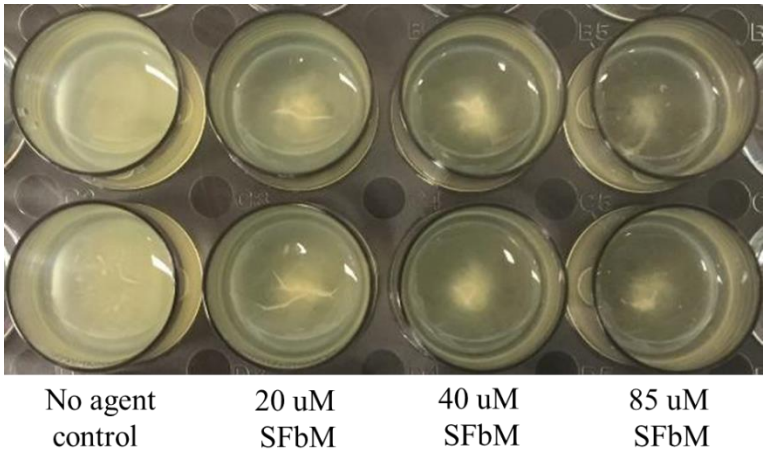

Figure 3.8 Treatment of rhamnolipids analogs on rhlA mutant affects the appearance of biofilm formed on 24 well plates under non-shaking condition.

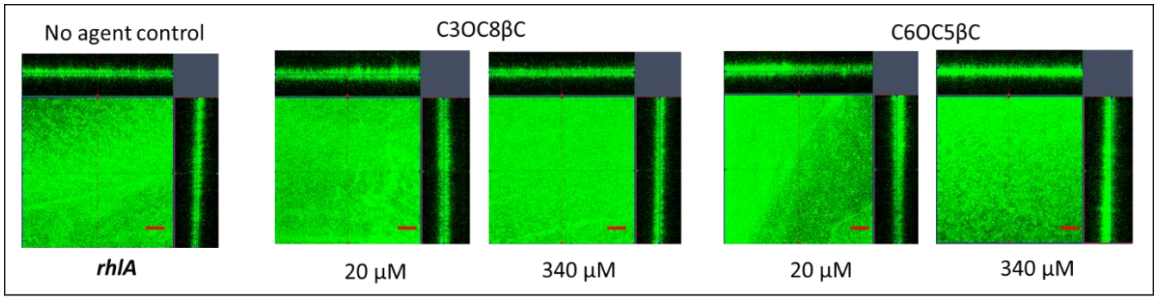

Figure 3.9 The effect of rhamnolipids analogs on biofilm formation by the *rhlA* mutant of P. aeruginosa in 48 h under 100 rpm shaking condition. Representative confocal laser scan microscopy (CLSM) images of biofilm formed by *rhlA*-EGFP (plasmid pSMC2 that expresses green fluorescence). Scale bar = 76 µm.

Next, we examined the biofilm formed by the *rhlA* mutant with intermediate concentrations between the low concentrations that caused the initial promotion and the high concentrations that caused the biofilm inhibition. To our surprise, at intermediate concentrations, the synthetic analogs SFβM (40 µM), SFβC (40 µM), and BPDeβm (40 µM) promoted biofilms formed by *rhlA* mutant to exhibit structural features of porosity more resembling the structured PAO1 biofilm formed under shaking than that without shaking (Figure 3.10). Without shaking, these structural features in the biofilm of rhlA mutant are likely caused by the presence of synthetic analogs rather than any other physical effect.

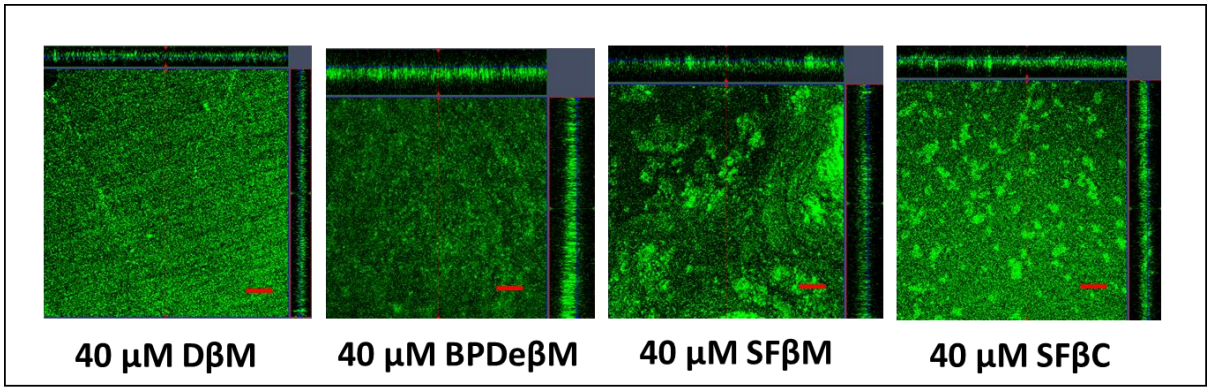

Figure 3.10 The effect of synthetic analogs of rhamnolipids on biofilm formation by the *rhlA* mutant of *P. aeruginosa* in 24 h under non-shaking condition. Representative confocal laser scan microscopy (CLSM) images of biofilm formed by *rhlA*- EGFP strain (expresses green fluorescence on plasmid pSMC2). Scale bar = 76 µm.

Wild-type PAO1 produces rhamnolipids, and under a flowing fluid[8] or shaking conditions, produces highly structured biofilms with channels. For *rhlA* mutant which does not produce rhamnolipid, however, our shaking experiment does not cause the bacteria to produce structured biofilm. Instead, two notable rhamnolipid analogs, SFβM and SFβC, at intermediate concentrations enabled *rhlA* mutant to make structured biofilms without shaking or under a flowing fluid. Figure 3.11 summarizes the effect of active synthetic analogs on biofilm structures of *rhlA* mutants. These fluid-filled voids give rise to the complex structure in a biofilm including pores and channels. Such structures are believed to be responsible for nutrient transport, cell-cell interactions, and even to support a degree of homeostasis.[36] The mechanism for the formation of these structures is still unclear although we know that rhamnolipids, and also its synthetic analogs, play a critical role.

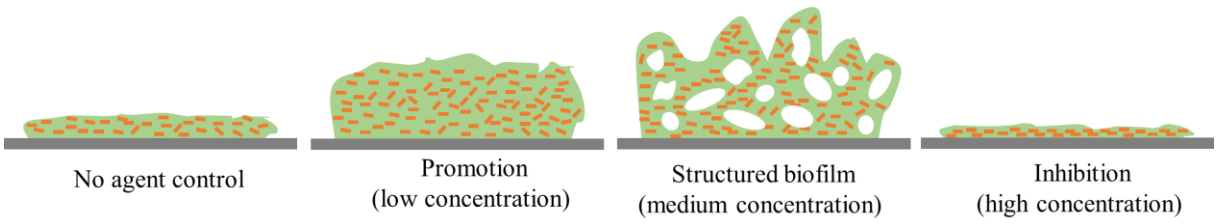

Figure 3.11 Schematic representation of synthetic analogs of rhamnolipids at modulating biofilm formed by the *rhlA* mutant.

Biofilm formation and swarming motility are both multi-cellular activities, and many of these multi-cellular activities are initiated or regulated by quorum sensing.[154-156] Here, we believe that both biofilm formation and swarming motility are also controlled

by chemical cues or signals such as rhamnolipids from the environment. These signals directly control whether swarming motility will occur or not, and what types of the internal structures of biofilm will be formed. It is not clear whether rhamnolipids and the synthetic analogs in our studies,[136, 138] are just signaling molecules that trigger the formation of pores and channels; or whether they also take part as a structural component to build and maintain the fluid void structures in a biofilm; or, whether they also act as anchors to which the bacteria attach in a biofilm. This subject is an ongoing area of research in our studies.

3.3. Conclusions

In this work, we found that synthetic rhamnolipid-analogs active for controlling swarming (inhibition and activation) also promote biofilm formation of a non-swarming strain, *rhlA* mutant, at relatively low concentration, but inhibit biofilm formation at high concentration. Agents that are inactive at controlling swarming motility are also not active in influencing the biofilm formation of the *rhlA* mutant. We also find that biofilm of PAO1 under shaking conditions exhibited porous structures, whereas under static conditions showed relatively uniform biofilms. Using this result as criteria for comparison between structured and nonstructured biofilms, we find that biofilm formation caused by the presence of rhamnolipid-analogs at intermediate concentrations also exhibited porous features. Together, these results suggest that synthetic rhamnolipid-analogs behave as signaling molecules and can substitute rhamnolipids for functional control. Among many other approaches,[157-158] chemical signaling that governs the

quorum sensing of bacteria has been a target for developing anti-bacterial as well as potential therapeutic agents.[147, 154, 159] We believe that a new approach of developing mimics and dominating agents of the environmental cues bears an enormous potential for developing therapeutic agents and chemical applications.

3.4 Materials and methods

3.4.1. Synthetic procedure

Synthesis of C_6OC_5OH: 0.51 g (12.9 mmol) of NaH (60% dispersion in mineral oil) was suspended in 10 mL of DMF and added to a solution of pentan-1,5-diol (2.69 g, 25.8 mmol) in DMF (6 ml). 1-bromohexane (1.33 g, 8.06 mmol) was then added drop by drop under argon and stirred overnight. The reaction mixture was quenched with deionized water and extracted with 1:1 hexane and ethyl acetate. Then the organic phase was concentrated *in vacuo* at 35 °C. The crude product was then purified by column chromatography. The product was obtained as colorless oil, 1.17 g, 73 %, Rf = (0.35, 45 % EtOAc in Hexane). ^{1}H NMR (400 MHz, CDCl3): δ 3.63 (t, 2H), 3.38 (t, 2H), 3.36 (t, 2H), 1.70-1.21 (m, 14H), 0.88 (t, J= 6.3 Hz, 3H). HRMS (ESI+): Cacld. for M^+: 189.1776, found: 189.1853

Synthesis of C_3OC_8OH: 0.51 g (12.9 mmol) of NaH (60% dispersion in mineral oil) was suspended in 10 mL of DMF and added to a solution of octan-1,8-diol (3.77 g, 25.8 mmol) in DMF (6 ml). 1- bromopropane (0.99 g, 8.06 mmol) was then added drop

by drop under argon and stirred overnight. The reaction mixture was quenched with deionized water and extracted with 1:1 hexane and ethyl acetate. Then the organic phase was concentrated *in vacuo* at 35 °C. The crude product was then purified by column chromatography. C_3OC_8OH was obtained as colorless oil, 1.13 g, 69 %, Rf = (0.37, 45 % EtOAc in Hexane). ^{1}H NMR (400 MHz, CDCl3): δ 3.63 (t, 2H), 3.36 (t, 2H), 3.34 (t, 2H), 1.66-1.20 (m, 14H), 0.88 (t, J= 6.3 Hz, 3H). HRMS (ESI+): Cacld. for M^+: 189.1776, found: 189.1853

Synthesis of acetylated-bromo-cellobiose: To an oven-dried round bottom flask, cellobiose (1.0 g, 2.8 mmol), AcBr (~3.6 mL, 44.4mmol), and AcOH (19 mL) were added and stirred at room temperature (25 °C) for ~ 1 h. The reaction mixture was concentrated *in vacuo* at 35 ºC and then co-evaporated three times with PhMe (2×10 mL, anhydrous). After removal of solvent, the flask was further heated *in vacuo* at 50 ºC for 15min to give a foamy solid, aceto-bromo-cellobiose. The crude aceto-bromo cellobiose was immediately used in next step without any further purification.

Synthesis of acetylated C_6OC_5βC and acetylated C_3OC_8βC: For obtaining β-anomer as the major product, the crude aceto-bromo cellobiose was dissolved in MeCN (10 mL) and 2 equivalents of C_6OC_5OH (1.05 g, 5.6 mmol) or C_3OC_8OH (1.05 g, 5.6 mmol) were added along with two equivalents of $FeCl_3$ (5.6 mmol). The reaction mixture was stirred vigorously for about ~45-60 mins at rt. After stirring at rt, aq KBr (10%, 25 mL) and then toluene (60 mL) were added under stirring. The organic phase was washed twice with aq KBr (10 %, 2×25 mL), once with aq $NaHCO_3$ (5 %, 25 mL) and twice with

H_2O (2×25 mL). The crude product was then purified by column chromatography using gradient elution (100 % hexane to 40 % ethyl acetate in hexane). Acetylated $C_6OC_5\beta C$ was obtained as Colorless powder, 0.42 g, 21.3 % (2-step), Rf = (0.36, 40 % EtOAc in Hexane). ^{1}H NMR (400 MHz, CDCl3): δ 5.20 (m, 3H), 4.93 (q, J1-2 = 8.4 Hz, 2H), 4.54-4.43 (m, 3H), 4.39 (dd, J1-3 = 12.9 Hz, J1-2 = 4.8 Hz, 1H), 4.13-4.02 (m, 2H), 3.87- 3.74 (m, 2H), 3.69-3.56(m, 2H), 3.44 (q, 1H), 3.38 (t, 2H) 3.36 (t, 2H) 2.13-1.99 (s, 7 X 3H), 1.70-1.21 (m, 14H), 0.88 (t, J= 6.3 Hz, 3H). Acetylated $C_3OC_8\beta C$ was obtained as colorless powder, 0.50 g, 23.1 % (2-step), Rf = (0.42, 40 % EtOAc in Hexane). 1H NMR (400 MHz, CDCl3): δ 5.20 (m, 3H), 4.93 (q, J1-2 = 8.4 Hz, 2H), 4.54-4.43 (m, 3H), 4.39 (dd, J1-3 = 12.9 Hz, J1-2 = 4.8 Hz, 1H), 4.13-4.02 (m, 2H), 3.87- 3.74 (m, 2H), 3.69-3.56(m, 2H), 3.44 (q, 1H), 3.36 (t, 2H), 3.34 (t, 2H), 1.66-1.20 (m, 14H), 0.88 (t, J= 6.3 Hz, 3H).

Synthesis of $C_6OC_5\beta C$ and $C_3OC_8\beta C$: The deprotection of acetyl groups was achieved by Zemplén deacetylation using MeONa/MeOH (10 mM solution) conditions followed by neutralization (pH ~6.5) over H+ amberlite resins. The resins were filtered off and products dried under high vacuum overnight. $C_6OC_5\beta C$ was obtained as colorless powder, 0.23 g, 87 %. ^{1}H NMR (300 MHz, CD_3OD): δ 4.36 (d, J = 7.8 Hz, 1H), 4.28 (d, J = 7.8 Hz, 1H), 3.82 (m, 4H), 3.69-3.47 (m, 4H), 3.40-3.25(m, 8H, overlapping with MeOH), 3.18-3.11 (m, 2H), 1.60-1.13 (m, 14H), 0.82 (t, J= 6.3 Hz, 3H). ^{13}C NMR (100 MHz, CD3OD): δ 103.2, 102.8, 79.3, 76.7, 76.4, 75.1, 75.0, 73.7, 73.5, 70.7, 70.4, 69.9, 69.3, 61.4, 60.5, 31.4, 29.3, 29.2, 29.1, 25.5, 22.3, 22.1, 13.0. HRMS (ESI) m/z: Calcd. $(C_{23}H_{44}O_{12})Na^+$: 535.2731; Found: 535.2728. $C_3OC_8\beta C$ was obtained as colorless

powder, 0.24 g, 91 %. ^{1}H NMR (300 MHz, CD_3OD): δ 4.33 (d, J = 7.8 Hz, 1H), 4.19 (d, J = 7.8 Hz, 1H), 3.78 (m, 4H), 3.63-3.39 (m, 4H), 3.40-3.25(m, 8H, overlapping with MeOH) 1.66-1.20 (m, 14H), 0.85 (t, J= 6.3 Hz, 3H). ^{13}C NMR (100 MHz, CD3OD): δ 103.2, 102.8, 79.3, 76.7, 76.4, 75.1, 75.0, 73.7, 73.4, 72.1, 70.4, 69.9, 69.3, 61.4, 60.5, 29.3, 29.3, 29.1, 29.1, 25.8, 25.6, 22.5, 9.5. HRMS (ESI) m/z: Calcd. $(C_{23}H_{44}O_{12})Na^{+}$: 535.2731; Found: 535.2728.

3.4.2. Bacterial strains

Wild-type *P. aeruginosa* PAO1 and PAO1-EGFP strains were obtained from Dr. Guirong Wang (Upstate Medical University, Syracuse). The non-swarming mutant of *P. aeruginosa*, *rhlA* (PW6886, *rhlA*-E08::ISphoA/hah) was obtained from PA two-allele library (PAO1 transposon mutant library).[156]

3.4.3. Crystal violet dye-based biofilm inhibition assay

Inhibitory effect of all the maltose hydrocarbons on the biofilm formation by *rhlA* mutant was determined by crystal violet dye based biofilm inhibition assays. An overnight culture of the *rhlA* mutant was subcultured to an OD_{600} of 0.01 into the LB medium. 200 µL of the subculture was aliquoted into the wells of 96-well polystyrene microtiter plate when it reached the OD_{600} of 0.1. Predetermined concentrations of the test compounds were then added to the respective wells containing subculture. Sample plates were wrapped in GLAD Press n' Seal® followed by incubation under stationary conditions for 24 h at 37 °C. After incubation, the media was discarded and the plates

were washed with water and dried for 1 h at 37 °C. The sample plates were stained with 200 μL of 0.1% aqueous solution of crystal violet (CV) and followed by incubation at ambient temperature for 20 min. The CV stain was then discarded and the plates were washed with water. The remaining biofilm adhered stain was re-solubilized with 200 μL of 30 % acetic acid. After the stain was dissolved (15 minutes), 100 μL of the solubilized CV was transferred from each well into the corresponding wells of a new polystyrene microtiter dish. Biofilm inhibition was quantified by measuring the OD_{600} of each well in which a negative control lane wherein no biofilm was formed served as a background and was subtracted out. The percent inhibition was calculated by the comparison of the OD_{600} for biofilm grown in the absence of compound (control) versus biofilm grown in the presence of compound under identical conditions. Biofilm inhibition assay with all the maltose derivatives was repeated four times and each data point in the graph is the average of values from 6 wells.

3.4.4. Confocal laser scanning microscopy (CLSM)

Biofilms were grown by inoculating the bacteria on polystyrene coupons (3/8 in. × 3/8 in.) with or without rhamnolipid analogs in a 24-well microtiter plate. The saran-wrapped plate was then incubated at 37 ºC with or without shaking. Each polystyrene coupon was then washed gently by dipping into 0.85 w/v% aqueous NaCl solutions twice and then placed on a microscope cover glass (50 x 24mm, No. 2, Fisher Scientific, Pittsburgh, PA). The biofilms were visualized using a Zeiss LSM 710 Confocal Laser

Scanning Microscope (Carl Zeiss, Jena, Germany). A 488 nm laser line was used to visualize biofilms formed by PAO1-EGFP and *rhlA*-EGFP strains.

3.4.5. Biofilm inhibition assay

An overnight culture of *rhlA* strain was subcultured to an OD_{600} of 0.01 in the LB medium. 200 µL of the subculture was aliquoted into the wells of 96-well polystyrene microtiter plate when it reached the OD_{600} of 0.1. The stock solutions of the test compounds in sterile water were added to the wells containing the subculture to achieve the predetermined concentrations. Sample plates were wrapped in polyvinylidene chloride (PVDC) and incubated without shaking for 24 h at 37 °C. After incubation, the media was discarded and the plates were washed with water and dried for 1 h at 37 °C. 200 µL of LB media and the test compounds were then added to the corresponding wells again. Sample plates were wrapped in PVDC and incubated without shaking for another 1 h at 37 °C. 100 µL of the media from each well was transferred into the corresponding wells of a new polystyrene microtiter plate. And the OD_{600} of each well was read by a microplate reader Elx800 (BIO-TEK Instruments, Inc., Winooski, VT, USA). A control lane containing pure LB media served as a background and was subtracted out. The percent bacteria in the biofilm was calculated by the comparison of the OD_{600} for bacteria grown in the absence of compound (control) versus bacteria grown in the presence of compound under identical conditions. Each data point in the graph is the average of values from 6 wells.

^{1}H NMR spectra

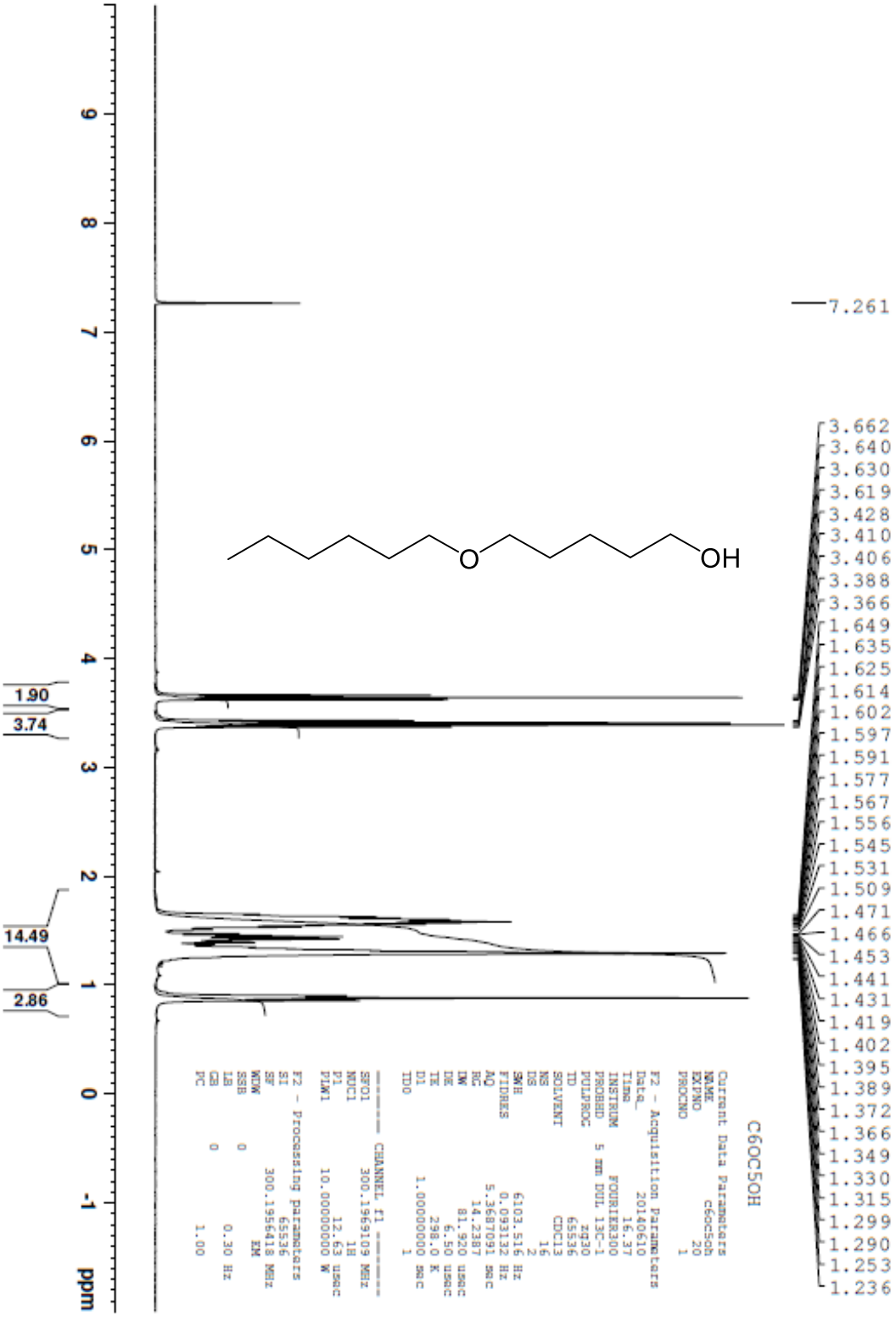

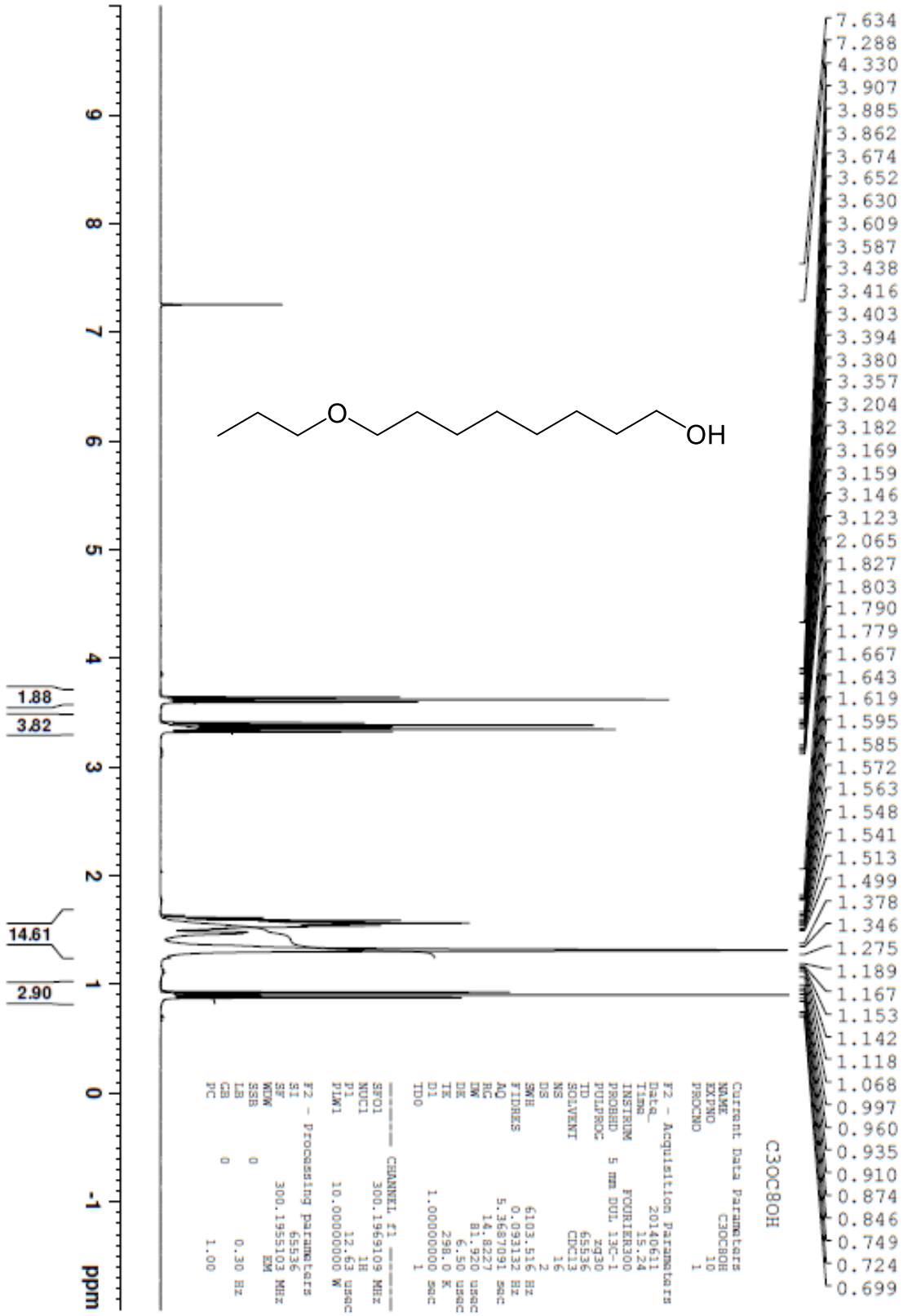
7.634
7.288
4.330
3.907
3.885
3.862
3.674
3.652
3.630
3.609
3.587
3.438
3.416
3.403
3.394
3.380
3.357
3.204
3.182
3.169
3.159
3.146
3.123
2.065
1.827
1.803
1.790
1.779
1.667
1.643
1.619
1.595
1.585
1.572
1.563
1.548
1.541
1.513
1.499
1.378
1.346
1.275
1.189
1.167
1.153
1.142
1.118
1.068
0.997
0.960
0.935
0.910
0.874
0.846
0.749
0.724
0.699
c3oc8oh
Current Data Parameters
NAME C3OC8OH
EXPNO 10
PROCNO 1
F2 - Acquisition Parameters
Date_ 20140611
Time 15.24
INSTRUM FOURIER300
PROBHD 5 mm DUL 13C-1
PULPROG zg30
TD 65536
SOLVENT CDCl3
NS 16
DS 2
SWH 6103.516 Hz
FIDRES 0.093132 Hz
AQ 5.3687091 sec
RG 14.8227
DW 81.920 usec
DE 6.50 usec
TE 298.0 K
D1 1.00000000 sec
TD0 1
====== CHANNEL f1 ======
SFO1 300.1969109 MHz
NUC1 1H
P1 12.63 usec
PLW1 10.00000000 W
F2 - Processing parameters
SI 65536
SF 300.1955103 MHz
WDW EM
SSB 0
LB 0.30 Hz
GB 0
PC 1.00
O
OH
1.88
3.82
14.61
2.90
9
8
7
6
5
4
3
2
1
0
-1
ppm

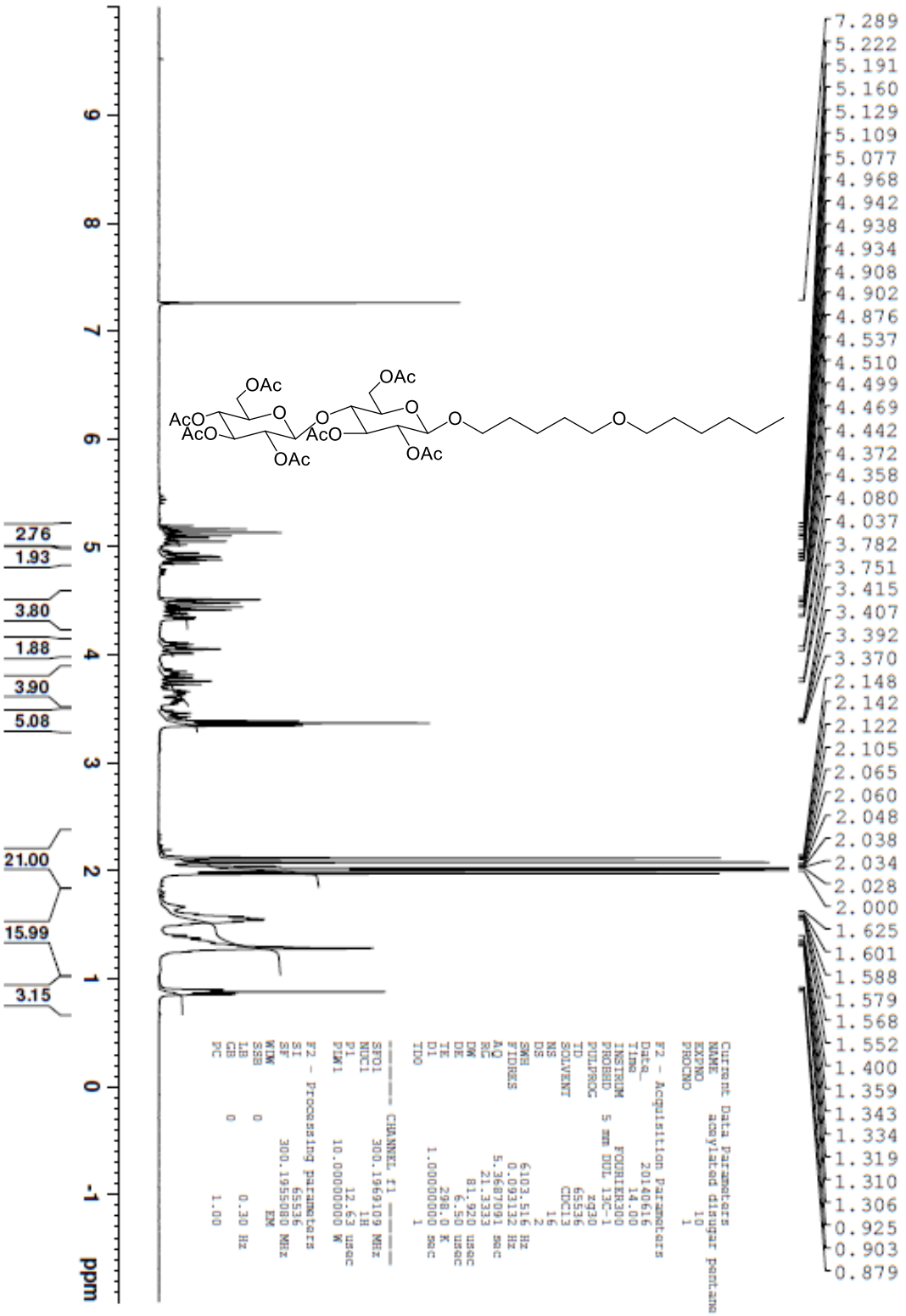
OAc
AcO
AcO
OAc
OAc
OAc
OAc
O
7.289
5.222
5.191
5.160
5.129
5.109
5.077
4.968
4.942
4.938
4.934
4.908
4.902
4.876
4.537
4.510
4.499
4.469
4.442
4.372
4.358
4.080
4.037
3.782
3.751
3.415
3.407
3.392
3.370
2.148
2.142
2.122
2.105
2.065
2.060
2.048
2.038
2.034
2.028
2.000
1.625
1.601
1.588
1.579
1.568
1.552
1.400
1.359
1.343
1.334
1.319
1.310
1.306
0.925
0.903
0.879
2.76
1.93
3.80
1.88
3.90
5.08
21.00
15.99
3.15
ppm
Current Data Parameters
NAME acylated disugar pentane product
EXPNO 10
PROCNO 1
F2 - Acquisition Parameters
Date_ 20140616
Time 14.00
INSTRUM FOURIER300
PROBHD 5 mm DUL 13C-1
PULPROG zg30
TD 65536
SOLVENT CDCl3
NS 16
DS 2
SWH 6103.516 Hz
FIDRES 0.093132 Hz
AQ 5.3687091 sec
RG 21.1333
DW 81.920 usec
DE 6.50 usec
TE 298.0 K
D1 1.00000000 sec
TD0 1
======== CHANNEL f1 ========
SFO1 300.1696109 MHz
NUCl 1H
P1 12.63 usec
PLW1 10.00000000 W
F2 - processing parameters
SI 65536
SF 300.1700000 MHz
WDW EM
SSB 0
LB 0.30 Hz
GB 0
PC 1.00

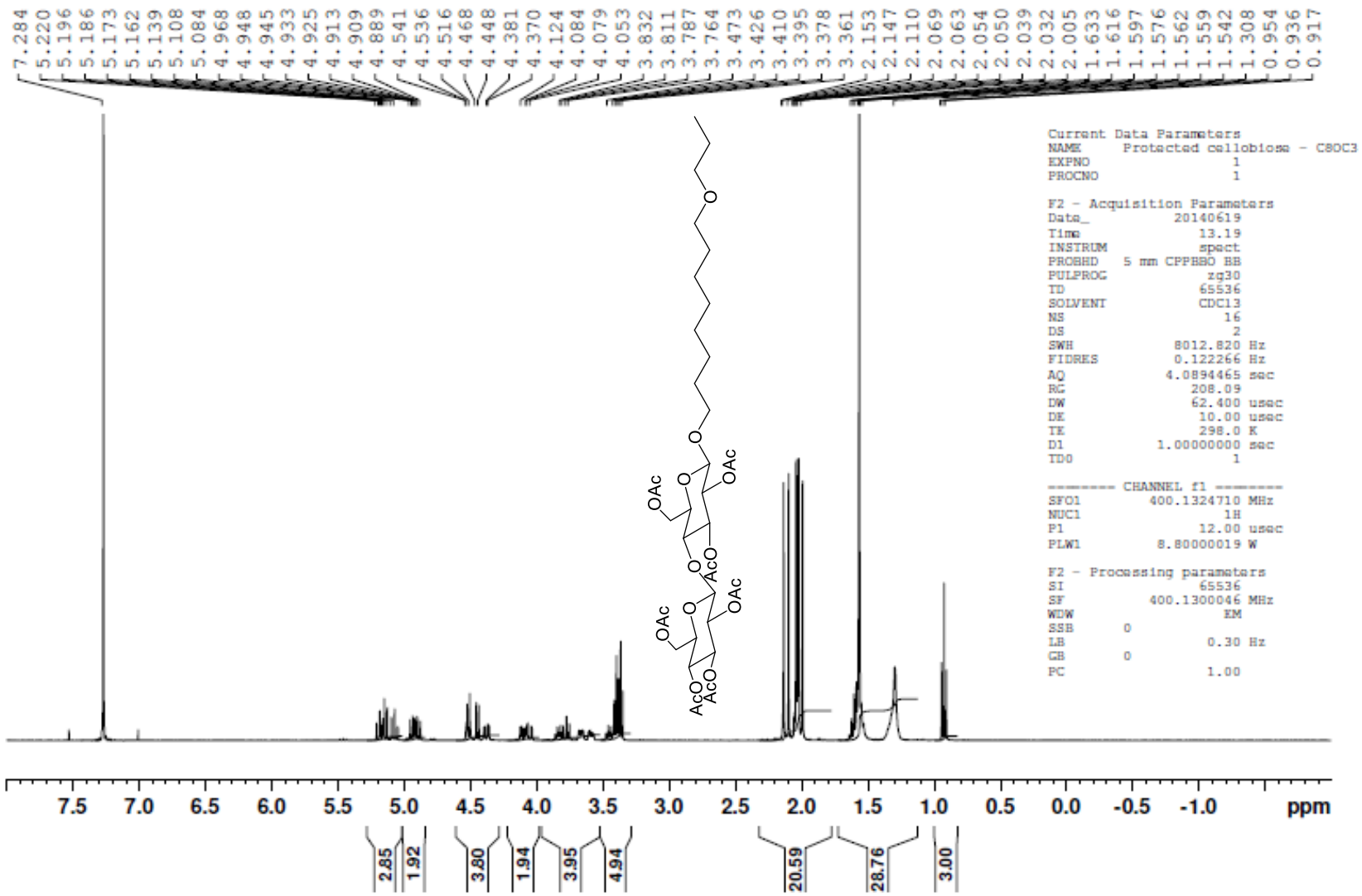
7.284
5.220
5.196
5.186
5.173
5.162
5.139
5.108
5.084
4.968
4.948
4.945
4.933
4.925
4.913
4.909
4.889
4.541
4.536
4.516
4.468
4.448
4.381
4.370
4.124
4.084
4.079
4.053
3.832
3.811
3.787
3.764
3.473
3.426
3.410
3.395
3.378
3.361
2.153
2.147
2.110
2.069
2.063
2.054
2.050
2.039
2.032
2.005
1.633
1.616
1.597
1.576
1.562
1.559
1.542
1.308
0.954
0.936
0.917
OAc
OAc
AcO
OAc
OAc
AcO
AcO
Current Data Parameters
NAME Protected cellobiose - C8OC3
EXPNO 1
PROCNO 1
F2 - Acquisition Parameters
Date_ 20140619
Time 13.19
INSTRUM spect
PROBHD 5 mm CPPBBO BB
PULPROG zg30
TD 65536
SOLVENT CDCl3
NS 16
DS 2
SWH 8012.820 Hz
FIDRES 0.122266 Hz
AQ 4.0894465 sec
RG 208.09
DW 62.400 usec
DE 10.00 usec
TE 298.0 K
D1 1.00000000 sec
TD0 1
CHANNEL f1
SFO1 400.1324710 MHz
NUC1 1H
P1 12.00 usec
PLW1 8.80000019 W
F2 - Processing parameters
SI 65536
SF 400.1300046 MHz
WDW EM
SSB 0
LB 0.30 Hz
GB 0
PC 1.00
7.5
7.0
6.5
6.0
5.5
5.0
4.5
4.0
3.5
3.0
2.5
2.0
1.5
1.0
0.5
0.0
-0.5
-1.0
ppm
2.85
1.92
3.80
1.94
3.95
4.94
20.59
28.76
3.00

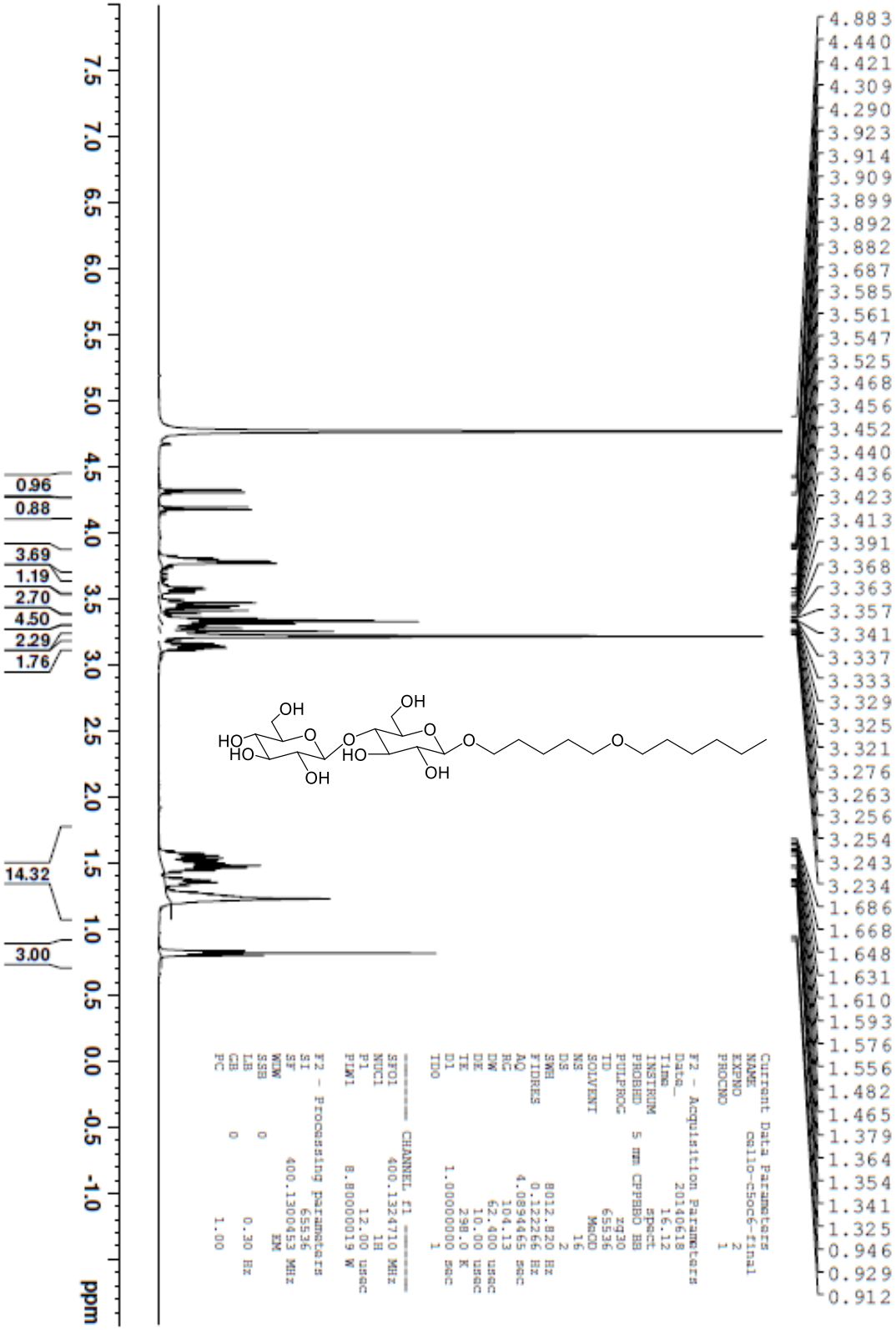
4.883
4.440
4.421
4.309
4.290
3.923
3.914
3.909
3.899
3.892
3.882
3.687
3.585
3.561
3.547
3.525
3.468
3.456
3.452
3.440
3.436
3.423
3.413
3.391
3.368
3.363
3.357
3.341
3.337
3.333
3.329
3.325
3.321
3.276
3.263
3.256
3.254
3.243
3.234
1.686
1.668
1.648
1.631
1.610
1.593
1.576
1.556
1.482
1.465
1.379
1.364
1.354
1.341
1.325
0.946
0.929
0.912
Current Data Parameters
NAME cello-c5oc6-final
EXPNO 2
PROCNO 1
F2 - Acquisition Parameters
Date_ 20140618
Time 16.12
INSTRUM spect
PROBHD 5 mm CPFBBO BB
PULPROG zg30
TD 65536
SOLVENT MeOD
NS 16
DS 2
SWH 8012.820 Hz
FIDRES 0.122266 Hz
AQ 4.0894465 sec
RG 104.13
DW 62.400 usec
DE 10.00 usec
TE 298.0 K
D1 1.00000000 sec
TD0 1
======== CHANNEL f1 ========
SFO1 400.1324710 MHz
NUC1 1H
P1 12.00 usec
PLW1 8.80000019 W
F2 - Processing parameters
SI 65536
SF 400.1300453 MHz
WDW EM
SSB 0
LB 0.30 Hz
GB 0
PC 1.00
0.96
0.88
3.69
1.19
2.70
4.50
2.29
1.76
14.32
3.00
7.5 7.0 6.5 6.0 5.5 5.0 4.5 4.0 3.5 3.0 2.5 2.0 1.5 1.0 0.5 0.0 -0.5 -1.0
ppm
OH
HO
HO
O
OH
O
HO
O
OH
O
O

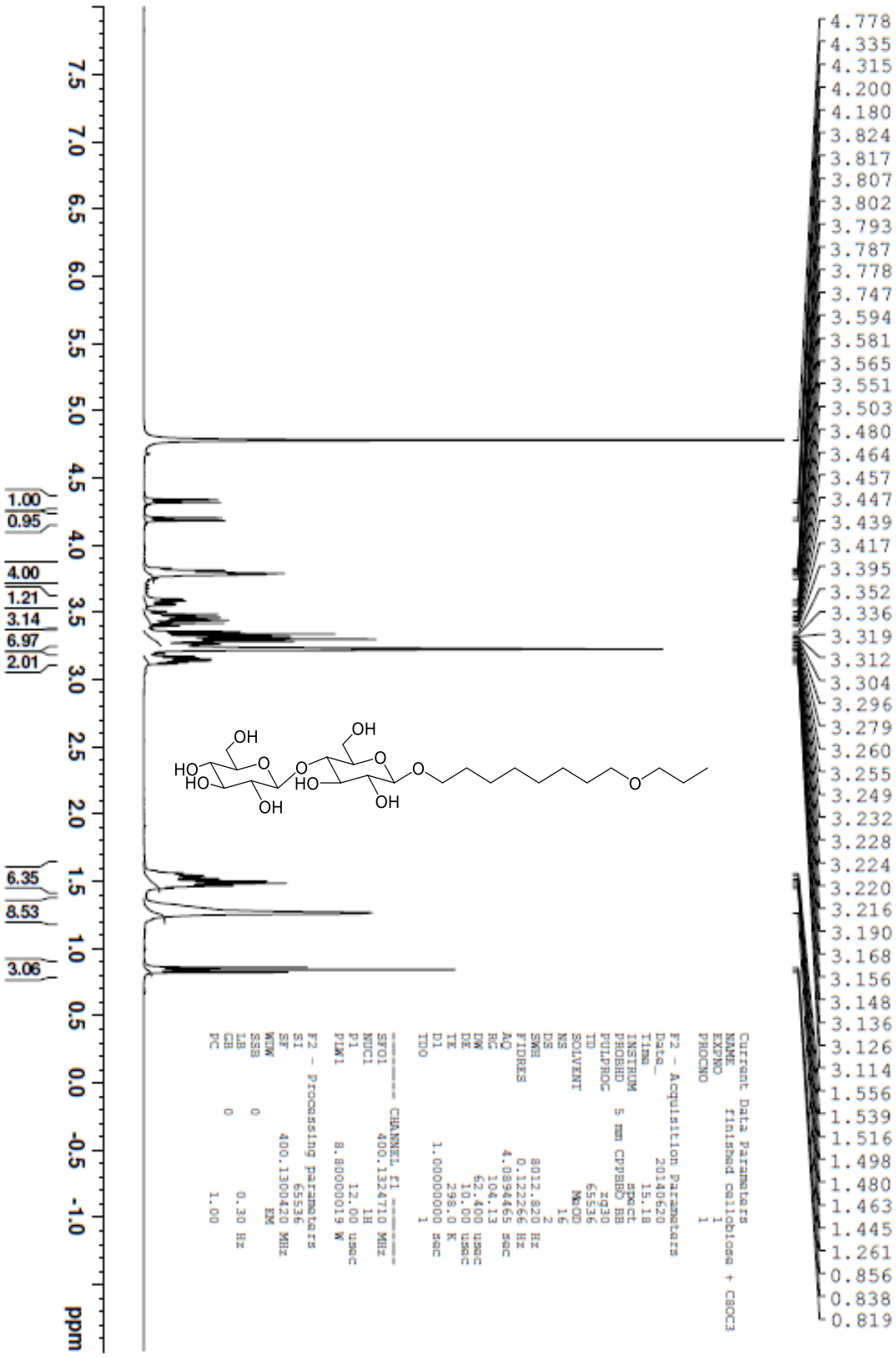
4.778
4.335
4.315
4.200
4.180
3.824
3.817
3.807
3.802
3.793
3.787
3.778
3.747
3.594
3.581
3.565
3.551
3.503
3.480
3.464
3.457
3.447
3.439
3.417
3.395
3.352
3.336
3.319
3.312
3.304
3.296
3.279
3.260
3.255
3.249
3.232
3.228
3.224
3.220
3.216
3.190
3.168
3.156
3.148
3.136
3.126
3.114
1.556
1.539
1.516
1.498
1.480
1.463
1.445
1.261
0.856
0.838
0.819
Current Data Parameters
NAME finished cellobiose + CDOCl3
EXPNO 1
PROCNO 1
F2 - Acquisition Parameters
Date_ 20140620
Time 15.18
INSTRUM spect
PROBHD 5 mm CPPBBO BB
PULPROG zg30
TD 65536
SOLVENT MeOD
NS 16
DS 2
SWH 8012.820 Hz
FIDRES 0.122266 Hz
AQ 4.0894465 sec
RG 104.13
DW 62.400 usec
DE 10.00 usec
TE 298.0 K
D1 1.00000000 sec
TD0 1
======== CHANNEL f1 ========
SFO1 400.1324710 MHz
NUC1 1H
P1 12.00 usec
PLW1 8.80000019 W
F2 - Processing parameters
SI 65536
SF 400.1300420 MHz
WDW EM
SSB 0
LB 0.30 Hz
GB 0
PC 1.00
1.00
0.95
4.00
1.21
3.14
6.97
2.01
6.35
8.53
3.06
7.5
7.0
6.5
6.0
5.5
5.0
4.5
4.0
3.5
3.0
2.5
2.0
1.5
1.0
0.5
0.0
-0.5
-1.0
ppm
OH
HO
HO
O
O
OH
HO
O
O
OH
O

^{13}C NMR Spectra

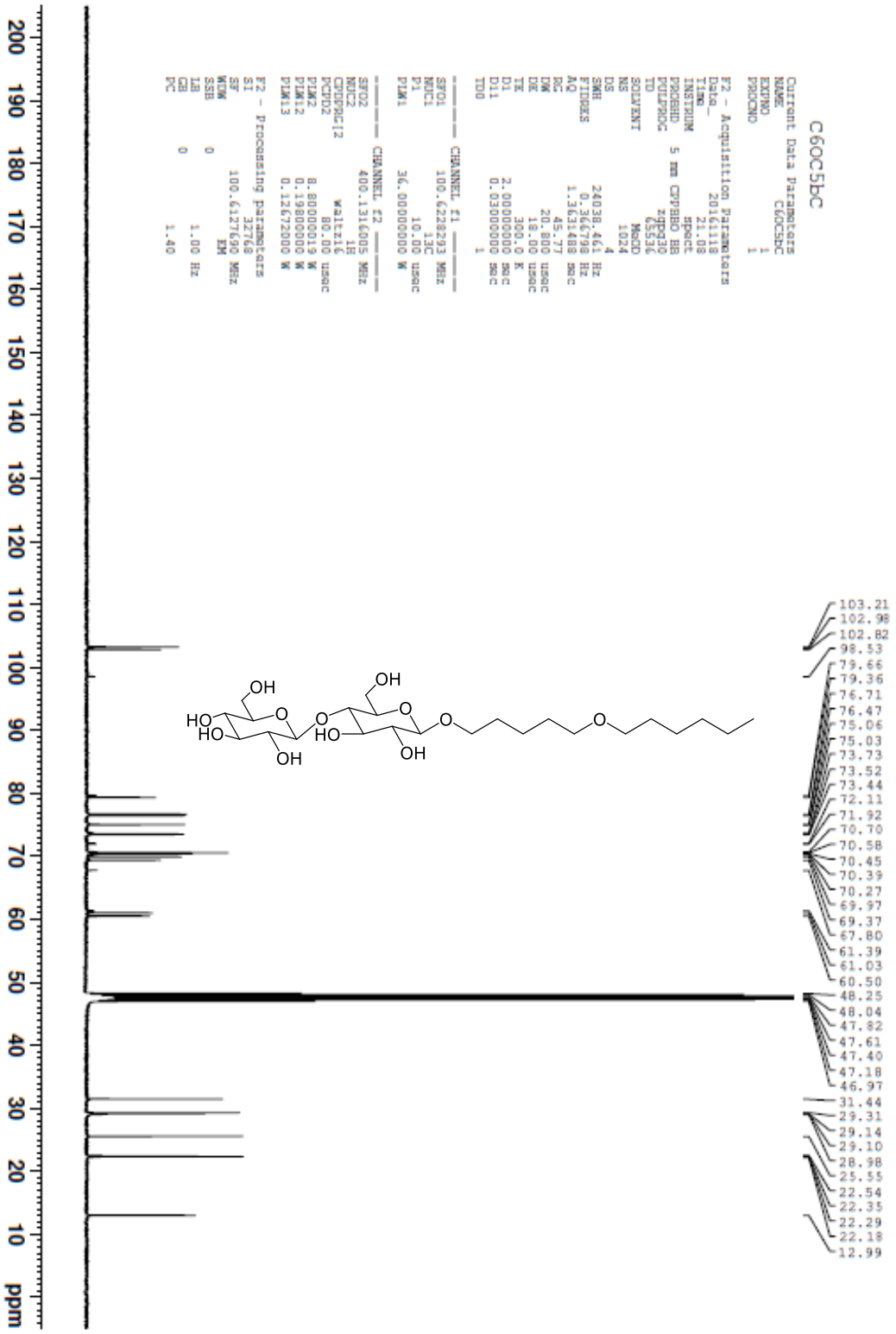

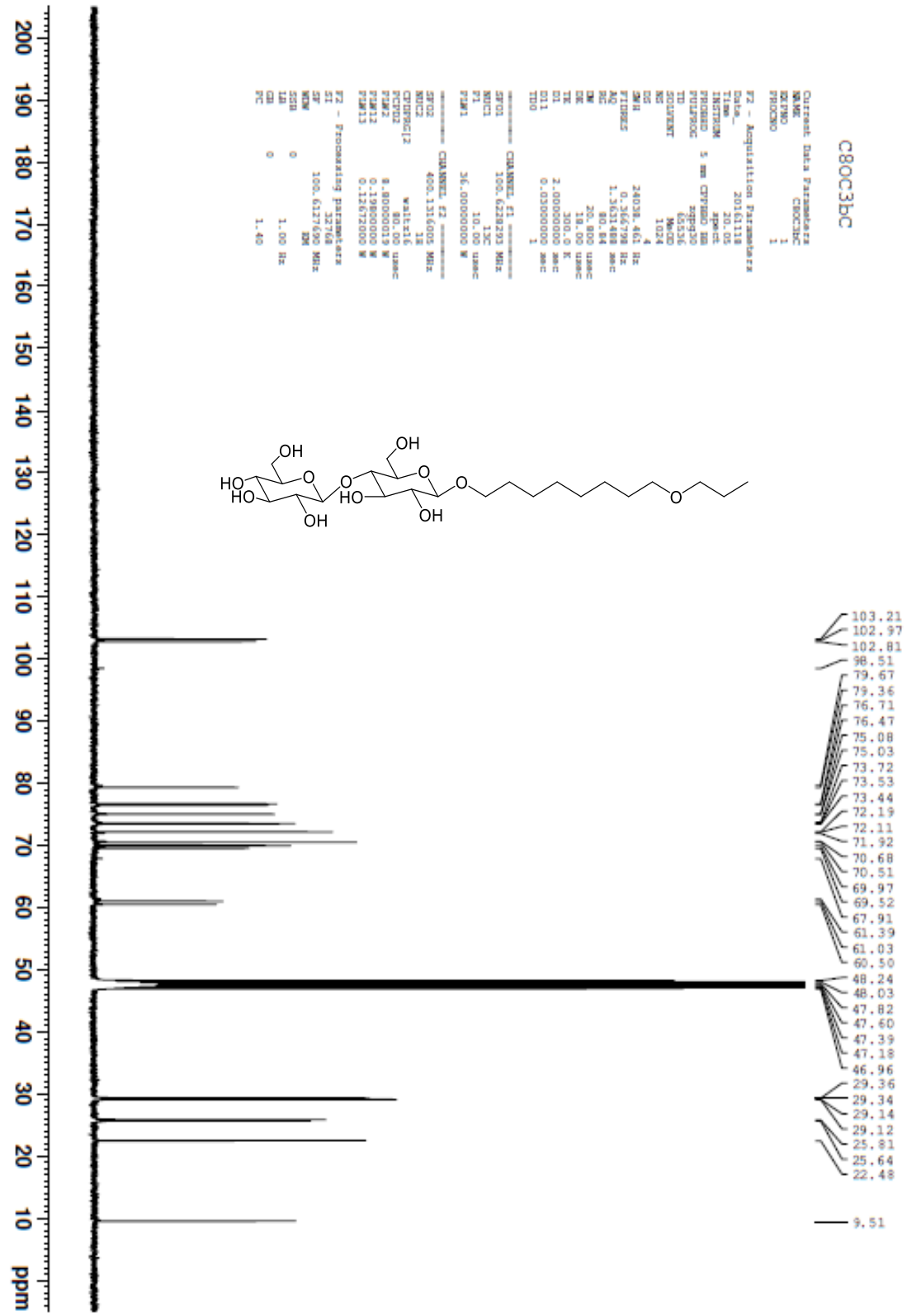
c8oc3bC
103.21
102.97
102.81
98.51
79.67
79.36
76.71
76.47
75.08
75.03
73.72
73.53
73.44
72.19
72.11
71.92
70.68
70.51
69.97
69.52
67.91
61.39
61.03
60.50
48.24
48.03
47.82
47.60
47.39
47.18
46.96
29.36
29.34
29.14
29.12
25.81
25.64
22.48
9.51
200
190
180
170
160
150
140
130
120
110
100
90
80
70
60
50
40
30
20
10
ppm

HRMS Spectra

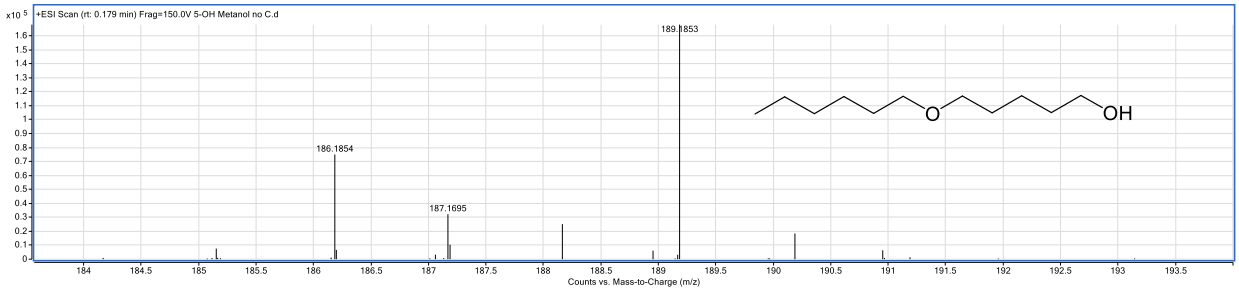

HRMS (ESI+): Cacld. for M^+: 189.1776, found: 189.1853

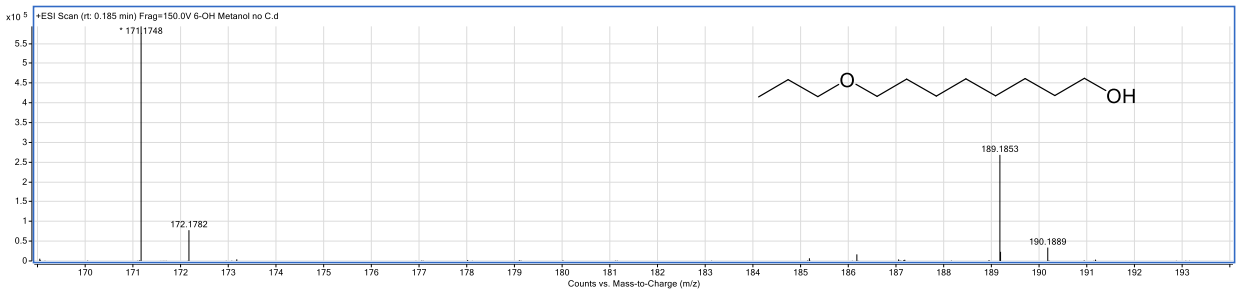

HRMS (ESI+): Cacld. for M^+: 189.1776, found: 189.1853

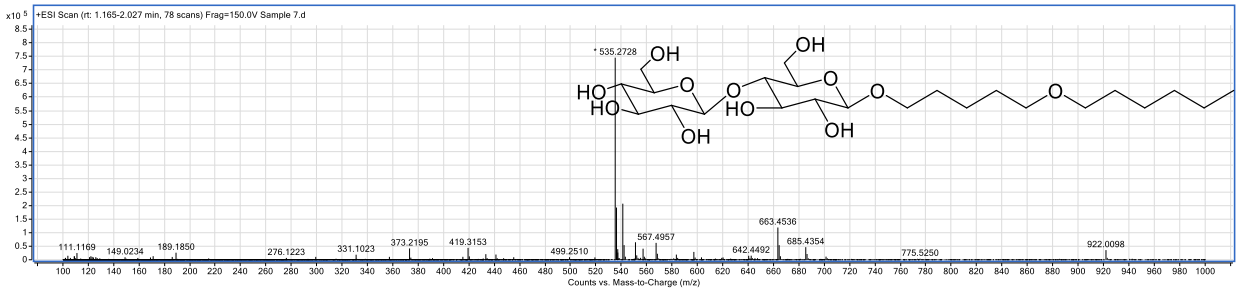

HRMS (ESI) m/z: Calcd. $(C_{23}H_{44}O_{12})Na^+$: 535.2731; Found: 535.2728.

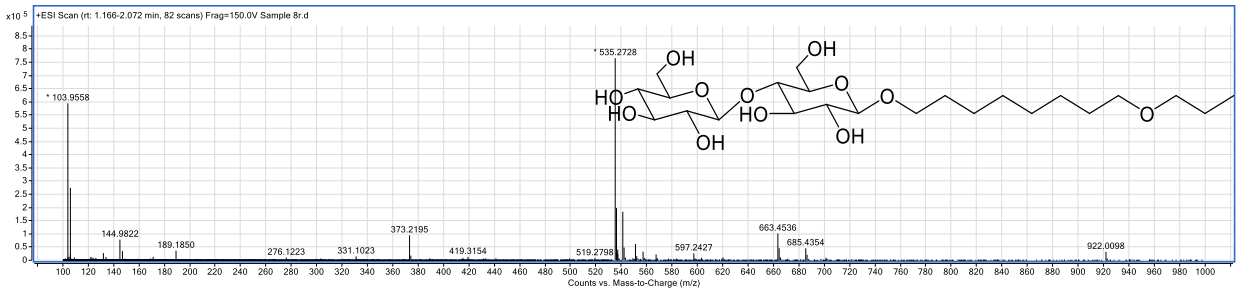

HRMS (ESI) m/z: Calcd. $(C_{23}H_{44}O_{12})Na^{+}$: 535.2731; Found: 535.27

Chapter 4 Synthetic Disaccharide Derivatives Inhibit Bacterial Antibiotic-Promoted Activities and Increase the Potency of Antibiotics to Remove Biofilms*

4.1. Introduction

4.1.1. A brief introduction of antibiotic resistance, tolerance, and persister

Antibiotic-treatment failure is typically attributed to antibiotic resistance.[77, 160] "Resistance" is used to describe the inherited ability of microorganisms to grow at high concentrations of an antibiotic, and can be quantified by the minimum inhibitory concentration (MIC) of the particular antibiotic,[161] Resistance is most often thought of as being attributable to mutations or exchange of antibiotic resistance genetic elements, although resistance may also be intrinsic and thus dependent on wild-type genes and innate properties of the cell.[162-163] For example, Gram-negative bacteria are intrinsically more resistant than Gram-positive cells to certain antibiotics like vancomycin due to the relatively less outer membrane permeability. Resistance mechanisms have been described by Lewis[164] as the means by which an antimicrobial agent is prevented from interacting with its intended target including antibiotic efflux pumps,[165] molecules (such as eDNA[166] and NdvB-derived periplasmic glucans[167]) that sequester antibiotics, and matrix β-lactamases[168].

In contrast, "tolerance", which is defined by Kester and Fortune, is used to describe the ability of microorganisms to survive transient exposure to high concentrations of an antibiotic without a change in the MIC, which is often achieved by

* The work in this chapter is a collaboration with Felicia Burns in Luk group. She synthesized and characterized the two molecules, 3,5-DMDβM and 3,5-DMDβC, used in this chapter. ^{1}HNMR and ^{13}CNMR collected by Felicia Burns were included for the purpose of completing the information.

slowing down an essential bacterial process.[169-170] In the presence of the antibiotic, tolerant bacteria cease to grow; however, they can start to grow and replicate once the antibiotic is removed.[171] Tolerance is an inherited rather than a non-inherited form of antibiotic resistance; tolerant cells are genetically different to the non-tolerant bacteria from which they are derived.[172-175] A measure of tolerance is the minimum bactericidal concentration (MBC), which is the lowest concentration of a bactericidal antimicrobial that will kill ≥99.9% of cells in a culture.[176] Mechanisms of tolerance are thought to somehow prevent the bactericidal agent from exerting its downstream toxic effects even though the agent has bound to its target.[164] Based on this definition, antibiotic tolerance mechanisms include reduced growth rate[177-178], the mechanisms that handle antibiotic-induced oxidative stress[179] and persister cells[180].

In contrast to resistance and tolerance, which are attributes of whole bacterial populations, 'persistence' is a term that describes the ability of a subpopulation of a clonal bacterial population to survive exposure to high concentrations of an antibiotic.[181] Persistence, was first reported for staphylococcal infections treated with penicillin and has since been observed in many bacterial species.[182] Despite being observed almost for decades, the mechanism behind persistence remains a puzzle. The reason might due to technical difficulties of working with a small fraction of cells expressing a temporary phenotype of uncertain functional significance.[183-184] In the 1980s, Harris and coworkers continued working on to search for genes that caused persister formation.[185-188] One of these persister mutations was mapped to the hipA gene. The hipA7 allelic strain produced ~1% persisters that survived treatment with ampicillin in exponential cultures, which is

approximately 1,000 times more persisters than the wild-type strain. The recent discovery of persisters in biofilms has led to a great interest in studying those unusual cells.[180, 189]

Bacteria have the potential to adapt to the environment, either under natural or laboratory condition.[190] Recent studies have shown that tolerance and persistence evolve rapidly under intermittent antibiotic exposure. Nathalie and coworkers reported resistance enhancement in bacterial populations under cyclic antibiotic treatments.[191] Maarten and Jan demonstrated that persistence is a highly evolvable trait that quickly adapts to drug-treatment frequency,[192] and that its evolutionary dynamics can be understood in the context of bet-hedging theory.[193-197] Hinrich and Gunther reported that *P. aeruginosa* adapts rapidly to high-level antibiotic stress and they expressed both collateral sensitivity and cross-resistance which was revealed by genomic and functional genetic analysis.[198] Evolution of resistance from tolerance indicates that new drugs or their combinations that decrease tolerance may intervene in the resistance evolution process.

4.1.2. The effect of sub-MIC antibiotics on P. aeruginosa biofilm formation

Pseudomonas aeruginosa forms biofilm with extreme tolerance to antibiotics in nosocomial infections, such as pneumonia and surgical site infections. The Diseases Society of America declared *Pseudomonas aeruginosa* is one of the six 'top-priority dangerous, drug-resistant microbes.[199] More than 60% of the bacterial infections currently treated by physicians are considered to involve biofilm formation.[128] Successful treatment in these cases depends on the effective removal of those biofilm materials. Since the discovery of penicillin, antibiotics have been proven to be effective in controlling serious bacterial infections.[63] Microbiologists have been using minimal inhibitory concentration (MIC) and the minimal bactericidal concentration (MBC) to

assess the effect of antibiotics against planktonic organisms. Table 4.1 showed MIC and MBC of 6 different antibiotics toward *P. aeruginosa*. As mentioned in chapter 1, antibiotics can act as signaling molecules that trigger transcription responses important for environmental survival in low concentrations.[75-76] While the growth of surrounding microorganisms could be inhibited at high concentrations of antibiotics are present.[77] Various studies have shown that sub-minimal inhibitory (sub-MIC) concentrations of some antibiotics can inhibit biofilm formation without killing the bacteria. Ichimiya and coworkers found that azithromycin can efficiently inhibit Pseudomonas aeruginosa biofilm formation at 1/128 of the MIC.[200-201] Low dose azithromycin therapy has been shown to improve lung function in cystic fibrosis patients.[202-204] The effect of low-dose azithromycin chemotherapy may be due to its ability to inhibit quorum sensing and alginate production of mucoid biofilms at sub-MIC concentrations.[205-207]

Table 4.1 MIC and MEC of different antibiotics for *P. aeruginosa*

Antibiotic	**MIC (mg/L)**	**MBC (mg/L)**	**Primary target**
Aztreonam	2[208]/16[209]	-	Penicillin-binding proteins
Chloramphenicol	-	1024[210]	50S ribosome (Protein translation)
Tetracycline	-	512[211]	30S ribosome (Protein translation)
Ciprofloxacin	1[212]	4[213]	Topoisomerase II (DNA gyrase), topoisomerase IV
Colistin	8~16[214]	64~128[214]	Cell membrane
Tobramycin	1[215]	~53[210]	30S ribosome (Protein translation)

However, there are numerous studies have shown that some antibiotics can induce biofilm formed by P. aeruginosa when present at concentrations below the MIC. Garey and coworkers[216] showed that sub-MIC concentrations of clarithromycin induced biofilm formation by 25-fold in 44 P. aeruginosa clinical isolates when tested at 1/32 to 1/2 MIC. Linares and coworkers[217] found that sub-MIC concentrations of tobramycin, ciprofloxacin, and tetracycline-induced P. aeruginosa biofilm formation by approximately 2-fold. Bagge and coworkers[218] also used microarray technology to study the effects of sub-MIC concentrations of the β-lactam antibiotic imipenem on P. aeruginosa biofilm formation. They identified 34 genes that were induced or repressed in biofilms exposed to 1/2 MIC imipenem. Five alginate metabolism-related genes (algD, algG, algJ, algF, and algA) were induced more than 10-fold by imipenem at 1/2 MIC. Hoffman and coworkers[42] found that sub-MIC concentrations of tobramycin readily induced P. aeruginosa biofilm formation while several other antibiotics including polymyxin B, chloramphenicol and carbenicillin had no effect on biofilm formation.[42] They found that all the mutants carried transposon insertions in a gene designated arr, which is an aminoglycoside response regulator that encodes a c-di-GMP phosphodiesterase that degrades c-di-GMP and reduces intracellular c-di-GMP concentrations, were defective in tobramycin-induced biofilm formation.[42] The results suggested that Aminoglycoside antibiotics such as tobramycin could act as first messengers that trigger changes—mediated either by binding directly to proteins such as Arr or indirectly through intermediary molecules—in the level of the second messenger c-di-GMP.[42]

4.1.3. Puzzle: Biofilm formation and swarming motility are inversely regulated but both activities can be induced by antibiotics

Switching between sessile and motile states is an important decision for the bacteria to ensure its survival.[48] However, external environmental stimuli that cause the transition from sessile to motile mode still remains unclear.[48, 219-220] As both swarming and biofilm formation are surface-associated multicellular behaviors that are controlled by bacterial quorum sensing, it is important to understand the relation between the two behaviors. SadB was originally identified as required for early biofilm formation, is also a negative effector of swarming motility. O'Toole and co-workers found that *sadB* gene of *P. aeruginosa* is most likely responsible for inversely regulating the swarming and biofilm formation through the chemotaxis cluster IV.[221-222] The authors also proposed that *P. aeruginosa* inversely regulates the surface-associated behaviors of biofilm formation and swarming by controlling both flagellar reversals and the production of the Pel polysaccharide. It has been observed that during the biofilm formation process bacterial cells were switched from one lifestyle to another to adapt to the new lifestyle.[223] For instance, during the biofilm formation process the cells of *P. aeruginosa* usually develop single polar flagella to assist the surface adherence process, while during swarming, *P. aeruginosa* seems to develop two polar flagella.[43, 219]

There are numerous studies have shown that antibiotics not only induce biofilm formation it can also induce swarming motility of *P. aeruginosa* when present at concentrations below the MIC. Hoffman and coworkers[42] found that sub-MIC concentrations of tobramycin readily induced P. aeruginosa biofilm formation. Garey and

coworkers[216] showed that sub-MIC concentrations of clarithromycin induced biofilm formation by 25-fold in 44 P. aeruginosa clinical isolates when tested at 1/32 to 1/2 MIC. Linares and coworkers found that sub-MIC of tobramycin increased bacterial swarming motility.[217] However, the mechanism of antibiotics inducing P. aeruginosa biofilm formation and swarming motility is still unclear.

4.1.4. The aim of the chapter

In this chapter, we have examined the effect of our synthetic disaccharide derivatives on sub-MIC antibiotic-promoted biofilm formation and swarming motility. The preliminary investigation by our previous lab members brought forward the hydrocarbon maltoside and cellobioside derivatives as potent biofilm and swarming inhibitors. Additionally, the fact that many saccharide-hydrocarbons are involved in bacterial surface recognition events further prompted us to explore the effect of our synthetic SFβM along with other potent leads 3,5-DMDβM and 3,5-DMDβC on sub-MIC antibiotic-promoted biofilm formation and swarming motility. Furthermore, we have examined the efficacy of two compounds SFβM and SF(EG)4OH in enhancing the bactericidal action of antibiotics colistin and tobramycin on biofilms grown on a polystyrene surface. In addition, to study drug tolerance and persister formation, we examined the ability of our molecules to eradicate drug tolerance and persisters induced by the presence of antibiotics using resazurin dye-based cell viability assay. To study the effect of our synthetic molecules, 3,5-DMDβM and 3,5-DMDβC, on the efficacy of

antibiotics to combat tobramycin-tolerant subpopulations, we examined the live and dead subpopulation of native and tobramycin promoted biofilms by confocal laser scanning microscope (CLSM).

4.2. Results and discussion

4.2.1. Library of molecules used in this study

In order to investigate the effect of our *synthetic* molecules on inhibiting antibiotic-promoted bacterial activities and increase the potency of antibiotics to kill bacteria in biofilms, a library of molecules was tested which has been listed in Figure 4.1. 2-ABI is a commercially available molecule. $SF(EG)_4OH$ and SFβM were designed and synthesized by our previous lab member Nischal. 3,5-DMDβM and 3,5-DMDβC were designed and synthesized by our current lab member Felicia Burns.

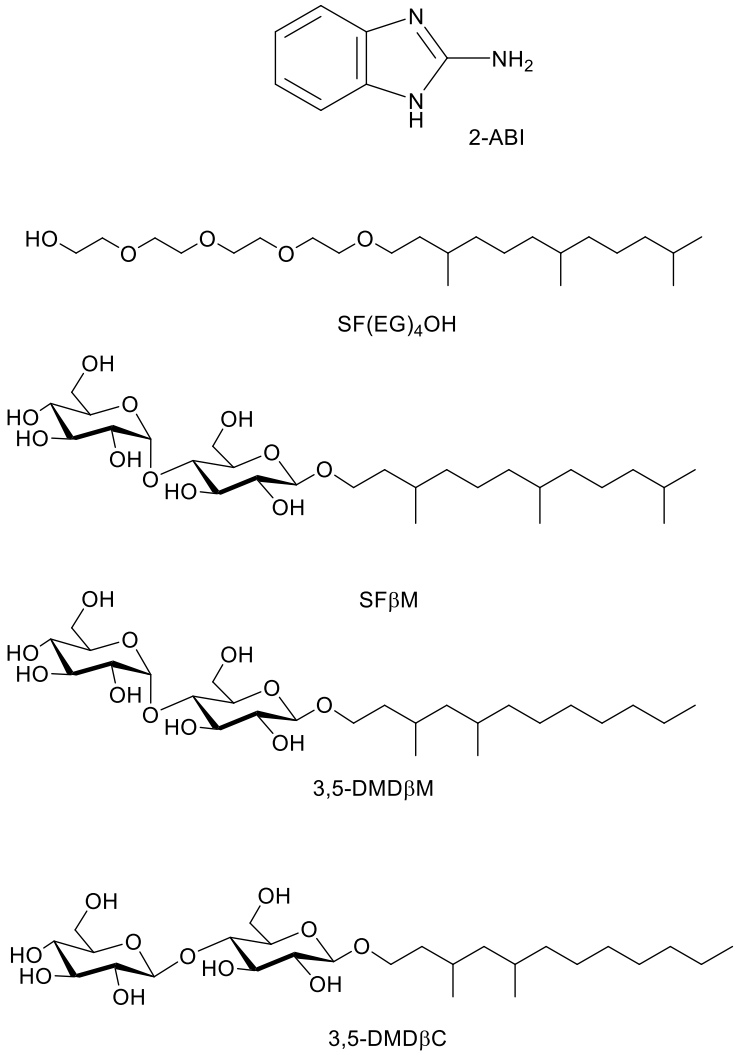

Figure 4.1 Collection of molecules used in this study. 3,5-DMDβM and 3,5-DMDβC are synthesized and characterized by Felicia Burns.

4.2.2. Disaccharide molecules having branched hydrocarbons inhibit tobramycin-promoted bacterial activities

Biofilm formation and swarming motility are two critical pathogen-related functions of bacteria.[221] Below the lethal concentration, tobramycin promotes both bioactivities by *P. aeruginosa*.[100] In contrast, our potent lead compound, SFβM, inhibit

both biofilm formation and swarming motility. The mechanism for these observations is not yet clear, but we have identified two proteins to which SFβM binds: Lectin A and pilin, which I will describe in detail in chapter 5 and 6. Here, we examined the influence of synthetic disaccharide derivatives supplemented with Las quorum sensing inhibitor ABI on normal biofilm and sub-MIC of tobramycin promoted biofilm formed by PAO1-EGFP strain under slow shaking condition (100 rpm). Biofilm inhibition activity of active disaccharide derivatives was verified by fluorescence-based biofilm assay. *P. aeruginosa* strain, PAO1-EGFP that constitutively expresses a green fluorescent protein (GFP) was allowed to grow on sterile polystyrene coupons for 24 h. The biofilms formed on the coupons grown in the presence and in absence of maltose derivatives were viewed under confocal laser scanning microscope (CLSM). The fluorescence observed indirectly indicates the amount of biofilm formed on the coupons. The biomass of biofilm was quantified using COMSTAT software. At 24 h, there is visibly less fluorescence signal for biofilm formed by the PAO1-EGFP strain which was treated with 40 μM SFβM/ABI, than biofilm formed without any added agents (Figure 4.2). For the sub-MIC of tobramycin promoted biofilm, there is visibly more fluorescence signal compared to biofilm formed without any added agents (Figure 4.2). In addition, adding 40 μM SFβM/ABI along with 0.3 μg/mL tobramycin, biofilms formed significantly less than sub-MIC of tobramycin promoted biofilm based on fluorescence signals. These results suggest that SFβM not only inhibited normal biofilm formed by PAO1-EGFP it also inhibited sub-MIC of tobramycin promoted biofilm. However, the remained portion of sub-MIC of tobramycin promoted biofilm after grown with 40 μM SFβM is still more than the remaining portion of 40 μM SFβM/ABI treated normal biofilm formed by PAO1-EGFP.

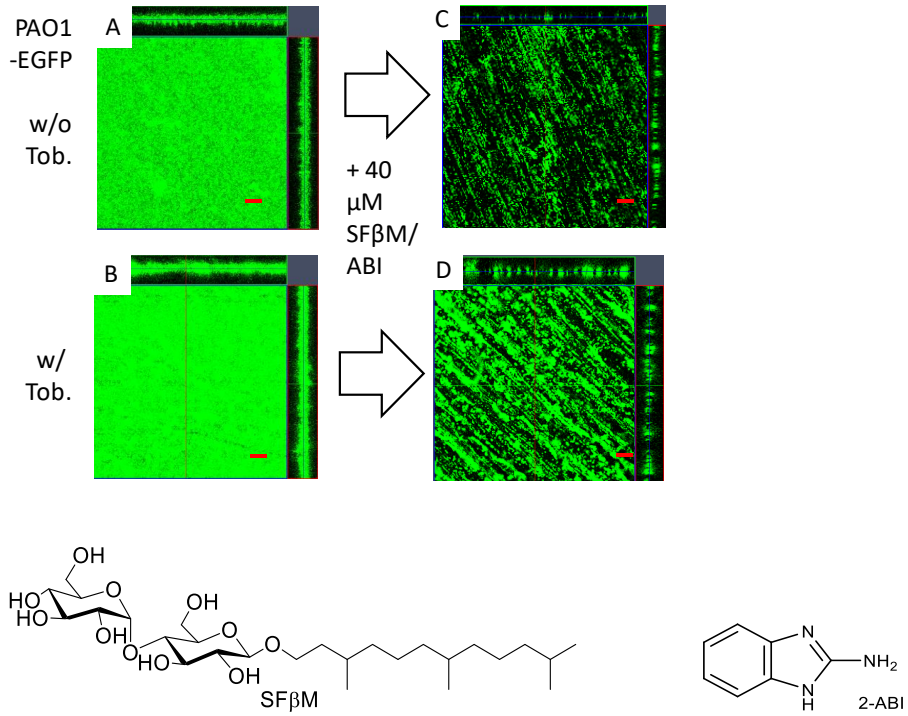

Figure 4.2 Representative confocal laser scanning microscopy (CLSM) micrographs of biofilm formed by PAO1-EGFP without (A) and with (B) Tobramycin (Tob) at a sub-MIC (0.3 µg/mL). Adjuvant molecules SFβM & 2-amino benzimidazole (2-ABI) (40 µM each) inhibit both native (C) and tobramycin-promoted biofilm (D). Biofilms were grown on polystyrene for 24 h with shaking (100 rpm). Scale bar = 30 µm. The thickness and biomass of biofilm were quantified using COMSTAT software.

Furthermore, the CLSM images show that the biofilm formed on the coupons in presence of 3,5-DMDβM and 3,5-DMDβC were significantly lower than those formed without agents (Figure 4.3). In the presence of 0.3 µg/mL tobramycin, which is the optimal condition for forming a sub-MIC antibiotic-promoted biofilm, the thickness was increased around 30%. When adding disaccharide derivatives, 3,5-DMDβM and 3,5-DMDβC, the thickness of the sub-MIC antibiotic-promoted biofilm were significantly decreased by around 50%.

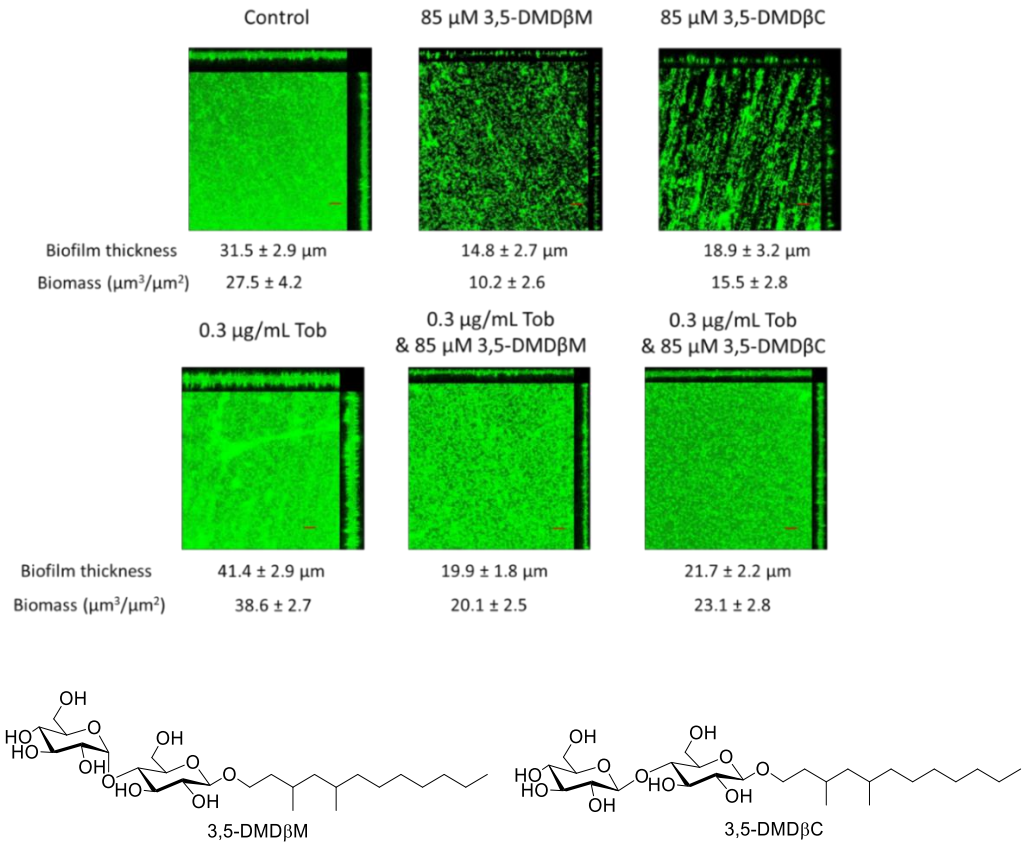

Figure 4.3 Representative confocal laser scanning microscopy (CLSM) micrographs of biofilm formed by PAO1-EGFP on polystyrene coupons; biofilms on the first row were grown in the absence of agents(control), and in the presence of 85 µM 3,5-DMDβM and 3,5-DMDβC. * Biofilms on the second row were grown under the same condition as the first row plus 0.3 µg/mL Tobramycin. Bacterial strain: PAO1-EGFP; Initial OD600: 0.01; Surface: Polystyrene; Time: 24 h; Shaking speed: 100 rpm; Scale bar: 30 µm. The thickness and biomass of biofilm was quantified using COMSTAT software.

* The work in this chapter is a collaboration with Felicia Burns in Luk group. She synthesized and characterized the two molecules, 3,5-DMDβM and 3,5-DMDβC, used in this chapter. ^{1}HNMR and ^{13}CNMR collected by Felicia Burns were included for the purpose of completing the information.

In addition, we examined the eradication effect of SFβM and amino benzimidazole on preformed native and tobramycin promoted biofilms. Specifically, we first grow a biofilm of PAO1-EGFP strain with and without 0.3 μg/mL of tobramycin for 24 h to establish an antibiotic-promoted biofilm and a native biofilm, respectively. For each biofilm, we then introduced fresh LB medium with and without 40 μM of SFβM or 40 μM 2-ABI or both. The thickness and biomass of biofilm were quantified using COMSTAT software. The results showed that during this second culture period, around 30-40 % of native biofilm was eradicated when 40 μM of SFβM was added. The biofilm thickness was decreased ~25% as well. However, 40 μM 2-ABI did not have any significant effect on either biofilm thickness or the biomass. Furthermore, the effect of adding both 40 μM of SFβM and 40 μM 2-ABI is similar to adding 40 μM of SFβM alone (Figure 4.4).

Eradication effect of SFβM and amino benzimidazole on preformed tobramycin promoted biofilms was tested using the similar way above. The results showed that during this second culture period, around 25 % of tobramycin promoted biofilm was eradicated when 40 μM of SFβM was added. However, the biofilm thickness was only decreased by ~10 %. 40 μM 2-ABI did not have any significant effect on either biofilm thickness or the biomass. Furthermore, the effect of adding both 40 μM of SFβM and 40 μM 2-ABI is similar to adding 40 μM of SFβM alone (Figure 4.5). The reason why antibiotic-promoted biofilms were slightly more difficult to eradicate than native biofilms is probably due to certain exopolymer acting as physical barriers and reduce the penetration of antibiotic into the deep part of biofilms, which allows more biofilm cells to survive and acquire tolerance.[214]

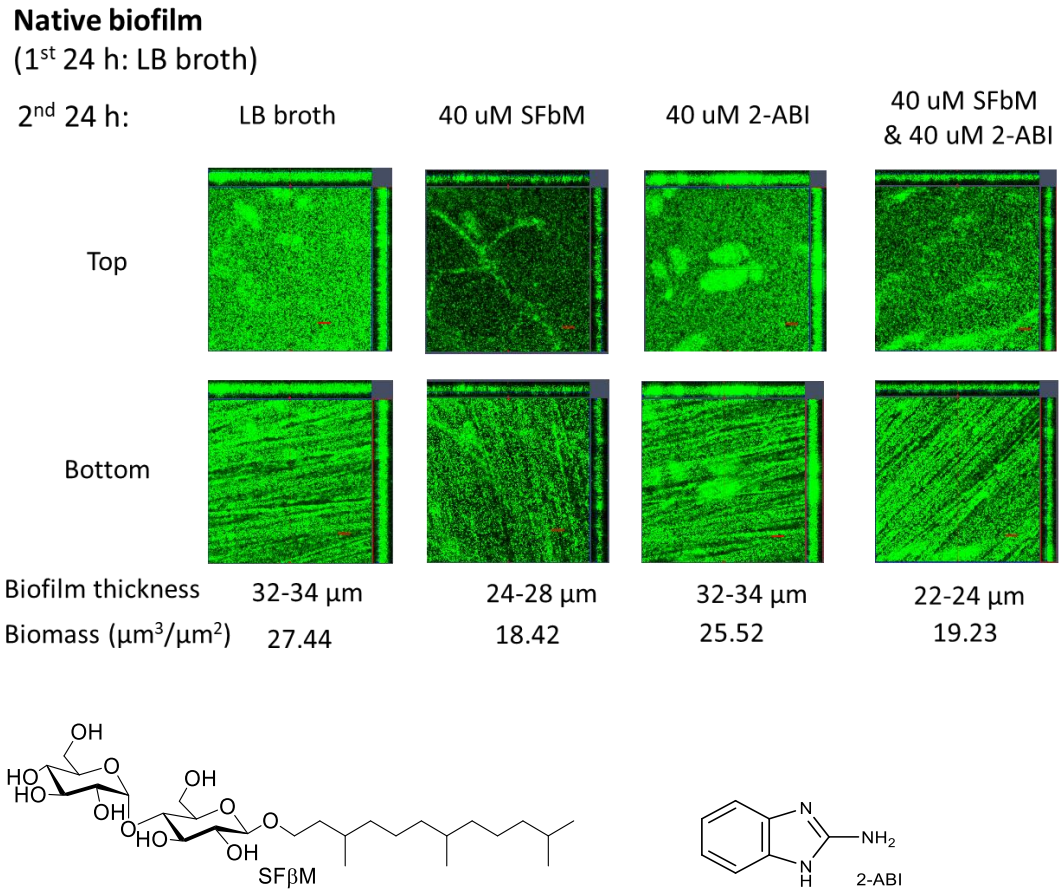

Figure 4.4 Representative confocal laser scanning microscopy (CLSM) micrographs of biofilm formed by PAO1-EGFP. Adjuvant molecules SFβM & amino benzimidazole (ABI) (40 µM each) inhibit native biofilm formation. Biofilms were grown on polystyrene for 24 h with shaking (100 rpm). Scale bar = 30 µm. The thickness and biomass of biofilm were quantified using COMSTAT software.

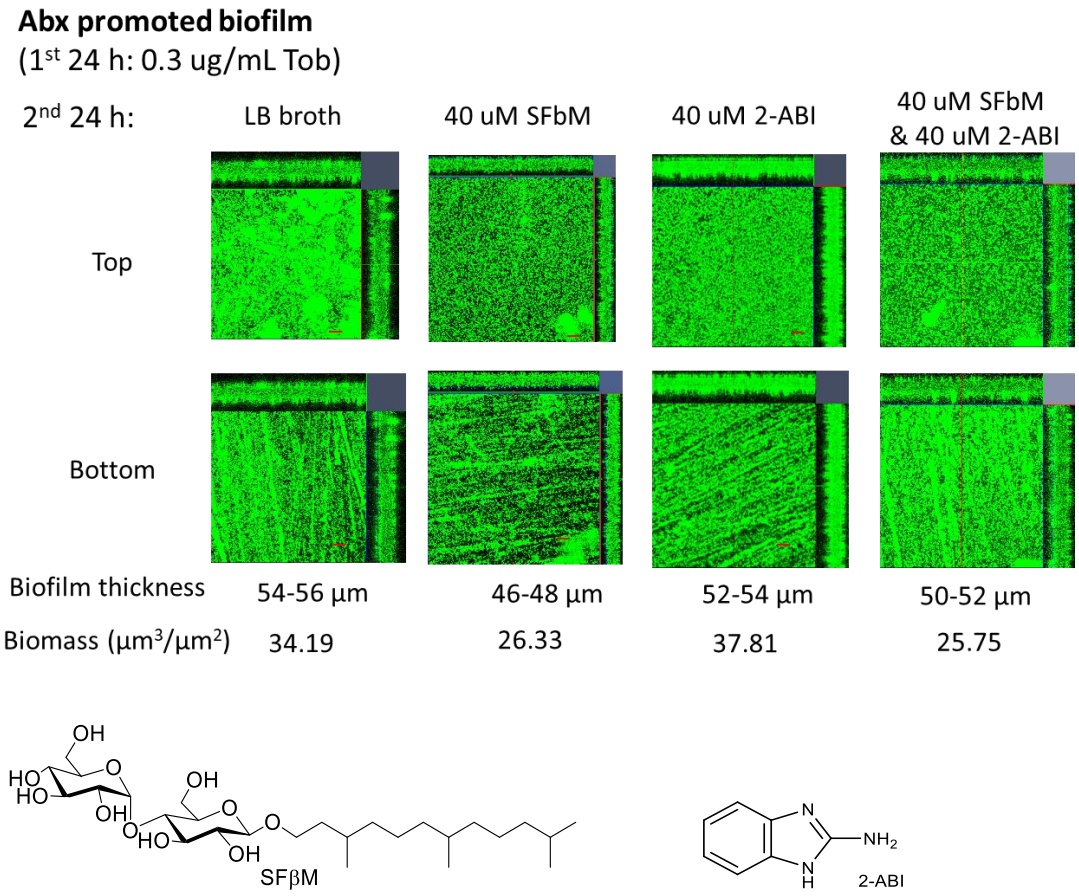

Figure 4.5 Representative confocal laser scanning microscopy (CLSM) micrographs of biofilm formed by PAO1-EGFP with Tobramycin (Tob) at a sub-MIC (0.3 µg/mL). Adjuvant molecules SFβM & amino benzimidazole (ABI) (40 µM each) inhibit tobramycin-promoted biofilm formation. Biofilms were grown on polystyrene for 24 h with shaking (100 rpm). Scale bar = 30 µm. The thickness and biomass of biofilm were quantified using COMSTAT software.

Swarming is a complex mode of translocation that is fundamentally different from other bacterial motilities like swimming and twitching. It has been reported that *P. aeruginosa* requires all of the following features to successfully swarm on a semisolid surface; quorum sensing, flagella, pili and production of biosurfactant rhamnolipids.[219]

PAO1 strain used in this study grows outward from the point of inoculation without forming any tendril patterns. Here, we examined the influence of synthetic disaccharide derivatives on normal and sub-MIC of tobramycin promoted swarming of PAO1 strain. It is evident from the images of swarm agar plates that the area or the diameter of PAO1 added with 20 µM SFβM was significantly smaller than PAO1 control without adding any agents (Figure 4.6). However, when adding 0.3 µg/mL of tobramycin, the swam area is slightly bigger than PAO1 control without adding any agents which indicate that the swarming of PAO1 is promoted by tobramycin. Furthermore, adding 20 µM SFβM along with 0.3 µg/mL of tobramycin significantly inhibits swarming of PAO1(Figure 4.6).

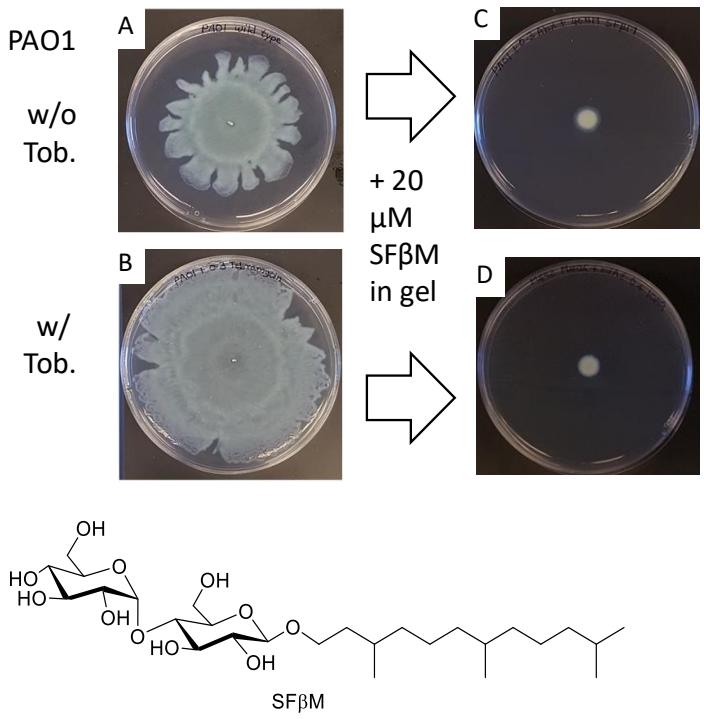

Figure 4.6 Swarming of PAO1 (A) is promoted by tobramycin (0.3 µg/mL) (B). Adding 20 µM SFβM to the swarm plates inhibits swarming without (C) and with (D) added tobramycin.

4.2.3. Synthetic agents acting as adjuvant compounds to enhance the activity of antibiotics against bacteria in biofilms on an abiotic surface

We also assessed the ability of our compounds to facilitate the killing of pre-formed biofilms in our co-culture model of PA biofilms on polystyrene surfaces. Here, we tested two antibiotics, colistin, and tobramycin, which were proven to be most effective against PA bacteria (see Figure 4.7). In this assay, biofilms were grown on polystyrene surfaces for 24 h to reach the mature state. Then predetermined concentrations of antibiotics (25 µg/mL, 30 µg/mL, 35 µg/mL colistin and 8 µg/mL, 16 µg/mL, 32 µg/mL tobramycin) and agents (50 µM SFβM and 50 µM $SF(EG)_4OH$) were added to those pre-formed biofilms and incubated for another 24 h. Survived bacteria were quantified by OD600 readings. For colistin, added synthetic agents significantly enhanced the efficacy of the antibiotics. When SFβM or $SF(EG)_4OH$ were added to 25 µg/mL and 35 µg/mL colistin, the survived bacteria within the biofilms were decreased by 75-85 % (Figure 4.8). However, the efficacy of SFβM or $SF(EG)_4OH$ in enhancing the action of tobramycin is not as good as colistin. The results showed the efficacy of two compounds in enhancing the action of colistin versus biofilms grown on a plastic surface, and modest enhancement of tobramycin (Figure 4.8).

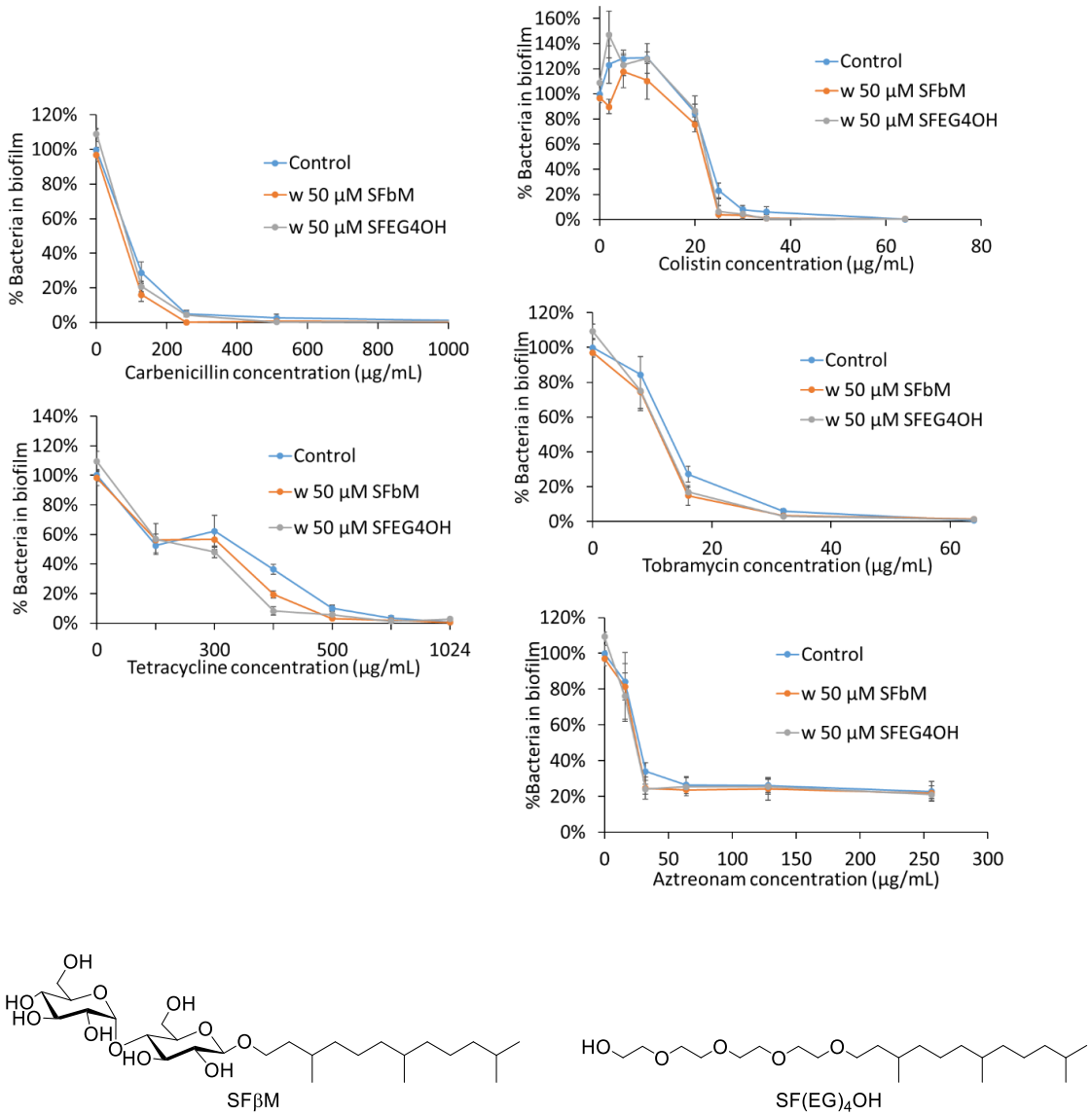

Figure 4.7 Adjuvant compounds enhance the activity of antibiotics versus biofilms on an abiotic surface. Shown is the impact of adjuvant compounds in combination with five antibiotics for a biofilm grown on an abiotic (polystyrene) surface.

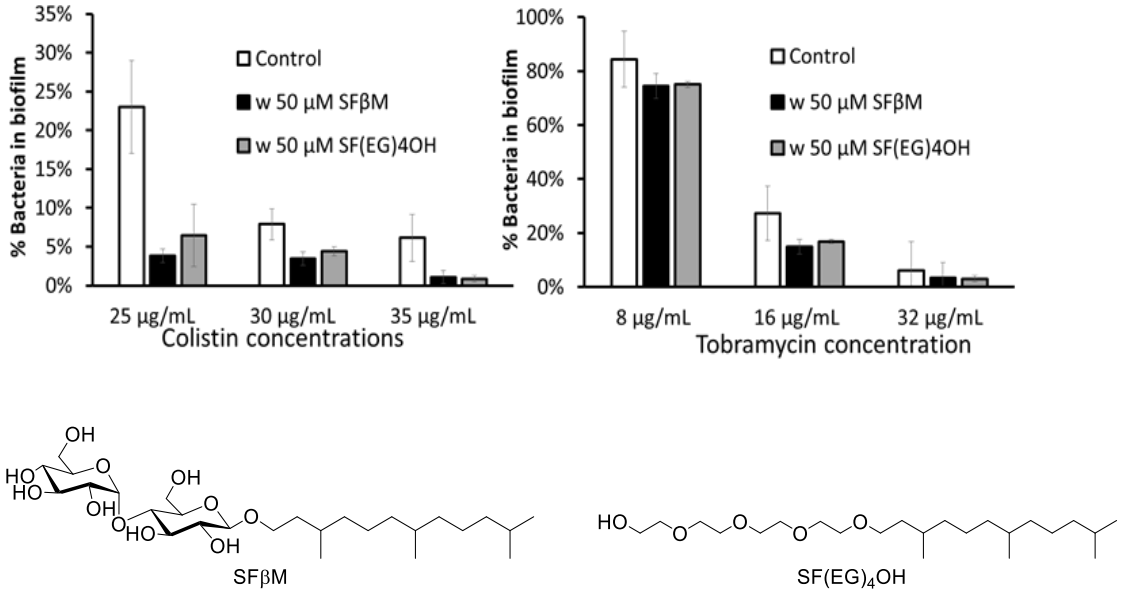

Figure 4.8 Adjuvant compounds enhance the activity of antibiotics versus biofilms on an abiotic surface. Shown is the impact of two different adjuvant compounds in combination with colistin (A) and tobramycin (B) for a biofilm grown on an abiotic (polystyrene) surface. Addition of either compound markedly enhances the % killing (Y-axis) of colistin.

Our molecules enable tobramycin to eradicate the drug-tolerant bacteria and nascent persisters often generated by treatment with this antibiotic. Thus, we have discovered a class of adjuvant agents for controlling antibiotic-induced problems of tolerance, induced persisters, and potentially, fully-developed resistance. To study drug tolerance and persister formation, we first grow a biofilm of PA strain PAO1 (a typical laboratory strain) on pegs[224] with and without 0.3 µg/mL of tobramycin for 24 h to establish

an antibiotic-promoted biofilm, which contains both drug-tolerant bacteria and nascent induced persisters, and a native biofilm, respectively. For each biofilm, we then introduced a fresh medium containing a high concentration of tobramycin (50 μg/mL) with and without 40 μM of SFβM +/- 40 μM ABI. During this second culture period with a high dose of tobramycin, we evaluate the effect of our molecules on tobramycin's killing of bacteria in biofilms as a function of time up to 24 h. Figure 4.9 shows that during the first 10-h versus a control biofilm, our molecules have a small, non-significant impact on tobramycin-mediated killing; no such enhancement is observed beyond 10 hrs (Figure 4.9.A). In contrast, for the tobramycin (0.3 μg/mL)-promoted biofilm,[100] we make three observations (Figure 4.9.B). First, without our molecules, a slower rate of killing was observed from the 2nd hour to the 12th hour when this biofilm was treated with tobramycin (50 μg/mL; Figure 4.9.B, bracket labeled "a"). This result is consistent with the existence of tobramycin-tolerant bacteria. Second, our molecules (SFβM/ABI) enabled the high dose of tobramycin (50 μg/mL) to kill tolerant bacteria that developed during the first 24-h culture with low antibiotic concentration (Figure 4.9.B, bracket labeled "b"). Third, for both control ("native") and tobramycin-induced biofilms, a plateau of killing was observed beyond ~12 h, but a higher resazurin dye signal (i.e., live bacteria)[225-226] is observed for the biofilm without our molecules compared to with SFβM/ABI (Figure 4.9.B). We confirmed that at the end of the high dose tobramycin treatment (50 μg/mL), viable bacteria could be detected in both treatments (with and without our agents). This result indicates that the existence of persisters in both biofilms (but with different amounts) for the last 12-h of high dose tobramycin treatment. To further confirm that these bacteria were persisters, we collected large amount of these bacteria (from 20 pegs when plateaus were reached),

sonicated them in saline water (to prevent phenotype reversion), concentrated to get the pellet, and cultured the pellet again in LB containing 10 µg/mL of tobramycin, and in fresh LB. Whereas there was no growth observed in LB containing 10 µg/mL tobramycin, bacteria from this treatment always regrow in fresh medium. Together, these finding and data from Figure 4.9.B suggest that our molecules enable tobramycin to kill and/or to prevent a portion of persisters in the drug-treated bacterial population.

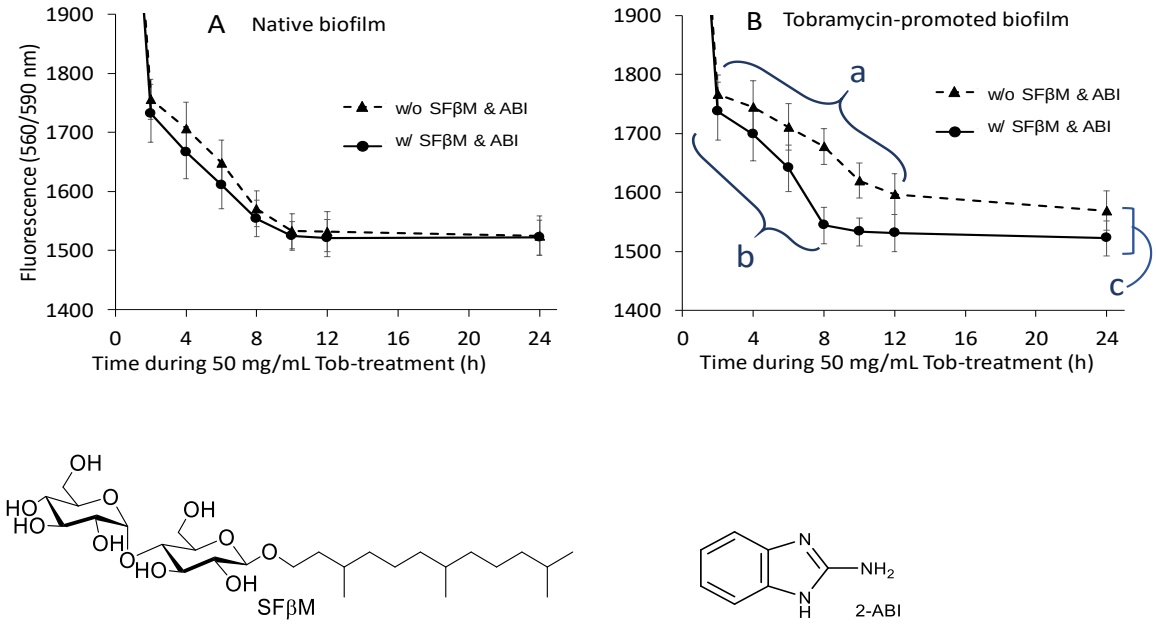

Figure 4.9 The fluorescence of resazurin dye showing live PA strain PAO1 in (A) native and (B) tobramycin (Tob, 0.3 µg/mL)-promoted biofilms, which were treated with 50 µg/mL Tob, and with (solid line) and without (dash line) 40 µM (~22 µg/mL) SFβM & 40 µM ABI at different times. Interpretation of panel B: "a" consists of susceptible and tolerant bacteria, plus persisters; "b", susceptible bacteria, plus persisters; "c", tobramycin -induced persisters.

4.2.4. Adjuvant compounds enhance the efficacy of antibiotics to combat tobramycin-tolerant subpopulations

To study the effect of adjuvant compounds on the efficacy of antibiotics to combat tobramycin-tolerant subpopulations, we first grow biofilms of PAO1 on polystyrene chips with and without 0.3 µg/mL of tobramycin for 24 h to establish native and antibiotic-promoted biofilms. In the next 24 h, we increased the concentration of tobramycin to 50 µg/mL with and without 85 µM 3,5-DMDβM or 3,5-DMDβC, and then we monitored the development of live and dead subpopulations of *P. aeruginosa* biofilms by confocal image acquisition. A 488 nm laser line was used to visualize live cells within the biofilms formed by PAO1-EGFP strain. Dead cells within the biofilm stained by propidium iodide were visualized by 635 nm laser line. The image analysis program COMSTAT was used to analyze images stained with the LIVE/DEAD viability stain by recognizing the relative biomass that fluoresces green (live) and red (dead) at levels above a user-defined threshold value and reports the percentage of biomass that is alive and the percentage of biomass that is dead in each slice in a stack of images. The areas of the biomass fluorescing green and red represented the relative amounts of living and dead biomass in a biofilm.

50 µg/mL tobramycin exposure to native biofilms led to a reduction in live cell biomass by ~50 %, and exposure to antibiotic-promoted biofilms led to a reduction in live cell biomass by ~40 % (Figure 4.10). We also examine the effect of the combination treatments with 85 µM 3,5-DMDβM or 3,5-DMDβC and tobramycin on native and

antibiotic-promoted biofilms. The results showed that the combination treatments lead to drastic change in live and dead cell subpopulation (Figure 4.10). 24 h of 50 μg/mL tobramycin exposure combined with 85 μM 3,5-DMDβM or 3,5-DMDβC to native biofilms caused live cell biomass further decreased by 50 % compared to when treated with 50 μg/mL tobramycin alone (Figure 4.10). However, adding 85 μM 3,5-DMDβM or 3,5-DMDβC in combine with 50 μg/mL tobramycin to the native biofilms caused a significant increase in dead cell biomass. There are 9 to 10 times more dead cells remained within the native biofilms after 24 h of 50 μg/mL tobramycin exposure combined with 85 μM 3,5-DMDβM or 3,5-DMDβC compared to when treated with 50 μg/mL tobramycin alone (Figure 4.10).

Similarly, the combination treatments with 85 μM 3,5-DMDβM or 3,5-DMDβC and tobramycin on antibiotic-promoted biofilms lead to drastic change in live and dead cell subpopulation as well (Figure 4.11). 24 h of 50 μg/mL tobramycin exposure combined with 85 μM 3,5-DMDβM or 3,5-DMDβC to antibiotic-promoted biofilms caused live cell biomass further decreased by 70 % compared to when treated with 50 μg/mL tobramycin alone (Figure 4.11). Dead cell biomass was significantly increased as well. There are 8 to 12 times more dead cells remained within the antibiotic-promoted biofilms after 24 h of 50 μg/mL tobramycin exposure combined with 85 μM 3,5-DMDβM or 3,5-DMDβC compared to when treated with 50 μg/mL tobramycin alone (Figure 4.11).

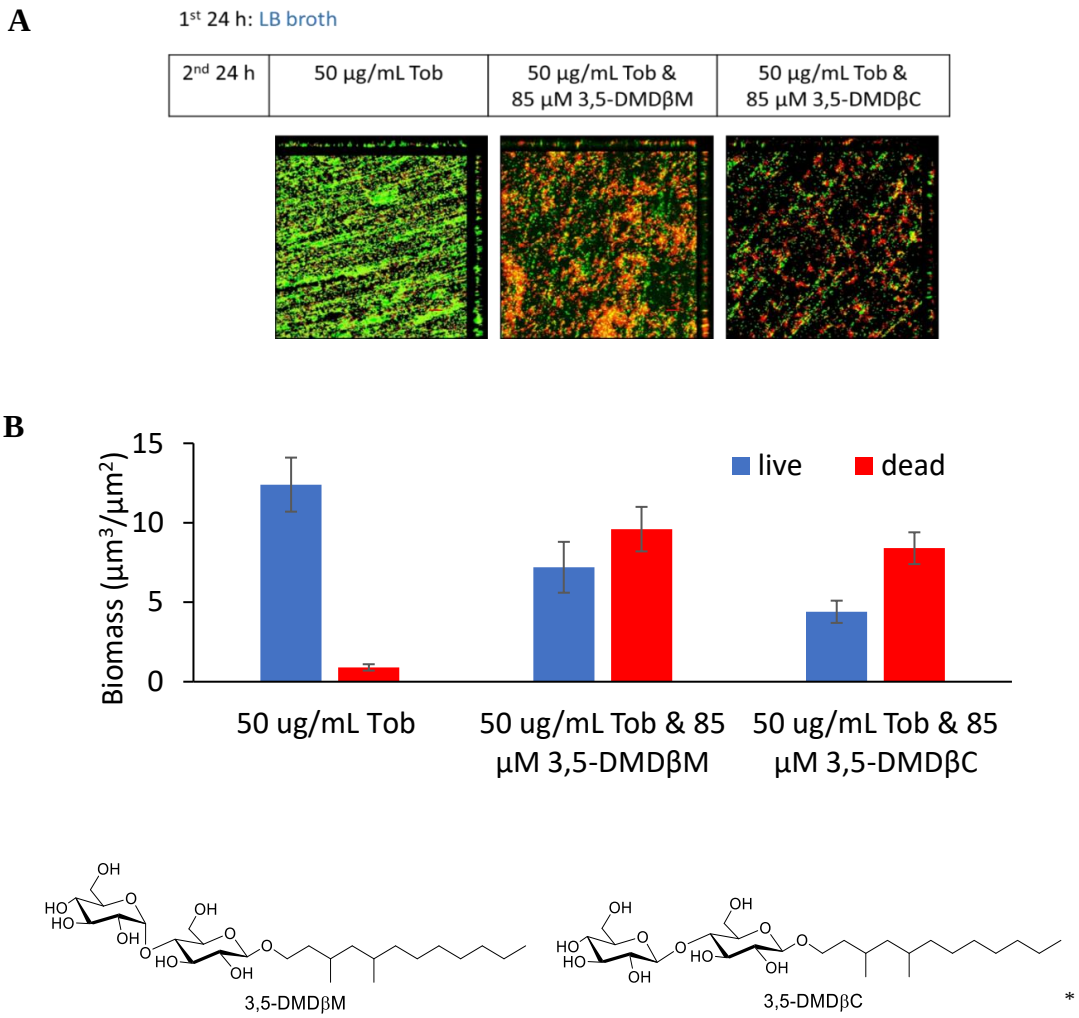

Figure 4.10 Confocal microscopy images of 2-day old native biofilms. Biofilms attached to polystyrene chips were stained using the LIVE/DEAD biofilm viability stain (A). The images are Z-stack projections indicating the thickness of the biofilms for strain PAO1-EGFP. Experiments were performed in triplicate, and a representative image for each condition is shown. Scale bar: 30 µm. The live and dead cell biomass of biofilm quantified using COMSTAT software (B).

* The work in this chapter is a collaboration with Felicia Burns in Luk group. She synthesized and characterized the two molecules, 3,5-DMDβM and 3,5-DMDβC, used in this chapter. ^{1}HNMR and ^{13}CNMR collected by Felicia Burns were included for the purpose of completing the information.

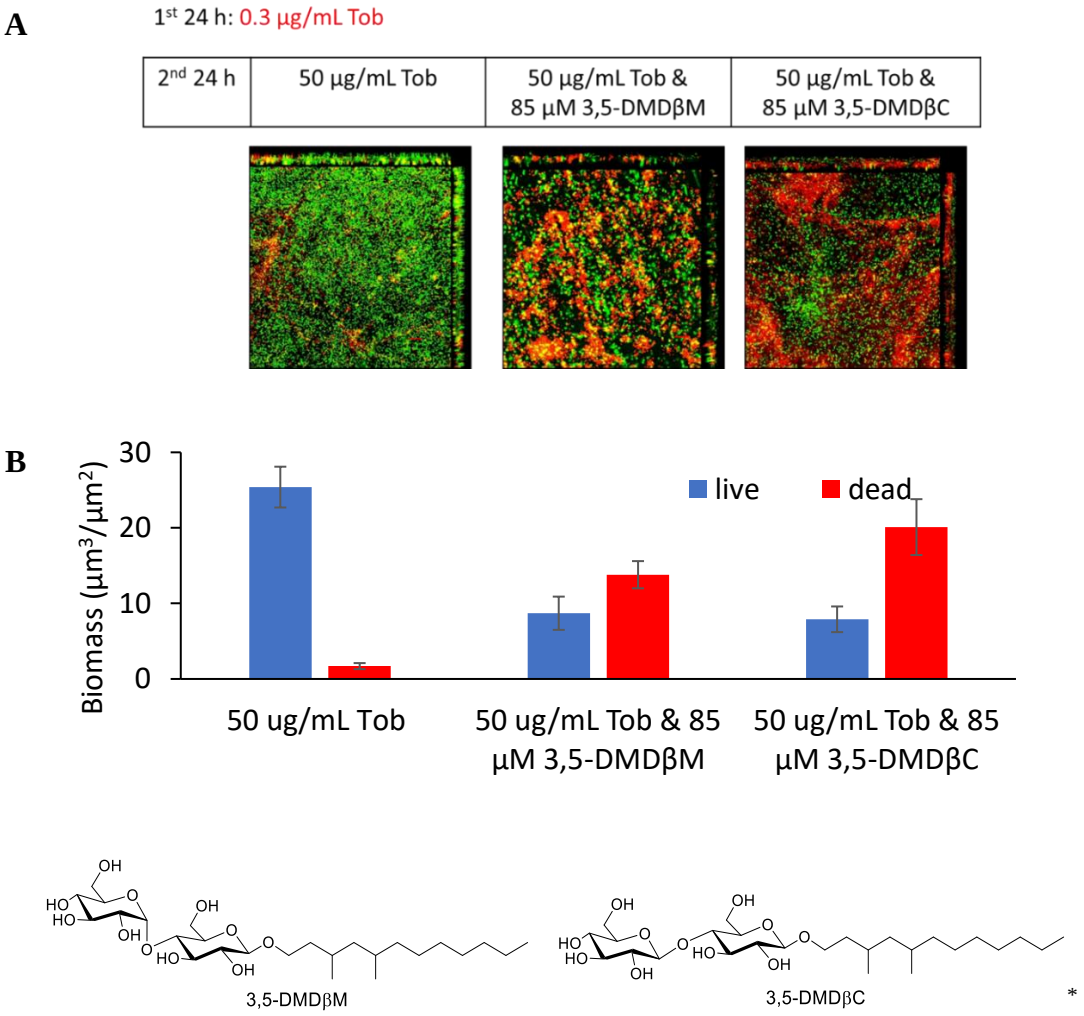

Figure 4.11 Confocal microscopy images of 2-day old antibiotic promoted biofilms. Biofilms attached to polystyrene chips were stained using the LIVE/DEAD biofilm viability stain(A). The images are Z-stack projections indicating the thickness of the biofilms for strain PAO1-EGFP. Experiments were performed in triplicate, and a representative image for each condition is shown. Scale bar: 30 µm. The live and dead cell biomass of biofilm quantified using COMSTAT software (B).

* The work in this chapter is a collaboration with Felicia Burns in Luk group. She synthesized and characterized the two molecules, 3,5-DMDβM and 3,5-DMDβC, used in this chapter. ^{1}HNMR and ^{13}CNMR collected by Felicia Burns were included for the purpose of completing the information.

4.3. Conclusion

In this chapter, we confirmed that our molecule, SFβM, inhibited both tobramycin-promoted biofilm formation and swarming motility, and thus SFβM overcomes the impact of tobramycin at controlling these two activities. 3,5-DMDβM and 3,5-DMDβC showed a similar effect on inhibiting both tobramycin-promoted biofilm formation and swarming motility. Thus, we can conclude that disaccharide molecules having branched hydrocarbons inhibit tobramycin-promoted bacterial activities. SFβM and $SF(EG)_4OH$ enhanced the bactericidal action of antibiotics colistin and tobramycin on biofilms grown on a polystyrene surface. In addition, SFβM/ABI enabled tobramycin to kill and to prevent a portion of persisters in the drug-treated bacterial population. Confocal microscopy study revealed that our synthetic molecules, 3,5-DMDβM and 3,5-DMDβC, can act as adjuvant compounds to enhance the efficacy of antibiotics to combat tobramycin-tolerant subpopulations. Thus, supplementing conventional antibiotic treatment with an adjuvant compound seems to be a promising therapy for eradicating biofilm-associated infections. Furthermore, our study showed that co-treatment of adjuvant compounds along with antibiotics is important to kill antibiotic-tolerant cells and prevent new persisters to form. It highlighted the importance of developing motility inhibitors that can be given to chronically infected patients, with the aim of constituting functional anti-biofilm chemotherapies.

4.4. Materials and Methods

4.4.1. Stock solutions

Stock solutions of all the agents were prepared in autoclaved water, sterilized by filtering through a 0.2 µm syringe filter, and stored at -20 °C in sealed vials. An appropriate amount of sterile water was added to controls in all assays to eliminate the solvent effect.

4.4.2. Bacterial strains

Wild-type *P. aeruginosa* PAO1 and PAO1-EGFP strains were obtained from Dr. Guirong Wang (Upstate Medical University, Syracuse). library (PAO1 transposon mutant library).[156]

4.4.3. Confocal laser scanning microscopy (CLSM)

Biofilms were grown by inoculating the bacteria on polystyrene coupons (3/8 in. × 3/8 in.) with or without agents in a 24-well microtiter plate. The saran-wrapped plate was then incubated at 37 ºC under 100 rpm shaking condition for 24 h. Inhibition of biofilm formation was directly observed. Eradication of preformed biofilm was performed after bacterial cultures were gently pipetted out and wells were washed, and fresh media was added containing predetermined concentrations of antibiotics and synthetic agents for another 24 h. Each polystyrene coupon was then washed gently by

dipping into 0.85 w/v% aqueous NaCl solutions twice and then placed on a microscope cover glass (50 x 24mm, No. 2, Fisher Scientific, Pittsburgh, PA). The biofilms were visualized using a Zeiss LSM 710 Confocal Laser Scanning Microscope (Carl Zeiss, Jena, Germany).

4.4.4. Swarming assay

Swarm agar plates were made using M8 medium supplemented with 0.2% glucose, 0.5% casamino acid, 1 mM $MgSO_4$ and solidified with 0.5 % Bacto agar. Bacterial culture with OD600 between 0.4 to 0.6 was inoculated as 3 µl aliquots. Swarm agar plates were incubated at 37 °C for 12 h and then incubated for an additional 12 h at rt. For each set of the experiment, all the swarm plates were poured from the same batch of agar and allowed to dry for 1 h before inoculation of bacteria.

4.4.5. Resazurin cell viability assay

On multi-array pegs, biofilms were grown for 24 h without and with 0.3 µg/mL tobramycin to form control and tobramycin -promoted biofilms, respectively. The medium was replaced with fresh medium supplemented with 50 µg/mL tobramycin, and without or with 40 µM SFβM & 40 µM 2-ABI and cultured for the times indicated. The biofilms were sonicated (15 min at 30 kHz). Resazurin was added to the sonicated culture, followed by quantifying the fluorescence at 590 nm.

^{1}H NMR spectra*

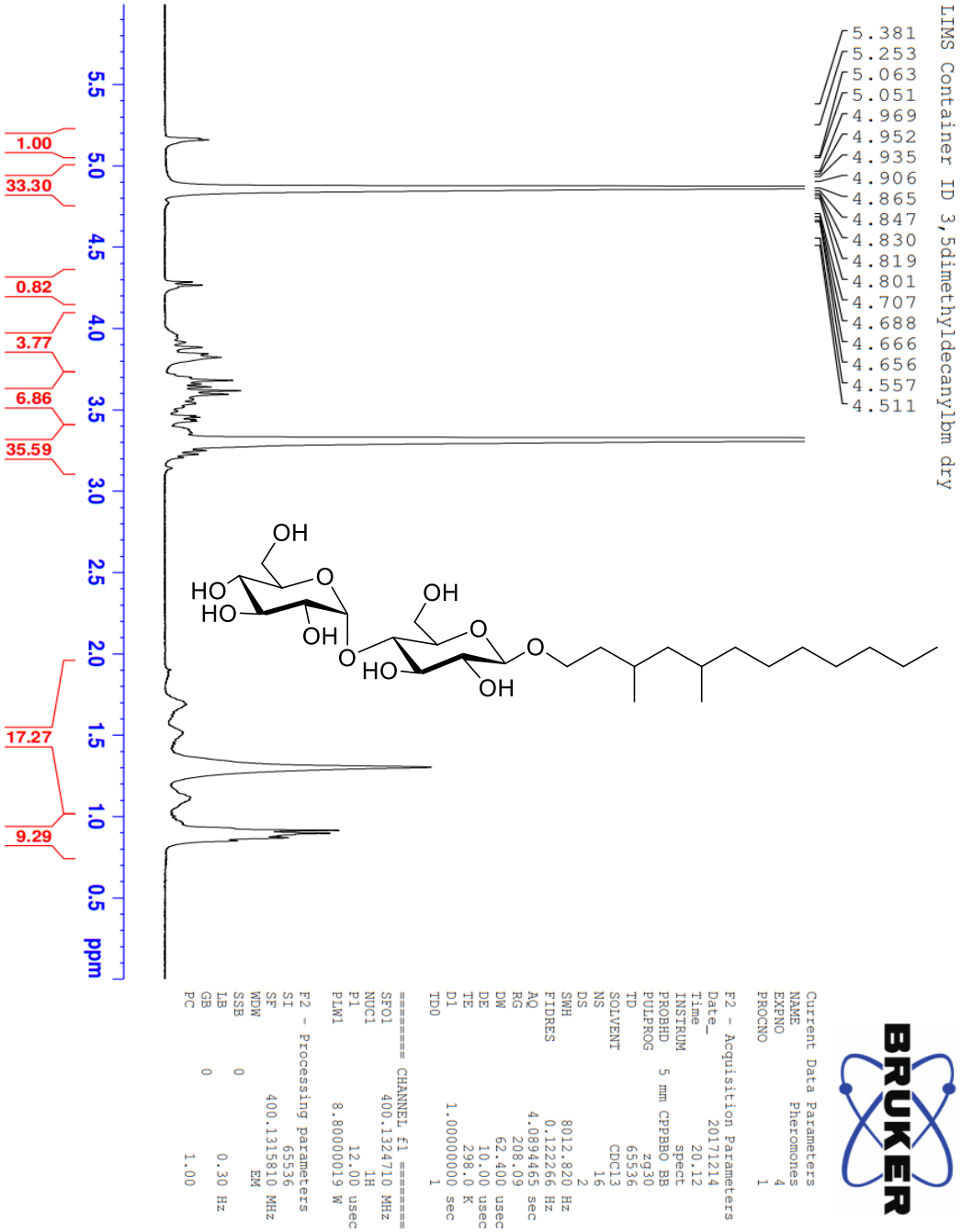

* This spectrum is collected by Felicia Burns.

LIMS Container ID 35bC

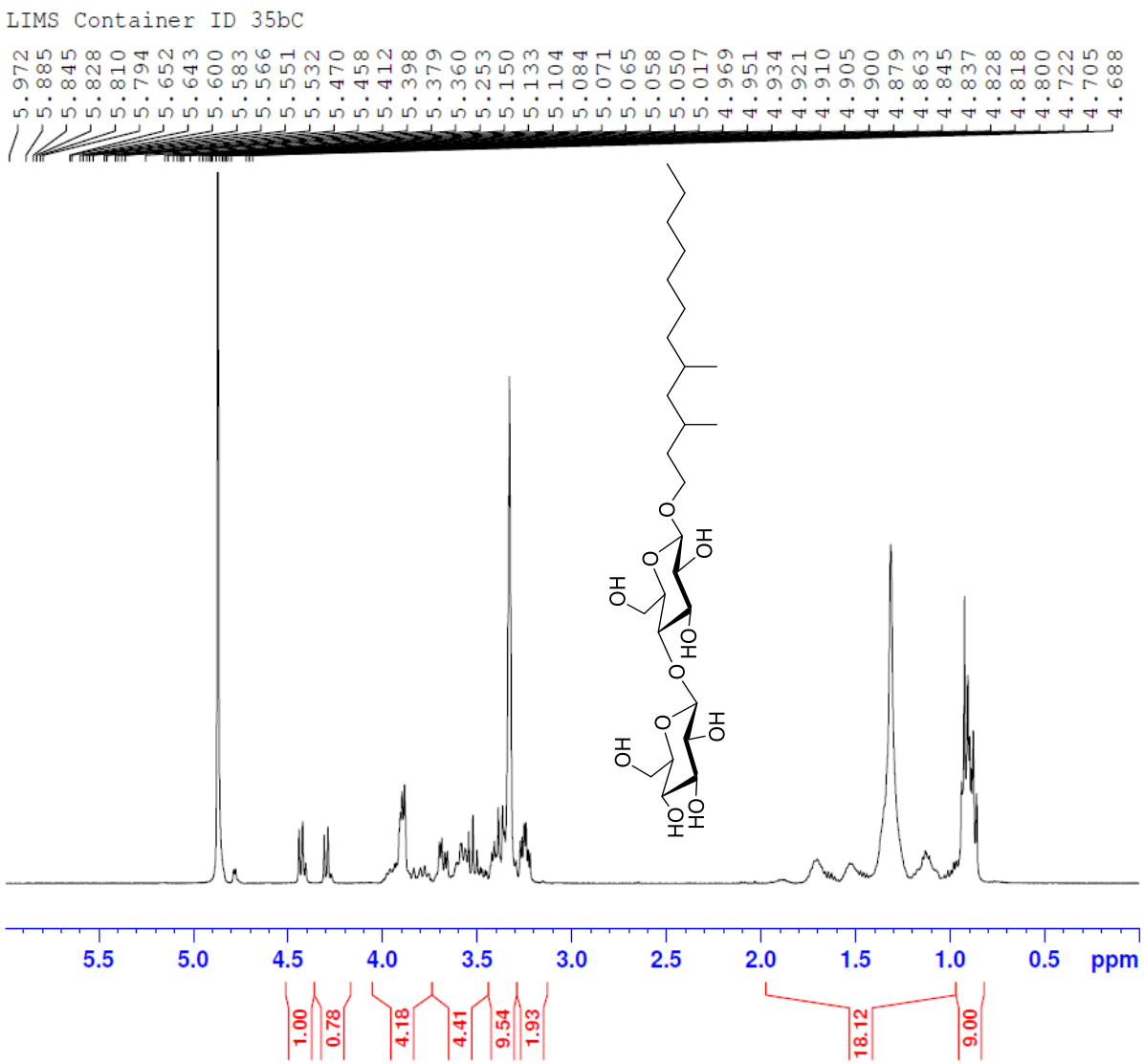

BRUKER

Current Data Parameters
NAME Pheromones
EXPNO 5
PROCNO 1

F2 - Acquisition Parameters
Date_ 20180317
Time 19.30 h
INSTRUM spect
PROBHD Z116098_0203 (
PULPROG zg30
TD 65536
SOLVENT CDCl3
NS 16
DS 2
SWH 8012.820 Hz
FIDRES 0.244532 Hz
AQ 4.0894465 sec
RG 91.52
DW 62.400 usec
DE 6.50 usec
TE 298.0 K
D1 1.00000000 sec
TD0 1
SFO1 400.1324708 MHz
NUC1 1H
P1 10.00 usec
PLW1 16.20000076 W

F2 - Processing parameters
SI 65536
SF 400.1315765 MHz
WDW EM
SSB 0
LB 0.30 Hz
GB 0
PC 1.00

^{13}C NMR Spectra*

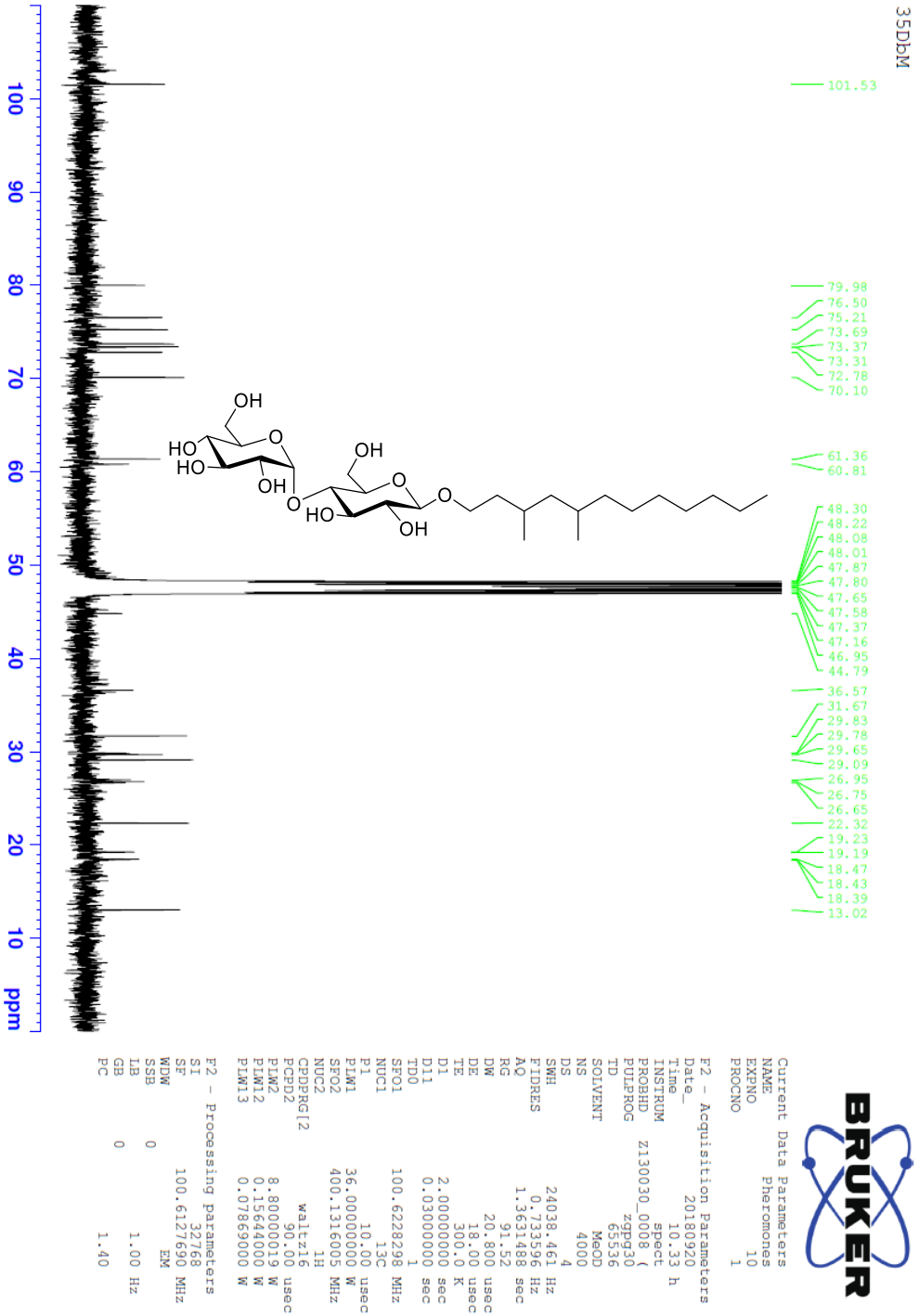

* This spectrum is collected by Felicia Burns.

LIMS Container ID 35DbC

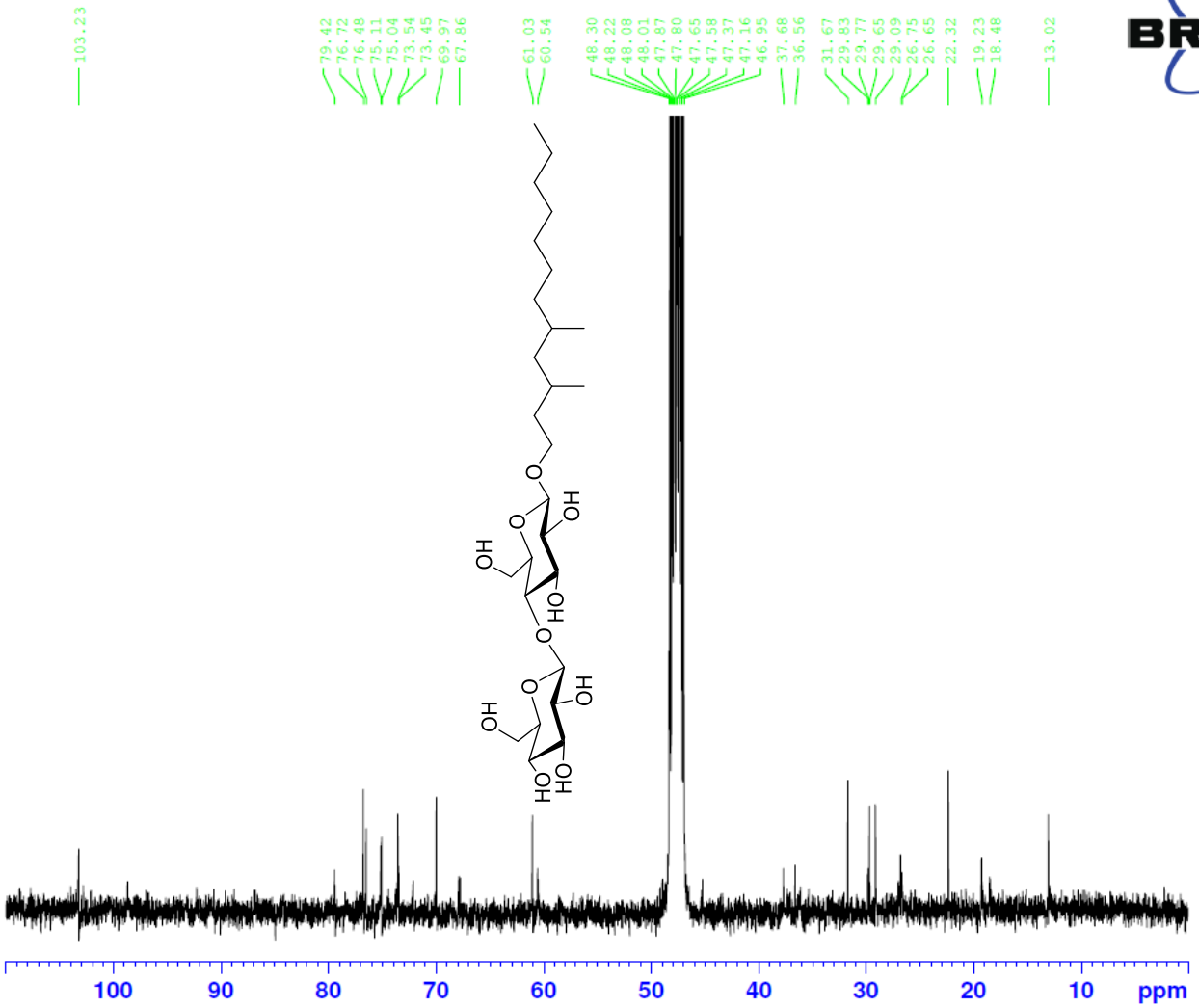

BRUKER

```
Current Data Parameters
NAME          Pheromones
EXPNO                  9
PROCNO                 1

F2 - Acquisition Parameters
Date_           20180920
Time                6.40 h
INSTRUM            spect
PROBHD   Z130030_0008 (
PULPROG          zgpg30
TD                65536
SOLVENT             MeOD
NS                  4000
DS                     4
SWH            24038.461 Hz
FIDRES          0.733596 Hz
AQ             1.3631488 sec
RG                 80.84
DW                20.800 usec
DE                18.00 usec
TE                300.0 K
D1             2.00000000 sec
D11            0.03000000 sec
TD0                    1
SFO1         100.6228298 MHz
NUC1                13C
P1                 10.00 usec
PLW1         36.00000000 W
SFO2         400.1316005 MHz
NUC2                1H
CPDPRG[2         waltz16
PCPD2              90.00 usec
PLW2          8.80000019 W
PLW12         0.15644000 W
PLW13         0.07869000 W

F2 - Processing parameters
SI                 32768
SF           100.6127690 MHz
WDW                   EM
SSB       0
LB                 1.00 Hz
GB        0
PC                 1.40
```

Chapter 5 Selective Binding of Synthetic Disaccharide Derivatives to LecA Revealed by Fluorescent Polarization*

5.1. Introduction

5.1.1. Background of Fluorescence polarization

Fluorescence polarization (FP) is a powerful method for probing protein-ligand interactions, that involve the interaction of small fluorescent ligands with large receptors.[227-228] In 1926, Francis Perrin first described the theoretical basis of fluorescence polarization.[229] In the 1950s, Gregorio Weber extended Perrin's theoretical work and developed the first instrumentation to measure fluorescence polarization, and applied it to study the interactions between dansyl chloride and bovine serum albumin.[230-232] Since then, the principles of fluorescence polarization have been applied extensively in assays to enable high-throughput screening of small molecule libraries for the purposes of probe development and drug discovery.[233-236] Fluorescence polarization assay is based on the rotational differences between the depolarization of the emitted light before and after the interaction of molecules.[237] A small fluorophore rotates in random directions, resulting in rapid depolarization of light, while a larger complex molecule rotates slower and depolarize light at a reduced rate. The difference in depolarization rate can be measured by fluorescence spectrometer. Specifically, the small fluorophore in solution is first excited by a linearly polarized light. The parallel and perpendicularly polarized components of the fluorescence emissions are measured. If the fluorophore is unbound, the polarization

* While I conducted all the experiments in this work, the idea of using fluorescent polarization to detect LecA binding to out molecules is initiated by Pankaj Patil, and he contributed substantially to the design of the experiments.

anisotropy value remains at a relatively low level. If it is bound to a larger receptor, its rotation is slowed, and the polarization anisotropy increases. In competition binding FP assays, the presence of unlabeled ligands or small molecule inhibitors of the interaction results in the displacement of the labeled fluorescent ligands, which increases the tumbling motion of the free fluorescent ligands in the solution, and a decrease in FP value can be detected.[238] It has been widely used in numerous studies to measure the binding affinity (IC_{50} or K_d measurement) of various receptors with their respective ligands.[239-241] Fluorescence polarization assay is a homogeneous assay which can perform very quickly since it does not require removal of unreacted reagents. Fluorescence polarization has emerged as a technique which allows for high throughput and in situ detection of the potency of a given competitive inhibitor.[237, 242-243]

5.1.2. Lectin protein of bacteria

Lectins are proteins that can bind specific carbohydrate structures which play important roles in interactions and communication between bacterial, mammalian, plant or fungi cells typically for recognition of glycan epitopes in multivalent carbohydrates and glycoprotein receptors.[244-245] Owing to carbohydrate binding specificity of lectins, they have a huge impact on cell adhesion and host cell cytotoxicity, thus play a crucial role in the pathogenic property of the parasite.[246-248] In the case of *P. aeruginosa*, the bacteria produce two lectins termed LecA (PA-IL) and LecB (PA-IIL).[249-250] These lectins appear to function in multistep adhesion events which involves proteolysis and elastolysis to be cloned and sequenced as well as cytotoxins for respiratory epithelial cells.[251-253] Galactose-

specific LecA is a tetrameric protein consisting of four 12.75-kDa subunits.[249, 254] LecB is about 12 ~13 kDa and exhibits a high specificity for fucose.[250, 255] LecA and LecB have both been shown to interact with the glycosphingolipid antigens, which is a huge factor for the infectivity and pathogenicity of *P. aeruginosa*.[256-257] The crystal structures of both lectins show homotetrameric assemblies and calcium ions mediating the recognition of their carbohydrate ligands.[257-259] LecA has an intermediate affinity for its monovalent d-galactose-derived ligands in the Kd = 50–100 μM range and Phenyl β-d-galactosides and derivatives at approximately 10 μM.[259-260] Recent studies revealed the affinities for LecA in the nanomolar range based on divalent galactoside compounds.[260-261] Here, we reveal the selective binding of maltose and cellobiose derivatives to the bacterial LecA by a fluorescence polarization-based assay.

5.1.3. The aim of the chapter

In this chapter, we designed and synthesized fluorescent-tag labeled ligand, βGal-aryl-Dansyl, for LecA protein. We examined the ligand-receptor binding between βGal-aryl-Dansyl and LecA by a fluorescence polarization-based assay and evaluated potential ligands for LecA by competitive fluorescence polarization assay.

5.2. Results and discussion

5.2.1. Design of fluorescent-tag labeled ligand for LecA protein

The fluorescent polarization has been developed and used to detect binding between LecA and two phenyl-linked reporter ligands by Alexander Titz and coworkers.[259] In their work, they synthesize two fluorescent molecules (See Figure 5.1).

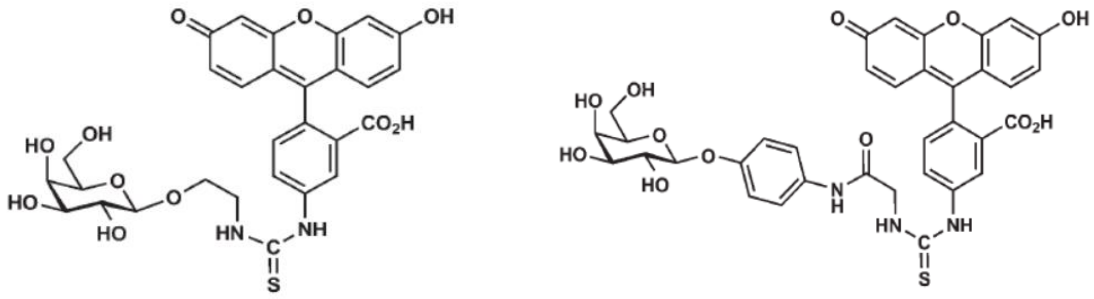

(K_d = 19.2 ± 4.8 μM) (K_d = 8.1 ± 2.1 μM)

Figure 5.1 Structures of fluorophore-tagged phenyl glycosides for LecA ligands. The listed dissociation constants are published in the literature.[259]

We design an efficient one-step synthesis of a fluorescently labeled ligand that would also bind to LecA. This molecule will be used to establish a fluorescence polarization assay with LecA. We explore this new structure because of the efficiency of the synthesis (72 % yield). The ligand βGal-aryl-Dansyl is a D-Galactose-based probe tethered with a dansyl group as the fluorescent part.

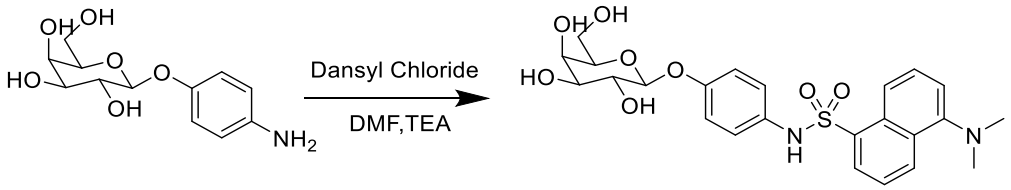

Scheme 5.1 New Fluorescent Ligand Molecule, βGal-aryl-Dansyl, for LecA – Efficient One-Step Synthesis

5.2.2. βGal-aryl-Dansyl binds to LecA with a K_d of 10.7 ± 0.8 μM, based on by fluorescence polarization

To evaluate the binding of βGal-aryl-Dansyl to LecA, a direct titration with increased amounts of LecA was performed along with increased amounts of BSA as a negative control. The ligand showed a dose-dependent increase in fluorescence polarization with increasing concentration of LecA, while did not show any significant effect on BSA (Figure 5.2). K_d value was obtained from a four-parameter fitting procedure to the dose-dependent increase in fluorescence polarization by using Origin software. The fitting equation is y = A1 + (A2-A1)/(1 + 10^((LOGx0-x)*p)), and A1 and A2 correspond to bottom and top asymptotes, p is the hill slope and LOGx0 is the center value when y=(A1+A1)/2. The model showed the fitted curve equation is: y=(0.12213-0.07179)/(1 + 10^((10.17-x)*0.052)), and the R^2=0.97. The calculated K_d of the binding of βGal-aryl-Dansyl to LecA is 10.17 ± 1.71 μM based on the direct binding curve derived from

fluorescence polarization assay, which is consistent with the reported K_d values of phenyl-β-galactoside derived ligands (K_d = 7.4 μM and 8.1 μM) in the low μM range.[18]

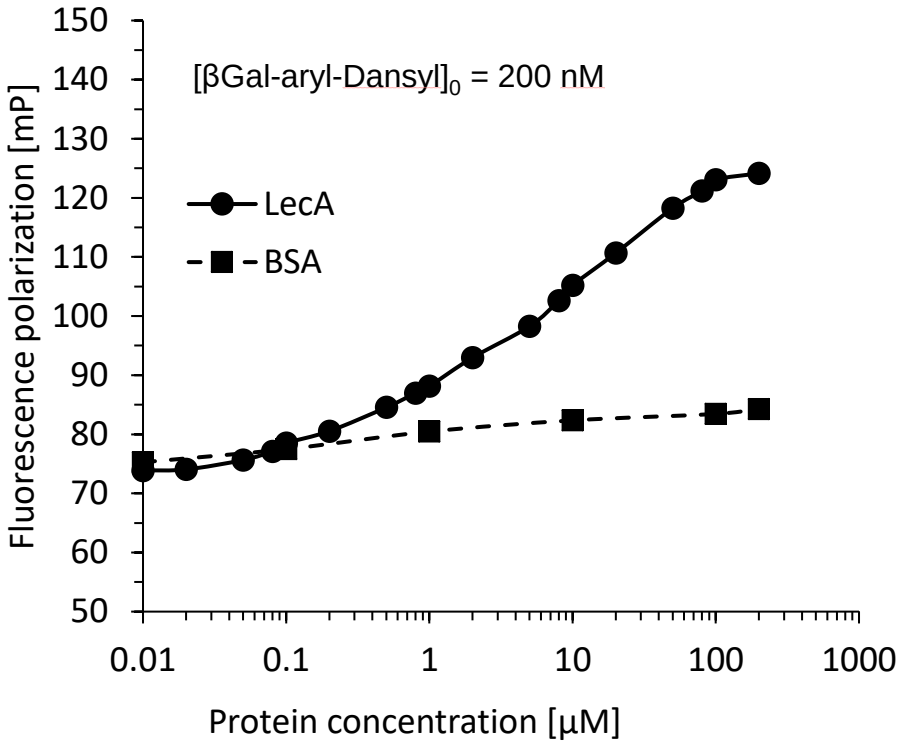

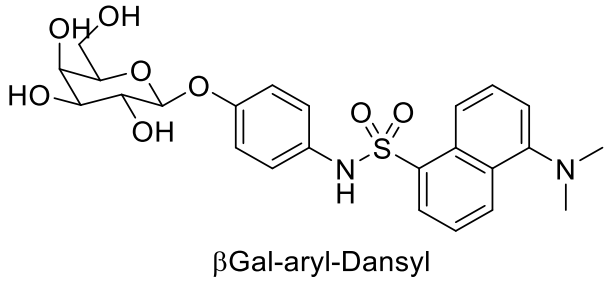

βGal-aryl-Dansyl

Figure 5.2 Direct Titration of βGal-aryl-Dansyl (200 nM) with Increasing [LecA] Revealed K_d of 10.17 ± 1.71μM. Dissociation constants were obtained from a four-parameter fitting procedure to the dose-dependent increase in fluorescence polarization.

5.2.3. The half maximal inhibitory concentrations (IC_{50}) *of synthetic molecules against βGal-aryl-Dansyl are between 10-20 μM*

The half maximal inhibitory concentration (IC_{50}) of our synthetic molecules against βGal-aryl-Dansyl were determined by competitive binding assay using FP. The basic principle of the assay is shown in the Figure 5.3.A. Basically, in a competition binding FP assays, the presence of unlabeled ligands or small molecule inhibitors of the interaction results in the displacement of the labeled fluorescent ligands, which increases the tumbling motion of the free fluorescent ligands in the solution, and a decrease in FP value can be detected. The results revealed that IC50 of SFβM and SFβC are both at ~15 μM, and DβM has an IC50 of ~19 μM. However, SFEG4OH and rhamnolipids did not show any binding ability toward LecA (Figure 5.3.B).

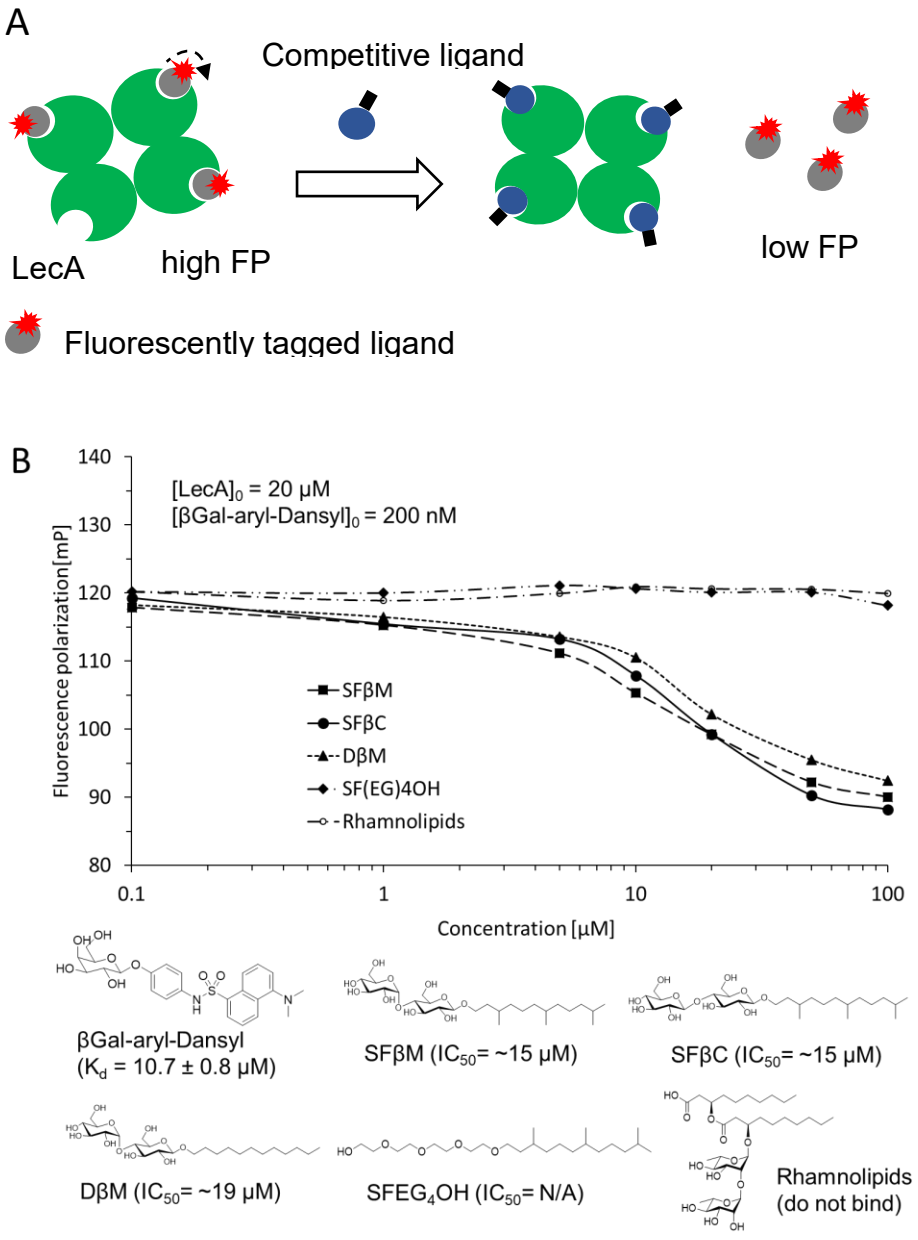

Figure 5.3 Competitive binding assay principle for monitoring LecA-ligand interaction using fluorescence polarization (A). Fluorescent polarization reading of solutions of LecA (final concentration: 20 µM) and βGal-aryl-Dansyl (200 nM) in 0.1M Tris-HCl pH

7.5 and 6 μM $CaCl_2$ with serial dilutions (0.1 μM to 100 μM) of test compounds, SFβM, SFβC, DβM and SFEG4OH (B). IC_{50} was obtained from a four-parameter variable slope model.

5.3. Conclusion

To conclude, we have used fluorescent polarization assay to show a fluorophore-derivatized disaccharide can bind to LecA. We also showed that our potent molecules can displace this fluorophore disaccharide from LecA, causing a decrease in fluorescence polarization. Together these results in chapter 6 suggest that SFβM is a chimeric ligand that binds to two different targets, LecA[101-102], and pili,[262] and also explains why two distinct processes (biofilm formation and swarming) are inhibited by the same molecule.

5.4. Materials and Methods

5.4.1. Synthesis of βGal-aryl-Dansyl

4-Aminophenyl β-D-galactopyranoside(0.12 g, 1.2 mmol) in anhydrous DMF (2 mL) was added to Et3N (0.53 g, 0.53 mmol) in anhydrous DMF (5mL) at 0 ºC. To this solution was added dansyl chloride (0.41 g, 1.5 mmol). After stirring at 0 ºC for 2 hr, the mixture was concentrated, and the residue obtained was subjected to the purification by column chromatography to yield a yellow solid product (0.44 g, 72 %). 1H NMR (400MHz, CDCl3): δ 8.47 (d, 1 H, dansyl), 8.24 (d, 1 H, dansyl), 8.20 (d, 1 H, dansyl), 7.65-7.69 (m, 2 H, dansyl), 7.39 (d, 1 H, dansyl), , 6.92–6.81 (m, 4H, ArH), 4.75 (d, J =

7.7 Hz, 1H), 4.37 (s, 2H, CH2NHR), 3.69 (d, J = 3.1 Hz, 1H), 3.58–3.46 (m, 5H), 2.84 (s, 6H,-CH3).

5.4.2. Direct binding of fluorescent ligands to LecA

The fluorescent ligands were dissolved in DMSO to a final concentration of 3 mg mL^{-1}. 2 mg LecA was dissolved in 1 mL of 0.1M Tris-HCl pH 7.5 and 6 μM $CaCl_2$. A serial dilution of LecA samples was prepared. The solution of one fluorescent ligand was added to a final concentration (final concentrations of βGal-aryl-Dansyl: 200 nM). After incubation for 1 h at r.t., fluorescence polarization was determined using Edinburgh FLS9801 Spectrometer. During measurement, the samples were illuminated with vertically polarized light at 330 nm (for βGal-aryl-Dansyl), and vertical and horizontal fluorescence components were measured, and the fluorescence polarization values were calculated subsequently.

5.4.3. Competitive binding assays

Typically, to a solution of LecA (final concentration: 20 μM) and fluorescent ligand (final concentrations of βGal-aryl-Dansyl: 200 nM; FITC-EG12-SF: 20 nM) in 0.1M Tris-HCl pH 7.5 and 6 μM $CaCl_2$, serial dilutions (0.1 μM to 100 μM) of test compounds (SFβM, SFβC, DβM, SFEG4OH) were added. After the addition of the reagents, the samples were incubated for 4–6 h at r.t. fluorescence polarization was determined using Edinburgh FLS9801 Spectrometer. During measurement, the samples

were illuminated with vertically polarized light at 330 nm (for βGal-aryl-Dansyl) and 490 nm (for FITC tagged fluorophore), and vertical and horizontal fluorescence components were measured, and the fluorescence polarization values were calculated subsequently.

^{1}H NMR spectra

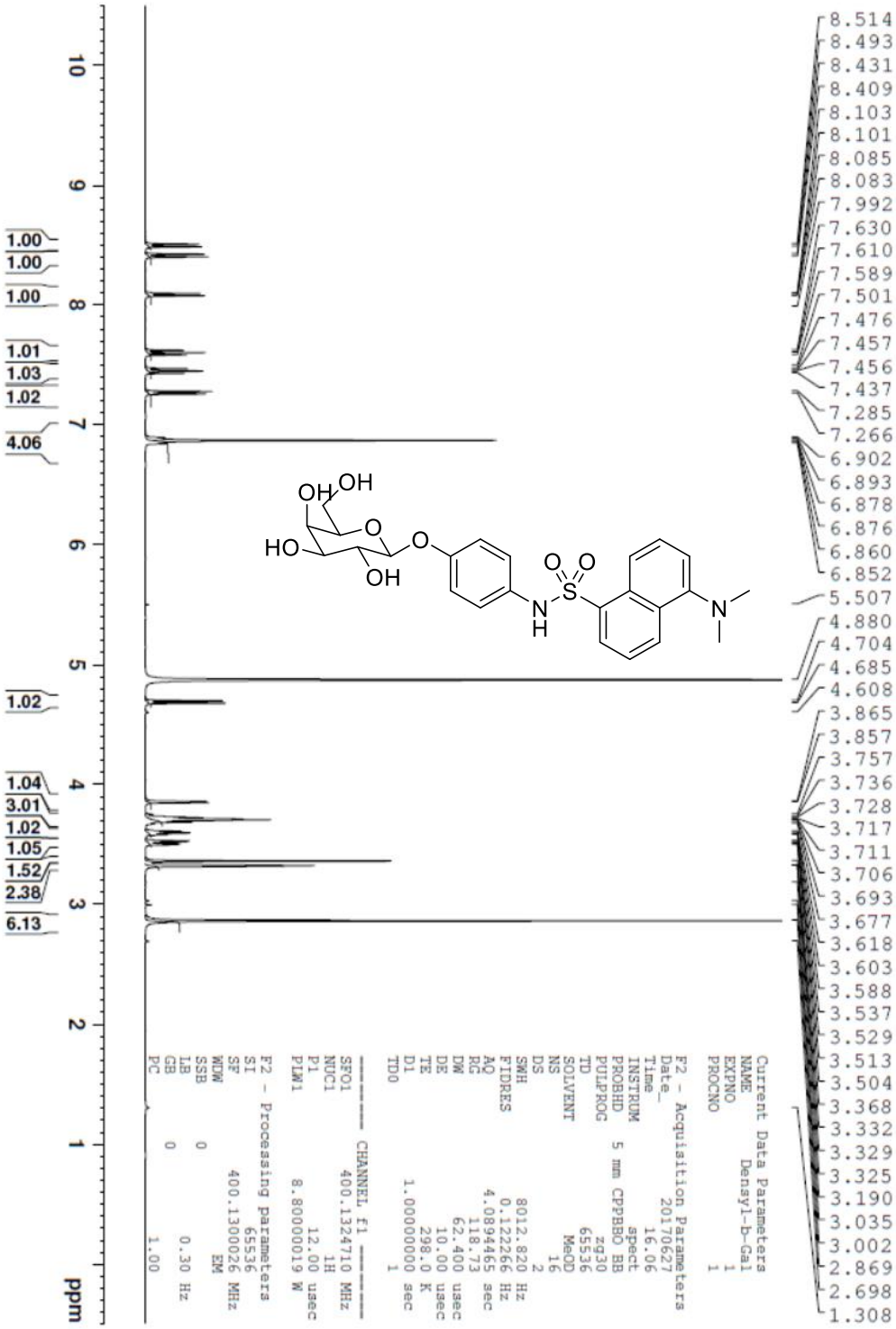
8.514
8.493
8.431
8.409
8.103
8.101
8.085
8.083
7.992
7.630
7.610
7.589
7.501
7.476
7.457
7.456
7.437
7.285
7.266
6.902
6.893
6.878
6.876
6.860
6.852
5.507
4.880
4.704
4.685
4.608
3.865
3.857
3.757
3.736
3.728
3.717
3.711
3.706
3.693
3.677
3.618
3.603
3.588
3.537
3.529
3.513
3.504
3.368
3.332
3.329
3.325
3.190
3.035
3.002
2.869
2.698
2.308
1.00
1.00
1.00
1.01
1.03
1.02
4.06
1.02
1.04
3.01
1.02
1.05
1.52
2.38
6.13
ppm
OH
OH
HO
O
O
OH
O
O
S
N
H
N
Current Data Parameters
NAME Densyl-b-Gal
EXPNO 1
PROCNO 1
F2 - Acquisition Parameters
Date_ 20170627
Time 16.06
INSTRUM spect
PROBHD 5 mm CPPBBO BB
PULPROG zg30
TD 65536
SOLVENT MeOD
NS 16
DS 2
SWH 8012.820 Hz
FIDRES 0.122266 Hz
AQ 4.0894465 sec
RG 118.73
DW 62.400 usec
DE 10.00 usec
TE 298.0 K
D1 1.00000000 sec
TD0 1
======== CHANNEL f1 ========
SFO1 400.1324710 MHz
NUC1 1H
P1 12.00 usec
PLW1 8.80000019 W
F2 - Processing parameters
SI 65536
SF 400.1300026 MHz
WDW EM
SSB 0
LB 0.30 Hz
GB 0
PC 1.00

Chapter 6 Pili-mediated Signaling Hypothesis and Validation.

6.1. Introduction

6.1.1. The attempt of using Pili as the vaccine target

Gram-negative bacterial surfaces have type IV pili, which can evoke the host immune response and are potential drug and vaccine targets.[263] Type IV pili are the assembly of pilin subunits, which generates a polymeric "machinery" that can mediate various cellular functions, including cell signaling, surface motility, microcolony, and biofilm formation, host-cell adhesion.[264-265] It has been reported that for many Gram-negative pathogens, disruption of pilus assembly can result in severely reduced virulence.[266-268] The Pseudomonas aeruginosa PAK pilin D-region is undergoing active investigation as a vaccine target because anti-D-region antibodies could potentially block the binding of a broad range of P. aeruginosa strains to the host-cell receptors.[269] However, despite high numbers of patients who may develop P. aeruginosa infections and the threat of antibiotic treatment failure due to bacterial resistance, there is surprisingly no P. aeruginosa vaccine currently available on the market, although many attempts have been made in the past, most of the published studies are preclinical, some describe results from phases I and II studies and only two vaccines have made it phase III studies in CF patients.[270-271]

6.1.2. Exploring bulky aliphatic chain of disaccharide derivatives for controlling bacterial multicellular activities

Based on the results from previous lab members in Luk's group, among different DSD, saturated farnesol disaccharide compound, like SFβM, has the highest anti-biofilm ability.[98-99] This observation leads us to explore even bulkier tail group to be attached on disaccharide, which might increase anti-biofilm ability even more. A well-defined binding pocket can bury the recognized ligands and exclude other molecules. The conformation of the binding pocket might match well for the bulky tail compounds. Furthermore, bulky tail DSD is relatively more difficult to assemble than non-bulky tail DSD, because bulky hydrophobic tail DSD is more difficult to satisfy the molecular *packing* requirements for forming a micelle than the non-bulky tail DSD. Since bulky tail DSD is hard to form a micelle, it is more likely to move around in a free molecule form. Hence, it has a higher chance to bind to the binding pocket (Figure 6.1).

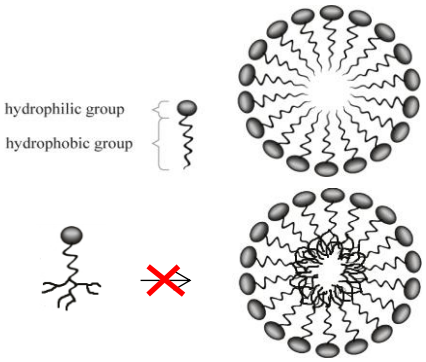

Figure 6.1 Representation of the hypothesis that bulky hydrophobic tail surfactant is more difficult to satisfy the molecular packing requirements for forming a micelle than the non-bulky tail surfactant.

Cholestanol is a neutral lipid that plays an essential role in the maintenance of the integrity of biologic membranes and serves as a precursor in the synthesis of many

endocrine mediators.[272] Recent clinical has demonstrated a possible linkage of cholestanol to prostatic cancer and benign prostatic hyperplasia.[273-275] Shinji and his coworker have found that chemically synthesized sugar-cholestanol compounds showed strong inhibiting activity against the proliferation of colorectal and gastric cancer cells.[276] In recent work, chemically synthesized sugar-cholestanols were demonstrated to possess potential multi-target anticancer activity against human esophageal cell lines because they induced apoptotic cell death of esophageal cancer cells.[277] Based on the past study led by Gauri and Nischal in Luk group, a bulky aliphatic chain of disaccharide derivatives, like SFβM, have the high anti-adhesion, and anti-biofilm formation and dispersion activity.[98, 149] We believe that bulky aliphatic chain that may cause higher potency than saturated farnesol at enabling disaccharide derivatives on controlling bacterial activity. We also speculate that inducing rigidity, multi-ring structures help limit conformation space, which might further increase the potency for disaccharide derivatives on controlling bacterial activity.

6.1.3. Covalent Ligation Strategy for Searching Pili Binding Sites

Covalent ligation has emerged as a valuable tool for the development of modified proteins and the study of binding activities since the techniques that allows covalent ligation have been developed over the last few decades.[278-280] The complementary use of both genetic and chemical methods has provided a large toolbox that allows us to immobilize, cross-link or tag proteins or even alter protein properties.[281] Covalent ligation is highly specific and appending various probes to these ligands is synthetically

straightforward and often does not reduce binding affinity for the protein targets since nature also uses a covalent modification of proteins to modulate their function which originated from millions of years of evolution, have adapted their structure for covalent binding to proteins.[282-283] The most straightforward method to covalently attach a small molecule to a protein sequence is to use a binding interaction. For example, Nolan and coworkers explored a fluorescein–SLF0 conjugate which was used to label several FKBP12(F36V) fusion proteins in NIH3T3 and COS-7.[284] Farinas and Verkman used antibody tags fused to localization signal sequences to target various hapten– fluorophore conjugates to specific subcellular compartments in live cells.[285] One approach is to engineer a mildly reactive functional group on the ligand molecule such that the ligand does not lose its binding activity to its receptor protein, and upon binding, the mildly reactive functional group will react covalently with a specific amino acid on the active binding site of the receptor. A few such mildly reactive functional groups are known to carry this binding enabled covalent conjugation. Chen and coworkers have surveyed a range of affinity probes for protein labeling.[286] Our initial design matches with their finding that epoxy has great potential for protein modification yield and efficiency.

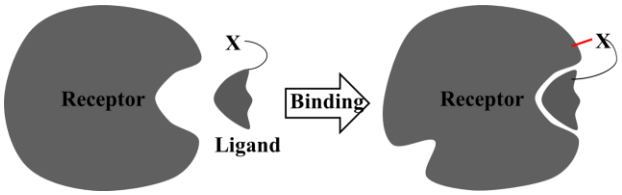

Figure 6.2 Schematic Representation Covalent Ligation upon Binding between Ligand and Receptor

6.1.4. Transmission electron microscopy of Surface Destructed Bacteria

The development of the transmission electron microscope (TEM), has increased the resolution limit over one thousand times greater than the conventional light microscope, which helped revolutionize many aspects of microbiology.[287] In general, a TEM system includes a fine electron beam, created by a high-voltage, electric current-heated tungsten filament, focused by magnetic lenses. The electron beam passes through an ultrathin plastic section, which impedes the beam in proportion to their respective degrees of electron density. The differential transmission of the electrons creates an image that is captured on a fluorescent screen. The first functional transmission electron microscope was developed in the early 1930s by Ruska who constructed an electron microscope with three magnetic lenses, condenser, objective, and projector.[288] After scientists fully developed new methods for preparation and new procedures for fixation, embedding, sectioning, and staining,[289-293] TEM has been used as a strong research tool in microbiology for high-resolution structural studies of bacteria and their appendages.[294] TEM technique also allowed significant advances in the understanding of infection

mechanisms, antibiotic tolerance, and biofilm geochemistry.[295-297] TEM has the advantage over scanning electron microscope (SEM), since a drastic preparation protocol of SEM sample preparation may eliminate appendages.[298] The TEM technique is widely used to study the morphology of bacterial cells and their surface structures, such as flagella and pili.[299-302]

6.1.5. Membrane Protein Study

Understanding of the properties of membranes is vital in many aspects of biology since membrane plays important roles in the functioning of cells such as organizing the shape of the organelles and the cells, the transport of ions, metabolites, and proteins across plasma membranes, and RNA transport across nuclear membrane.[303-305] Recently, the complete genome sequencing estimated the transmembrane proteins represent over 30 % of total proteins.[306-307] To understand how membrane proteins work and to generate drugs that target specific sites within the protein, it is important to purify the protein to fully characterize it. However, membrane proteins are difficult to purify for the following reasons. First, most membrane proteins are present at low levels; and second, they are embedded in the lipid bilayer and require detergents to become soluble in aqueous systems.[308] Large proteins whose molecular weight is above 250 kDa can be easily separated as their individual subunits using simple centrifugation, while very small proteins require special buffer systems in the second dimension to resolve proteins with apparent masses less than 8 kDa.[309] Hydrophobic proteins which include the key cell-surface proteins, many of which are assumed to play important roles in cell adhesion, cell

recognition, and cell differentiation require special systems such as extraction by using urea, CHAPS, DTT, and alkaline buffers or sucrose density gradient centrifugation.[309-312] Among them, alkaline extraction has gained widespread popularity as an easy and efficient method for selectively stripping extrinsic proteins off membranes without affecting the disposition of integral components.[312]

6.1.6. The aim of the chapter

In this chapter, we explored the effect of ChC3βM on these biological activities by *P. aeruginosa*. In addition, to search the hypothetical receptor to gain insight into the mechanism of ligand-receptor interactions, we also synthesized TEGβM and TGMEβM to test their effect on biological activities by *P. aeruginosa*. To study the potential interaction between our molecules and pili proteins, we designed and synthesized active agents containing a functional group that can react with an amine group, which can covalently and permanently attach to the receptor protein only when the physical ligand-receptor binding takes place. In addition, we also tested the effect of externally added pili on the swarming motility of P. aeruginosa to support the mechanistic study of the pili as the receptor (or one of the receptors) that will bind to rhamnolipids and our synthetic agents, and upon binding, causing the bacterial activities. Furthermore, to study the effect of our synthetic agents on the morphology of bacterial surfaces we have imaged bacterial surfaces using a transmission electron microscope. In addition, we studied the membrane protein composition using an alkaline buffer extraction method and then visualized by the SDS-PAGE gel.

6.2. Results and discussion

6.2.1. Cholestanol-sugar compound has activity at relatively low concentration but with low potency

Quantification of PAO1 biofilm was done by crystal violet (CV) dye-based assay after 24h of inoculation with and without maltose derivatives. We found that synthesized ChC3βM exhibited biofilm inhibition activity against *P. aeruginosa*. At 10~20 μM concentration, ChC3βM showed 60% biofilm inhibition. However, when the concentration is higher, the biofilm inhibition rate decreased to 30%. Surprisingly, when the concentration is reduced to nM level, ChC3βM still showed 20~30% biofilm inhibition (Fig. 6.3).

If we assume that an optical density (OD) reading of 1 corresponds to 10^9 bacteria per ml. This value is true for E. coli. Because *E. coli* and *P. aeruginosa* are similar in shape and dimension, we adopted this value for our estimation. Thus, as OD=1 corresponds to 10^9 bacteria/ml, there are $2*10^7$ bacteria in a well containing 200 μL solution when OD=0.1. After 24 h incubation, the OD is approximately 1, which corresponds to $2*10^8$ bacteria in 200 μL. For the ChC3βM molecules, there are $1.2*10^{14}$ molecules in 200 μL of a 1 μM-solution. So even the concentration is reduced to 1 nM, the molecule number, $1.2*10^{11}$, is still about 1000-fold higher than bacteria number ($2*10^8$). Thus, if we can reach IC50 at nM level, it would a significant improvement for anti-biofilm drug development.

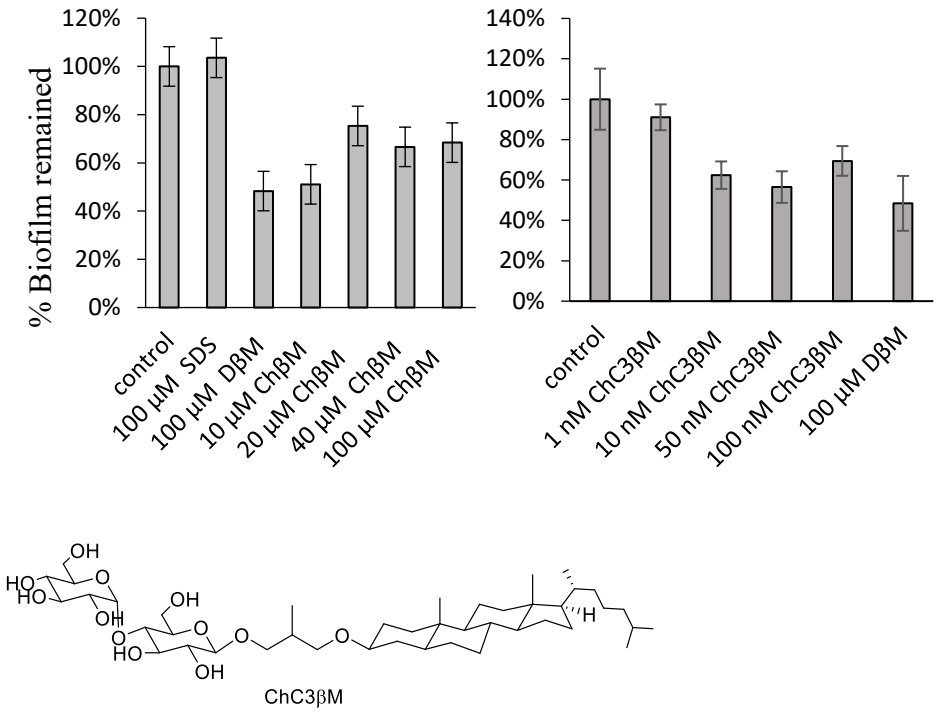

Figure 6.3 Inhibition of biofilm by ChC3βM at different concentrations on PAO1 measured by CV dye assay. The compound showed biofilm inhibition activity at relatively low concentration but with low potency.

6.2.2. Disaccharide oligo-ethylene glycol has an insignificant effect on bacteria

For synthesized DSD, TEGβM and TGMEβM, we tested their effect on swarming motilities of PAO1 and rhlA on agar plates. According to the result of swarming assay, TEGβM and TGMEβM have no effect on swarming motilities of both PAO1 and rhlA

(Figure 6.4 and Figure 6.5). The steric and electronic structure of the aliphatic tail is concluded to have great importance on the ability of these compounds to control bacterial activities. In addition, C6OC5-β–Cellobiose, and C3OC8-β–Cellobiose have an insignificant effect on the activities of P. aeruginosa (See chapter 3). Those results lead us to hypothesize that there is a ligand-receptor mechanism involved with these signaling molecules. The structure of the aliphatic side chain is important in the binding of these compounds to the receptor, explaining why the introduction of a single ether linkage obliterates the potency of our compounds since binding sites are often highly sensitive to the molecular details of its ligands.

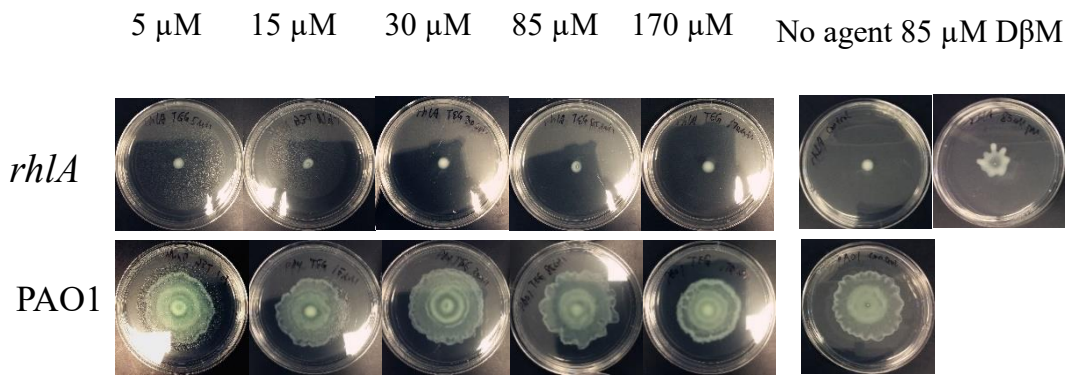

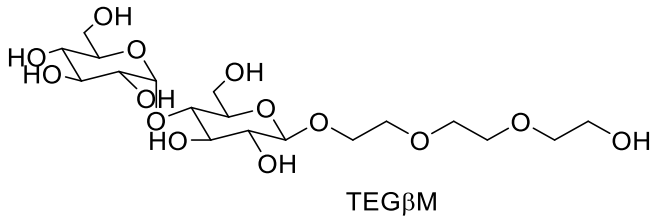

TEGβM

Figure 6.4 Images of swarming motilities of PAO1 and rhlA on agar plates containing different concentrations of TEGβM. The compound does not promote swarming of *rhlA* or promote tendril formation in PAO1.

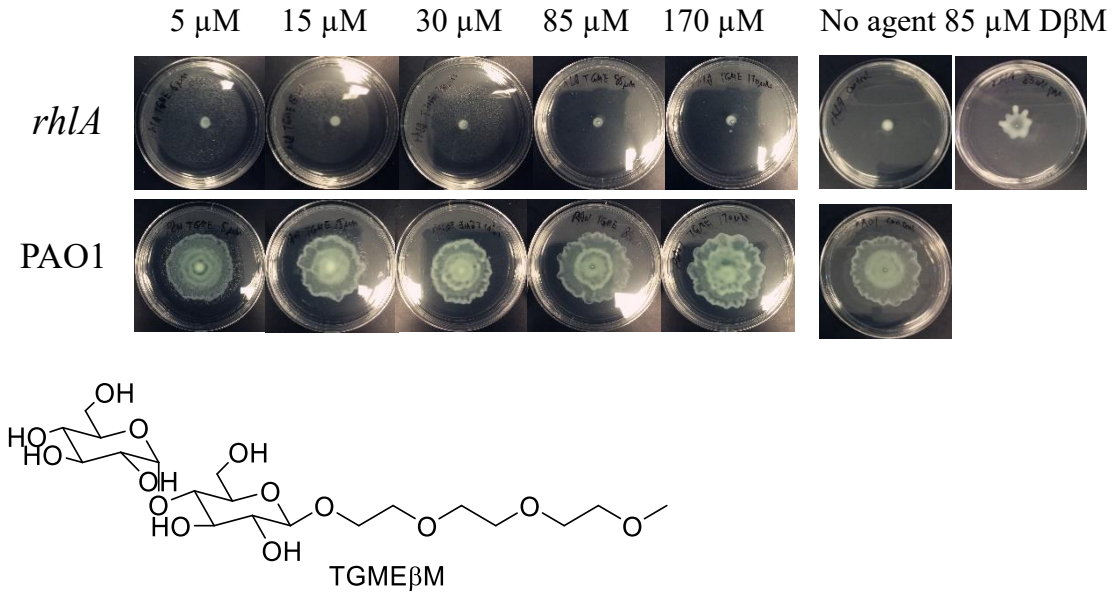

Figure 6.5 Images of swarming motilities of PAO1 and rhlA on agar plates containing different concentrations of TGMEβM. The compound does not promote swarming of *rhlA* or promote tendril formation in PAO1.

6.2.3. The specific covalent ligating agent can bind to pilin, but not other proteins

PA1244 is a wild-type clinically isolated strain of Pseudomonas aeruginosa, which is hyper-piliated.[313] P. aeruginosa strain 1244N3 is a mutant of PA1244 that is unable to produce pilin due to an inactivated rpoN gene.[314] When inserted with plasmid pPAC46, PA1244N3 could produce glycosylated pilin. Plasmid pPAC46 contains the strain 1244 pilA and pilO genes under the control of a tac promoter. We successfully purified a large amount of pili proteins using a P. aeruginosa PA1244N3/pPAC46 strain.

Based on the preliminary results of MALDI-MS experiment, we have confirmed that pili can be covalently modified by our agent available of covalent ligation, while other proteins, like BSA and lysozyme, were not covalently modified by the same agent. (Figure 6.6) In addition, among SF(EG)n-epoxy (n=3, 4, 5), SF(EG)4-epoxy has the highest yield for covalent ligation with Pili protein (Figure 6.7).

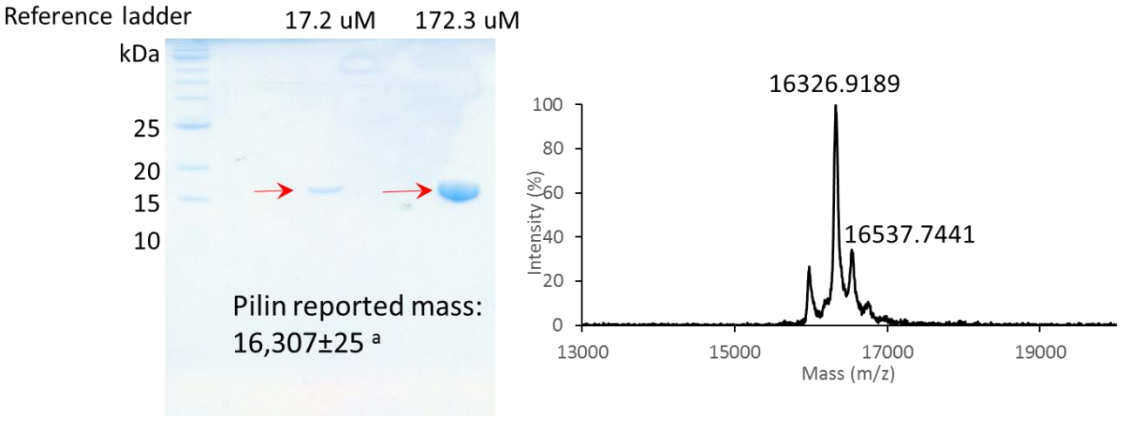

Figure 6.6 SDS-PAGE gel image of purified pili protein and the MALDI-MS results. Expressed Pili Protein from PA1244N3(pPAC46) Matches the Reported Mass of 16,307±25 (ref: James G. Smedley, Erica Jewell, Jennifer Roguskie, Joseph Horzempa, Andrew Syboldt, Donna Beer Stolz, and Peter Castric,* Influence of pilin glycosylation on Pseudomonas aeruginosa 1244 pilus function[J]. Infection and immunity, 2005, 73(12): 7922-7931.)

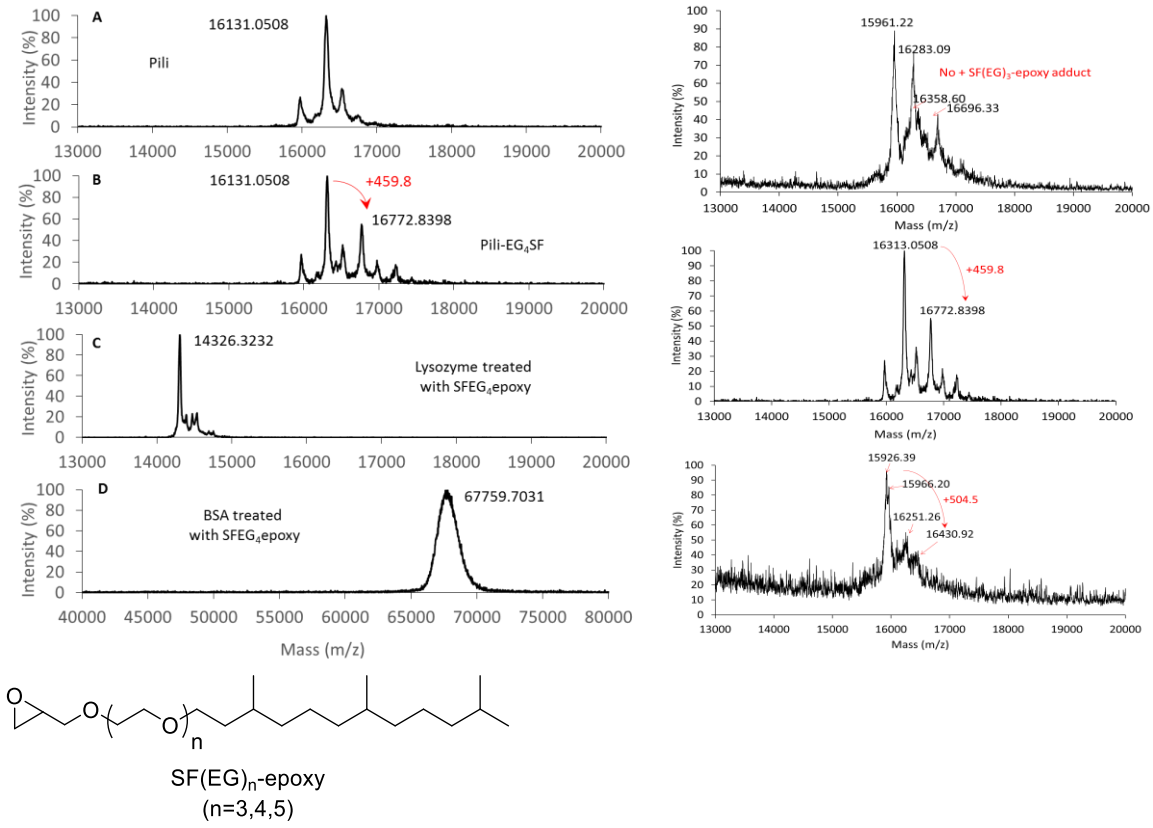

Figure 6.7 MALDI-MS Result Indicates Pili is Covalently Modified by SF(EG)4-epoxy (MW=459) in PBS (pH 8.2). Among SF(EG)n-epoxy (n=3, 4, 5), SF(EG)4-epoxy has the highest yield for covalent ligation with Pili protein.

6.2.4. Supporting evidence of ligand-receptor binding between DSD and pili protein by swarming assay

To support that pili could be the receptor that binds to rhamnolipids, and our synthetic agents, we conducted an experiment where pili protein was applied on the surface of the soft agar gel used for observing the swarming motility of wild-type P.

aeruginosa, PAO1. If swarming is initiated by ligand-receptor binding between rhamnolipids (or our molecules) and pili protein on the bacterium surfaces, then the presence of pili proteins on the agar gel (outside the bacteria) will sequester the natural molecules (rhamnolipids) secreted by the bacteria, and thus inhibit the bacteria's swarming motility. If bacterial swarming is a physical effect, the presence of pili protein will unlikely not reduce the swarming motilities. Controls of other proteins (BSA) were used to observe any nonspecific effect due to the presence of proteins on the gel. The results indicate that pili protein inhibits swarming motility of PAO1, while BSA does not inhibit the swarming motility of PAO1. (See Figure 6.8)

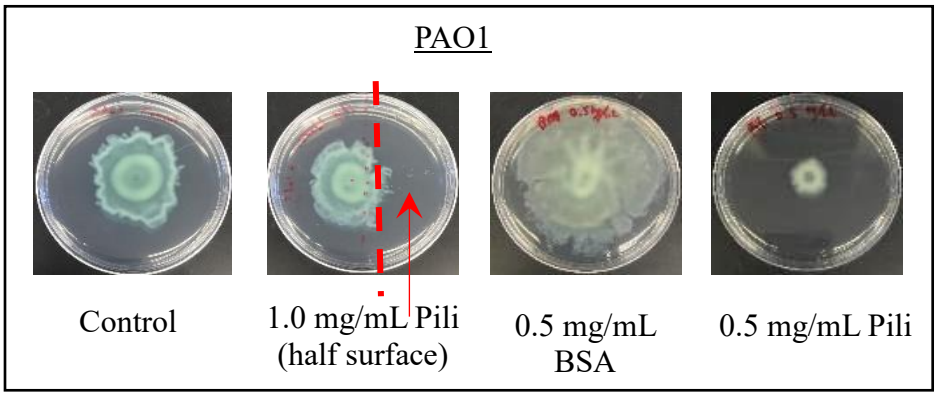

Figure 6.8 Pili protein inhibits swarming motility of PAO1 while BSA does not. After the agar was cooled to r. t. and solidified, 1 mL of the corresponding solution was evenly spread on the surface and dried for 1 h. Then 3 µL of the PAO1 culture (OD = 0.4 - 0.6) was spotted on the center. Pictures were taken after the plates were put in 37 ℃ incubators for 12 h and then 22℃ for another 12 h.

Previous lab member Gauri in Luk lab has examined the effect of a class of synthetic analogs of rhamnolipids at controlling (promoting and inhibiting) the swarming motility of a non-rhamnolipid-producing strain – *rhlA* – of *P. aeruginosa*. When the swarming gel was supplemented with 85 uM DβM, the non-swarming PA strain *rhlA* will swarm on the agar gel plate. Here we tested the effect of added pili protein on Swarming Motility of rhlA in the Presence of 85 µM DβM. The results showed that the externally added pili protein significantly reduced the swarm area of rhlA in the presence of 85 µM DβM (Figure 6.9). In contrast, externally added BSA protein did not show any significant inhibition on the swarming motility of rhlA in the presence of 85 µM DβM (Figure 6.9). Those results support our proposed mechanism of ligand-receptor binding between rhamnolipids (or our molecules) and pili protein.

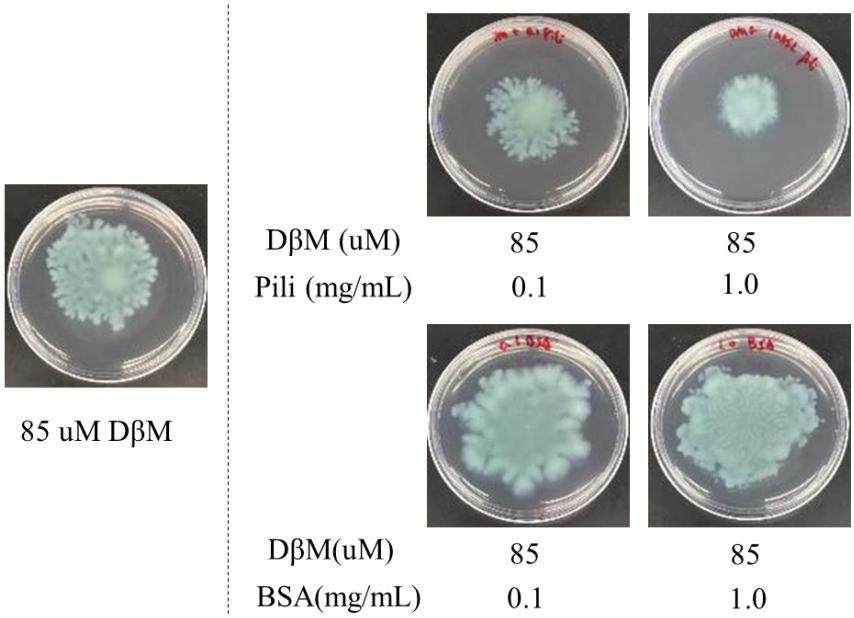

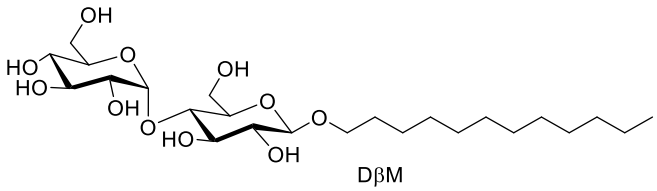

Figure 6.9 Pili protein inhibits swarming motility of rhlA in the presence of 85 μM DβM while BSA does not. Predetermined concentrations of agents were added when preparing the swarming agar plates. After the agar was cooled to r. t. and solidified, 1 mL of the corresponding solution was evenly spread on the surface and dried for 1 h. Then 3 μL of the rhlA culture (OD = 0.4 - 0.6) was spotted on the center. Pictures were taken after the plates were put in 37 ℃ incubators for 12 h and then 22℃ for another 12 h.

However, there is another possibility that the externally added pili can act as a pili inhibitor which can inhibit swarming motility by pili-pili interaction. To rule out such an alternative mechanism of inhibition effect, we proposed another experiment to confirm whether ligand-Pili interaction or pili-pili interaction is dominating in the inhibition effect

of externally added pili protein (Figure 6.10). Predetermined concentrations of SFβM were added in the swarming agar plates. Then 1 mL of 1.0 mg/mL of pili solutions were spread on the agar plate and dried for 1 h. Controls of other proteins (BSA) were used to observe any nonspecific effect due to the presence of proteins on the gel. PAO1 bacteria were inoculated on the agar plates followed by 12 h incubation under 37 C and then another 12 h under r.t. At 15 μM, SFβM inhibits swarming motility of PAO1. However, under the same condition plus the externally added pili, the swarming inhibition effect of SFβM was neutralized and the swarming pattern showed up again. Although the swarming area of the re-promoted PAO1 is not as pronounced as the no agent control of PAO1 swarming, the swarming re-promotion effect is still evident (Figure 6.11). The results confirmed that pili protein inhibits swarming motility of PAO1 by ligand-Pili interaction instead of pili-pili interaction.

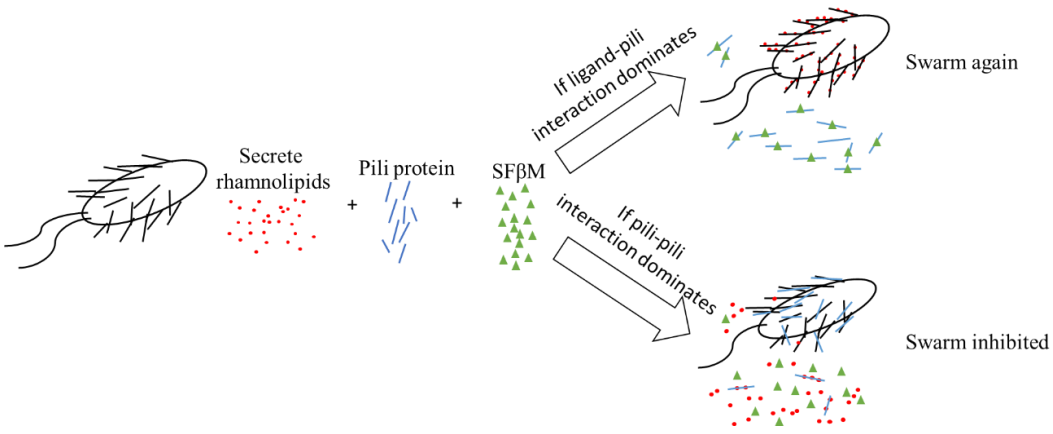

Figure 6.10 Mechanism hypothesis: ligand-pili interaction or pili-pili interaction?

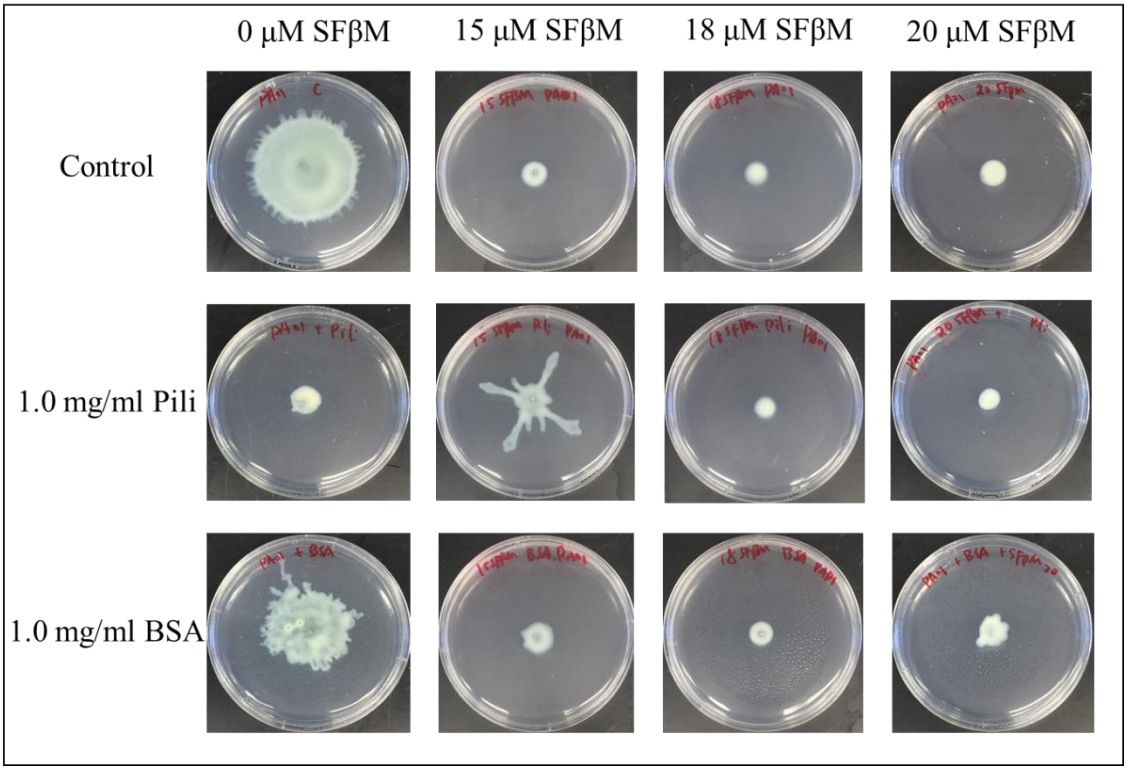

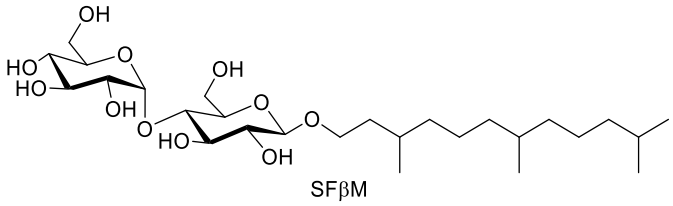

Figure 6.11 Add swarm-inhibitor (SFβM) with pili in gel cause re-promotion of swarming motility of PAO1. Predetermined concentrations of agents were added when preparing the swarming agar plates. After the agar was cooled to r. t. and solidified, 1 mL of the corresponding solution was evenly spread on the surface and dried for 1 h. Then 3 μL of the PAO1 culture (OD = 0.4 - 0.6) was spotted on the center. Pictures were taken after the plates were put in 37 ℃ incubators for 12 h and then 22℃ for another 12 h.

6.2.5. Bulky DSDs Like SRβM and rhamnolipids Modulate PA14 Swarming while other potent agents that can control PAO1 and rhlA swarming have weak effects

PA14 always exhibit tendril formation when they swarm on a soft agar gel, whereas PAO1 swarm evenly outward radially, resulting in a circle pattern. There are currently no reported chemicals that control the swarming of PA14. However, we did find that natural product rhamnolipids inhibit the swarming of PA14 starting at around 60 μM (Figure 6.12). Surprisingly, the potent agents that can modulate the swarming motilities of PAO1, like DβM and BPDeβM, did not show any control of the swarming motility of PA14. However, SRβM modulated the swarming motility of PA14. For this molecule, swarming motility of PA14 was inhibited at relatively low concentration, 10 μM, but reactivated again as the concentration was increased. The swarming motility reached a second maximum at 60 μM and then started to decrease again. A second inhibition was observed at 170 μM. These results indicate that while pili structures vary between different mutants and different strains. Such an oscillation effect of chemicals on biological activities was described by Eberhard[150] and coworkers for quorum sensing molecules for Photobacterium fischeri. This oscillation in swarming pattern activity due to the difference in chemical concentration is symbolic of an oscillatory response by the bacteria to the chemical stimuli.[151]

Oscillations are ubiquitous in nature and occur in physical, chemical and biological systems that are periodically repeating variations of some measure or quantity about a central value or between two or more different states.[151] At the cellular level, an oscillating system consists of three parts: the oscillator, which generates the oscillatory

output; the input pathways that regulates the oscillator in response to external or internal signals; and output pathways that couple information about the state of the oscillator to downstream targets in order to generate the oscillatory output.[151] There are two types of bacterial oscillators: Temporal oscillators which incorporate the periodic accumulation or activity of a protein to drive temporal cycles such as the cell and circadian cycles,[315] and spatial oscillator which incorporate the periodic variation in the localization of a protein to define subcellular positions such as the site of cell division[316-317] and the localization of DNA.[318] However, the mechanisms of how these oscillators are designed and function are still unclear.

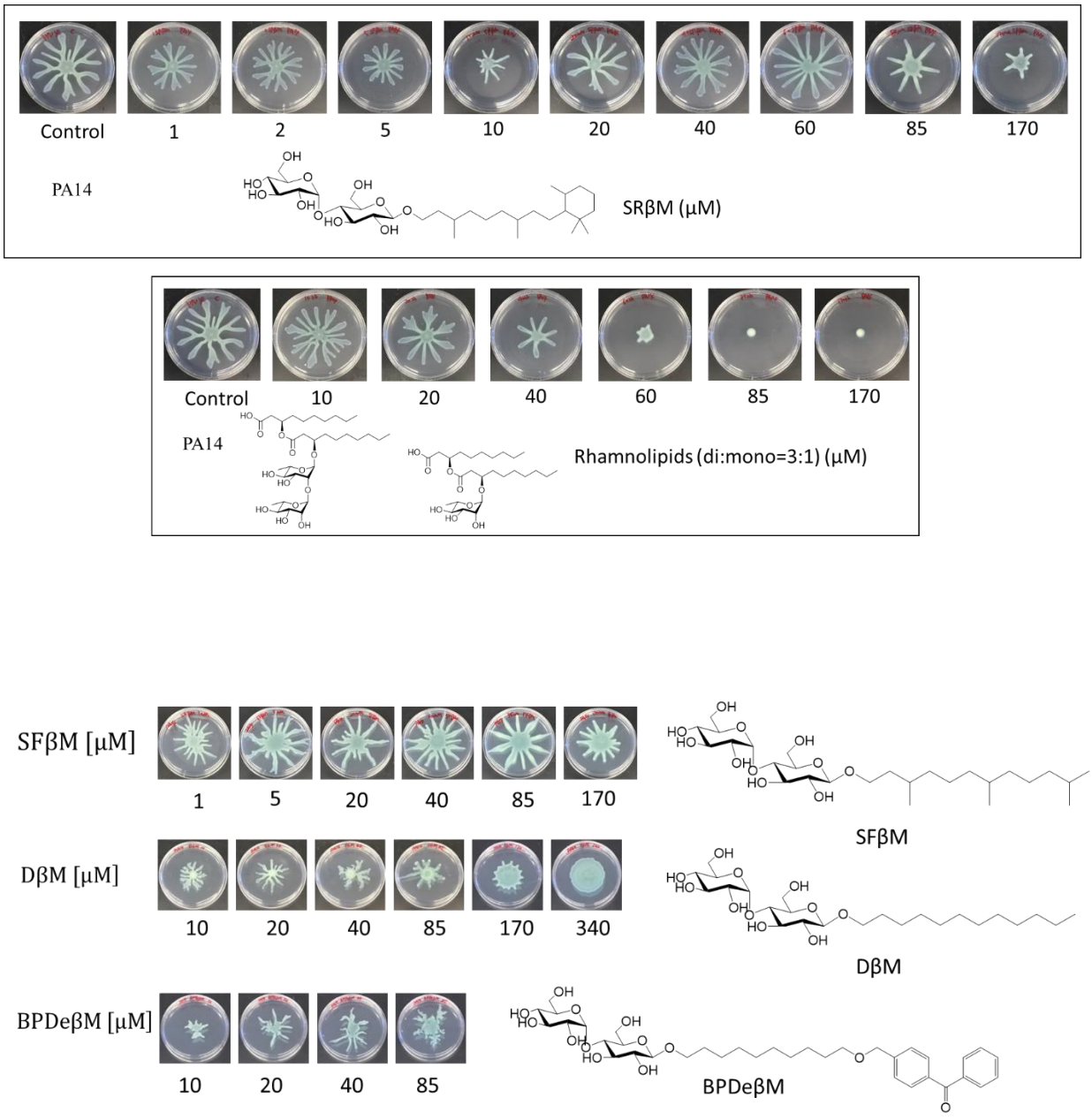

Figure 6.12 Images of P. aeruginosa PA14 strain inoculated on the M8 swarm agar (0.5 % agar) plates with and without 85 μM of DSDS. Pictures were taken 24 h after the inoculation of bacteria on the plates.

6.2.6. Synthetic agents can destruct the bacterial surface of PAO1 and PA14

To observe the effects of our molecules on the bacterial surfaces by using TEM, we cultured PAO1 with 20 μM of SFβM, and PA14 with 85 μM of SRβM and 170 μM of rhamnolipids (a mixture of 3:1 di- and mono-rhamnolipids) in LB media to an optical density about 0.4 to 0.5. We choose these polar hydrocarbons and concentrations because these conditions inhibited the swarming motilities of PAO1 and PA14. The bacterial culture solutions were directly placed on the copper grids for TEM, rinsed and then stained with uranyl acetate. Figure 6.13 showed that intact bacteria of PAO1 and PA14 with some appendages readily visible for PAO1. In presence of 20 μM SFβM for PAO1, a drastic effect was observed on the surfaces of the bacteria. Debris was released from the bacteria, with some debris still attached to the bacteria. Similar phenomena were observed for PA14. With 85 μM SRβM, some debris was seen; and with 170 μM rhamnolipids, a considerable amount of debris was seen at the two polar ends of the PA14 strain. We note that at these conditions, the bacteria were not dead, but their pathogenic activities were grossly altered.

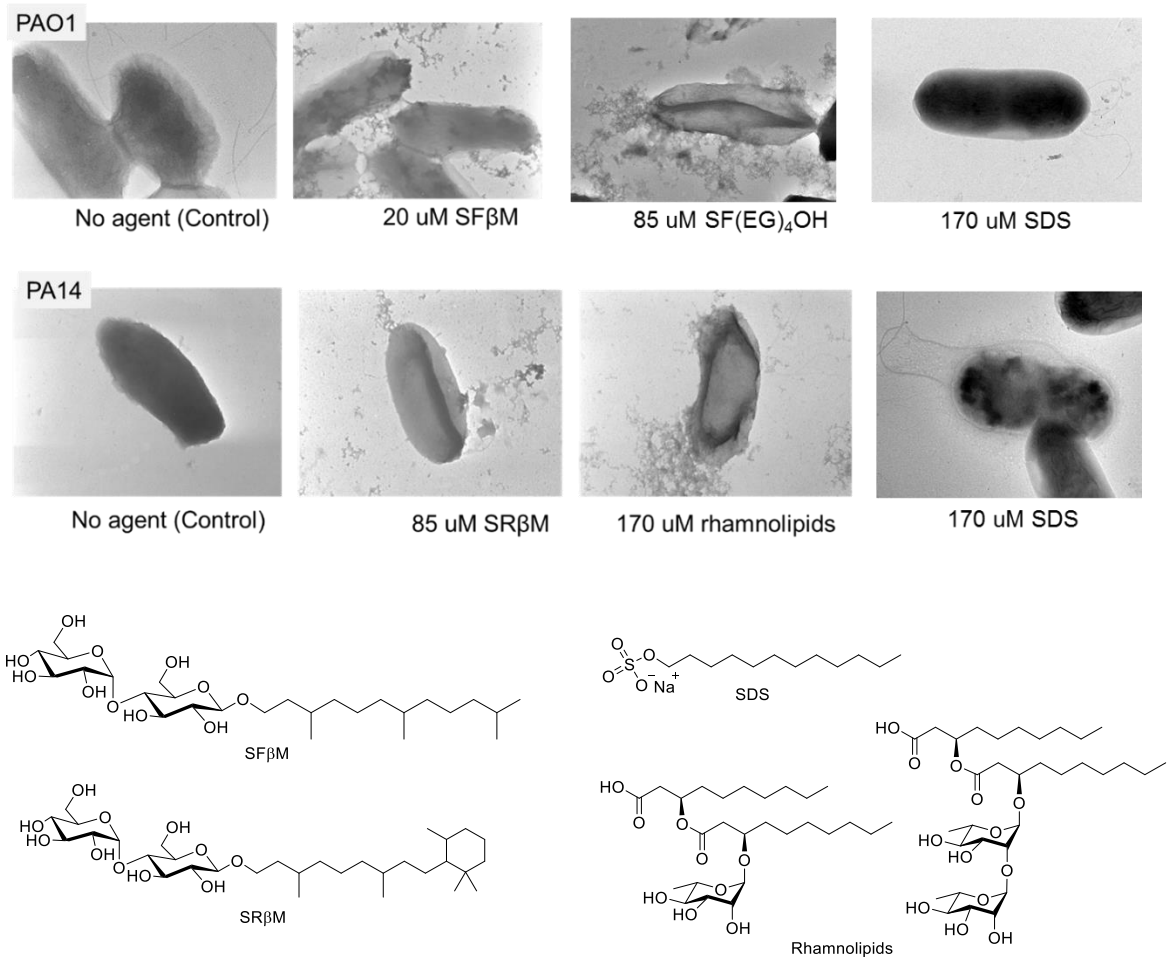

Figure 6.13 Transmission electron microscopy of PAO1, PA14, and Mucoid PA strain with and without treatment with their active agents in 4-h culture (OD=0.5). The samples were stained with 0.5% (wt/vol) uranyl acetate.

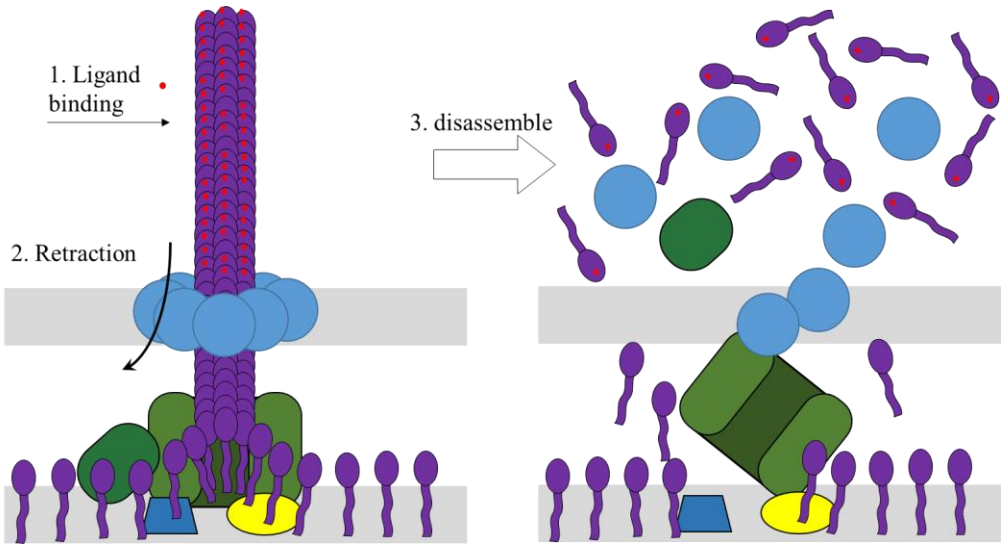

Figure 6.14 Hypothesis of Ligand Binding Causing Pili Assembly and Engine in Membrane to Disassemble

In addition, to support the observation that our molecules disrupted the bacterial surfaces using TEM, we also examined the membrane protein composition using an alkaline buffer extraction method and then visualized by the SDS-PAGE gel. The result showed alkaline buffer extracted a sample of PAO1 treated with 45 μM SFβM had a significant decrease in protein expression at ~15 kDa than no agent control sample which indicates the disrupted protein is most likely to be pili protein since the molecular weight of pili protein is ~15-16 kDa region (Figure 6.15). As for the cause of the increase in the protein expression at ~34 kDa and ~55 kDa range is not clear. However, the possible surface protein that has a molecular weight of 34~55 kDa can be Putative pili assembly chaperone, Type IV pili twitching motility protein PilT, Phosphate-binding protein PstS or Pili assembly chaperone (see Table 6.1). These results support the hypothesis that our

molecules target the pili assemblies of the bacteria, and because of the control of bioactivities, induced a wide range of bacterial signaling events.

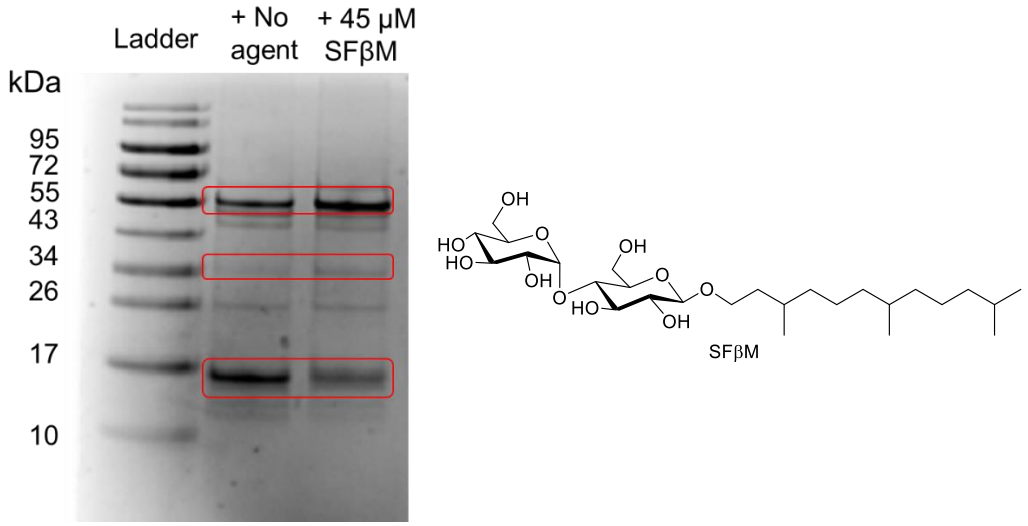

Figure 6.15 SDS-PAGE gel image of alkaline buffer extracted bacterial surface protein composition. Samples were prepared from PAO1 bacteria cultures grown with and without agents and purified by alkaline buffer extraction.

Table 6.1 List of 9 possible surface proteins at 30-50 kDa range in *Pseudomonas aeruginosa* species (source; http://www.uniprot.org/uniprot/)

Protein names	Gene names	Mass
Putative pili assembly chaperone	PAMH19_0553	32,356
Phosphate-binding protein PstS	pstS	34,474
Twitching mobility protein (Twitching motility protein PilT) (Type IV pili twitching motility protein PilT)	pilT_2 pilT_3...	38,021
Alkaline phosphatase L (L-AP) (EC 3.1.3.1) (Low molecular weight phosphatase) (Protein DING)	phoA2 dinG	40,663
Type IV pili twitching motility protein PilT	AO896_17845	42,537
Type IV pili twitching motility protein PilT	AO964_26870	42,560
Pili assembly chaperone	BKN49_11215	46,978
Pili assembly chaperone	AO964_18715	49,769
Pili assembly chaperone	AO896_02295	49,983

6.2.7. The synthetic agent can inhibit twitching motilities of P. aeruginosa in solution

In order to have direct observation of the effect of our molecules on the motilities of bacteria at the level of an individual bacterium, we observe the motility of individual bacterium of P. aeruginosa that express fluorescent proteins PAO1-EGFP under a confocal microscope. We discovered that without the presence of our agents, in every second, there is about 7% of bacteria will either move in or out of the focal plane of the fluorescence due to swimming or twitching motilities. However, in the presence of SFβM

(10 µM, 6.1 µg/mL) and over the duration of 1 second, the entire bacteria population is not motile (Figure 6.16). This inhibition of bacterial solution-based twitching and swimming motility further supports that our agents bind to pili, and perhaps also flagella, and inhibit the dynamic of these appendages (extension and retraction for pili, and rotation for flagella).

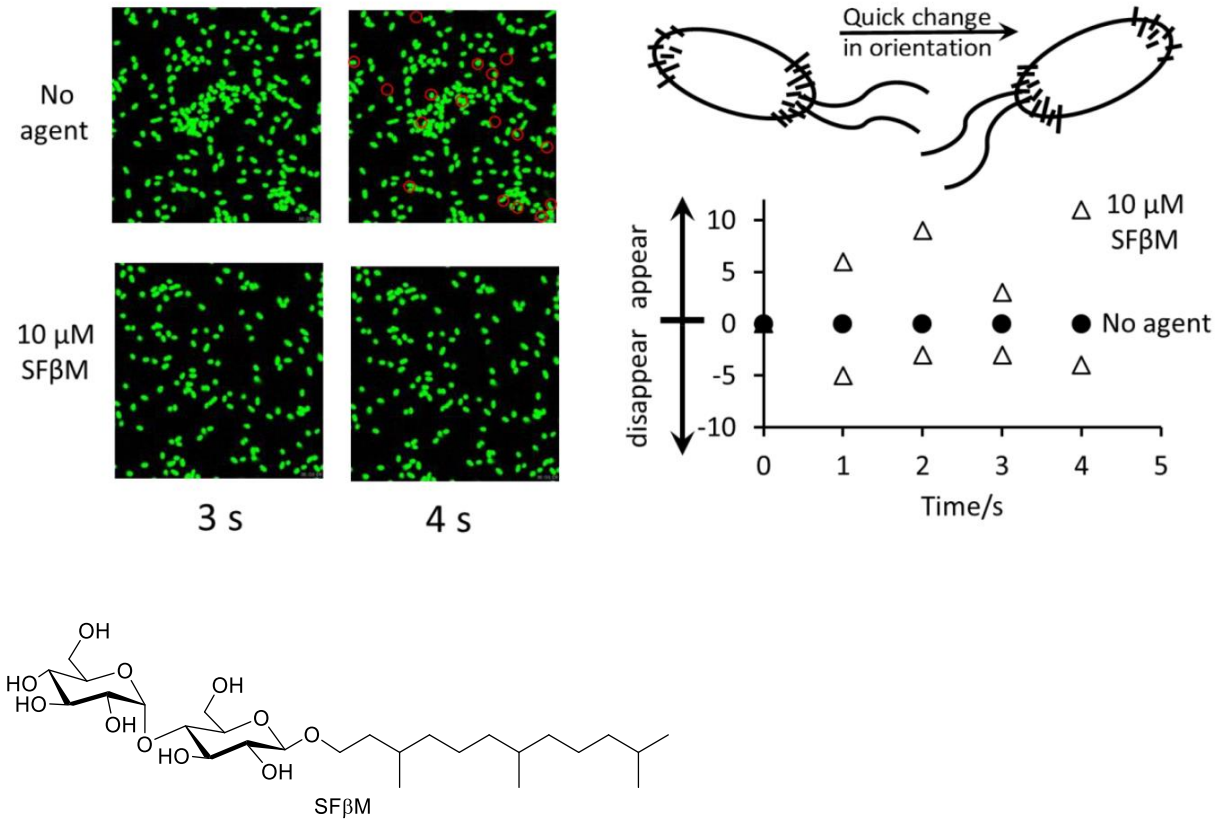

Figure 6.16 One-second time lapse of confocal fluorescence of PAO1-EGFP (OD= 0.3 to 0.4) with and without 10 µM SFβM in the media. The images at the 3rd and 4th second were shown; the red circles indicate changes: bacteria that move bacteria into (appear) and out of (disappear) the focal plane due to the twitching motion. The numbers of "appear" and "disappear" bacteria are plotted for the bacterial sample without the agent (empty triangles) and sample with 10 µM SFβM (filled circle).

6.2.8. Attempts at making a fluorescently tagged pilin ligand

In order to obtain more direct evidence of ligand-receptor binding between our molecules and pili appendage on bacterial surfaces, we designed ligand molecules with covalently attached fluorescent tags, and explore their use of direct observation of fluorescently active surface appendages on bacteria, and of fluorescent polarization.

In the past, such direct observations were obtained by modifying the amino acid of pilin monomers with cysteine amino acid, which will covalent attach to a fluorescent label. This approach enables a "live" observation of the dynamics and biology of the pili appendages. Another approach involves direct binding of a fluorescently active antibody to pilin of the pili appendage and makes a direct observation on the microscope.

Because our indirect evidence suggests that our molecules bind to pili assembly on bacterial surfaces, we explore the following design of fluorescently labeled ligand molecules. Synthesis schemes for two fluorescent tagged DSDs, Pyrenyl-C_{11}-βM (**18**) and UmDeβM (**24**) were shown in Scheme 6.1. However, the separation of Pyrenyl-C_{11}-βM encountered the major difficulty that most of the compound was stuck with the resin in the last deacylation step. According to the ^{1}H NMR spectra of the Pyrenyl-C_{11}-βM (**18**), most of the -OH peaks were disappeared from the final product. UmDeβM (**24**) has been successfully synthesized and the swarming assay was tested for this molecule. Unfortunately, UmDeβM did not show any modulating effect on the swarming motility of both PAO1 and rhlA strains of *Pseudomonas aeruginosa* (Figure 6.17).

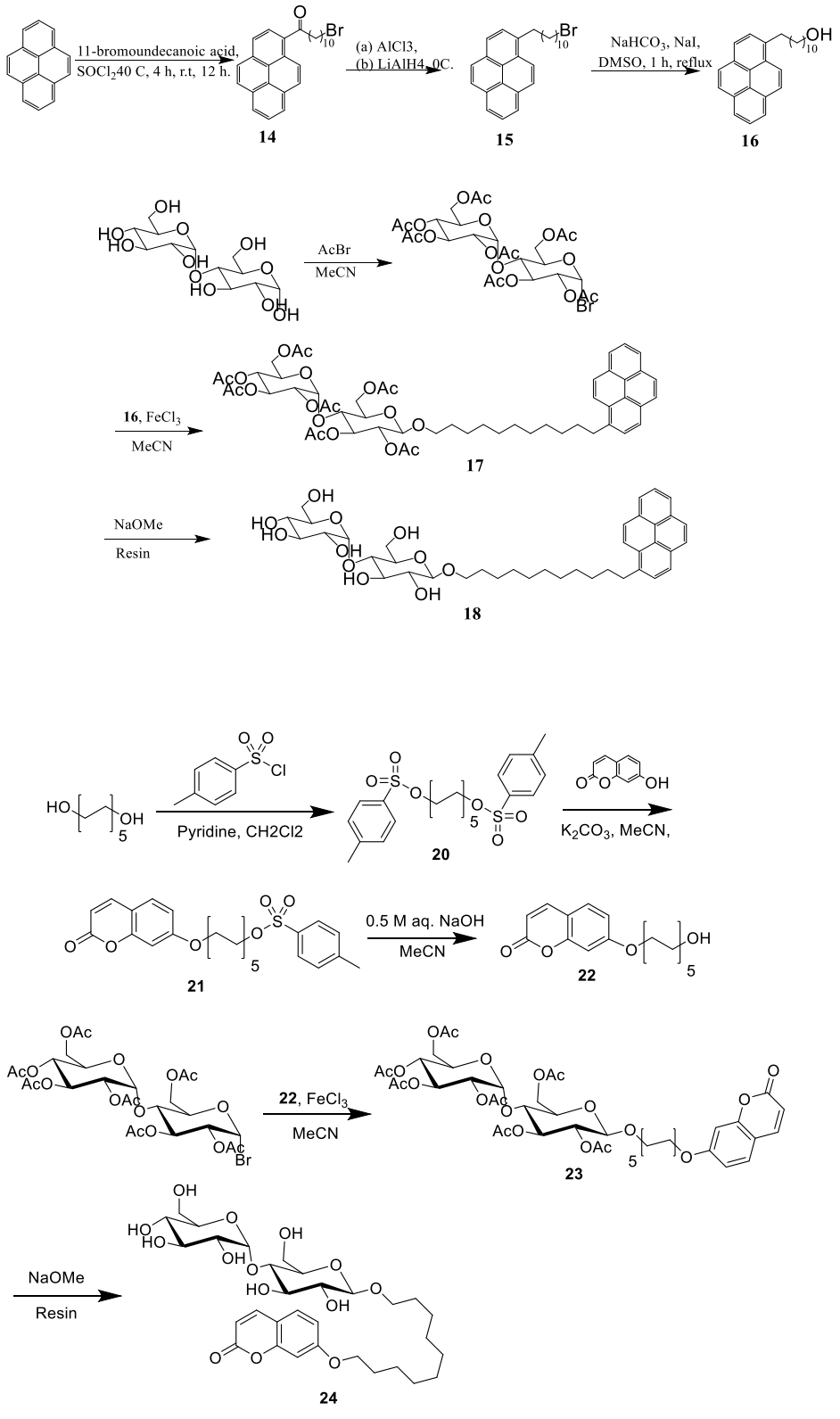

Scheme 6.1. Synthesis schemes for fluorescent-tagged DSDs

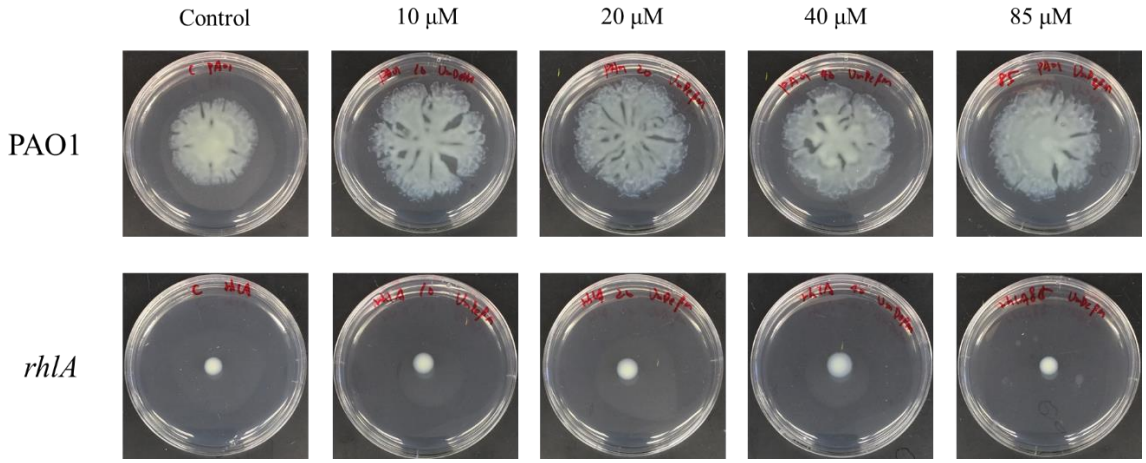

Figure 6.17 Images of swarming motilities of PAO1 and rhlA on agar plates containing different concentrations of UmDeβM. The compound does not promote swarming of *rhlA* or promote tendril formation in PAO1.

6.3. Conclusions

Molecules capable of covalent ligation were designed and synthesized, and their multiple biological effects on P. aeruginosa bacteria were tested. The results show that one of our synthetic molecules SF(EG)4-epoxy is nontoxic and no biofilm Inhibition effect but capable of controlling bacterial swarming of PAO1. Pili protein was successfully purified by using P. aeruginosa bacteria strain that can overproduce pili proteins. To study the potential interaction between our synthetic molecules and pilin proteins, mixing experiment were done by using the pili protein and several other proteins (Lysozyme and BSA) with the synthetic molecule SF(EG)4-epoxy, which is capable of covalent ligation. The results indicate that SF(EG)4-epoxy can covalently attach to the receptor protein ONLY when the ligand-receptor take place. Swarming motility of P. aeruginosa was tested with protein solutions (Pili protein and BSA) spread

on agar gel. Pili protein inhibits swarming of PAO1 and also inhibits swarming of rhlA in the presence of 85 μM DβM (this condition was supposed to promote swarming of rhlA). While BSA does not inhibit swarming of PAO1, and rhlA in the presence of 85 μM DβM. The results further indicate that pili are the receptor (or one of the receptors) that will bind to rhamnolipids and our synthetic agents, and upon binding, causing the bacterial activities. We also imaged damaged pili on bacterial surfaces using TEM. These results indicate that pili appendage is the target of SFβM.

6.4. Materials and Methods

6.4.1. Stock solutions of generic surfactants and maltose derivatives

A stock solution of all the agents was prepared in autoclaved water, sterilized by filtering through a 0.2 μm 16 syringe filter, and stored at -20 °C in sealed vials. An appropriate amount of sterile water was added to controls in all assays to eliminate the solvent effect.

6.4.2. Swarming assay

Swarm agar plates were made using M8 medium supplemented with 0.2% glucose, 0.5% casamino acid, 1 mM MgSO4 and solidified with 0.5 % Bacto agar. Bacterial culture with OD600 between 0.4 to 0.6 was inoculated as 3 μl aliquots. Swarm agar plates were incubated at 37 °C for 12 h and then incubated for an additional 12 h at

rt. For each set of the experiment all the swarm plates were poured from the same batch of agar and allowed to dry for 1 h before inoculation of bacteria.

6.4.3. Crystal violet dye-based biofilm inhibition assay

Inhibitory effect of all the maltose hydrocarbons on *P. aeruginosa* biofilm formation was determined by crystal violet dye-based biofilm inhibition assays. An overnight culture of wild-type *P. aeruginosa* (PAO1) was subcultured to an OD600 of 0.01 into the 95/5 M9+/LB medium (The places where only LB medium has been used is indicated in the figure caption). 200 µL of the subculture was aliquoted into the wells of 96 well polystyrene microtiter plate when it reached the OD600 of 0.1. Predetermined concentrations of the test compounds were then added to the respective wells containing subculture. Sample plates were wrapped in GLAD Press n' Seal® followed by incubation under stationary conditions for 24 h at 37 °C. After incubation, the media was discarded, and the plates were washed with water and dried for 1 h at 37 °C. The sample plates were stained with 200 µL of 0.1% aqueous solution of crystal violet (CV) and followed by incubation at ambient temperature for 20 min. The CV stain was then discarded, and the plates were washed with water. The remaining biofilm adhered stain was re-solubilized with 200 µL of 30 % acetic acid. After the stain was dissolved (15 minutes), 100 µL of the solubilized CV was transferred from each well into the corresponding wells of a new polystyrene microtiter dish. Biofilm inhibition was quantified by measuring the OD600 of each well in which a negative control lane wherein no biofilm was formed served as a background and was subtracted out. The percent inhibition was calculated by the

comparison of the OD600 for biofilm grown in the absence of compound (control) versus biofilm grown in the presence of compound under identical conditions.

6.4.4. Solution-based bacteria twitching assay.

An overnight culture of bacteria was subcultured to an OD_{600} of 0.01 into the LB medium containing predetermined concentrations of the test compounds. 10 µL of the subculture was transferred onto a glass slide when it reached the OD_{600} of 0.3-0.4. Twitching motilities were visualized using a Zeiss LSM 710 Confocal Laser Scanning Microscope (Carl Zeiss, Jena, Germany). A 488 nm laser line was used to visualize twitching motilities of PAO1-EGFP strain.

6.4.5. Ligand-Pili receptor conjugation reactions.

300 µL of $SF(EG)_4$-epoxy (50 equiv., 1.6 mg) from a stock solution of 11.5 mM in deionized water (18.2 MΩ.cm) was added to a 1 mL solution containing 1 mg/mL lysozyme (14307 Da) or pili protein (15648 Da) or *bovine serum albumin* protein (~66000 Da) in PBS pH 8.2 (reaction buffer). The reaction mixture was shaken at 250 rpm for 24 h at ambient temperature in a shaker-incubator. These samples were sent out for MALDI-MS at Rutgers University (http://cabm-ms.cabm.rutgers.edu/) to characterize the potential covalent modification of the proteins.

6.4.6. Transmission electron microscopy.

A small number of bacteria from the edge or the center of the colony on the swarming plate was picked using a sterile toothpick and dispersed in PBS buffer by gently touching the toothpick to the liquid for 5 s. A droplet of the bacterial suspension was placed onto a copper TEM grid. After waiting for 15 min, the remaining solution was wicked away using a piece of filter paper. The samples were then rinsed with 2 ml of 2 mM HEPES buffer (pH 6.8) followed by a rinse with 1 ml of MilliQ water. The samples were then stained by placing a drop of 0.5% (wt/vol) uranyl acetate onto the samples and removing the excess by wicking with filter paper after 3 to 5 min. TEM pictures were imaged using a 120 kV field FEI T12 Spirit TEM Equipped with a LaB6 filament, single and double tilt holder, an SIS Megaview III CCD camera, and a STEM dark field and bright field detector, along with analysis and imaging software.

6.4.7. Alkaline buffer extraction.

Set up overnight cultures for *P. aeruginosa* from frozen stocks. Conditions: 10 ml LB broth in 50 ml Falcon tube at 37 °C shaking at 200 rpm. Next day, set up fresh cultures from the overnight cultures in new LB broth using a 1:100 ratio dilution, and grow at 37 °C shaking at 200 rpm until the exponential growth phase (0.4 - 0.6 OD_{600}). Centrifuge the culture at 3,000 x *g* for 5 min at 4 °C. Discard the supernatant and gently resuspend the pellet in 10 ml of PBS. Centrifuge at 3,000 x *g* for 10 min at 4 °C, discard supernatant and resuspend pellet in 3 ml 20 mM Tris pH 7.4. Centrifuge at 3,000 x *g* for 10 min at 4 °C , discard the supernatant and resuspend the pellet in 0.1 M Na_2CO_3. Keep on ice for 30 min.

Use 1 mL syringe pass cells suspension through a >22-gauge needle 10 times (or other gentle cells lyse methods). Centrifuge 3,000 x *g* for 20 min at 4 °C to remove unlysed cells. Resuspend the pellet in 0.1 M Na_2CO_3, re-extract as above and pool the supernatants. Combine the supernatants and neutralize by adding HCl drop by drop. The supernatant is transferred to a fresh tube and centrifuged at 30,000 *x g* for 40 minutes at 4 °C. Take off the supernatant and the left pellets are ready for running SDS-PAGE.

6.4.8. Synthetic procedures

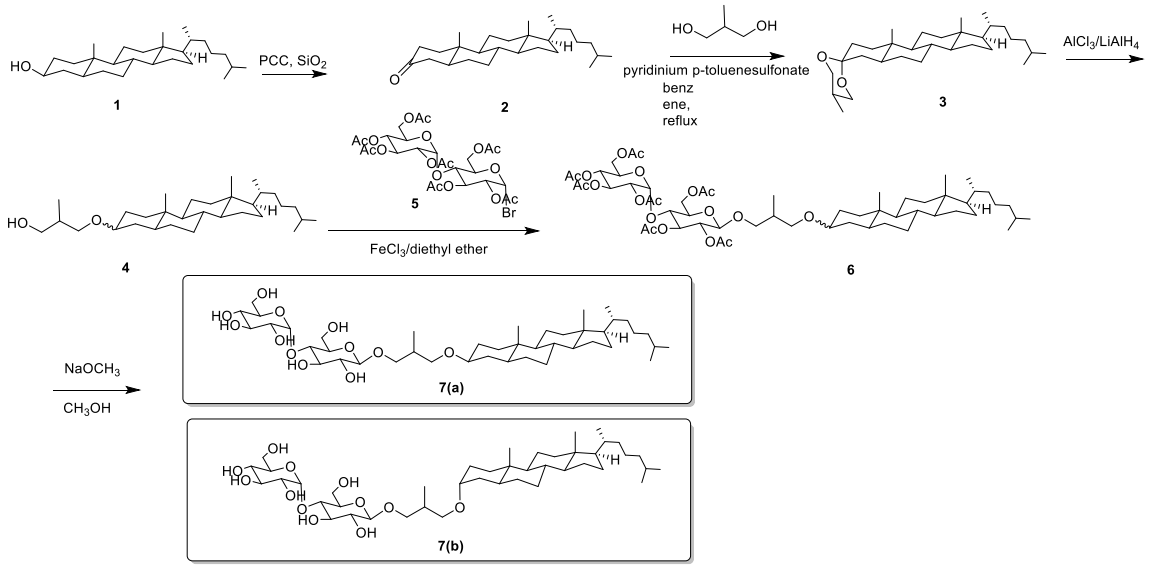

Scheme 6.2. Synthesis scheme for ChC3βM

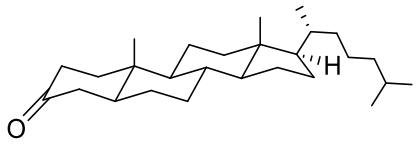

β-cholestanone (2)

Lit. ref. for characterization data: *Org. Lett.* **2013**, *15*, 992-995.

To a suspension of pyridinium chlorochromate (2.21 g, 10.29 mmol) and silica gel (2.21 g) in 10 mL dichloromethane, β-cholestanol (1) (2.0 g, 5.14 mmol) dissolved in 10 mL dichloromethane was added. The resulting black/orange solution was stirred at room temperature for 4 h. The reaction mixture was then filtered through a bed of silica gel. The residue was washed with dichloromethane. The filtrate was concentrated to afford β-cholestanone (1.91 g, 96%) as a white solid. White powder; TLC: Rf = 0.36 (10% ethyl acetate/90% hexanes); ^{1}H NMR ($CDCl_3$, 400 MHz): δ 2.37-2.30 (m, 3H), 2.26-0.85 (m, 40H), 0.68 (s, 3H).

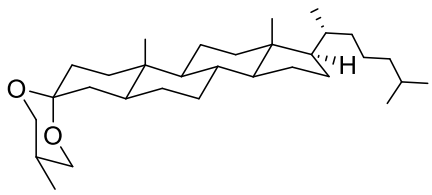

(3)

A solution of **2** (1.5 g, 3.88 mmol) and 1, 3-butanediol (1.0 g, 11.1 mmol) was refluxed overnight under toluene (25 ml) in the presence of pyridinium p-toluenesulfonate (50 mg). Molecular sieve (type 3A) was added to remove water formed during the reaction. Concentration and silica gel chromatography (elution with 3% ethyl acetate in hexane) afforded **3** (1.5 g, 3.31 mmol, 85%) as a white solid. TLC: Rf = 0.60 (5% ethyl acetate/95%

hexanes); ^{1}H NMR ($CDCl_3$, 400 MHz): δ 3.82-3.74(m, 2H), 3.61(m, 1H), 3.50(m, 1H), 2.26-0.85 (m, 47H), 0.68 (s, 3H).

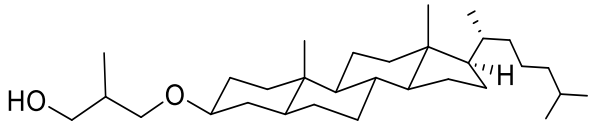

(4a)

Add **3** (1.2 g, 2.6 mmol) in 8 mL anhydrous ether to a previously prepared solution of LiAIH(0.30 g, 7.5 mmol) and A1C1$_3$ (0.35 g, 2.5 mmol) in 8 mL anhydrous ether. The reduction was allowed to proceed at room temperature for 12 h. Then 15% aqueous KOH was added dropwise to decompose the complex and form a colorless precipitate which was readily removed by filtration. Concentration and silica gel chromatography (elution with 3% ethyl acetate in hexane) afforded **4a** (0.62 g, 1.3 mmol, 50%). TLC: Rf = 0.70 (15% ethyl acetate/85% hexanes); ^{1}H NMR ($CDCl_3$, 400 MHz): δ 3.50-3.70(m, 4H), 3.38-3.30(m, 1H), 2.26-0.55 (m, 50H).

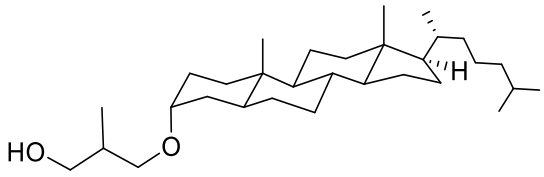

(4b)

Add **3** (1.2 g, 2.6 mmol) in 8 mL anhydrous ether to a previously prepared solution of LiAIH(0.30 g, 7.5 mmol) and A1C1$_3$ (0.35 g, 2.5 mmol) in 8 mL anhydrous

ether. The reduction was allowed to proceed at room temperature for 12 h. Then 15% aqueous KOH was added dropwise to decompose the complex and form a colorless precipitate which was readily removed by filtration. Concentration and silica gel chromatography (elution with 3% ethyl acetate in hexane) afforded **4b** (0.30 g, 1.3 mmol, 24%). TLC: Rf = 0.65 (15% ethyl acetate/85% hexanes); ^{1}H NMR ($CDCl_3$, 400 MHz): δ 3.64-3.58(m, 3H), 3.45-3.37(m, 1H), 3.24-3.15(m, 1H), 2.26-0.50 (m, 50H).

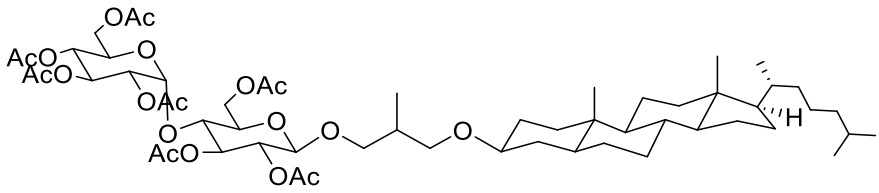

(6a)

Maltose (0.2 g, 0.5mmol), AcBr (~0.6mL, 8 mmol), and AcOH (5mL) were added to an oven dried round bottom flask and stirred at room temperature (25 ^{0}C) for ~ 1 h. The reaction mixture was concentrated in vacuo at 35 ^{0}C and then co-evaporated three times with PhMe (2×10 mL, anhydrous). After removal of solvent, the flask was further heated in vacuo at 50 ^{0}C for 15min to give a foamy solid, aceto-bromo sugar. The crude aceto-bromo sugars were immediately used in next step without any further purification.

Crude aceto-bromo sugars were the dissolved in MeCN (10mL) and 4a (1.0mmol, 2 equivalents) were added along with acid 2-equivalents of a Lewis catalyst $FeCl_3$. The reaction mixture was stirred vigorously for about ~45-60 mins at rt. After stirring at rt, aq KBr (10%, 25mL) and then PhMe (60mL) were added under stirring. The organic phase

was washed twice with aq KBr (10%, 2×25mL), once with aq $NaHCO_3$ (5%, 25mL) and twice with H_2O (2×25mL). The crude product was then purified by column chromatography using gradient elution (100 % hexane to 35 % ethyl acetate in hexane). Concentration and silica gel chromatography afforded **6a** (0. 22g, 0.2 mmol, 20%) TLC: Rf = 0.45 (35% ethyl acetate/65% hexanes); ^{1}H NMR ($CDCl_3$, 400 MHz): δ 5.43-5.33 (m, 2H), 5.29-5.26 (m, 1H), 5.09-5.02(m, 1H), 4.89-4.79 (m, 2H), 4.52 – 4.45 (m, 2H), 4.29 – 4.21 (m, 2H), 4.06-3.93 (m, 3H), 3.88 – 3.68 (m, 2H), 3.52 – 3.35 (m, 2H), 3.30-3.15(m, 2H) 2.15 – 2.01 (s, 7 × 3 H), 2.26-0.50 (m, 50H).

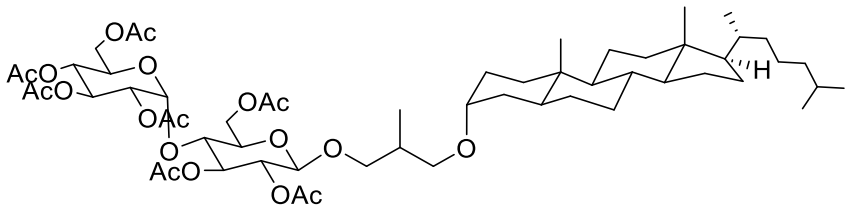

(6b)

Maltose (0.2 g, 0.5mmol), AcBr (~0.6mL, 8 mmol), and AcOH (5mL) were added to an oven dried round bottom flask and stirred at room temperature (25 ^{0}C) for ~ 1 h. The reaction mixture was concentrated *in vacuo* at 35 ^{0}C and then co-evaporated three times with PhMe (2×10 mL, anhydrous). After removal of solvent, the flask was further heated in vacuo at 50 ^{0}C for 15min to give a foamy solid, aceto-bromo sugar. The crude aceto-bromo sugars were immediately used in next step without any further purification.

Crude aceto-bromo sugars were the dissolved in MeCN (10mL) and 4a (1.0mmol, 2 equivalents) were added along with acid 2-equivalents of a Lewis catalyst $FeCl_3$. The reaction mixture was stirred vigorously for about ~45-60 mins at rt. After stirring at rt, aq KBr (10%, 25mL) and then PhMe (60mL) were added under stirring. The organic phase was washed twice with aq KBr (10%, 2×25mL), once with aq $NaHCO_3$ (5%, 25mL) and twice with H_2O (2×25mL). The crude product was then purified by column chromatography using gradient elution (100 % hexane to 35 % ethyl acetate in hexane). Concentration and silica gel chromatography afforded **6b** (0. 37g, 0.35 mmol, 32%) TLC: Rf = 0.40 (35% ethyl acetate/65% hexanes); ^{1}H NMR ($CDCl_3$, 400 MHz): δ 5.43-5.33 (m, 2H), 5.29-5.26 (m, 1H), 5.09-5.02(m, 1H), 4.89-4.79 (m, 2H), 4.52 – 4.45 (m, 2H), 4.29 – 4.21 (m, 2H), 4.06-3.93 (m, 3H), 3.88 – 3.68 (m, 2H), 3.55 – 3.32 (m, 3H), 3.32-3.17(m, 1H) 2.15 – 2.01 (s, 7 × 3 H), 2.26-0.50 (m, 50H).

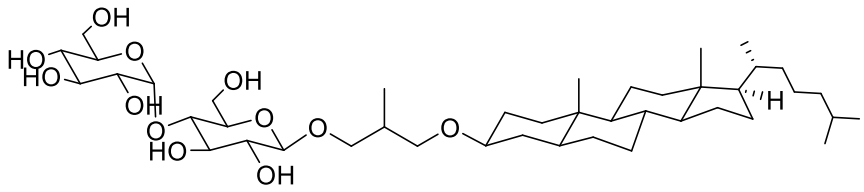

(7a)

Zemplén deacetylation. For all acetylated sugar-derivatized hydrocarbon molecules, the deprotection of alcoholic groups was achieved by Zemplén deacetylation using MeONa/MeOH (10 mM solution) conditions followed by neutralization (pH ~6.5) over H+ amberlite resins. The resins were filtered off and products dried under high vacuum overnight. White solid, Yield: **7a** (0.07 g, 88 %), ^{1}H-NMR (CD_3OD, 400 MHz):

δ 5.17 (d, *J* = 3.6 Hz, 1H), 4.28 (d, *J* = 7.8 Hz, 1H), 3.92-3.78 (m, 4 H), 3.72 – 3.15 (m, 15H, overlapping with CD_3OD), 2.26-0.50 (m, 50H).

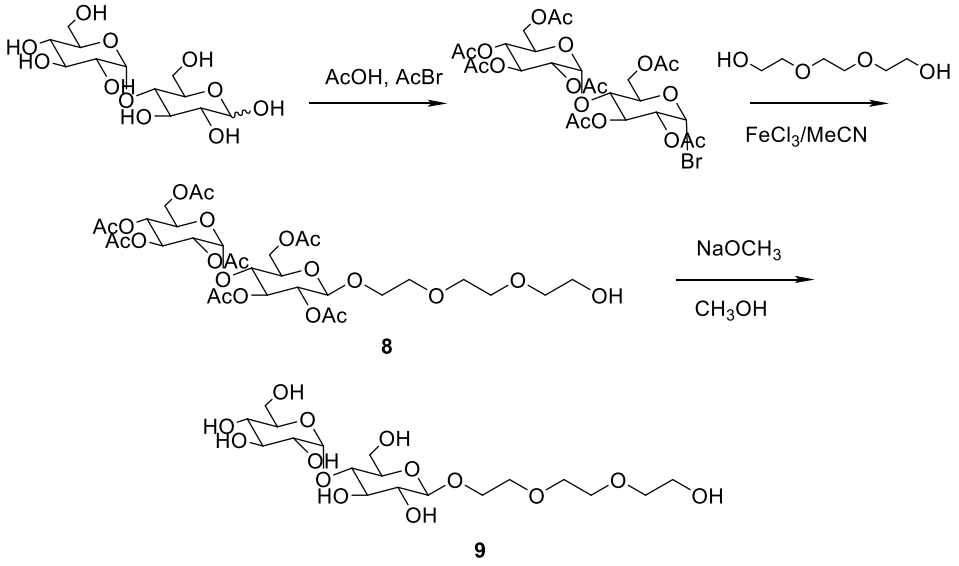

Scheme 6.3. Synthesis scheme for TEGβM

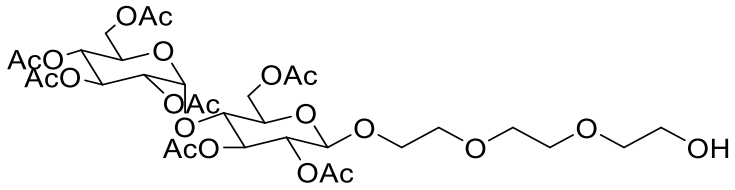

(8)

Maltose (1.0 g, 2.8mmol), AcBr (~3.6mL, 44.4mmol), and AcOH (19mL) were added to an oven dried round bottom flask and stirred at room temperature (25 ^{0}C) for ~

1 h. The reaction mixture was concentrated *in vacuo* at 35 ^{0}C and then co-evaporated three times with PhMe (2×10 mL, anhydrous). After removal of solvent, the flask was further heated in vacuo at 50 ^{0}C for 15min to give a foamy solid, aceto-bromo sugar. The crude aceto-bromo sugars were immediately used in next step without any further purification.

Crude aceto-bromo sugars were then dissolved in MeCN (10mL) and TEG (5.6mmol, 2 equivalents) were added along with acid 2-equivalents of a Lewis catalyst $FeCl_3$. The reaction mixture was stirred vigorously for about ~45-60 mins at rt. After stirring at rt, aq KBr (10%, 25mL) and then PhMe (60mL) were added under stirring. The organic phase was washed twice with aq KBr (10%, 2×25mL), once with aq $NaHCO_3$ (5%, 25mL) and twice with H2O (2×25mL). The crude product was then purified by column chromatography using gradient elution (100 % hexane to 50 % ethyl acetate in hexane). Concentration and silica gel chromatography afforded **8** (0.6 g, 0.8 mmol, 29%) TLC: Rf = 0.55 (50% ethyl acetate/50% hexanes); ^{1}H NMR ($CDCl_3$, 400 MHz): δ 5.62-5.55(m, 1H), 5.38-5.30(m, 2H), 5.08-4.95(m, 1H), 4.86-4.80(m, 1H), 4.70-4.65(m, 1H), 4.52-4.45(m, 1H), 4.30-4.17(m, 3H), 4.12-3.98(m, 3H), 3.93-3.88(m, 1H), 2.15 – 2.01 (s, 7 × 3 H).

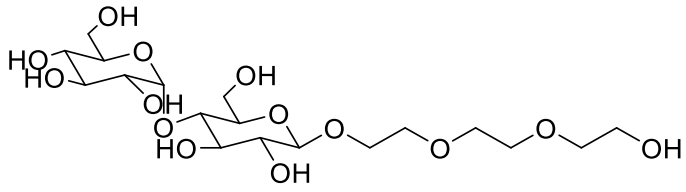

(9)

Zemplén deacetylation. For all acetylated sugar-derivatized hydrocarbon molecules, the deprotection of alcoholic groups was achieved by Zemplén deacetylation using MeONa/MeOH (10 mM solution) conditions followed by neutralization (pH ~6.5) over H+ amberlite resins. The resins were filtered off and products dried under high vacuum overnight. White solid. Yield: **9** (0.35 g, 85 %), ^{1}H NMR ($CDCl_3$, 400 MHz): δ 5.20-5.16 (m, 1H), 4.26-4.21 (m, 1H), 3.97-3.88 (m, 1H), 3.82-3.40 (m, 17H), 3.38-3.27(m, 2H),3.22-3.12 (m, 4H).

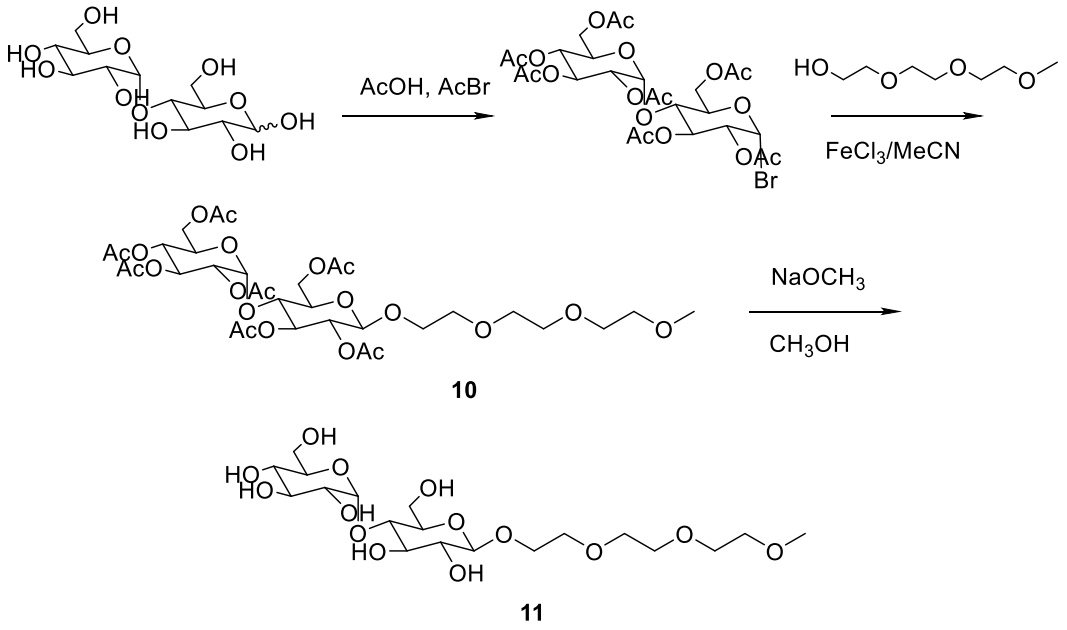

Scheme 6.4. Synthesis scheme for TGMEβM

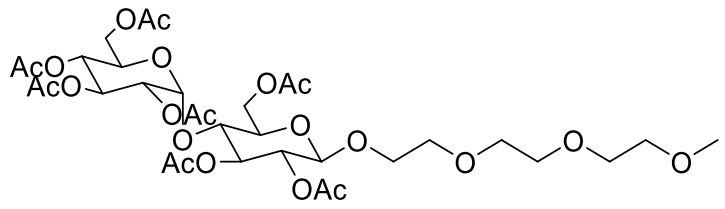

(10)

Maltose (1.0 g, 2.8mmol), AcBr (~3.6mL, 44.4mmol), and AcOH (19mL) were added to an oven dried round bottom flask and stirred at room temperature (25 ^{0}C) for ~ 1 h. The reaction mixture was concentrated *in vacuo* at 35 ^{0}C and then co-evaporated three times with PhMe (2×10 mL, anhydrous). After removal of solvent, the flask was further heated in vacuo at 50 ^{0}C for 15min to give a foamy solid, aceto-bromo sugar. The crude aceto-bromo sugars were immediately used in next step without any further purification.

Crude aceto-bromo sugars were the dissolved in MeCN (10mL) and TGME (5.6mmol, 2 equivalents) were added along with acid 2-equivalents of a Lewis catalyst $FeCl_3$. The reaction mixture was stirred vigorously for about ~45-60 mins at rt. After stirring at rt, aq KBr (10%, 25mL) and then PhMe (60mL) were added under stirring. The organic phase was washed twice with aq KBr (10%, 2×25mL), once with aq $NaHCO_3$ (5%, 25mL) and twice with H_2O (2×25mL). The crude product was then purified by column chromatography using gradient elution (100 % hexane to 50 % ethyl acetate in hexane). Concentration and silica gel chromatography afforded **10** (0.6 g, 0.8 mmol, 29%) TLC: Rf = 0.55 (50% ethyl acetate/50% hexanes); ^{1}H NMR ($CDCl_3$, 400 MHz): δ 5.62-5.40(m, 2H), 5.38-5.22(m, 1H), 5.08-4.95(m, 1H), 4.90-4.78(m, 2H), 4.65-4.60(m,

1H), 4.52-4.45(m, 1H), 4.30-4.17(m, 2H), 3.93-3.85(m, 5H), 3.76-3.52(m, 11H), 3.38 (s, 3H), 2.15 – 2.01 (s, 7 × 3 H).

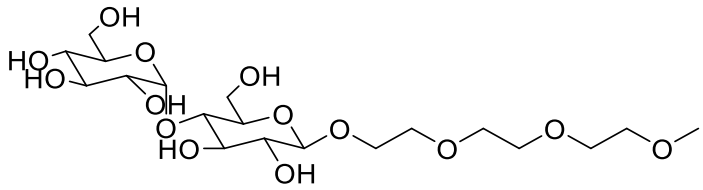

(11)

Zemplén deacetylation. For all acetylated sugar-derivatized hydrocarbon molecules, the deprotection of alcoholic groups was achieved by Zemplén deacetylation using MeONa/MeOH (10 mM solution) conditions followed by neutralization (pH ~6.5) over H+ amberlite resins. The resins were filtered off and products dried under high vacuum overnight. ^{1}H-NMR (CD_3OD, 400 MHz): δ 5.20-5.16 (m, 1H), 4.26-4.21 (m, 1H), 3.97-3.88 (m, 1H), 3.82-3.40 (m, 20H), 3.38 (s, 3H),3.36-3.24 (m, 3H).

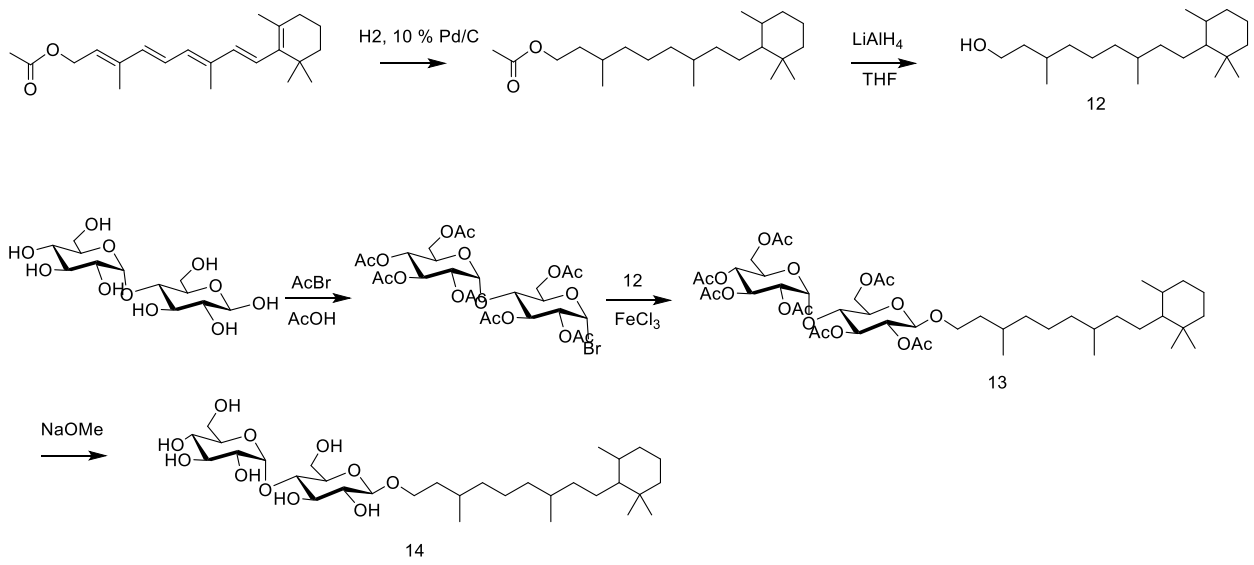

Scheme 6.5. Synthesis scheme for SRβM

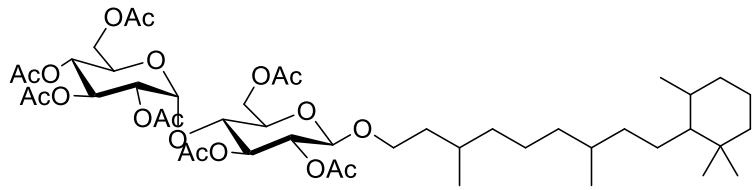

(14)

Add 1 equivalent of retinol acetate and 10 equivalents of 10% Pd/C in EtOAc. Hydrogenation is proceeded under *125 psi* hydrogen. The reaction was filtered over celite and washed with EtOAc to remove any excess product in the celite. Slowly add 1 equiv. LAH to a solution of saturated retinol acetate in THF(0.2M) at 0ºC. Allow to warm to room temperature and stir for 16h. The reaction was filtered over celite and the filtrate was concentrated to dryness without further purifications.

To an oven dried round bottom flask, disaccharide (maltose, cellobiose) (1.0 g, 2.8mmol), AcBr (~3.6mL, 44.4mmol), and AcOH (19mL) were added and stirred at

room temperature (25 ^{0}C) for ~ 1 h. The reaction mixture was concentrated *in vacuo* at 35 ^{0}C and then co-evaporated three times with PhMe (2×10 mL, anhydrous). After removal of solvent, the flask was further heated in vacuo at 50 ^{0}C for 15min to give a foamy solid, aceto-bromo sugar. The crude aceto-bromo sugars were immediately used in next step without any further purification. The crude aceto-bromo sugars were then dissolved in MeCN (10mL) and saturated retinol (5.6mmol, 2 equivalents) were added along with two equivalents of $FeCl_3$.The reaction mixture was stirred vigorously for about ~45-60 mins at rt. After stirring at rt, aq KBr (10%, 25mL) and then PhMe (60mL) were added under stirring. The organic phase was washed twice with aq KBr (10%, 2×25mL), once with aq $NaHCO_3$ (5%, 25mL) and twice with H_2O (2×25mL). The crude product was then purified by column chromatography using gradient elution (100 % hexane to 35 % ethyl acetate in hexane). Concentration and silica gel chromatography afforded **14** (0. 37g, 0.35 mmol, 32%) TLC: Rf = 0.40 (35% ethyl acetate/65% hexanes); ^{1}H NMR ($CDCl_3$, 400 MHz): δ 5.43-5.33 (m, 2H), 5.29-5.26 (m, 1H), 5.09-5.02(m, 1H), 4.89-4.79 (m, 2H), 4.52–4.45 (m, 2H), 4.29–4.21 (m, 2H), 4.06-3.93 (m, 3H), 3.88–3.68 (m, 2H), 3.55 – 3.32 (m, 3H), 3.32-3.17(m, 1H) 2.15-2.01 (s, 7 × 3 H), 1.52-0.83 (m, 37H aliphatic chain).

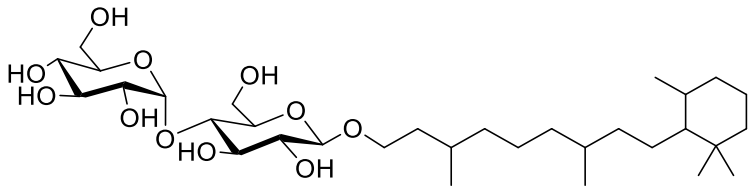

(15)

The deprotection of acetyl groups was achieved by Zemplén deacetylation using MeONa/MeOH (10 mM solution) conditions followed by neutralization (pH ~6.5) over H+ amberlite resins. The resins were filtered off and products dried under high vacuum overnight. 1H-NMR (CD_3OD, 400 MHz): δ 5.17 (br, s, 1H), 4.27 (d, J = 9 Hz, 1H), 3.95-3.92 (m, 4H), 3.88-3.43 (m, 6H, overlap with CD3OD peak), 3.27-3.20 (m, 4H), 1.60-0.88 (m, 37H aliphatic chain).

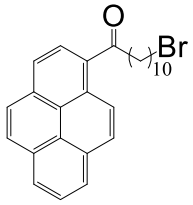

(16)

1-(1-pyrenyl)-11-bromo-1-undecanone

In a 5 mL round bottom flask, 1.8 mL (24.8 mmol) of thionyl chloride was added to 1.0 g (3.8 mmol) of 11-bromoundecanoic acid. The mixture was heated at 40°C for 4 h and then stirred at room temperature for 12 h. After removal of the excess of thionyl chloride by rotavap, the residual colorless oil was dissolved in 6 mL of dry CH2Cl2, transferred in a two neck round bottom flask, and cooled to 0°C in an ice bath. Upon addition of 0.72 g (3.6 mmol) of pyrene and 0.57 g (4.3 mmol) of AlCl3, the reaction was stirred for 5 h at 0°C. The reaction mixture was then poured on an ice/water/Et2O mixture. The organic layer was washed three times with water and dried over Mg2SO4. After removal of solvent, purification of the crude product on silica gel, using

hexane/Et2O (9:1) as eluent, yielded the intermediate product I as a yellow solid (98%). ^{1}H NMR ($CDCl_3$, 400 MHz): 8.93 (d, 1H, Ar), 7.92-8.31 (m, 8H, Ar), 3.44 (t, 2H, CH2 ω), 3.22 (t, 2H, CH2 α), 1.94 (m, 2H, CH2 ω-1), 1.22-1.53 (m, 14H, aliphatic chain).

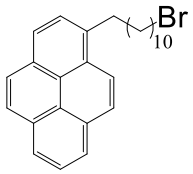

(17)

11-(1-pyrenyl)-1-bromoundecene was prepared according to a reported procedure. Briefly, in a two-neck, round bottom flask fitted with a reflux condenser, 0.45 g (3.4 mmol) of $AlCl_3$ dissolved in 5 mL of dry Et_2O were added dropwise to a 1 M solution of LiAlH4 in dry Et_2O. Then, 0.5 g (1.1 mmol) of **16** dissolved in 10 mL of dry CH_2Cl_2 were added dropwise to the mixture cooled to 0 °C in an ice bath, and the reaction mixture was stirred at room temperature and monitored by TLC (hexane/Et_2O 9:1) until disappearance of **16** (~3 h). The reaction was quenched by the addition of 10 mL of Et_2O and 10 mL of water; the organic layer was washed several times with HCl 1 M and dried over Mg_2SO_4. Removal of the solvent yielded a yellow solid (90%). ^{1}H NMR ($CDCl_3$, 400 MHz): 7.74-8.22 (m, 9H, Ar), 3.3 (m, 4H), 1.1-1.9 (m, 18H, aliphatic chain).

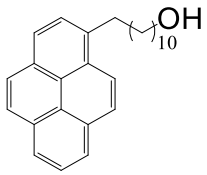

(18)

A mixture of **17** (200mg, 0.56mmol) and $NaHCO_3$ (320mg, 3.8mmol) in DMSO (3.8mL) was heated to reflux for 1 h. Then saturated $NaHCO_3$ solution and CH_2Cl_2 were added at room temperature. The organic layer was extracted with saturated NaCl solution, dried ($MgSO_4$), and evaporated and the residue was purified by flash chromatography (hexane/ EtOAc 3:1) to give 97 mg (59%) as a colorless solid. ^{1}H NMR ($CDCl_3$, 400 MHz): δ 9.77(t, 1H), 7.72-8.24 (m, 9H, Ar), 3.32(t, 2H), 2.41(t, 2H), 1.14-1.92 (m, 18H).

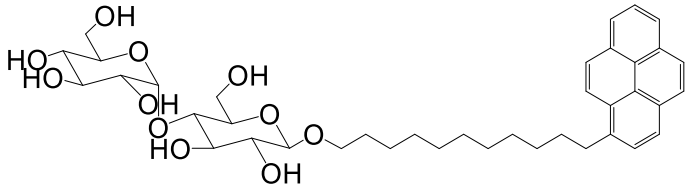

(19)

(Need repeat)

Maltose (1.0 g, 2.8mmol), AcBr (~3.6mL, 44.4mmol), and AcOH (19mL) were added to an oven dried round bottom flask and stirred at room temperature (25 ^{0}C) for ~ 1 h. The reaction mixture was concentrated *in vacuo* at 35 ^{0}C and then co-evaporated three times with PhMe (2×10 mL, anhydrous). After removal of solvent, the flask was further heated in vacuo at 50 ^{0}C for 15min to give a foamy solid, aceto-bromo sugar. The

crude aceto-bromo sugars were immediately used in next step without any further purification.

Crude aceto-bromo sugars were then dissolved in MeCN (10mL) and **18** (5.6mmol, 2 equivalents) were added along with acid 2-equivalents of a Lewis catalyst $FeCl_3$. The reaction mixture was stirred vigorously for about ~45-60 mins at rt. After stirring at rt, aq KBr (10%, 25mL) and then PhMe (60mL) were added under stirring. The organic phase was washed twice with aq KBr (10%, 2×25mL), once with aq $NaHCO_3$ (5%, 25mL) and twice with H_2O (2×25mL). The crude product was then purified by column chromatography using gradient elution (100 % hexane to 50 % ethyl acetate in hexane). Concentration and silica gel chromatography afforded the acetylated product (0.6 g, 0.8 mmol, 29%). The deprotection of acetyl groups was achieved by Zemplén deacetylation using MeONa/MeOH (10 mM solution) conditions followed by neutralization (pH ~6.5) over H+ amberlite resins. The resins were filtered off and products dried under high vacuum overnight. 1H NMR (400 MHz, MeOD) showed the product is not pure, need to synthesize this again.

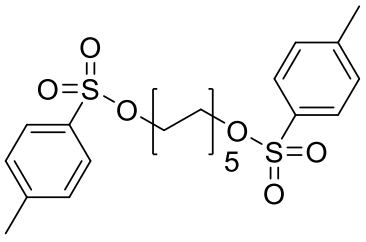

1,10-Decanediol di-*p*-tosylate, $TsOC_{10}H_{20}OTs$ **(20)**

In an overnight oven-dried round bottom flask, 1, 10-decanediol (1 g, 5.7 mmol) and 4-toluenesulfonyl chloride (2.3 g, 12 mmol) were dissolved in dry dichloromethane (60 ml) at 0 °C. Upon the addition of pyridine (0.94 g, 12 mmol) the reaction mixture was allowed to stir vigorously under argon environment and warmed to room temperature overnight. The reaction mixture was concentrated *in vacuo*. The reaction crude was diluted with 1:1 H_2O:CH_2Cl_2 (120 ml). The organic layer was washed with brine (3*30 ml) and dried over Na_2SO_4. Upon removal of solvents, 1,10-Decanediol di-p-tosylate was afforded as a white solid (2.29 g, 4.8 mmol, 98%). TLC: R_f=0.48 (hexanes:ethyl acetate, 7:3). ^{1}H NMR ($CDCl_3$, 400 MHz): δ 7.79 (4H, d, J=8 Hz, -$C_2H_4C_2$**H**$_4$CS-), 7.34 (4H, d, J=8 Hz, CH_3CC_2**H**$_4C_2H_4$-), 4.00 (4H, t, J=6.8 Hz, TsOC**H**$_2CH_2$-), 2.45 (6H, s, -PhC**H**$_3$), 1.62 (4H, p, J=6.8 Hz, $TsOCH_2$C**H**$_2$-), 1.2 (6H, s, b, Aliphatic), 1.18 (6H, s, b, Aliphatic).

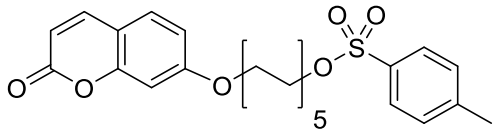

Um$OC_{10}H_{20}$OTs **(21)**

In an overnight oven-dried round bottom flask, umbelliferone (0.162 g, 1 mmol) was dissolved in dry MeCN (10 ml), and K_2CO_3 (0.140 g, 1 mmol) was added. The reaction mixture was stirred at room temperature for 15 minutes, then treated with 1, 10-decandiol ditosylate (1.01 g, 2.1 mmol). The reaction mixture was heated with an oil bath to 65 ˚C and allowed to stir vigorously at for 12 h under Ar environment. After cooling, the reaction mixture was concentrated, diluted with 1:1 CH_2Cl_2: H_2O (20 ml). The

organic layer was washed with brine, dried over $MgSO_4$, and concentrated *in vacuo*. The reaction crude was diluted with CH_2Cl_2, mixed with SiO_2 (80%). Upon removal of the solvent, the crude mixture was purified with flash chromatography (hexane: ethyl acetate, 3:1) to give Umbelliferone Decanol Tosylate Ether as a colorless oil (0.223g, 0.47 mmol, 47%). TLC: R_f=0.34 (hexanes:ethyl acetate, 7:3). ^{1}H NMR ($CDCl_3$, 400 MHz): δ 7.80 (2H, d, J=8.4 Hz, -$C_2H_4C_2$**H**$_4$CS-), 7.64 (1H, d, J=9.6 Hz, -CH=C**H**C-), 7.37 (2H, d, J=8.4 Hz, CH_3CC_2**H**$_4C_2H_4$-), 7.35 (1H, d, J=6.8 Hz, -CHC**H**C(OH)-), 6.84 (1H, dd, J=8.8, 2.4 Hz, -CC**H**CH-), 6.81 (1H, d, J=2 Hz, -CC**H**C(OH)-), 6.25 (1H, d, J=9.6 Hz, -OC(=O)C**H**=CHC-), 4.03 (2H, t, J=6.8 Hz, UmOC**H**$_2CH_2$-), 4.0 (2H, t, J=6.8 Hz, TsOC**H**$_2CH_2$-), 2.46 (3H, s, -PhC**H**$_3$), 1.81 (2H, p, J=6.8 Hz, Aliphatic), 1.65 (2H, p, J=6.8 Hz, Aliphatic), 1.69 (2H, d, J=7.6 Hz), 1.45 (2H, p, J=6.8 Hz, Aliphatic), 1.2-1.4 (8H, m, Aliphatic).

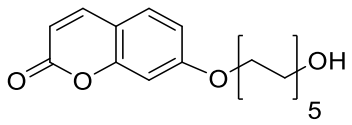

UmDe Alcohol, $UmOC_{10}H_{20}OH$ **(22)**

In a clean and dry round bottom flask, UmDe Tosylate (0.443 g, 0.937 mmol) was dissolved in a stirring mixture of 0.5 M aq. NaOH (2 ml, 2 mmol) and MeCN (8 ml). The reaction mixture was heated with an oil bath to 78 ˚C and allowed to stir vigorously at for 12 h. After cooling, the reaction mixture was quenched with 0.5 M HCl (2 ml, 2 mmol), concentrated, then diluted with 1:1 CH_2Cl_2: H_2O (20 ml). The organic layer was washed

with brine, water, and dried over $MgSO_4$, and concentrated *in vacuo*. Upon removal of the solvent, the crude mixture was purified with flash chromatography (hexane: ethyl acetate, 7:3) to give UmDe Alcohol as a white solid (26 mg, 0.082 mmol, 8.6%). TLC: R_f=0.24 (hexanes:ethyl acetate, 7:3). ^{1}H NMR ($CDCl_3$, 400 MHz): δ 7.64 (1H, d, J=9.6 Hz, -CH=C**H**C-), 7.36 (1H, d, J=6.8 Hz, -CHC**H**C(OH)-), 6.84 (1H, dd, J=8.8, 2.4 Hz, -CC**H**CH-), 6.81 (1H, d, J=2 Hz, -CC**H**C(OH)-), 6.25 (1H, d, J=9.6 Hz, -OC(=O)C**H**=CHC-), 4.02 (2H, t, J=6.4 Hz, UmOC**H**$_2$CH$_2$-), 3.66 (2H, t, J=6.4 Hz, HOC**H**$_2$CH$_2$-), 1.84 (2H, t, J=6.8 Hz, Aliphatic), 1.6-1.4 (10H, m, Aliphatic), 1.36 (8H, s, Aliphatic).

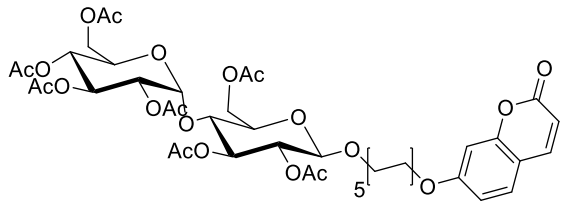

Per-acetyl UmDeβM **(23)**

To an oven dried round bottom flask, maltose (0.072 g, 0.2 mmol) was dissolved in AcOH (2 ml), then treated with AcBr (~0.30 mL, 4.0 mmol). The reaction mixture was allowed to stir at room temperature (25 ºC) for ~ 1 h. The reaction mixture was concentrated *in vacuo* at 35 ºC. After removal of solvent, the reaction crude was co-evaporated with anhydrous toluene (2×3 mL) at 40 ºC to further remove residual acetic acid to give aceto-bromo sugars as a foamy solid. The crude aceto-bromo maltose was immediately used in next step without any further purification. The crude aceto-bromo maltose (~0.2 mmol) was dissolved in MeCN (10mL) along with $UmOC_{10}H_{20}OH$ (0.096

g, 0.3 mmol). To this reaction mixture was added two $FeCl_3$ (0.033 g, 0.4 mmol). The reaction mixture was stirred vigorously for about 60 mins at rt. Then 10% aq. KBr (3 ml) and toluene (5 ml) were added under stirring. The organic phase was subsequently washed with 10% aq. KBr (2×3 ml), 5% aq $NaHCO_3$ (5%, 3 ml), and H_2O (2×3 ml). Upon removal of solvent, the crude mixture was purified with flash chromatography (hexane: ethyl acetate, 1:1) to give Per-acetyl UmDeβM as a white solid (19 mg, 0.020 mmol, 10%). TLC: Rf=0.29 (hexanes:ethyl acetate, 1:1). ^{1}H NMR ($CDCl_3$, 400 MHz): δ 7.64 (1H, d, J=9.6 Hz, -CH=C**H**C-), 7.37 (1H, d, J=8.4 Hz, -CHC**H**C(OH)-), 6.84 (1H, dd, J=8.8, 2.4 Hz, -CC**H**CH-), 6.81 (1H, d, J=2 Hz, -CC**H**C(OH)-), 6.25 (1H, d, J=9.2 Hz, -OC(=O)C**H**=CHC-), 5.43-5.34 (2H, m, maltose), 5.26 (1H, t, J = 9.2 Hz, anomeric), 5.07 (1H, t, J = 9.6 Hz, anomeric), 4.89-4.80 (2H, m, maltose), 4.53-4.46 (2H, m, maltose), 4.28-4.22 (2H, m, maltose), 4.07-3.96 (2H, m, UmOC**H**$_2$CH$_2$-), 4.07-3.96 (2H, m, MOC**H**$_2$CH$_2$-), 4.07-3.96 (1H, m, -CHC**H**$_2$OAc), 3.85 (1H, m, -CHC**H**$_2$OAc), 3.67 (1H, m, -CHC**H**$_2$OAc), 3.47 (1H, m, -CHC**H**$_2$OAc), 2.15-2.01 (7 x 3H, s, C**H**$_3$C(=O)O-),1.81 (2H, t, J=7.6 Hz, Aliphatic), 1.47 (2, t, J=7.6 Hz, Aliphatic), 1.45-1.25 (16H, m, Aliphatic).

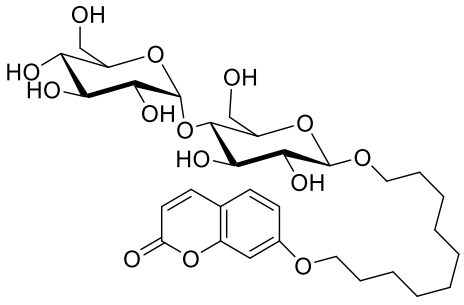

UmDeβM **(24)**

To an oven dried round bottom flask, per-acetyl UmDeβM (30 mg, 32.02 mmol) was dissolved in 10 mM CH3ONa/CH3OH (10 ml). The reaction was allowed to stirred at room temperature under argon environment for 12 hours; then followed by neutralization (pH ~6.5) over H+ amberlite resins. After the resins were filtered off, the filtrate was concentrated *in vacuo* at 35 ºC to afford UmDeβM as a light-yellow solid (14 mg, 21.78 mmol, 66%). TLC: Rf=0.18 (methanol). 1H NMR (CD_3OD, 400 MHz): δ 7.88 (1H, d, J=9.2 Hz, -CH=C**H**C-), 7.53 (1H, d, J=8.4 Hz, -CHC**H**C(OH)-), 6.92 (1H, dd, J=8.8, 2.4 Hz, -CC**H**CH-), 6.89 (1H, d, J=2 Hz, -CC**H**C(OH)-), 6.24 (1H, d, J=9.2 Hz, -OC(=O)C**H**=CHC-), 4.26 (1H, d, J = 9.2 Hz, anomeric), 3.90-3.83 (5H, m, maltose), 4.07 (2H, t, J=6.4 Hz, UmOC**H**$_2$CH$_2$-), 3.81 (1H, t, J = 6.4 Hz, anomeric), 3.80-3.65 (5H, m, maltose), 3.61 (2H, J=9.6 Hz, MOC**H**$_2$CH$_2$-), 3.6-3.5 (2H, m, -CHC**H**$_2$OH), 3.3-3.2 (2H, m, -CHC**H**$_2$OH), 1.81 (2H, t, J=7.2 Hz, Aliphatic), 1.62 (2H, t, J=7.6 Hz, Aliphatic), 1.50 (2H, m, Aliphatic), 1.35 (10H, bs, Aliphatic).

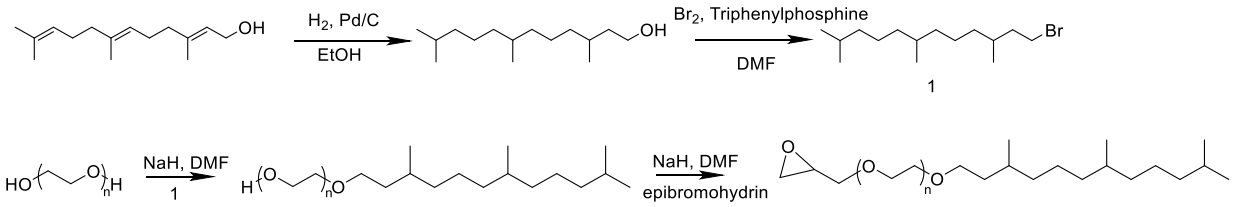

Scheme 6.6. Synthesis scheme for SF(EG)$_n$-epoxy (n=3,4,5)

General procedure for the synthesis of $SF(EG)_nOH$ (n=3, 4, 5)

Saturated farnesol (1 equiv.) and triphenylphosphine (1.1 equiv.) were dissolved in DMF under nitrogen atmosphere. Bromine was added drop by drop until the solution turned orange in color and flask temperature was maintained below 55 ºC. Reaction was allowed to stir at rt for additional 12 h. Reaction mixture was concentrated in vacuo and the resulting product was purified over column chromatography (15% EtOAc/hexanes) to afford the desired product SFBr. Then $(EG)_nOH$ (n=3, 4, 5) (2 equiv.) was dissolved in dry DMF and cooled to 0 ºC for 5 min. To the reaction mixture was added NaH (60% dispersion in mineral oil) (1 equiv.) at 0 °C and the reaction was further stirred for one hour. SFBr (1 equiv.) was added and the mixture was stirred at rt overnight. Reaction mixture was concentrated in vacuo and then dissolved in Et_2O (15 mL). Organic layer was washed with water (10 mL x 3), brine and dried over Na2SO4. Organic phase was filtered and concentrated in vacuo. The reaction mixture was purified by column chromatography (40 % EtOAc/ Hexane) to afford SF(EG)nOH (n=3, 4, 5).

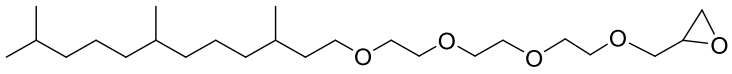

$SF(EG)_3$-epoxy **(25)**

$SF(EG)_3OH$ (0.11 g, 0.30 mmol) was dissolved in 1 mL dry DMF and cooled to 0 ºC for 5 min. To the reaction mixture was added NaH (60% dispersion in mineral oil) (0.04 g, 0.33 mmol) at 0 °C and the reaction was further stirred for one hour. Epibromohydrin (0.05 g, 0.33 mmol) was added and the mixture was stirred at rt overnight. Reaction mixture was concentrated in vacuo and then dissolved in Et_2O (5 mL). Organic layer was

washed with water (10 mL x 3), brine and dried over Na_2SO_4. Organic phase was filtered and concentrated in vacuo. The reaction mixture was purified by column chromatography (25 % EtOAc/ Hexane) to afford **25** (0.06 g, 47%). ^{1}H NMR (400 MHz, $CDCl_3$) δ 3.73 (dd, 1H), 3.70-3.63 (m, 9H), 3.60-3.53(m, 1H), 3.51-3.38(m, 3H), 3.21-3.12 (m, 1H), 2.84-2.77(m, 1H), 2.65-2.60 (m, 1H), 1.64-1.08 (m, 19H), 0.94-0.89 (m, 12H).

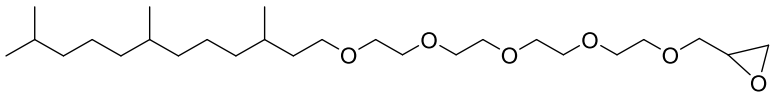

SF(EG)$_4$-epoxy **(26)**

SF(EG)$_4$OH (0.22 g, 0.60 mmol) was dissolved in 2 mL dry DMF and cooled to 0 ºC for 5 min. To the reaction mixture was added NaH (60% dispersion in mineral oil) (0.08 g, 0.66 mmol) at 0 °C and the reaction was further stirred for one hour. Epibromohydrin (0.10 g, 0.66 mmol) was added and the mixture was stirred at rt overnight. Reaction mixture was concentrated in vacuo and then dissolved in Et_2O (10 mL). Organic layer was washed with water (10 mL x 3), brine and dried over Na_2SO_4. Organic phase was filtered and concentrated in vacuo. The reaction mixture was purified by column chromatography (40 % EtOAc/ Hexane) to afford **26** (0.13 g, 45%). ^{1}H NMR (400 MHz, $CDCl_3$) δ 3.73 (dd, 1H), 3.70-3.63 (m, 13H), 3.60-3.53(m, 1H), 3.51-3.38(m, 3H), 3.21-3.12 (m, 1H), 2.84-2.77(m, 1H), 2.65-2.60 (m, 1H), 1.64-1.08 (m, 19H), 0.94-0.89 (m, 12H).

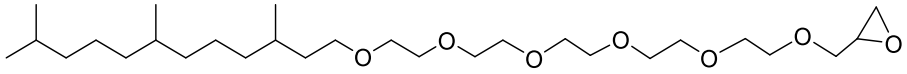

SF(EG)$_5$-epoxy **(27)**

SF(EG)$_5$OH (0.17 g, 0.40 mmol) was dissolved in 1 mL dry DMF and cooled to 0 ºC for 5 min. To the reaction mixture was added NaH (60% dispersion in mineral oil) (0.05 g, 0.44 mmol) at 0 °C and the reaction was further stirred for one hour. Epibromohydrin (0.07 g, 0.44 mmol) was added and the mixture was stirred at rt overnight. Reaction mixture was concentrated in vacuo and then dissolved in Et_2O (5 mL). Organic layer was washed with water (10 mL x 3), brine and dried over Na_2SO_4. Organic phase was filtered and concentrated in vacuo. The reaction mixture was purified by column chromatography (25 % EtOAc/ Hexane) to afford **27** (0.06 g, 47%). ^{1}H NMR (400 MHz, $CDCl_3$) δ 3.73 (dd, 1H), 3.70-3.63 (m, 17H), 3.60-3.53(m, 1H), 3.51-3.38(m, 3H), 3.21-3.12 (m, 1H), 2.84-2.77(m, 1H), 2.65-2.60 (m, 1H), 1.64-1.08 (m, 19H), 0.94-0.89 (m, 12H).

^{1}H NMR spectra

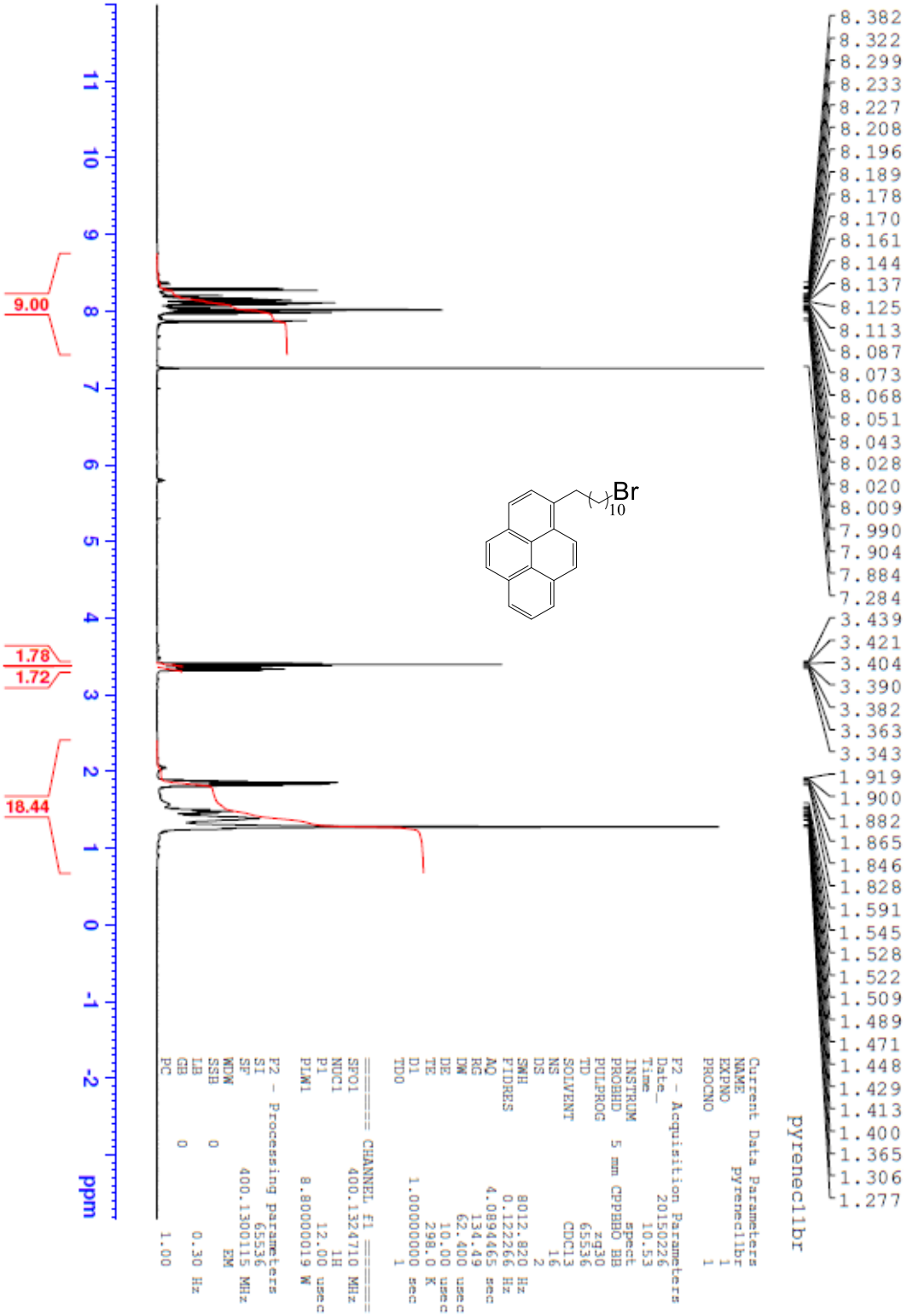

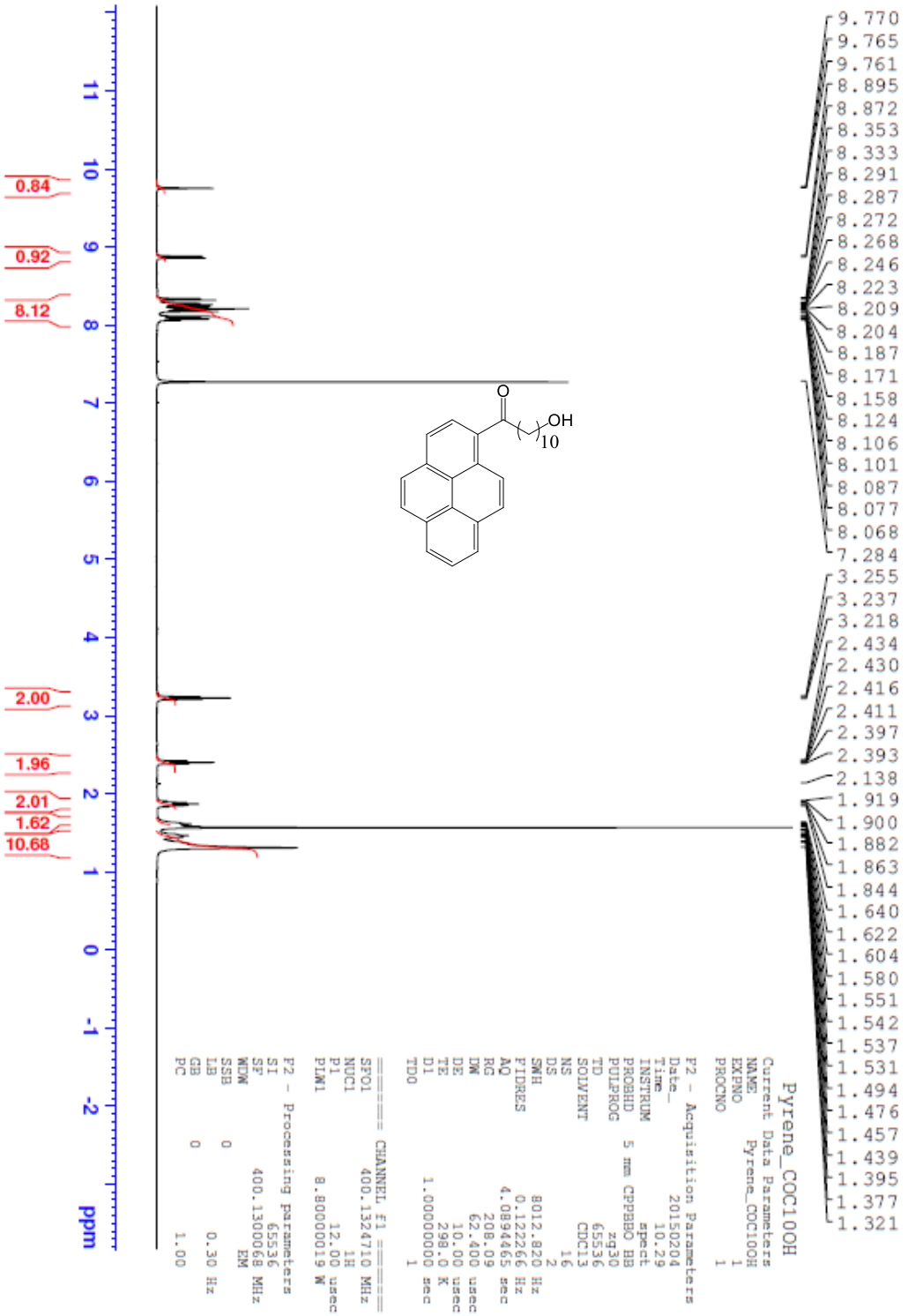
9.770
9.765
9.761
8.895
8.872
8.353
8.333
8.291
8.287
8.272
8.268
8.246
8.223
8.209
8.204
8.187
8.171
8.158
8.124
8.106
8.101
8.087
8.077
8.068
7.284
3.255
3.237
3.218
2.434
2.430
2.416
2.411
2.397
2.393
2.138
1.919
1.900
1.882
1.863
1.844
1.640
1.622
1.604
1.580
1.551
1.542
1.537
1.531
1.494
1.476
1.457
1.439
1.395
1.377
1.321
Pyrene_COC10OH
Current Data Parameters
NAME Pyrene_COC10OH
EXPNO 1
PROCNO 1
F2 - Acquisition Parameters
Date_ 20150204
Time 10.29
INSTRUM spect
PROBHD 5 mm CPPBBO BB
PULPROG zg30
TD 65536
SOLVENT CDCl3
NS 16
DS 2
SWH 8012.820 Hz
FIDRES 0.122266 Hz
AQ 4.0894465 sec
RG 208.09
DW 62.400 usec
DE 10.00 usec
TE 298.0 K
D1 1.00000000 sec
TD0 1
======== CHANNEL f1 ========
SFO1 400.1324710 MHz
NUC1 1H
P1 12.00 usec
PLW1 8.80000019 W
F2 - Processing parameters
SI 65536
SF 400.1300068 MHz
WDW EM
SSB 0
LB 0.30 Hz
GB
PC 1.00
0.84
0.92
8.12
2.00
1.96
2.01
1.62
10.68
O
OH
10
11
10
9
8
7
6
5
4
3
2
1
0
-1
-2
ppm

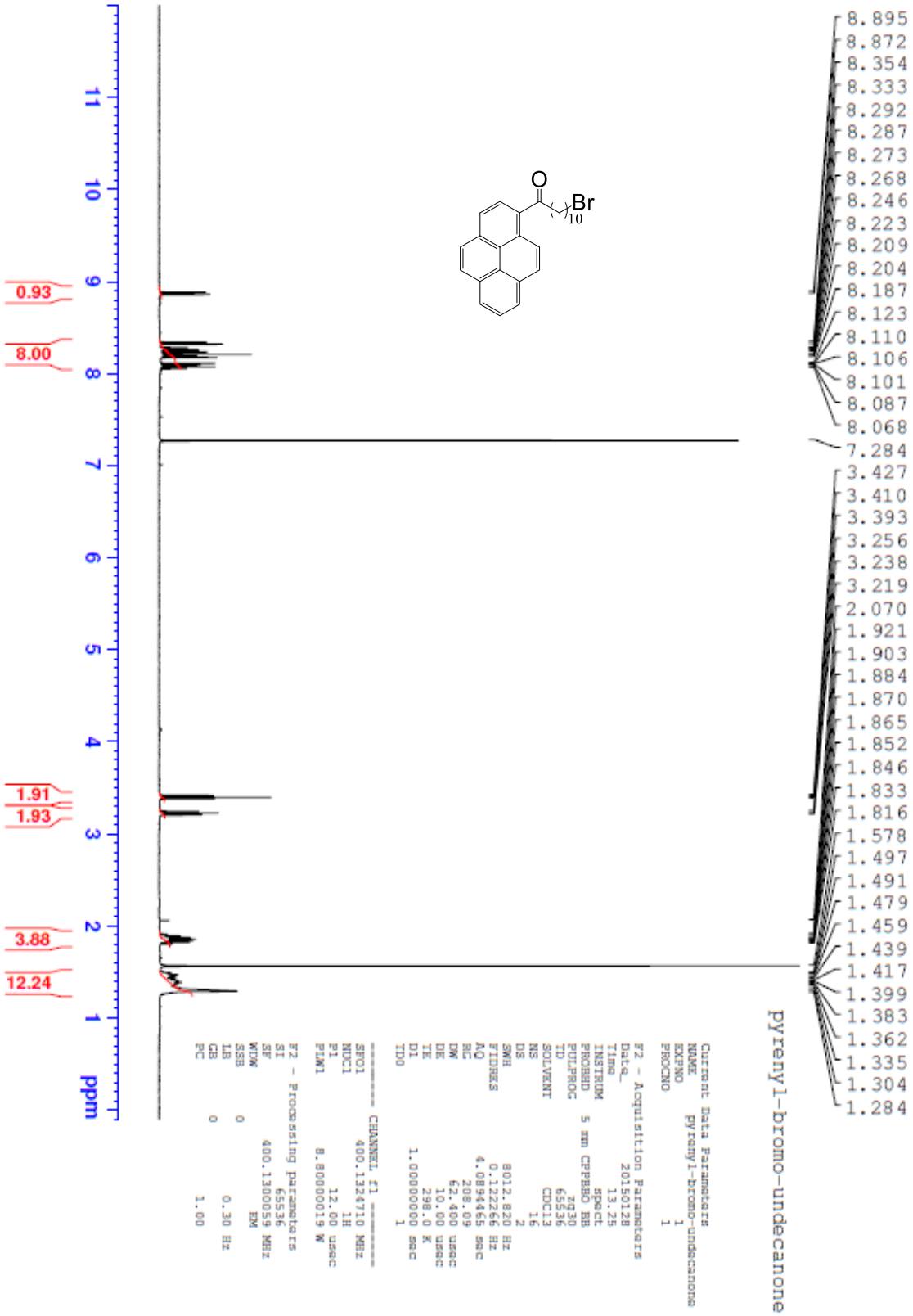
pyrenyl-bromo-undecanone
8.895
8.872
8.354
8.333
8.292
8.287
8.273
8.268
8.246
8.223
8.209
8.204
8.187
8.123
8.110
8.106
8.101
8.087
8.068
7.284
3.427
3.410
3.393
3.256
3.238
3.219
2.070
1.921
1.903
1.884
1.870
1.865
1.852
1.846
1.833
1.816
1.578
1.497
1.491
1.479
1.459
1.439
1.417
1.399
1.383
1.362
1.335
1.304
1.284
0.93
8.00
1.91
1.93
3.88
12.24
ppm
Br
10

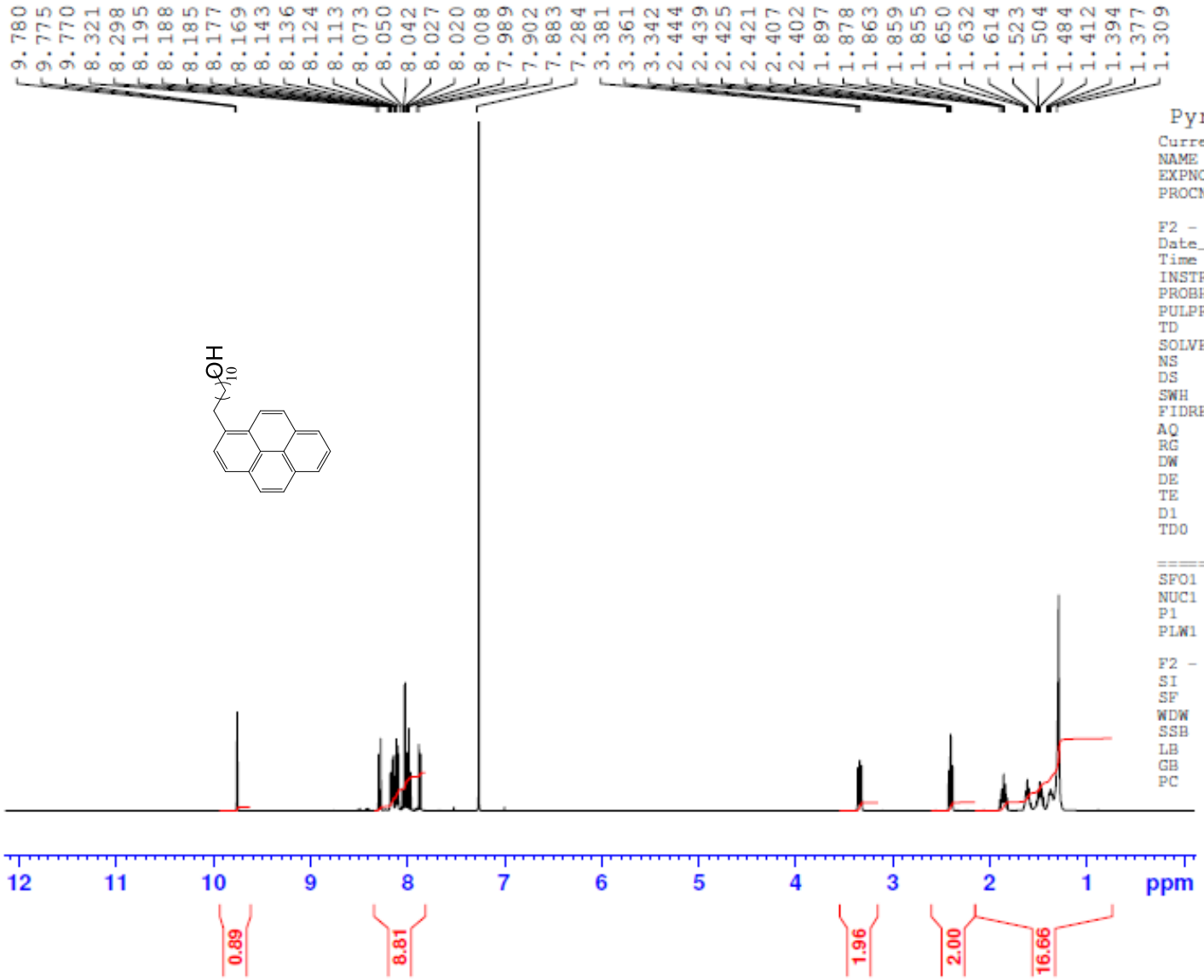

PyreneC11OH

Current Data Parameters

NAME	PyreneC11OH
EXPNO	1
PROCNO	1

F2 - Acquisition Parameters

Date_	20150302
Time	13.46
INSTRUM	spect
PROBHD	5 mm CPPBBO BB
PULPROG	zg30
TD	65536
SOLVENT	CDCl3
NS	16
DS	2
SWH	8012.820 Hz
FIDRES	0.122266 Hz
AQ	4.0894465 sec
RG	208.09
DW	62.400 usec
DE	10.00 usec
TE	298.0 K
D1	1.00000000 sec
TD0	1

====== CHANNEL f1 ======

SFO1	400.1324710 MHz
NUC1	1H
P1	12.00 usec
PLW1	8.80000019 W

F2 - Processing parameters

SI	65536
SF	400.1300079 MHz
WDW	EM
SSB	0
LB	0.30 Hz
GB	0
PC	1.00

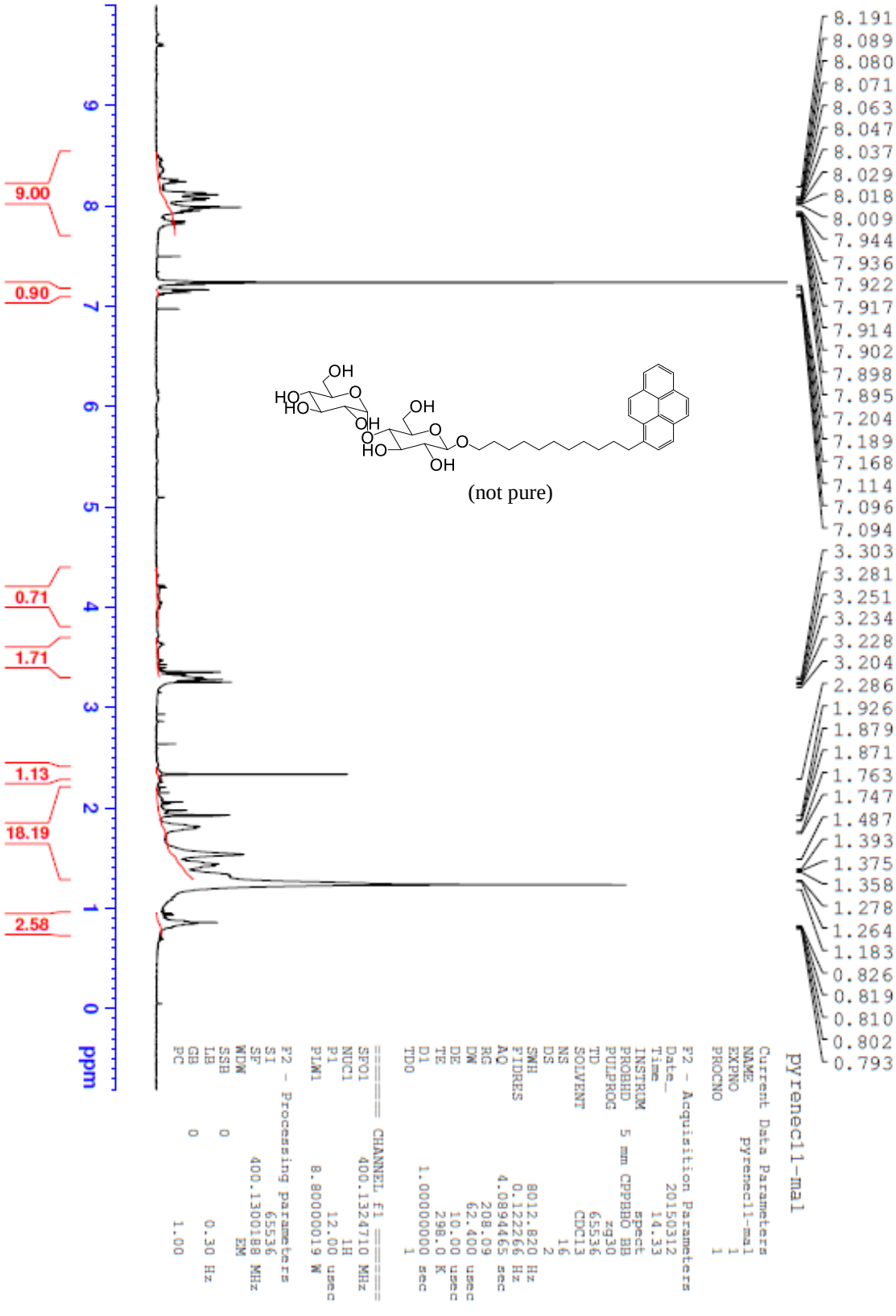
pyrenec11-mal
8.191
8.089
8.080
8.071
8.063
8.047
8.037
8.029
8.018
8.009
7.944
7.936
7.922
7.917
7.914
7.902
7.898
7.895
7.204
7.189
7.168
7.114
7.096
7.094
3.303
3.281
3.251
3.234
3.228
3.204
2.286
1.926
1.879
1.871
1.763
1.747
1.487
1.393
1.375
1.358
1.278
1.264
1.183
0.826
0.819
0.810
0.802
0.793
9.00
0.90
0.71
1.71
1.13
18.19
2.58
ppm
(not pure)

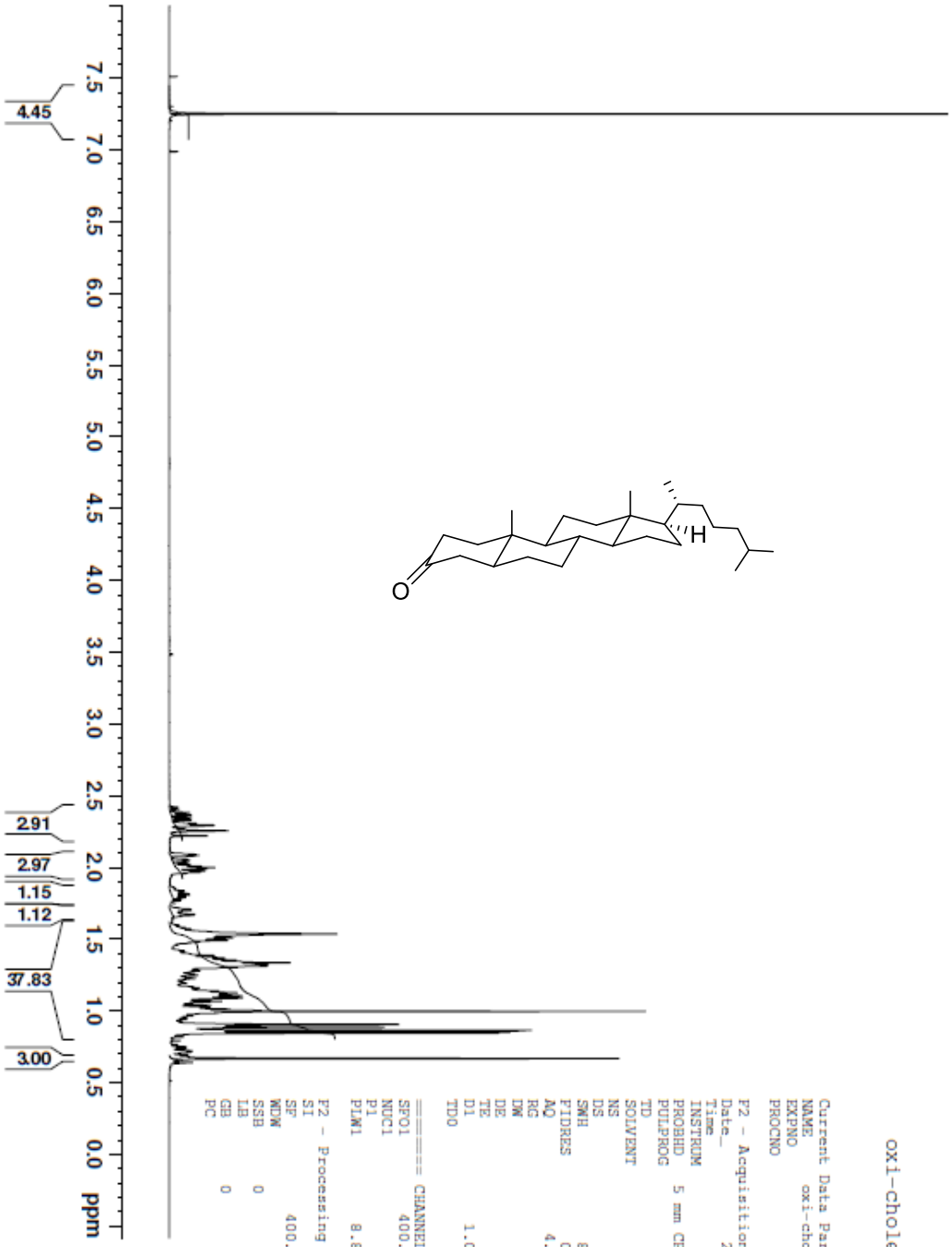
oxi-cholesterol
Current Data Parameters
NAME oxi-cholesterol
EXPNO 2
PROCNO 1
F2 - Acquisition Parameters
Date_ 20140510
Time 17.47
INSTRUM spect
PROBHD 5 mm CPPBBO BB
PULPROG zg30
TD 65536
SOLVENT CDCl3
NS 16
DS 2
SWH 8012.820 Hz
FIDRES 0.122266 Hz
AQ 4.0894465 sec
RG 208.09
DW 62.400 usec
DE 10.00 usec
TE 298.0 K
D1 1.00000000 sec
TD0 1
======== CHANNEL f1 ========
SFO1 400.1324710 MHz
NUC1 1H
P1 12.00 usec
PLW1 8.80000019 W
F2 - Processing parameters
SI 65536
SF 400.1300141 MHz
WDW EM
SSB 0
LB 0.30 Hz
GB 0
PC 1.00
4.45
2.91
2.97
1.15
1.12
37.83
3.00
7.5
7.0
6.5
6.0
5.5
5.0
4.5
4.0
3.5
3.0
2.5
2.0
1.5
1.0
0.5
0.0
ppm
O
H

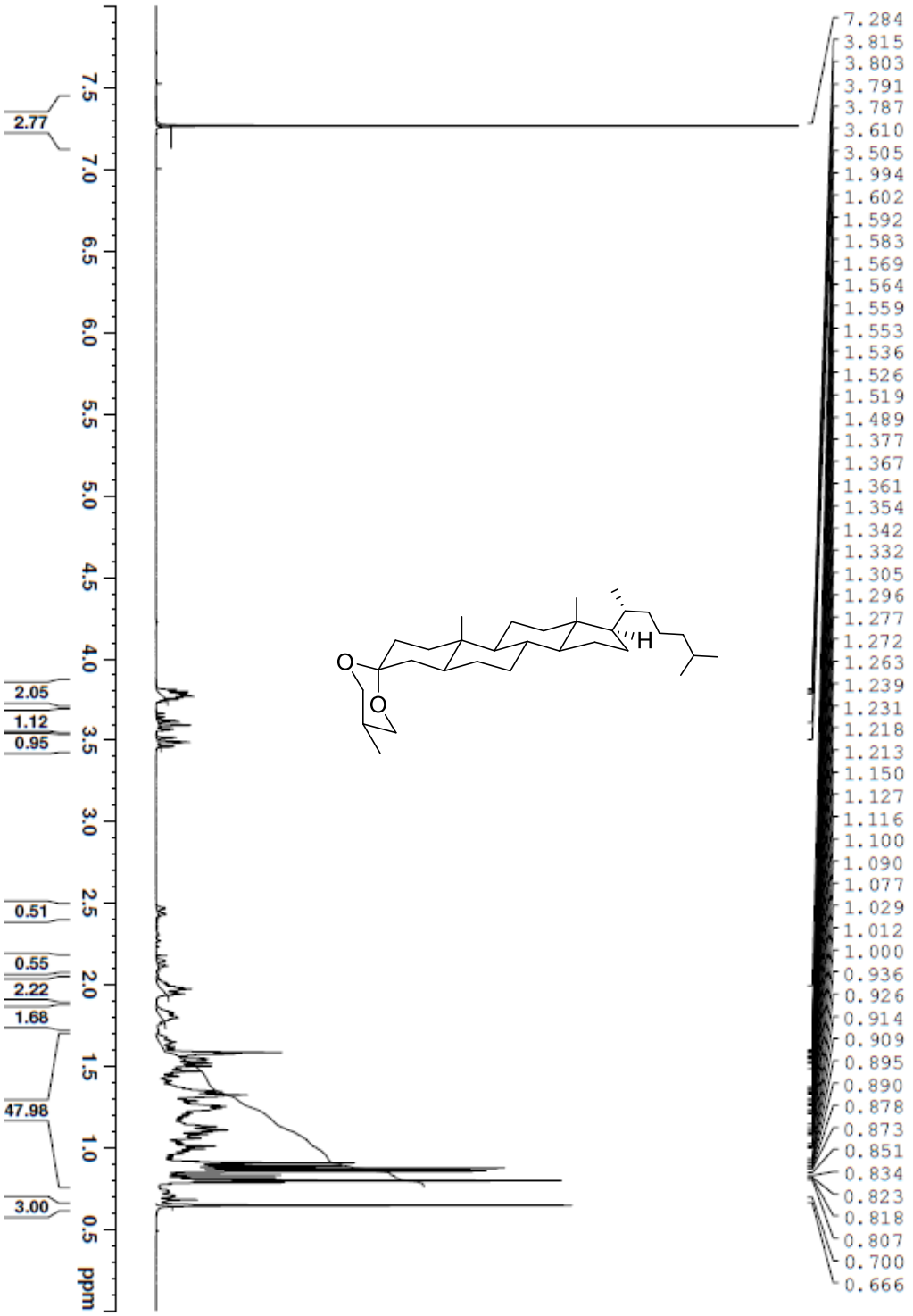
7.284
3.815
3.803
3.791
3.787
3.610
3.505
1.994
1.602
1.592
1.583
1.569
1.564
1.559
1.553
1.536
1.526
1.519
1.489
1.377
1.367
1.361
1.354
1.342
1.332
1.305
1.296
1.277
1.272
1.263
1.239
1.231
1.218
1.213
1.150
1.127
1.116
1.100
1.090
1.077
1.029
1.012
1.000
0.936
0.926
0.914
0.909
0.895
0.890
0.878
0.873
0.851
0.834
0.823
0.818
0.807
0.700
0.666
2.77
2.05
1.12
0.95
0.51
0.55
2.22
1.68
47.98
3.00
7.5
7.0
6.5
6.0
5.5
5.0
4.5
4.0
3.5
3.0
2.5
2.0
1.5
1.0
0.5
ppm
O
O
H

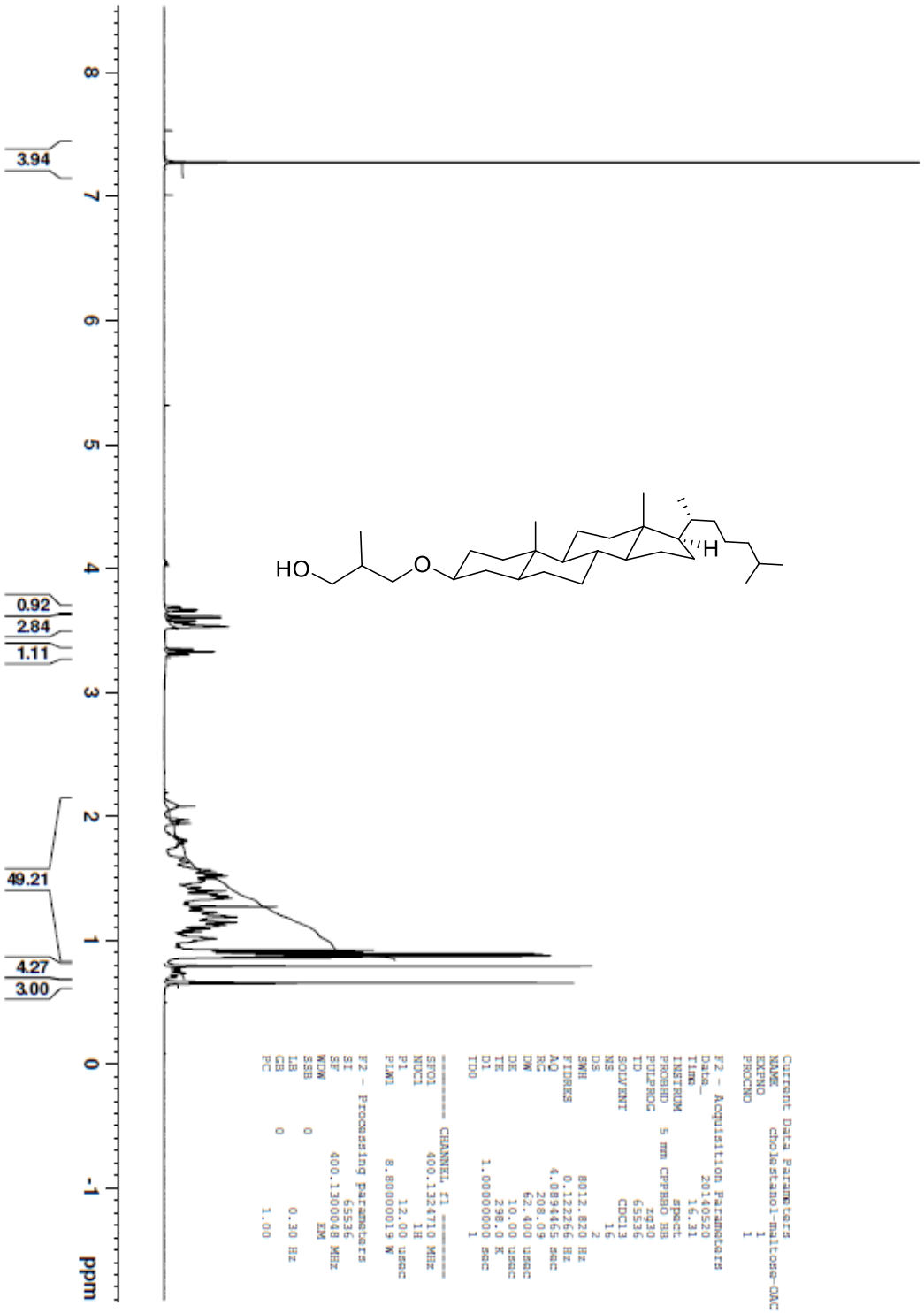
3.94
0.92
2.84
1.11
49.21
4.27
3.00
8
7
6
5
4
3
2
1
0
-1
ppm
HO
O
H
Current Data Parameters
NAME cholestanol-maltose-OAC
EXPNO 1
PROCNO 1
F2 - Acquisition Parameters
Date_ 20140520
TIME 16.31
INSTRUM spect
PROBHD 5 mm CPPBBO BB
PULPROG zg30
TD 65536
SOLVENT CDCl3
NS 16
DS 2
SWH 8012.820 Hz
FIDRES 0.122266 Hz
AQ 4.0894465 sec
RG 208.09
DW 62.400 usec
DE 10.00 usec
TE 298.0 K
D1 1.00000000 sec
TD0 1
======== CHANNEL f1 ========
SFO1 400.1324710 MHz
NUC1 1H
P1 12.00 usec
PLW1 8.80000019 W
F2 - Processing parameters
SI 65536
SF 400.1300048 MHz
WDW EM
SSB 0
LB 0.30 Hz
GB 0
PC 1.00

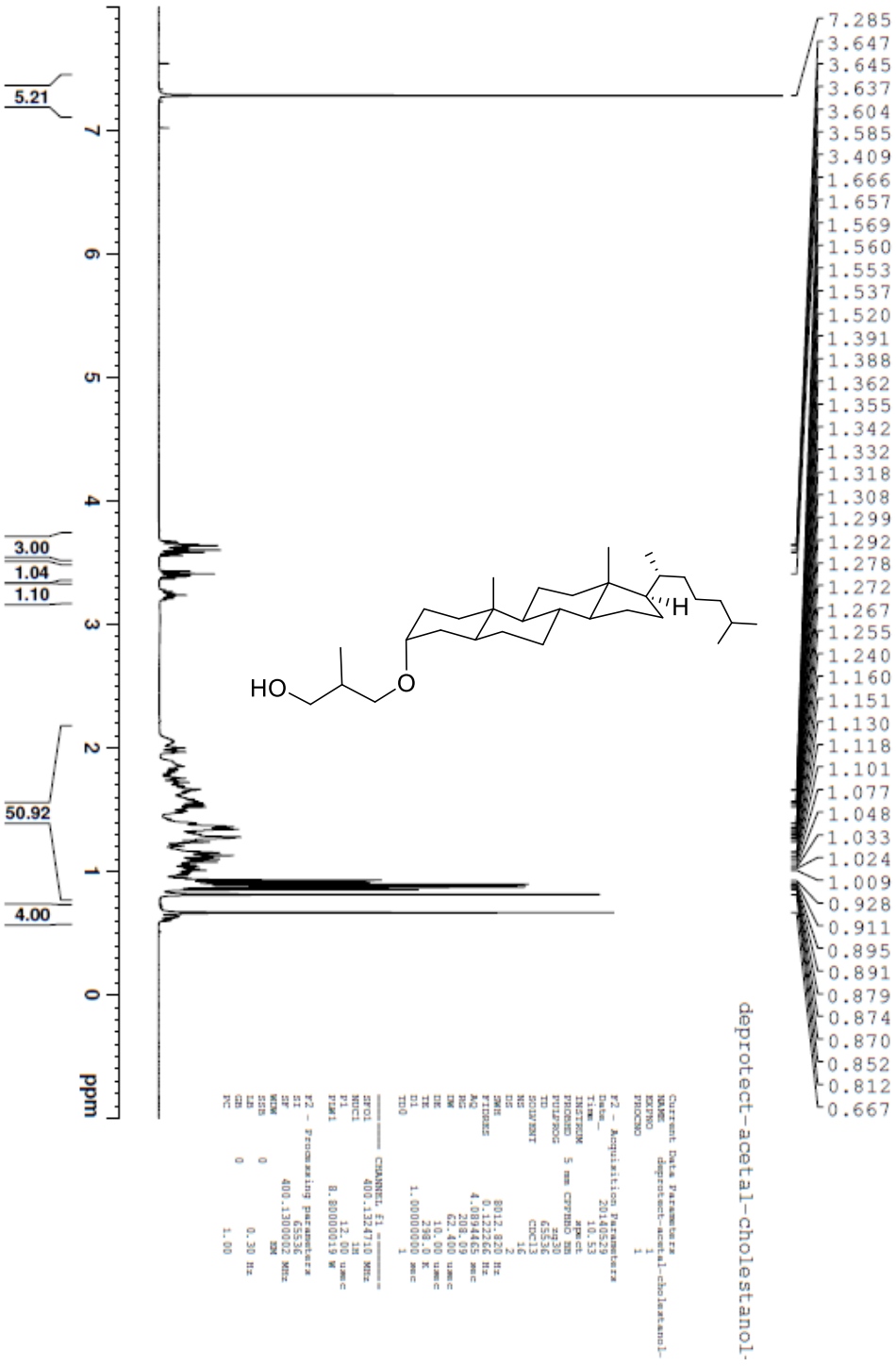
5.21
3.00
1.04
1.10
50.92
4.00
ppm
HO
O
H
7.285
3.647
3.645
3.637
3.604
3.585
3.409
1.666
1.657
1.569
1.560
1.553
1.537
1.520
1.391
1.388
1.362
1.355
1.342
1.332
1.318
1.308
1.299
1.292
1.278
1.272
1.267
1.255
1.240
1.160
1.151
1.130
1.118
1.101
1.077
1.048
1.033
1.024
1.009
0.928
0.911
0.895
0.891
0.879
0.874
0.870
0.852
0.812
0.667
deprotect-acetal-cholestanol-

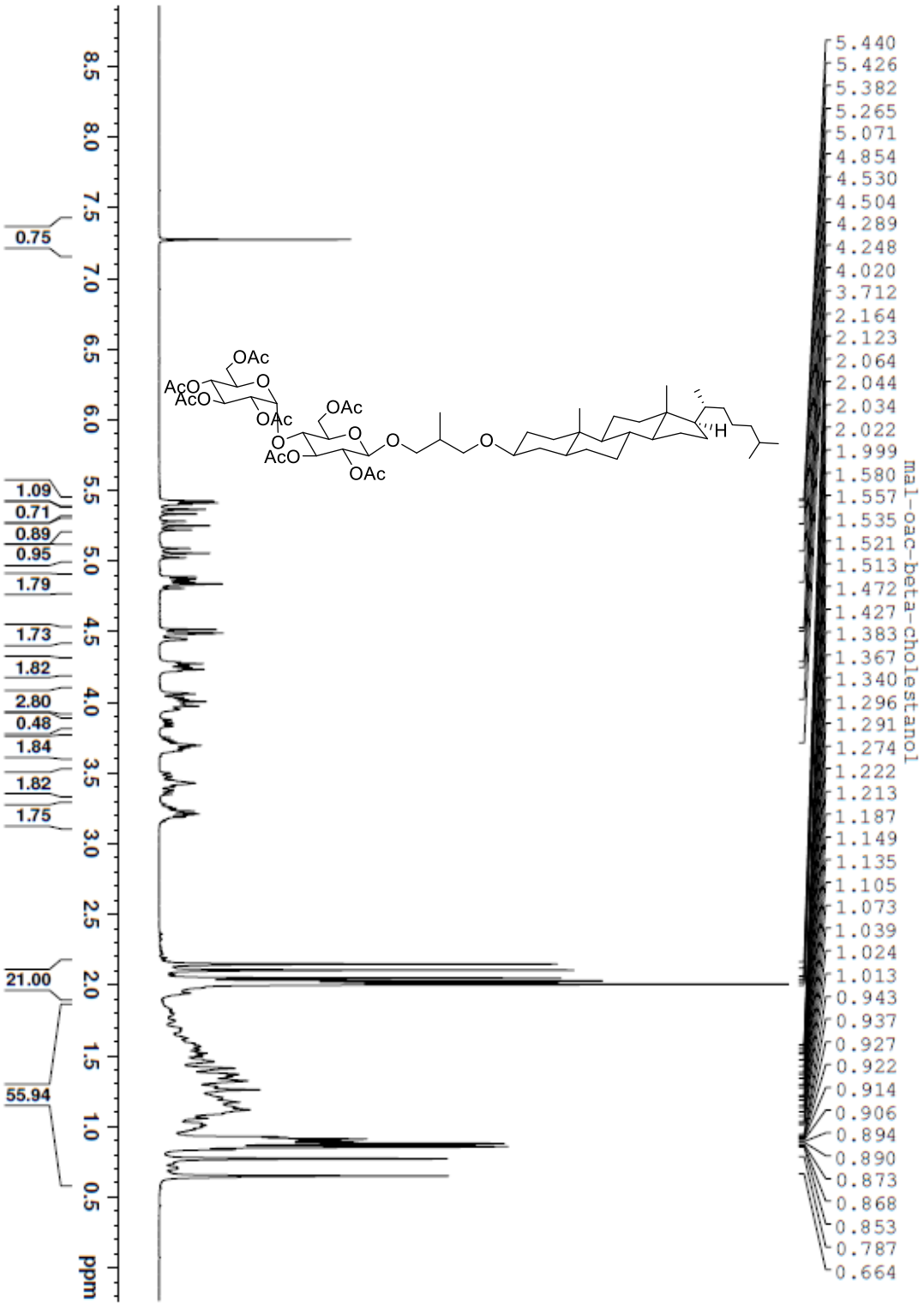
OAc
AcO
AcO
OAc
OAc
O
AcO
OAc
O
O
O
H
0.75
1.09
0.71
0.89
0.95
1.79
1.73
1.82
2.80
0.48
1.84
1.82
1.75
21.00
55.94
8.5
8.0
7.5
7.0
6.5
6.0
5.5
5.0
4.5
4.0
3.5
3.0
2.5
2.0
1.5
1.0
0.5
ppm
5.440
5.426
5.382
5.265
5.071
4.854
4.530
4.504
4.289
4.248
4.020
3.712
2.164
2.123
2.064
2.044
2.034
2.022
1.999
1.580
1.557
1.535
1.521
1.513
1.472
1.427
1.383
1.367
1.340
1.296
1.291
1.274
1.222
1.213
1.187
1.149
1.135
1.105
1.073
1.039
1.024
1.013
0.943
0.937
0.927
0.922
0.914
0.906
0.894
0.890
0.873
0.868
0.853
0.787
0.664
mal-oac-beta-cholestanol

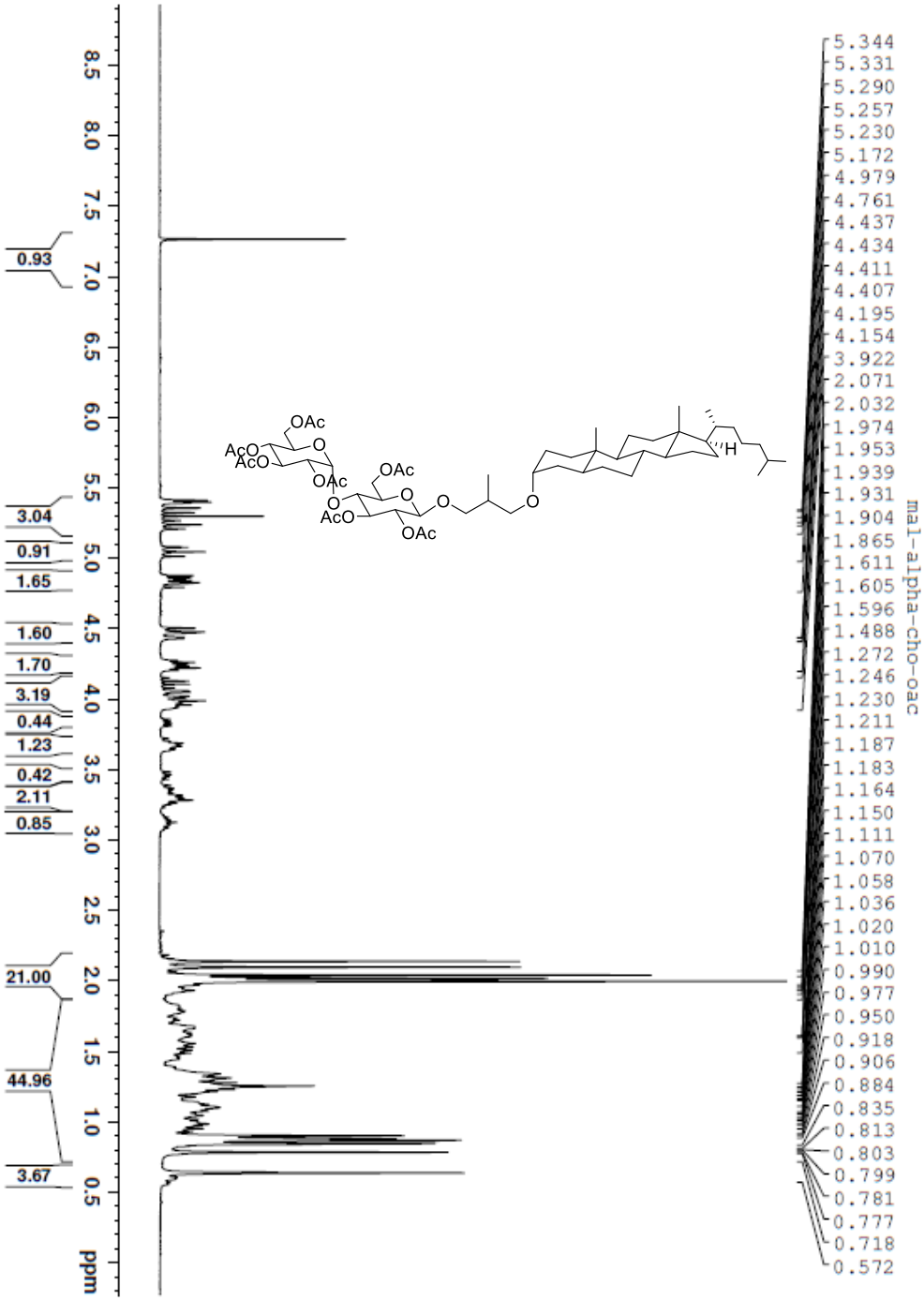
8.5
8.0
7.5
7.0
6.5
6.0
5.5
5.0
4.5
4.0
3.5
3.0
2.5
2.0
1.5
1.0
0.5
ppm
0.93
3.04
0.91
1.65
1.60
1.70
3.19
0.44
1.23
0.42
2.11
0.85
21.00
44.96
3.67
OAc
AcO
AcO
OAc
O
OAc
O
AcO
OAc
O
O
O
H
5.344
5.331
5.290
5.257
5.230
5.172
4.979
4.761
4.437
4.434
4.411
4.407
4.195
4.154
3.922
2.071
2.032
1.974
1.953
1.939
1.931
1.904
1.865
1.611
1.605
1.596
1.488
1.272
1.246
1.230
1.211
1.187
1.183
1.164
1.150
1.111
1.070
1.058
1.036
1.020
1.010
0.990
0.977
0.950
0.918
0.906
0.884
0.835
0.813
0.803
0.799
0.781
0.777
0.718
0.572
mal-alpha-cho-oac

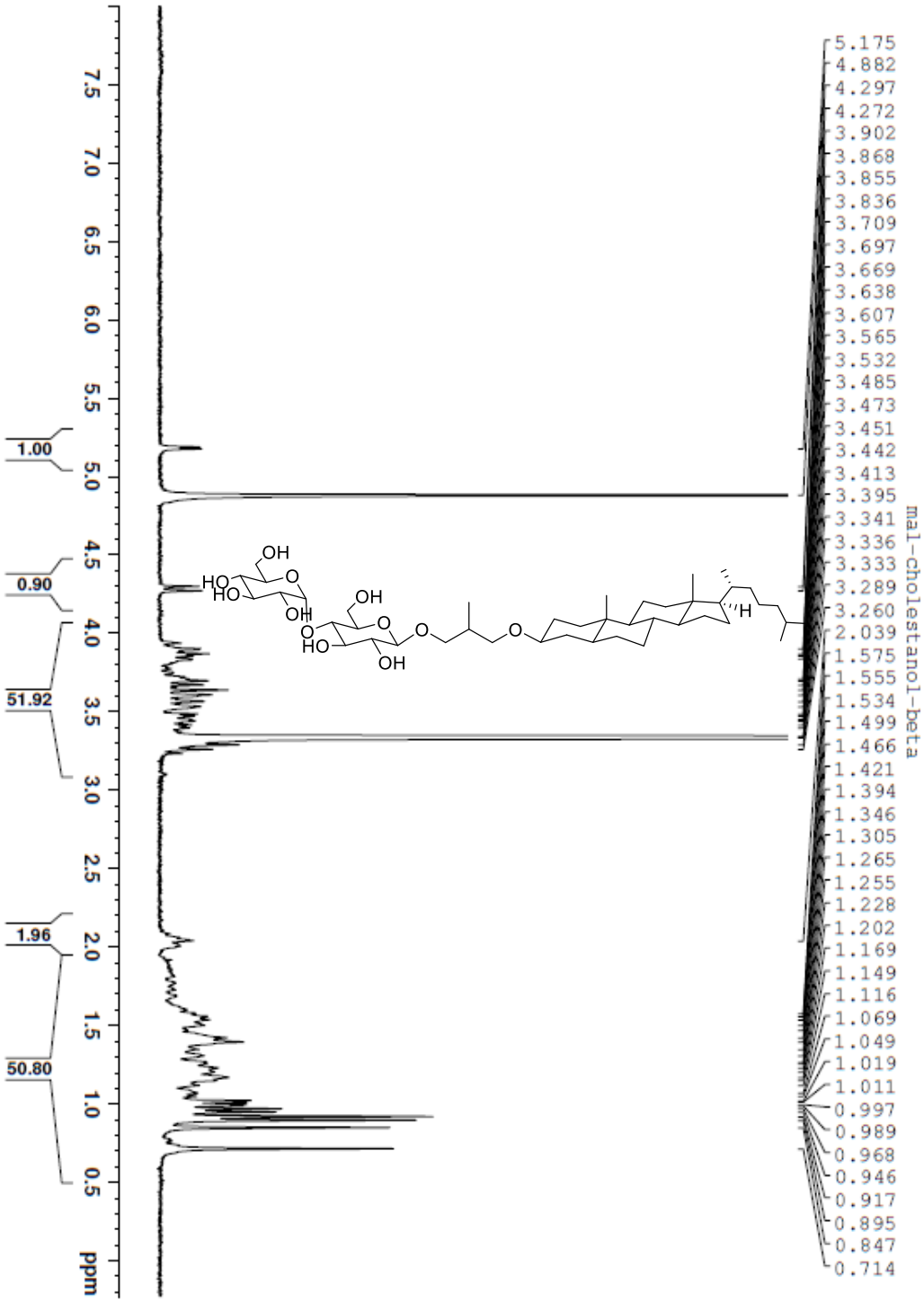
1.00
0.90
51.92
1.96
50.80
7.5
7.0
6.5
6.0
5.5
5.0
4.5
4.0
3.5
3.0
2.5
2.0
1.5
1.0
0.5
ppm
OH
HO
HO
O
OH
OH
O
O
HO
OH
O
O
H
5.175
4.882
4.297
4.272
3.902
3.868
3.855
3.836
3.709
3.697
3.669
3.638
3.607
3.565
3.532
3.485
3.473
3.451
3.442
3.413
3.395
3.341
3.336
3.333
3.289
3.260
2.039
1.575
1.555
1.534
1.499
1.466
1.421
1.394
1.346
1.305
1.265
1.255
1.228
1.202
1.169
1.149
1.116
1.069
1.049
1.019
1.011
0.997
0.989
0.968
0.946
0.917
0.895
0.847
0.714
mal-cholestanol-beta

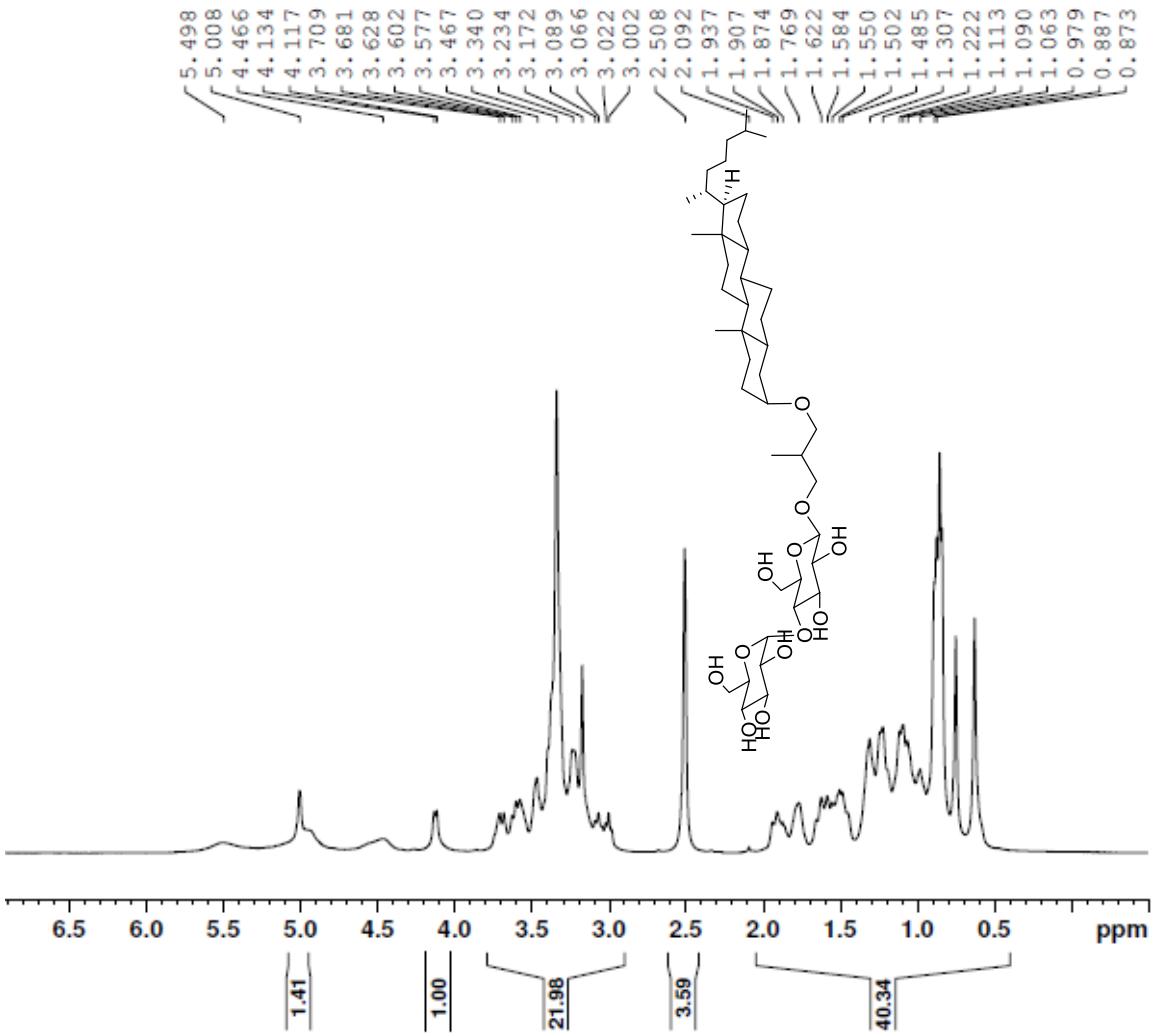

alpha-cholestanol-mal

```
Current Data Parameters
NAME      alpha-cholestanol-mal
EXPNO                         1
PROCNO                        1

F2 - Acquisition Parameters
Date_              20140620
Time                  16.26
INSTRUM               spect
PROBHD    5 mm CPPBBO BB
PULPROG                zg30
TD                    65536
SOLVENT                DMSO
NS                       16
DS                        2
SWH                8012.820 Hz
FIDRES             0.122266 Hz
AQ                 4.0894465 sec
RG                     66.01
DW                    62.400 usec
DE                    10.00 usec
TE                    298.0 K
D1              1.00000000 sec
TD0                       1

======== CHANNEL f1 ========
SFO1            400.1324710 MHz
NUC1                    1H
P1                    12.00 usec
PLW1             8.80000019 W

F2 - Processing parameters
SI                    65536
SF              400.1300000 MHz
WDW                     EM
SSB         0
LB                     0.30 Hz
GB          0
PC                     1.00
```

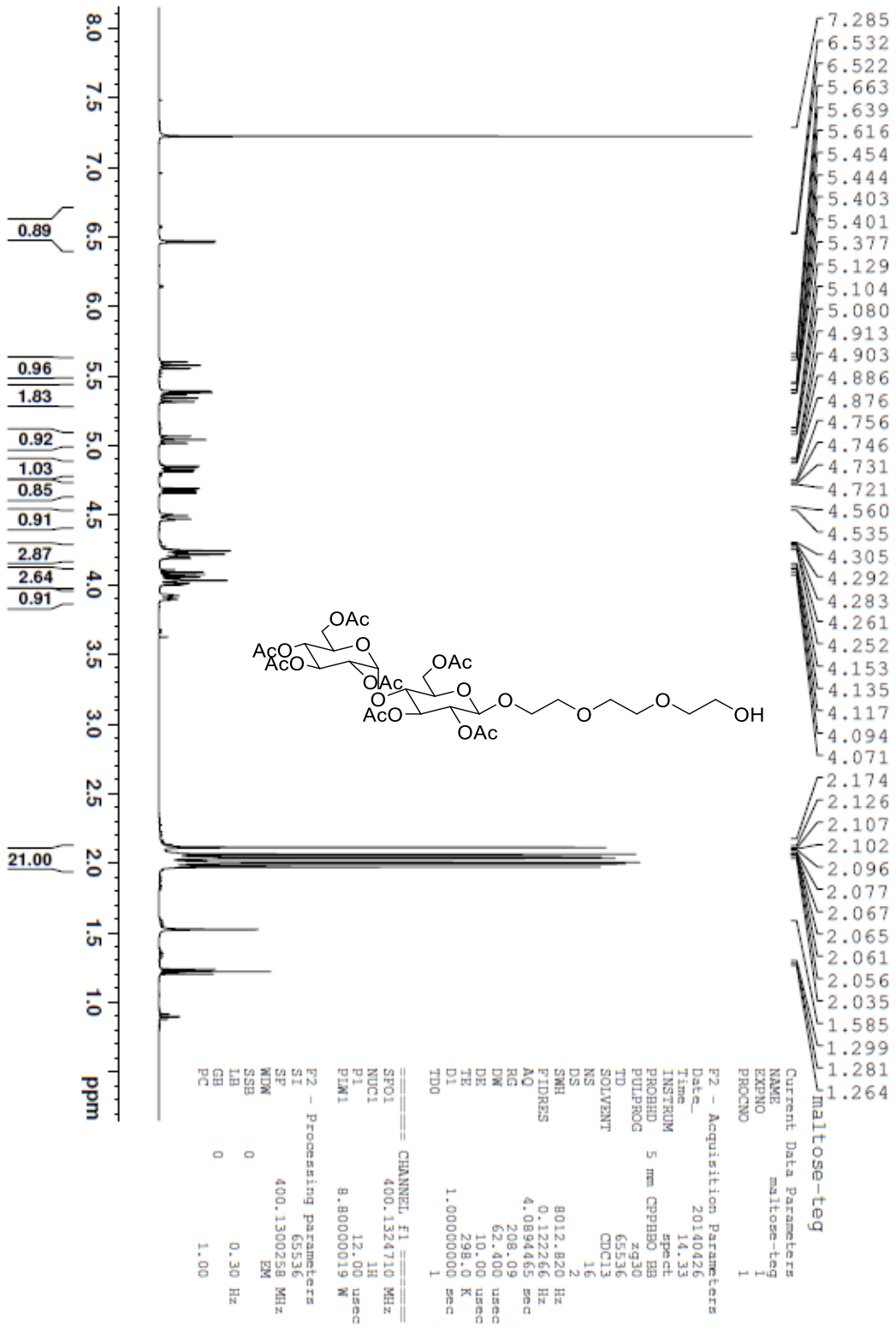
7.285
6.532
6.522
5.663
5.639
5.616
5.454
5.444
5.403
5.401
5.377
5.129
5.104
5.080
4.913
4.903
4.886
4.876
4.756
4.746
4.731
4.721
4.560
4.535
4.305
4.292
4.283
4.261
4.252
4.153
4.135
4.117
4.094
4.071
2.174
2.126
2.107
2.102
2.096
2.077
2.067
2.065
2.061
2.056
2.035
1.585
1.299
1.281
1.264
maltose-teg
Current Data Parameters
NAME maltose-teg
EXPNO 1
PROCNO 1
F2 - Acquisition Parameters
Date_ 20140426
Time 14.33
INSTRUM spect
PROBHD 5 mm CPPBBO BB
PULPROG zg30
TD 65536
SOLVENT CDCl3
NS 16
DS 2
SWH 8012.820 Hz
FIDRES 0.122266 Hz
AQ 4.0894465 sec
RG 208.09
DW 62.400 usec
DE 10.00 usec
TE 298.0 K
D1 1.00000000 sec
TD0 1
======== CHANNEL f1 ========
SFO1 400.1324710 MHz
NUC1 1H
P1 12.00 usec
PLW1 8.80000019 W
F2 - Processing parameters
SI 65536
SF 400.1300258 MHz
WDW EM
SSB 0
LB 0.30 Hz
GB 0
PC 1.00
0.89
0.96
1.83
0.92
1.03
0.85
0.91
2.87
2.64
0.91
21.00
8.0
7.5
7.0
6.5
6.0
5.5
5.0
4.5
4.0
3.5
3.0
2.5
2.0
1.5
1.0
ppm
OAc
AcO
AcO
OAc
OAc
AcO
O
O
O
O
O
O
O
OH

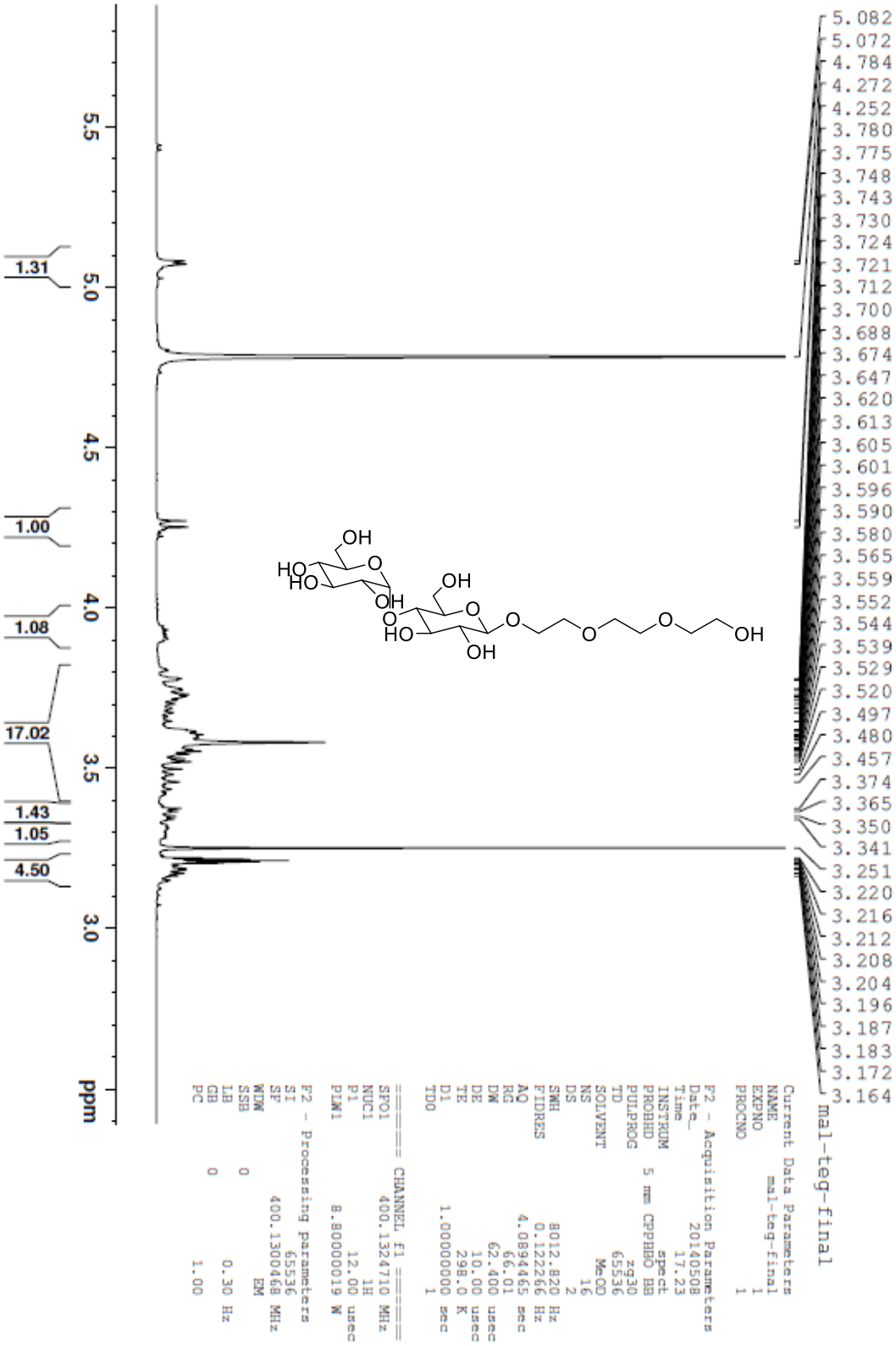
mal-teg-final
5.082
5.072
4.784
4.272
4.252
3.780
3.775
3.748
3.743
3.730
3.724
3.721
3.712
3.700
3.688
3.674
3.647
3.620
3.613
3.605
3.601
3.596
3.590
3.580
3.565
3.559
3.552
3.544
3.539
3.529
3.520
3.497
3.480
3.457
3.374
3.365
3.350
3.341
3.251
3.220
3.216
3.212
3.208
3.204
3.196
3.187
3.183
3.172
3.164
Current Data Parameters
NAME mal-teg-final
EXPNO 1
PROCNO 1
F2 - Acquisition Parameters
Date_ 20140508
Time 17.23
INSTRUM spect
PROBHD 5 mm CPPBBO BB
PULPROG zg30
TD 65536
SOLVENT MeOD
NS 16
DS 2
SWH 8012.820 Hz
FIDRES 0.122266 Hz
AQ 4.0894465 sec
RG 66.01
DW 62.400 usec
DE 10.00 usec
TE 298.0 K
D1 1.00000000 sec
TD0 1
======== CHANNEL f1 ========
SFO1 400.1324710 MHz
NUC1 1H
P1 12.00 usec
PLW1 8.80000019 W
F2 - Processing parameters
SI 65536
SF 400.1300468 MHz
WDW EM
SSB 0
LB 0.30 Hz
GB 0
PC 1.00
1.31
1.00
1.08
17.02
1.43
1.05
4.50
5.5
5.0
4.5
4.0
3.5
3.0
ppm
OH
HO
HO
O
OH
O
HO
OH
O
O
O
O
OH

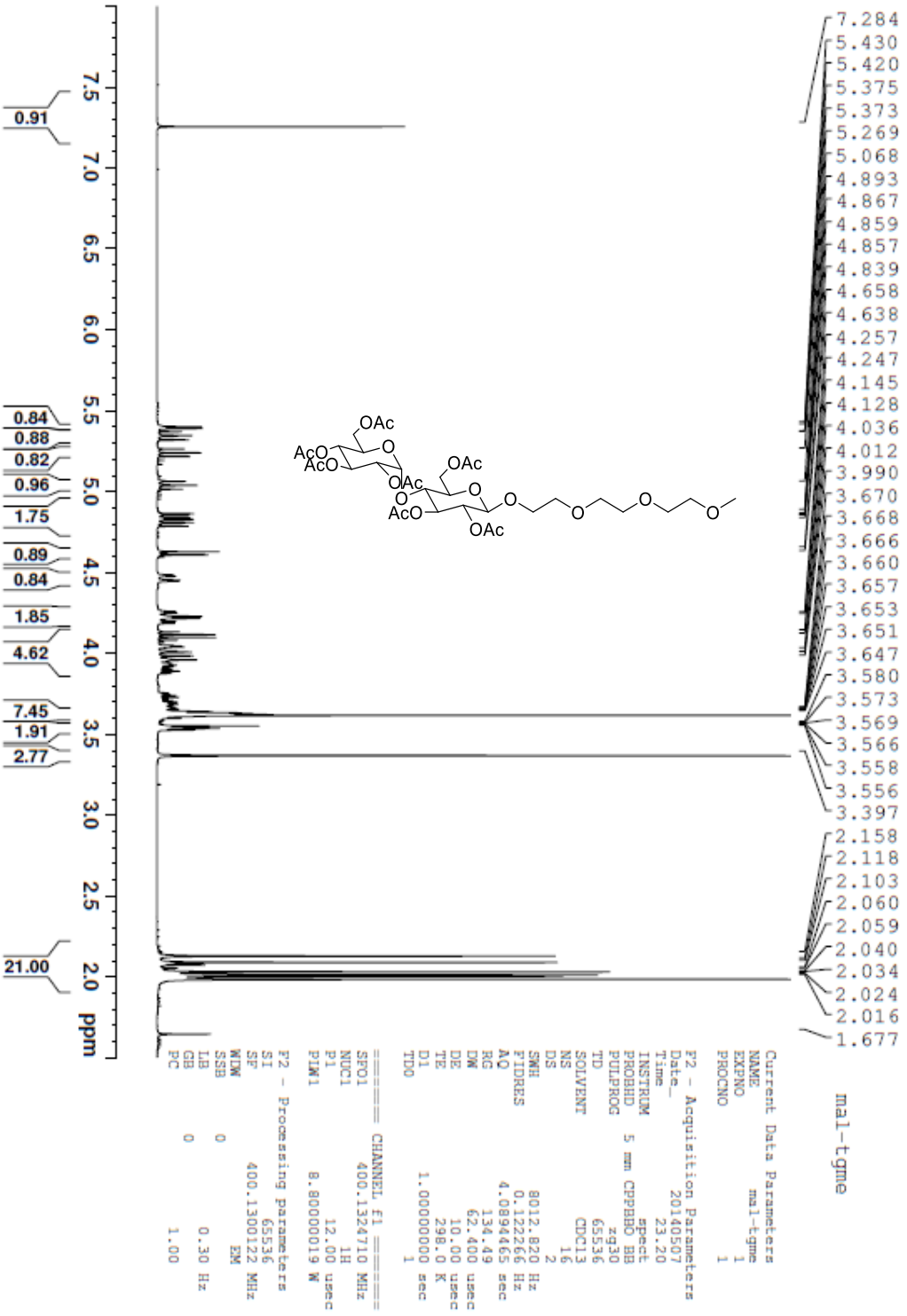
7.284
5.430
5.420
5.375
5.373
5.269
5.068
4.893
4.867
4.859
4.857
4.839
4.658
4.638
4.257
4.247
4.145
4.128
4.036
4.012
3.990
3.670
3.668
3.666
3.660
3.657
3.653
3.651
3.647
3.580
3.573
3.569
3.566
3.558
3.556
3.397
2.158
2.118
2.103
2.060
2.059
2.040
2.034
2.024
2.016
1.677
mal-tgme
0.91
0.84
0.88
0.82
0.96
1.75
0.89
0.84
1.85
4.62
7.45
1.91
2.77
21.00
ppm
OAc
AcO
AcO
OAc
OAc
AcO
OAc
O
Current Data Parameters
NAME mal-tgme
EXPNO 1
PROCNO 1
F2 - Acquisition Parameters
Date_ 20140507
Time 23.20
INSTRUM spect
PROBHD 5 mm CPPBBO BB
PULPROG zg30
TD 65536
SOLVENT CDCl3
NS 16
DS 2
SWH 8012.820 Hz
FIDRES 0.122266 Hz
AQ 4.0894465 sec
RG 134.49
DW 62.400 usec
DE 10.00 usec
TE 298.0 K
D1 1.00000000 sec
TD0 1
======== CHANNEL f1 ========
SFO1 400.1324710 MHz
NUC1 1H
P1 12.00 usec
PLW1 8.80000019 W
F2 - Processing parameters
SI 65536
SF 400.1300122 MHz
WDW EM
SSB 0
LB 0.30 Hz
GB 0
PC 1.00

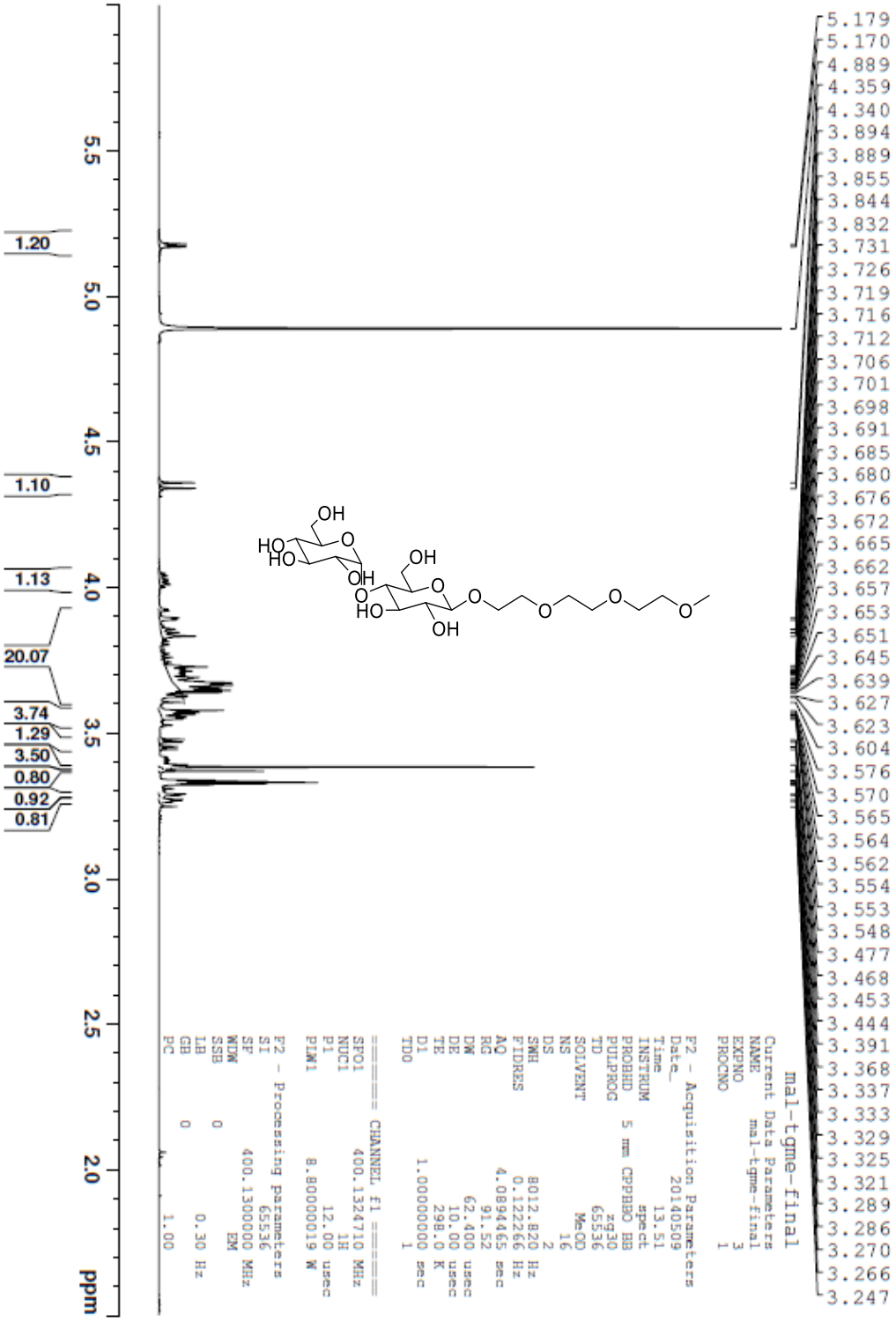
5.179
5.170
4.889
4.359
4.340
3.894
3.889
3.855
3.844
3.832
3.731
3.726
3.719
3.716
3.712
3.706
3.701
3.698
3.691
3.685
3.680
3.676
3.672
3.665
3.662
3.657
3.653
3.651
3.645
3.639
3.627
3.623
3.604
3.576
3.570
3.565
3.564
3.562
3.554
3.553
3.548
3.477
3.468
3.453
3.444
3.391
3.368
3.337
3.333
3.329
3.325
3.321
3.289
3.286
3.270
3.266
3.247
mal-tgme-final
Current Data Parameters
NAME mal-tgme-final
EXPNO 3
PROCNO 1
F2 - Acquisition Parameters
Date_ 20140509
Time 13.51
INSTRUM spect
PROBHD 5 mm CPPBBO BB
PULPROG zg30
TD 65536
SOLVENT MeOD
NS 16
DS 2
SWH 8012.820 Hz
FIDRES 0.122266 Hz
AQ 4.0894465 sec
RG 91.52
DW 62.400 usec
DE 10.00 usec
TE 298.0 K
D1 1.00000000 sec
TD0 1
======== CHANNEL f1 ========
SFO1 400.1324710 MHz
NUC1 1H
P1 12.00 usec
PLW1 8.80000019 W
F2 - Processing parameters
SI 65536
SP 400.1300000 MHz
WDW EM
SSB 0
LB 0.30 Hz
GB 0
PC 1.00
1.20
1.10
1.13
20.07
3.74
1.29
3.50
0.80
0.92
0.81
5.5
5.0
4.5
4.0
3.5
3.0
2.5
2.0
ppm
OH
HO
HO
O
OH
OH
O
O
HO
OH
O
O
O
O

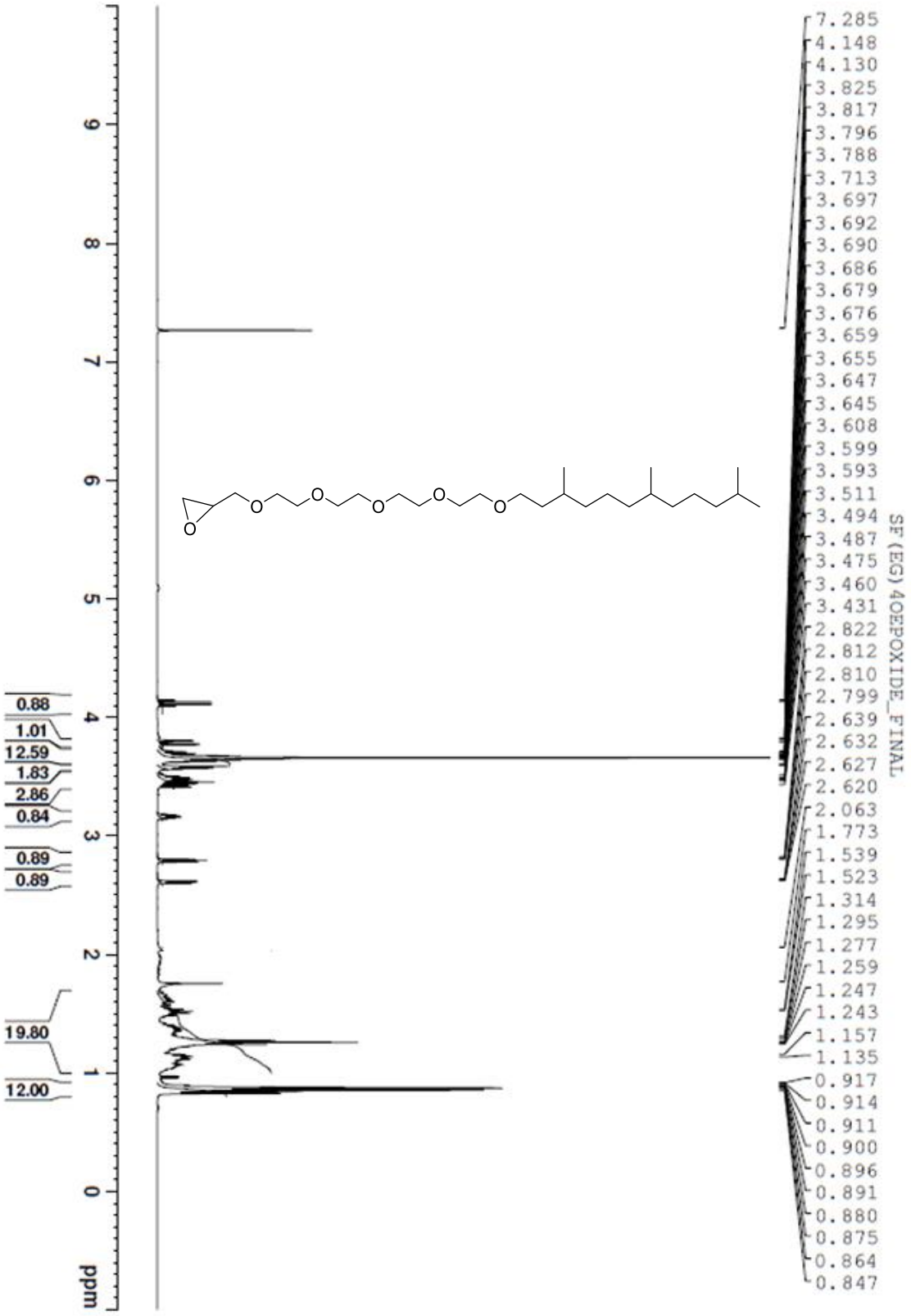
7.285
4.148
4.130
3.825
3.817
3.796
3.788
3.713
3.697
3.692
3.690
3.686
3.679
3.676
3.659
3.655
3.647
3.645
3.608
3.599
3.593
3.511
3.494
3.487
3.475
3.460
3.431
2.822
2.812
2.810
2.799
2.639
2.632
2.627
2.620
2.063
1.773
1.539
1.523
1.314
1.295
1.277
1.259
1.247
1.243
1.157
1.135
0.917
0.914
0.911
0.900
0.896
0.891
0.880
0.875
0.864
0.847
SF(EG)4OEPOXIDE_FINAL
0.88
1.01
12.59
1.83
2.86
0.84
0.89
0.89
19.80
12.00
O
O
O
O
O
O
ppm

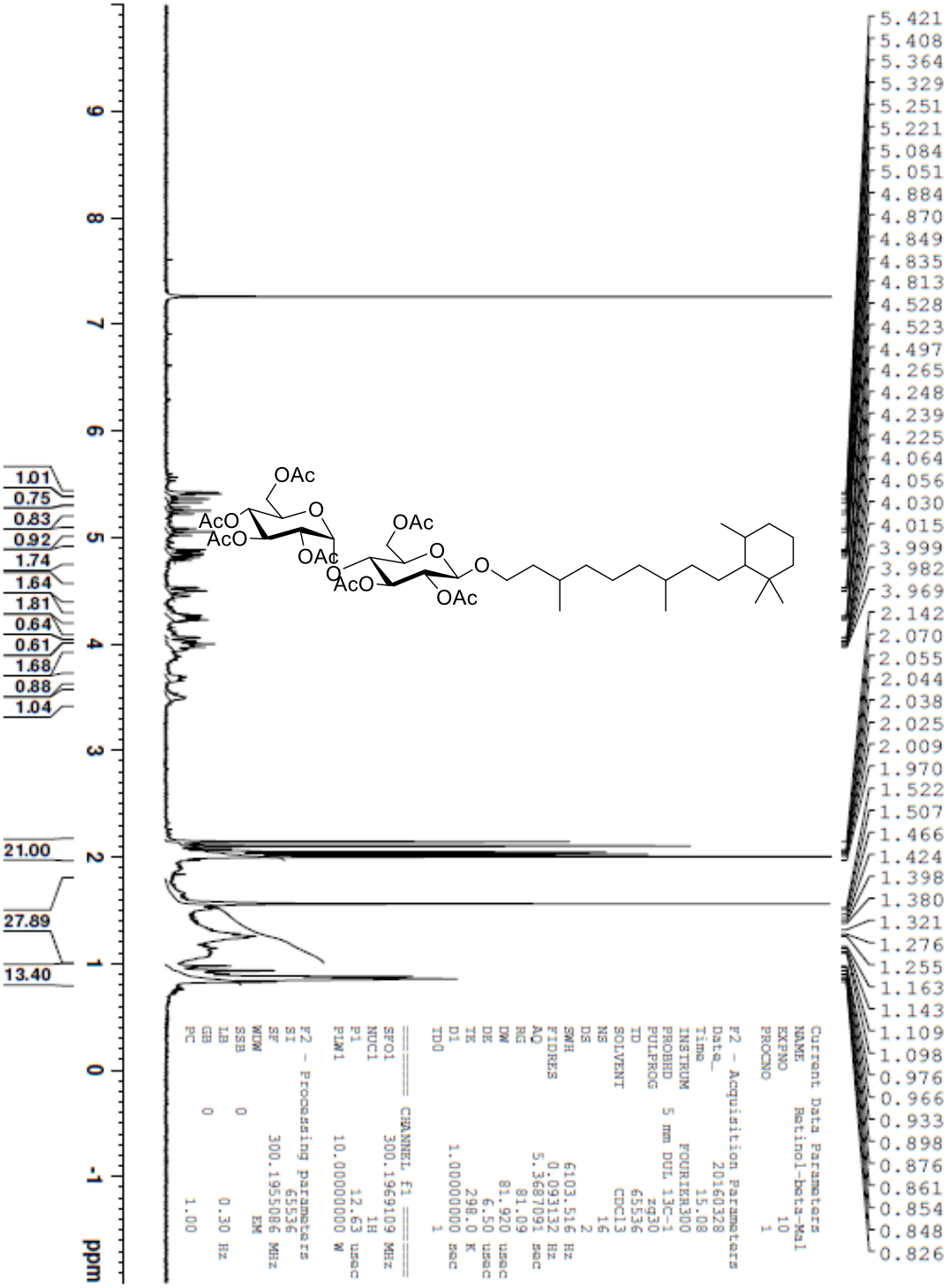
OAc
AcO
AcO
OAc
OAc
AcO
OAc
O
O
1.01
0.75
0.83
0.92
1.74
1.64
1.81
0.64
0.61
1.68
0.88
1.04
21.00
27.89
13.40
9
8
7
6
5
4
3
2
1
0
-1
ppm
5.421
5.408
5.364
5.329
5.251
5.221
5.084
5.051
4.884
4.870
4.849
4.835
4.813
4.528
4.523
4.497
4.265
4.248
4.239
4.225
4.064
4.056
4.030
4.015
3.999
3.982
3.969
2.142
2.070
2.055
2.044
2.038
2.025
2.009
1.970
1.522
1.507
1.466
1.424
1.398
1.380
1.321
1.276
1.255
1.163
1.143
1.109
1.098
0.976
0.966
0.933
0.898
0.876
0.861
0.854
0.848
0.826
Current Data Parameters
NAME Retinol-beta-Mal
EXPNO 10
PROCNO 1
F2 - Acquisition Parameters
Date_ 20160328
Time 15.08
INSTRUM FOURIER300
PROBHD 5 mm DUL 13c-1
PULPROG zg30
TD 65536
SOLVENT CDCl3
NS 16
DS 2
SWH 6103.516 Hz
FIDRES 0.093132 Hz
AQ 5.3687091 sec
RG 81.09
DW 81.920 usec
DE 6.50 usec
TE 298.0 K
D1 1.00000000 sec
TD0 1
======== CHANNEL f1 ========
SFO1 300.1969109 MHz
NUC1 1H
P1 12.63 usec
PLW1 10.00000000 W
F2 - Processing parameters
SI 65536
SF 300.1955086 MHz
WDW EM
SSB 0
LB 0.30 Hz
GB 0
PC 1.00

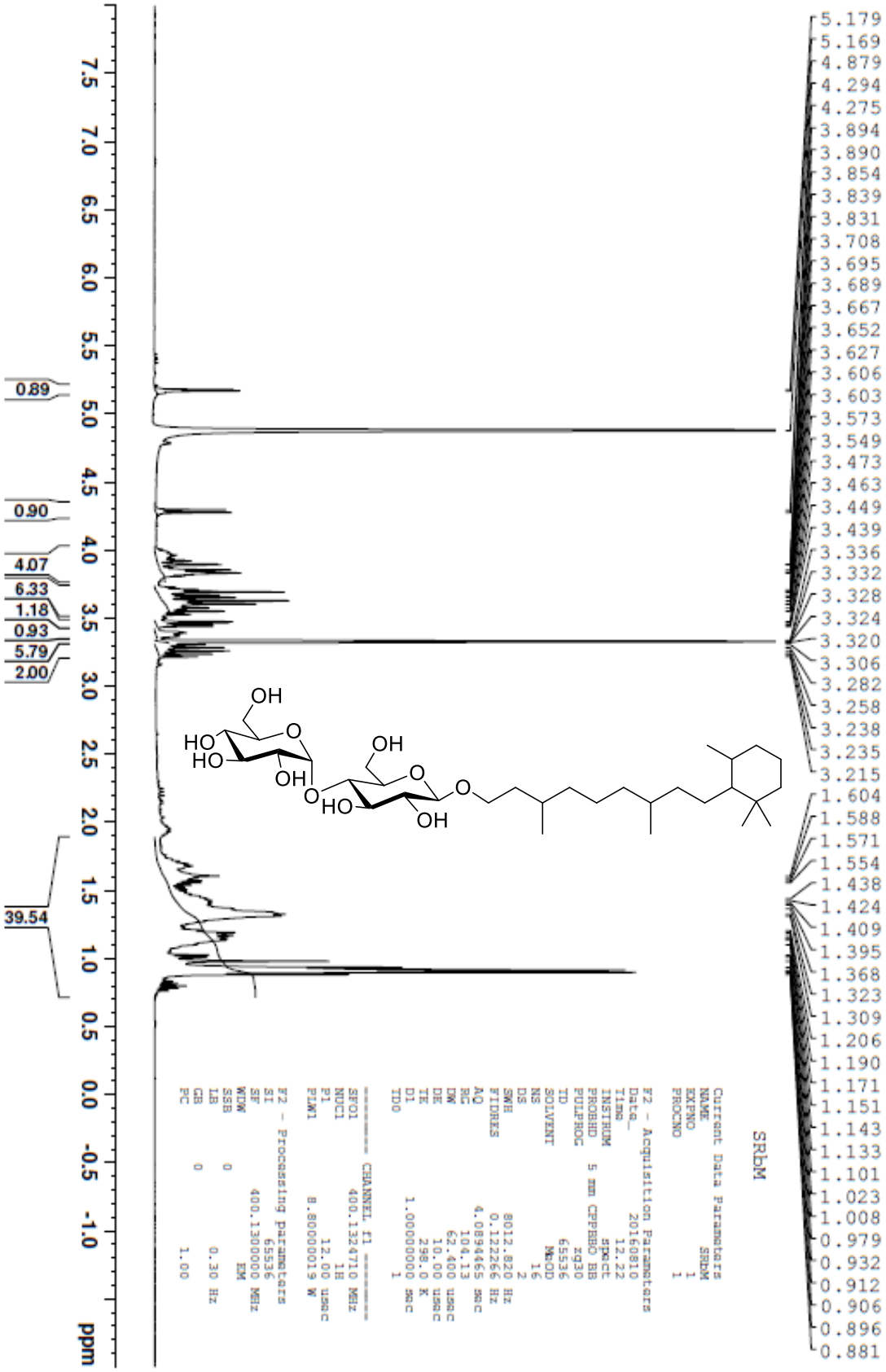
0.89
0.90
4.07
6.33
1.18
0.93
5.79
2.00
39.54
ppm
SRbM
OH
HO
HO
OH
O
O
OH
HO
OH
O
O
5.179
5.169
4.879
4.294
4.275
3.894
3.890
3.854
3.839
3.831
3.708
3.695
3.689
3.667
3.652
3.627
3.606
3.603
3.573
3.549
3.473
3.463
3.449
3.439
3.336
3.332
3.328
3.324
3.320
3.306
3.282
3.258
3.238
3.235
3.215
1.604
1.588
1.571
1.554
1.438
1.424
1.409
1.395
1.368
1.323
1.309
1.206
1.190
1.171
1.151
1.143
1.133
1.101
1.023
1.008
0.979
0.932
0.912
0.906
0.896
0.881

WL.1.27 diOTs SM Col. @400

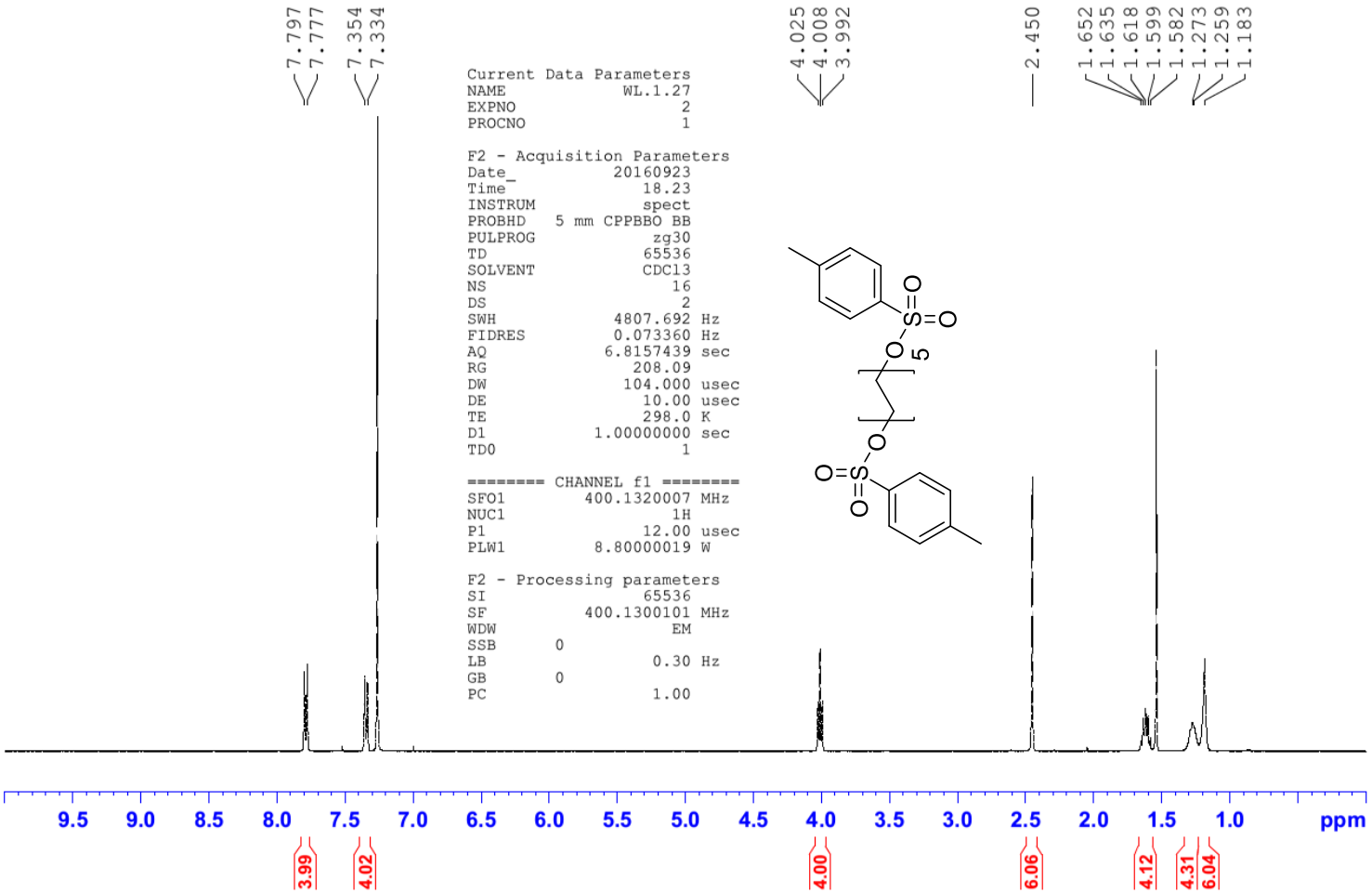

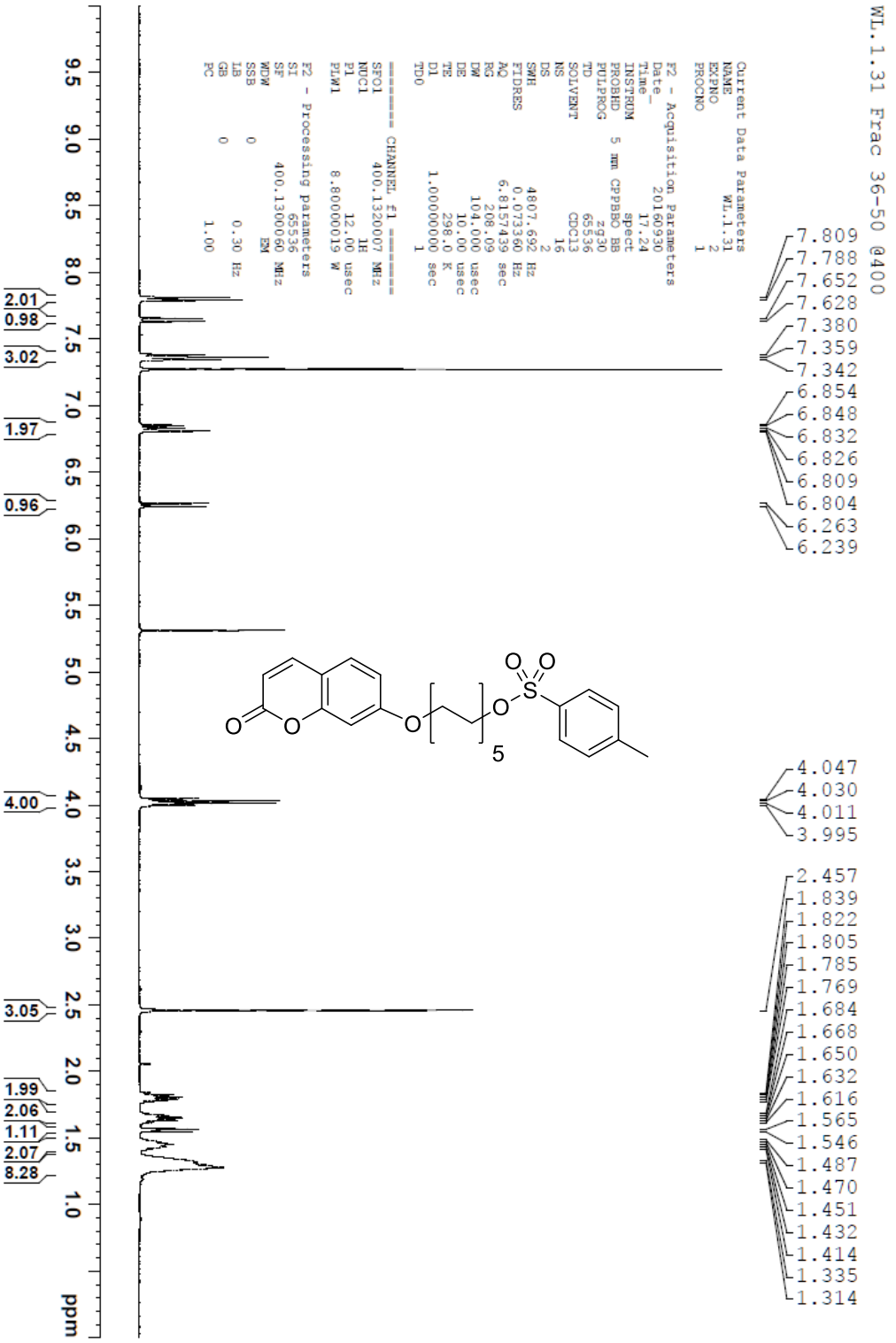
WL.1.31 Frac 36-50 @400
7.809
7.788
7.652
7.628
7.380
7.359
7.342
6.854
6.848
6.832
6.826
6.809
6.804
6.263
6.239
4.047
4.030
4.011
3.995
2.457
1.839
1.822
1.805
1.785
1.769
1.684
1.668
1.650
1.632
1.616
1.565
1.546
1.487
1.470
1.451
1.432
1.414
1.335
1.314
2.01
0.98
3.02
1.97
0.96
4.00
3.05
1.99
2.06
1.11
2.07
8.28
ppm
5

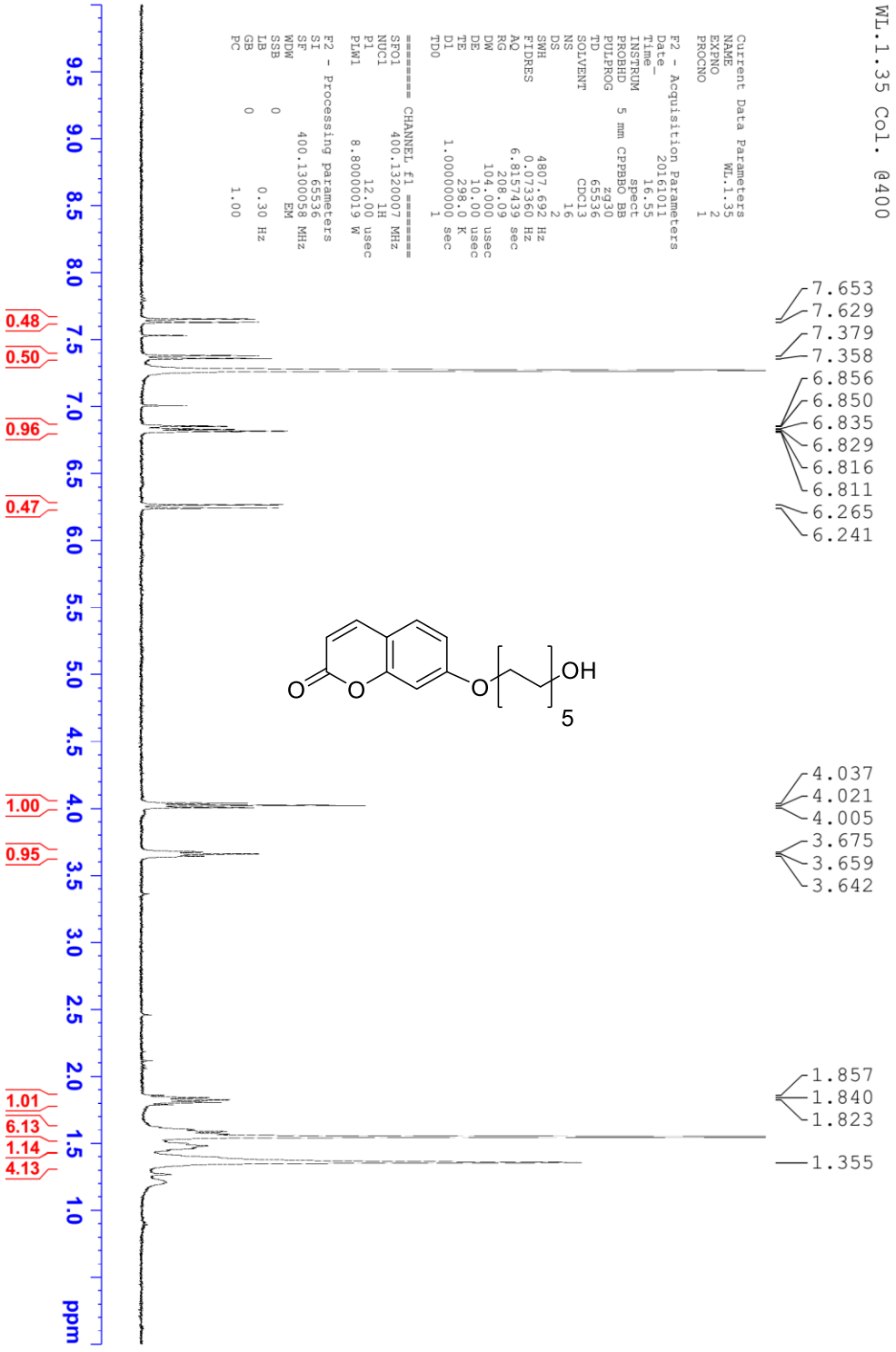
WL.1.35 Col. @400
7.653
7.629
7.379
7.358
6.856
6.850
6.835
6.829
6.816
6.811
6.265
6.241
4.037
4.021
4.005
3.675
3.659
3.642
1.857
1.840
1.823
1.355
0.48
0.50
0.96
0.47
1.00
0.95
1.01
6.13
1.14
4.13
ppm
OH
5

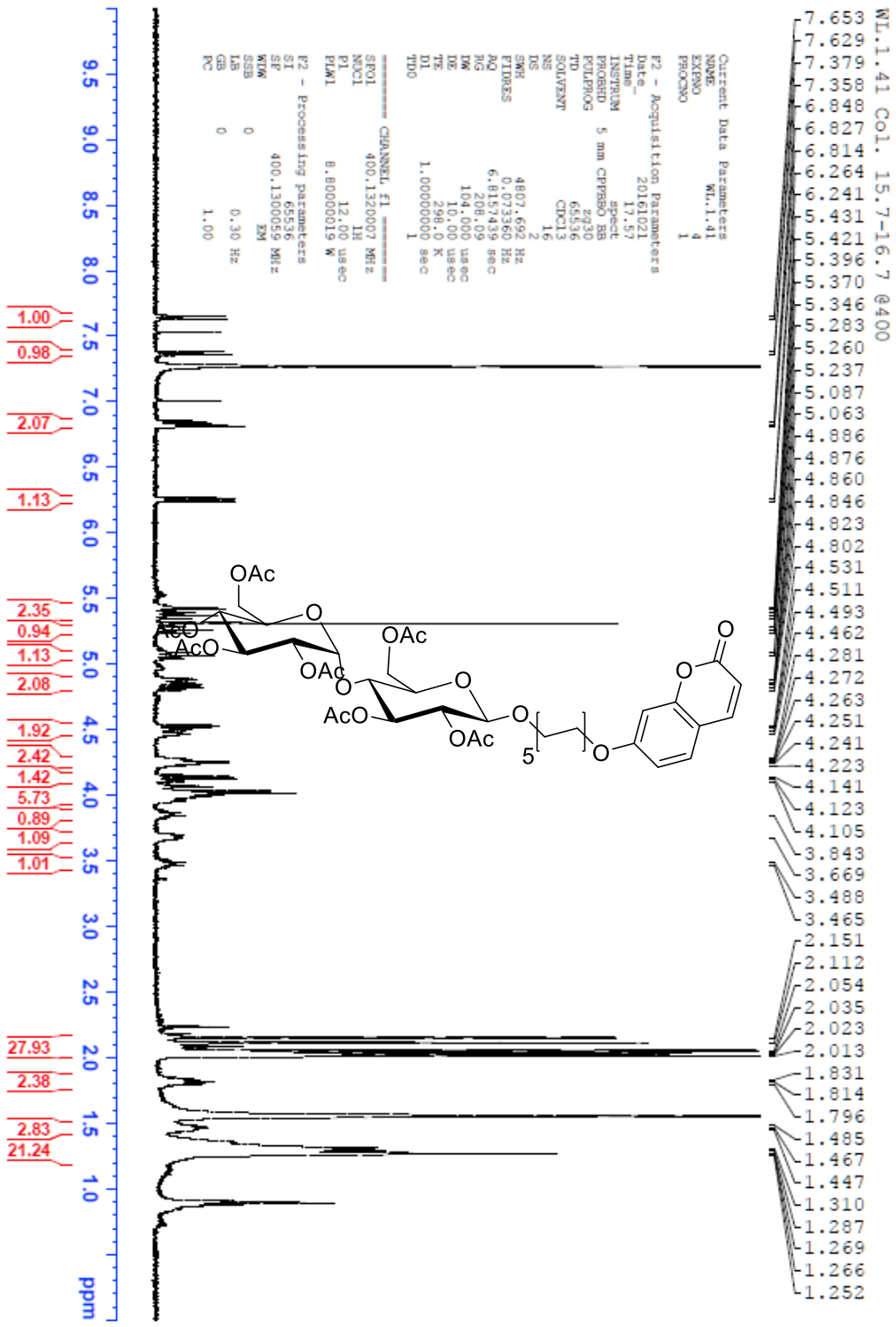
WL.1.41 Col. 15.7-16.7 @400
7.653
7.629
7.379
7.358
6.848
6.827
6.814
6.264
6.241
5.431
5.421
5.396
5.370
5.346
5.283
5.260
5.237
5.087
5.063
4.886
4.876
4.860
4.846
4.823
4.802
4.531
4.511
4.493
4.462
4.281
4.272
4.263
4.251
4.241
4.223
4.141
4.123
4.105
3.843
3.669
3.488
3.465
2.151
2.112
2.054
2.035
2.023
2.013
1.831
1.814
1.796
1.485
1.467
1.447
1.310
1.287
1.269
1.266
1.252
Current Data Parameters
NAME WL.1.41
EXPNO 4
PROCNO 1
F2 - Acquisition Parameters
Date_ 20161021
Time 17.57
INSTRUM spect
PROBHD 5 mm CPPBBO BB
PULPROG zg30
TD 65536
SOLVENT CDCl3
NS 16
DS 2
SWH 4807.692 Hz
FIDRES 0.073360 Hz
AQ 6.8157439 sec
RG 208.09
DW 104.000 usec
DE 10.00 usec
TE 298.0 K
D1 1.00000000 sec
TD0 1
======== CHANNEL f1 ========
SFO1 400.1320007 MHz
NUC1 1H
P1 12.00 usec
PLW1 8.80000019 W
F2 - Processing parameters
SI 65536
SF 400.1300059 MHz
WDW EM
SSB 0
LB 0.30 Hz
GB 0
PC 1.00
1.00
0.98
2.07
1.13
2.35
0.94
1.13
2.08
1.92
2.42
1.42
5.73
0.89
1.09
1.01
27.93
2.38
2.83
21.24
ppm
OAc
AcO
AcO
OAc
O
O
AcO
OAc
OAc
O
O
O
O
5
O
O

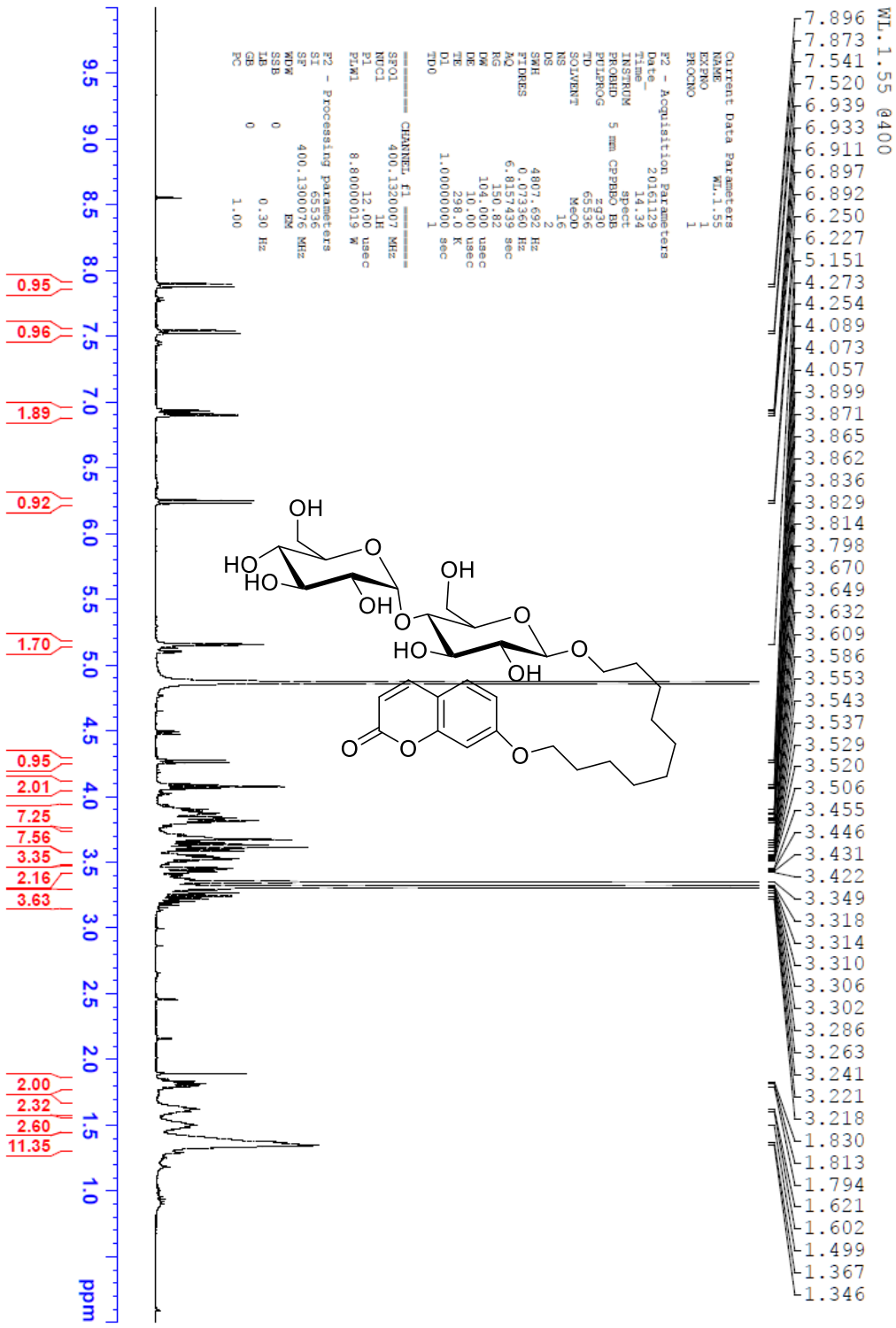
WL.1.55 @400
7.896
7.873
7.541
7.520
6.939
6.933
6.911
6.897
6.892
6.250
6.227
5.151
4.273
4.254
4.089
4.073
4.057
3.899
3.871
3.865
3.862
3.836
3.829
3.814
3.798
3.670
3.649
3.632
3.609
3.586
3.553
3.543
3.537
3.529
3.520
3.506
3.455
3.446
3.431
3.422
3.349
3.318
3.314
3.310
3.306
3.302
3.286
3.263
3.241
3.221
3.218
1.830
1.813
1.794
1.621
1.602
1.499
1.367
1.346
0.95
0.96
1.89
0.92
1.70
0.95
2.01
7.25
7.56
3.35
2.16
3.63
2.00
2.32
2.60
11.35
ppm
OH
HO
HO
O
OH
O
OH
HO
O
OH
O
O
O
O

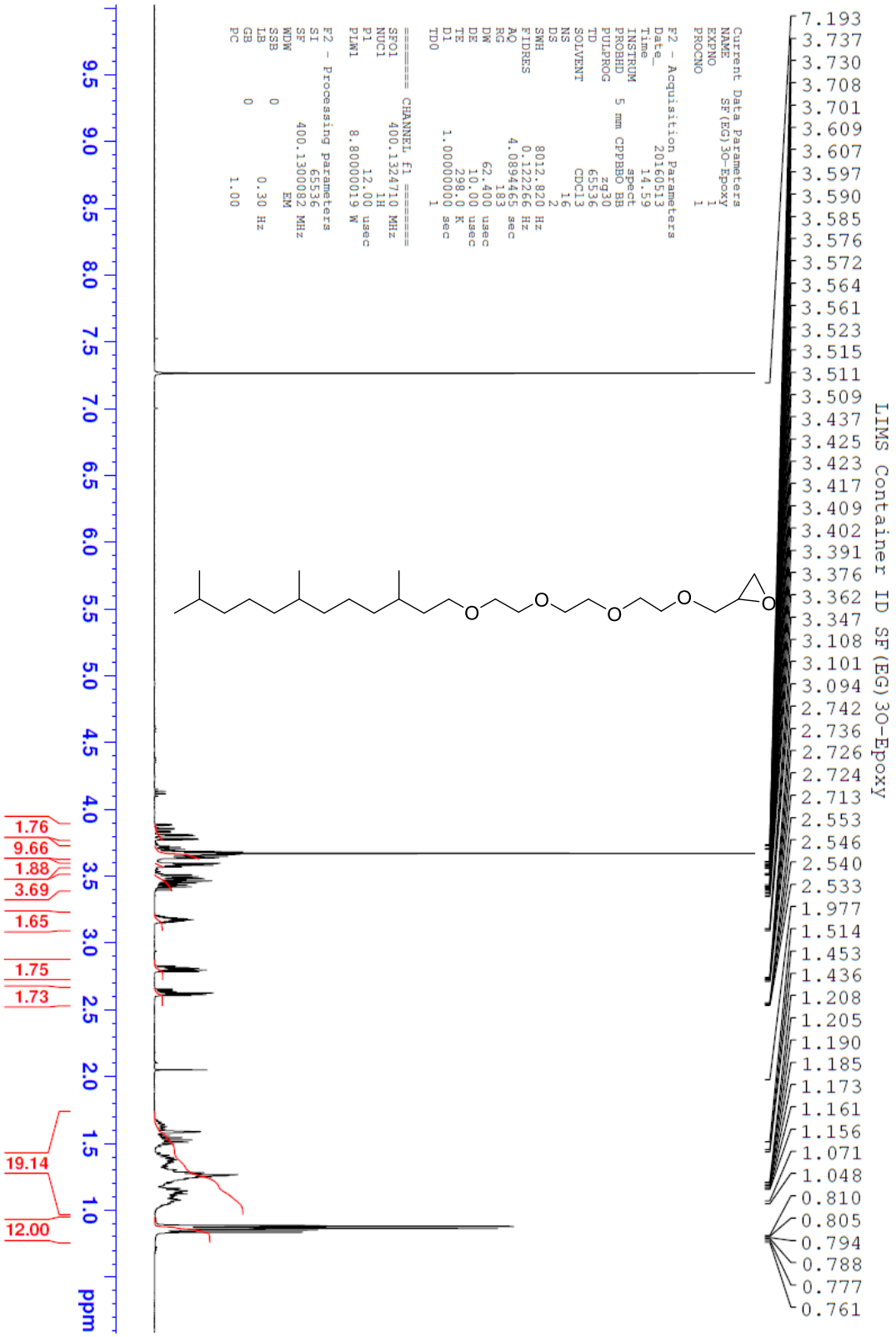
LIMS Container ID SF(EG)3O-Epoxy
7.193
3.737
3.730
3.708
3.701
3.609
3.607
3.597
3.590
3.585
3.576
3.572
3.564
3.561
3.523
3.515
3.511
3.509
3.437
3.425
3.423
3.417
3.409
3.402
3.391
3.376
3.362
3.347
3.108
3.101
3.094
2.742
2.736
2.726
2.724
2.713
2.553
2.546
2.540
2.533
1.977
1.514
1.453
1.436
1.208
1.205
1.190
1.185
1.173
1.161
1.156
1.071
1.048
0.810
0.805
0.794
0.788
0.777
0.761
Current Data Parameters
NAME SF(EG)3O-Epoxy
EXPNO 1
PROCNO 1
F2 - Acquisition Parameters
Date_ 20160513
Time 14.59
INSTRUM spect
PROBHD 5 mm CPPBBO BB
PULPROG zg30
TD 65536
SOLVENT CDCl3
NS 16
DS 2
SWH 8012.820 Hz
FIDRES 0.122266 Hz
AQ 4.0894465 sec
RG 183
DW 62.400 usec
DE 10.00 usec
TE 298.0 K
D1 1.00000000 sec
TD0 1
======== CHANNEL f1 ========
SFO1 400.1324710 MHz
NUC1 1H
P1 12.00 usec
PLW1 8.80000019 W
F2 - Processing parameters
SI 65536
SF 400.1300082 MHz
WDW EM
SSB 0
LB 0.30 Hz
GB 0
PC 1.00
1.76
9.66
1.88
3.69
1.65
1.75
1.73
19.14
12.00
9.5 9.0 8.5 8.0 7.5 7.0 6.5 6.0 5.5 5.0 4.5 4.0 3.5 3.0 2.5 2.0 1.5 1.0
ppm

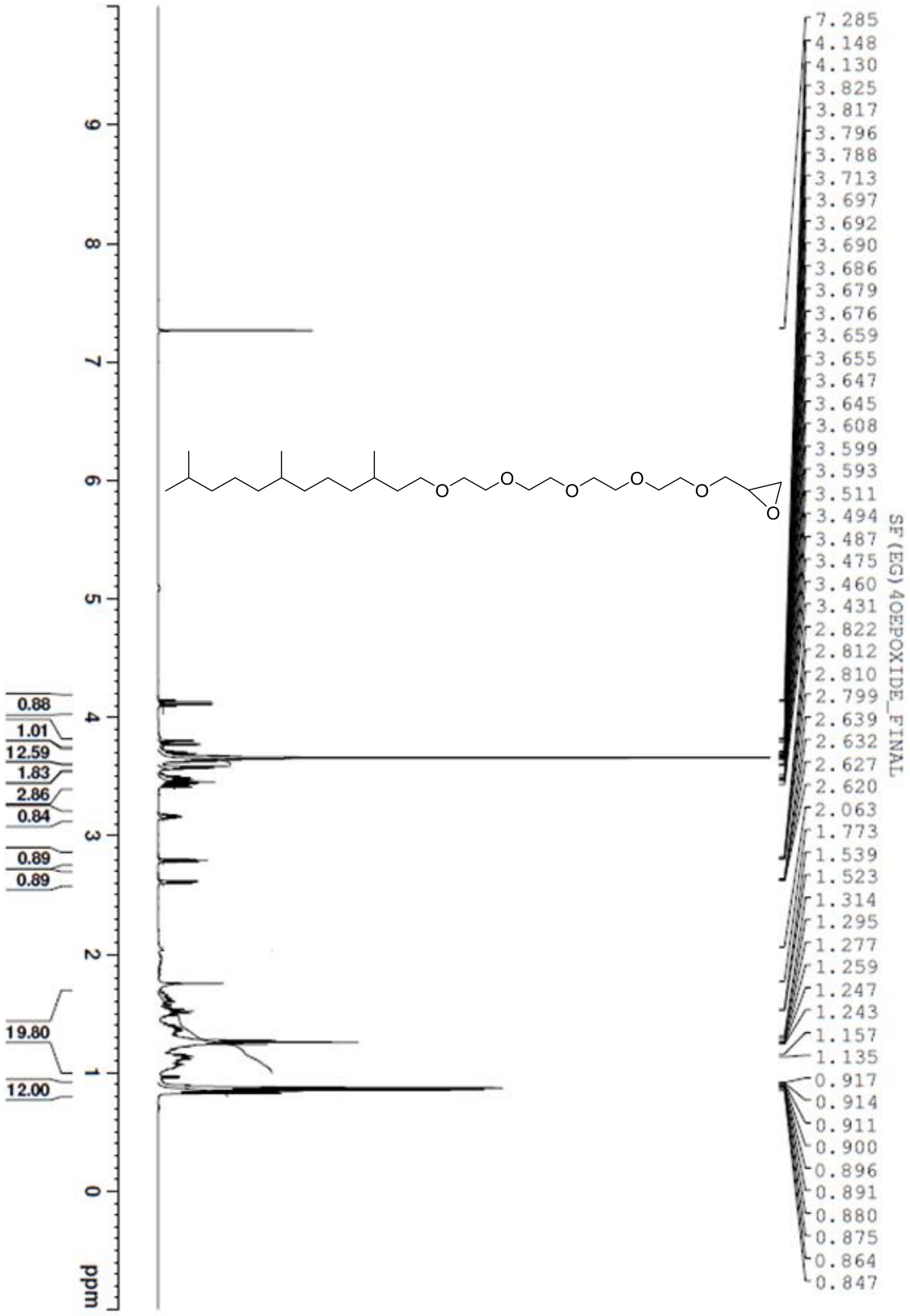
7.285
4.148
4.130
3.825
3.817
3.796
3.788
3.713
3.697
3.692
3.690
3.686
3.679
3.676
3.659
3.655
3.647
3.645
3.608
3.599
3.593
3.511
3.494
3.487
3.475
3.460
3.431
2.822
2.812
2.810
2.799
2.639
2.632
2.627
2.620
2.063
1.773
1.539
1.523
1.314
1.295
1.277
1.259
1.247
1.243
1.157
1.135
0.917
0.914
0.911
0.900
0.896
0.891
0.880
0.875
0.864
0.847
SF(EG)4OEPOXIDE_FINAL
0.88
1.01
12.59
1.83
2.86
0.84
0.89
0.89
19.80
12.00
O
O
O
O
O
O
ppm
9
8
7
6
5
4
3
2
1
0

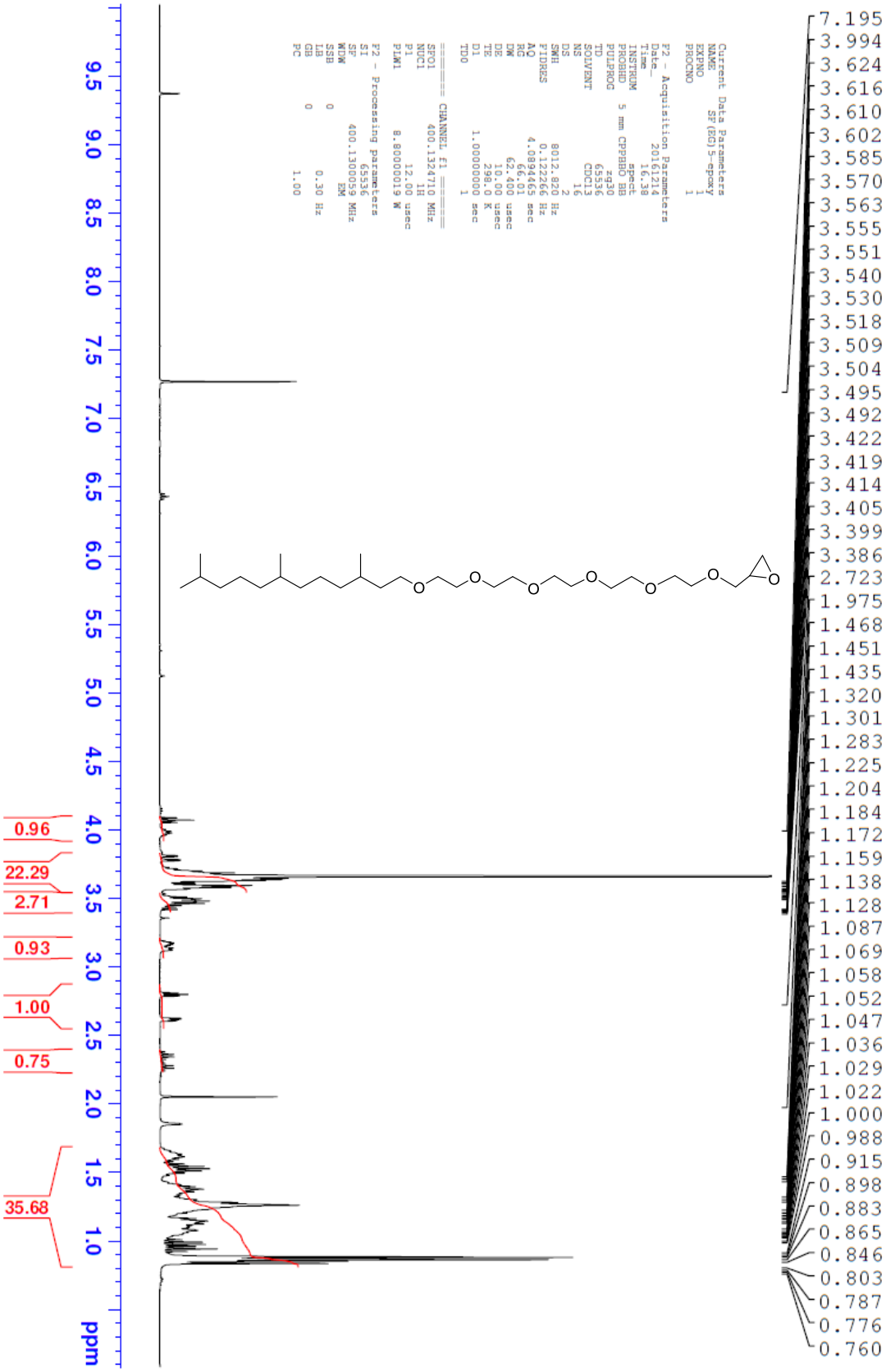
7.195
3.994
3.624
3.616
3.610
3.602
3.585
3.570
3.563
3.555
3.551
3.540
3.530
3.518
3.509
3.504
3.495
3.492
3.422
3.419
3.414
3.405
3.399
3.386
2.723
1.975
1.468
1.451
1.435
1.320
1.301
1.283
1.225
1.204
1.184
1.172
1.159
1.138
1.128
1.087
1.069
1.058
1.052
1.047
1.036
1.029
1.022
1.000
0.988
0.915
0.898
0.883
0.865
0.846
0.803
0.787
0.776
0.760
0.96
22.29
2.71
0.93
1.00
0.75
35.68
ppm

HRMS Spectra

Mass Spectrum List Report

Analysis Info

Analysis Name	G:\Data\apexdata050516\SRBM-OAc_pos_000001.d	Acquisition Date	5/5/2016 4:40:40 PM
Method	Neg_DOM_032112	Operator	Administrator
Sample Name	SRBM-OAc	Instrument	apex-IV
Comment	SRBM-OAc in 1:1 MeOH:THF with NaCl added		

Sample name: SRBM-OAc
Exact mass of $C_{46}H_{74}O_{18}Na^+$ = 937.476737 m/z
Exact mass Observed = 937.476395 m/z
Difference < -1.0 ppm

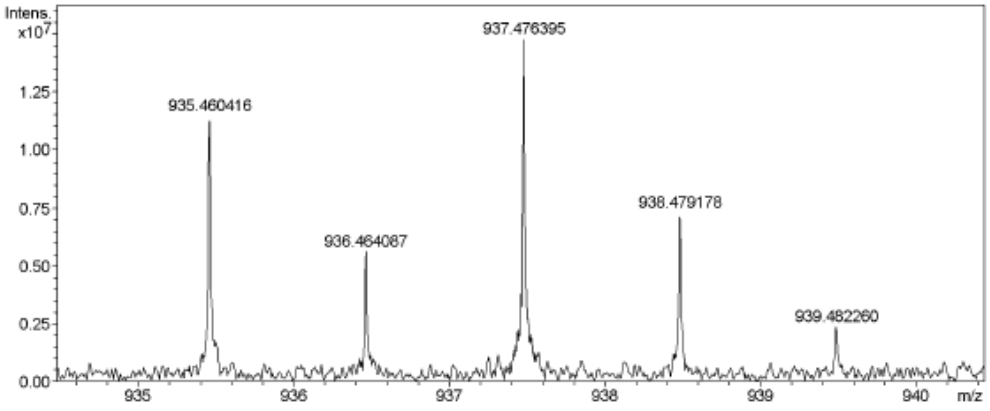

HRMS (ESI+): Cacld. for M^+: 937.476737, found: 937.476395

Mass Spectrum List Report

Analysis Info

Analysis Name	G:\Data\apexdata061716\Retinol-B-Mal_pos_000001.d	Acquisition Date	6/17/2016 5:40:19 PM
Method	Neg_DOM_032112	Operator	Administrator
Sample Name	Retinol-B-Mal	Instrument	apex-IV
Comment	Retinol-B-Mal in THF:MeOH with NaCl added		

Sample Name	Retinol-B-Mal		
Exact Mass of	$C_{32}H_{60}O_{11}Na^+$	= 643.402784	m/z
Mass Observed		= 643.402634	m/z
Difference < -1.0 ppm			

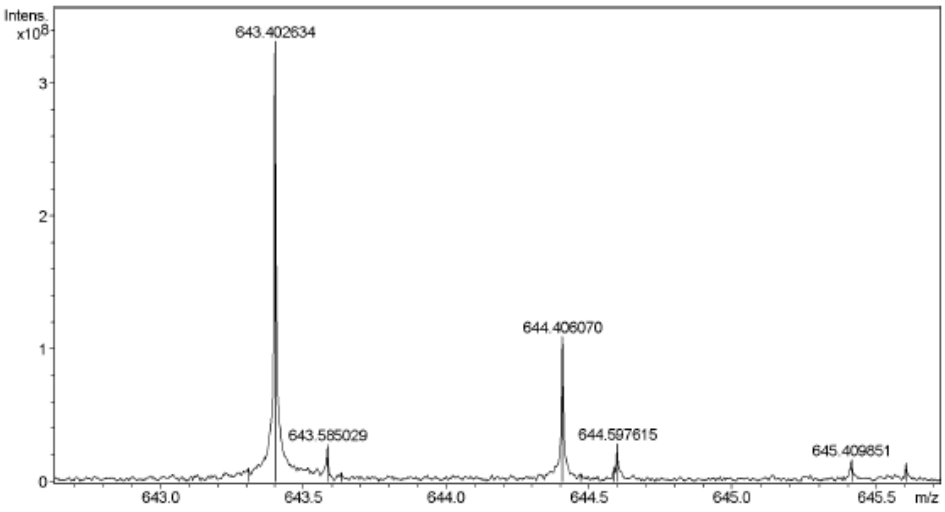

HRMS (ESI+): Cacld. for M^+: 643.402784, found: 643.402634

References

1. Botzenhart, K.; Döring, G., Ecology and epidemiology of Pseudomonas aeruginosa. In *Pseudomonas aeruginosa as an Opportunistic Pathogen*, Springer: 1993; pp 1-18.

2. Bodey, G. P.; Bolivar, R.; Fainstein, V.; Jadeja, L., Infections caused by Pseudomonas aeruginosa. *Reviews of infectious diseases* **1983,** *5* (2), 279-313.

3. Govan, J. R.; Deretic, V., Microbial pathogenesis in cystic fibrosis: mucoid Pseudomonas aeruginosa and Burkholderia cepacia. *Microbiological reviews* **1996,** *60* (3), 539-574.

4. Wagner, V. E.; Iglewski, B. H., P. aeruginosa biofilms in CF infection. *Clinical reviews in allergy & immunology* **2008,** *35* (3), 124-134.

5. Oliver, A.; Cantón, R.; Campo, P.; Baquero, F.; Blázquez, J., High frequency of hypermutable Pseudomonas aeruginosa in cystic fibrosis lung infection. *Science* **2000,** *288* (5469), 1251-1253.

6. Singh, P. K.; Schaefer, A. L.; Parsek, M. R.; Moninger, T. O.; Welsh, M. J.; Greenberg, E., Quorum-sensing signals indicate that cystic fibrosis lungs are infected with bacterial biofilms. *Nature* **2000,** *407* (6805), 762-764.

7. Hancock, R. E., Resistance mechanisms in Pseudomonas aeruginosa and other nonfermentative gram-negative bacteria. *Clinical Infectious Diseases* **1998,** *27* (Supplement_1), S93-S99.

8. Breidenstein, E. B.; de la Fuente-Núñez, C.; Hancock, R. E., Pseudomonas aeruginosa: all roads lead to resistance. *Trends in microbiology* **2011,** *19* (8), 419-426.

9. Sautter, R.; Ramos, D.; Schneper, L.; Ciofu, O.; Wassermann, T.; Koh, C.-L.; Heydorn, A.; Hentzer, M.; Høiby, N.; Kharazmi, A., A complex multilevel attack on Pseudomonas aeruginosa algT/U expression and algT/U activity results in the loss of alginate production. *Gene* **2012,** *498* (2), 242-253.

10. Terry, J. M.; Piña, S. E.; Mattingly, S. J., Environmental conditions which influence mucoid conversion Pseudomonas aeruginosa PAO1. *Infection and immunity* **1991,** *59* (2), 471-477.

11. Ramphal, R.; Pier, G. B., Role of Pseudomonas aeruginosa mucoid exopolysaccharide in adherence to tracheal cells. *Infection and immunity* **1985,** *47* (1), 1-4.

12. Ramphal, R.; Sadoff, J.; Pyle, M.; Silipigni, J., Role of pili in the adherence of Pseudomonas aeruginosa to injured tracheal epithelium. *Infection and immunity* **1984,** *44* (1), 38-40.

13. Mathee, K.; Ciofu, O.; Sternberg, C.; Lindum, P. W.; Campbell, J. I.; Jensen, P.; Johnsen, A. H.; Givskov, M.; Ohman, D. E.; Søren, M., Mucoid conversion of Pseudomonas aeruginos by hydrogen peroxide: a mechanism for virulence activation in the cystic fibrosis lung. *Microbiology* **1999,** *145* (6), 1349-1357.

14. Ryan Withers, T.; Heath Damron, F.; Yin, Y.; Yu, H. D., Truncation of type IV pilin induces mucoidy in Pseudomonas aeruginosa strain PAO579. *Microbiologyopen* **2013,** *2* (3), 459-470.

15. Laharrague, P.; Corberand, J.; Fillola, G.; Gleizes, B.; Fontanilles, A.; Gyrard, E., In vitro effect of the slime of Pseudomonas aeruginosa on the function of human polymorphonuclear neutrophils. *Infection and immunity* **1984,** *44* (3), 760-762.

16. Oliver, A.; Weir, D., Inhibition of bacterial binding to mouse macrophages by Pseudomonas alginate. *Journal of clinical & laboratory immunology* **1983,** *10* (4), 221-224.

17. Ruhen, R.; Holt, P.; Papadimitriou, J., Antiphagocytic effect of Pseudomonas aeruginosa exopolysaccharide. *Journal of clinical pathology* **1980,** *33* (12), 1221.

18. Schwarzmann, S.; Boring, J. R., Antiphagocytic effect of slime from a mucoid strain of Pseudomonas aeruginosa. *Infection and immunity* **1971,** *3* (6), 762-767.

19. Martin, D.; Schurr, M.; Mudd, M.; Govan, J.; Holloway, B.; Deretic, V., Mechanism of conversion to mucoidy in Pseudomonas aeruginosa infecting cystic fibrosis patients. *Proceedings of the National Academy of Sciences* **1993,** *90* (18), 8377-8381.

20. Boucher, J.; Yu, H.; Mudd, M.; Deretic, V., Mucoid Pseudomonas aeruginosa in cystic fibrosis: characterization of muc mutations in clinical isolates and analysis of clearance in a mouse model of respiratory infection. *Infection and immunity* **1997,** *65* (9), 3838-3846.

21. Wood, L. F.; Ohman, D. E., Identification of genes in the σ22 regulon of Pseudomonas aeruginosa required for cell envelope homeostasis in either the planktonic or the sessile mode of growth. *MBio* **2012,** *3* (3), e00094-12.

22. Ramsey, D. M.; Wozniak, D. J., Understanding the control of Pseudomonas aeruginosa alginate synthesis and the prospects for management of chronic infections in cystic fibrosis. *Molecular microbiology* **2005,** *56* (2), 309-322.

23. DeVries, C. A.; Ohman, D. E., Mucoid-to-nonmucoid conversion in alginate-producing Pseudomonas aeruginosa often results from spontaneous mutations in algT,

encoding a putative alternate sigma factor, and shows evidence for autoregulation. *Journal of bacteriology* **1994,** *176* (21), 6677-6687.

24. Hauser, A. R.; Jain, M.; Bar-Meir, M.; McColley, S. A., Clinical significance of microbial infection and adaptation in cystic fibrosis. *Clinical microbiology reviews* **2011,** *24* (1), 29-70.

25. Wood, L. F.; Ohman, D. E., Use of cell wall stress to characterize σ22 (AlgT/U) activation by regulated proteolysis and its regulon in Pseudomonas aeruginosa. *Molecular microbiology* **2009,** *72* (1), 183-201.

26. Wood, L. F.; Leech, A. J.; Ohman, D. E., Cell wall‐inhibitory antibiotics activate the alginate biosynthesis operon in Pseudomonas aeruginosa: roles of σ 22 (AlgT) and the AlgW and Prc proteases. *Molecular microbiology* **2006,** *62* (2), 412-426.

27. Govan, J.; Harris, G., Pseudomonas aeruginosa and cystic fibrosis: unusual bacterial adaptation and pathogenesis. *Microbiological sciences* **1986,** *3* (10), 302-308.

28. Pritt, B.; O'brien, L.; Winn, W., Mucoid Pseudomonas in cystic fibrosis. *American journal of clinical pathology* **2007,** *128* (1), 32-34.

29. Hentzer, M.; Teitzel, G. M.; Balzer, G. J.; Heydorn, A.; Molin, S.; Givskov, M.; Parsek, M. R., Alginate overproduction affects Pseudomonas aeruginosa biofilm structure and function. *Journal of bacteriology* **2001,** *183* (18), 5395-5401.

30. Hengzhuang, W.; Wu, H.; Ciofu, O.; Song, Z.; Høiby, N., Pharmacokinetics/pharmacodynamics of colistin and imipenem on mucoid and nonmucoid Pseudomonas aeruginosa biofilms. *Antimicrobial agents and chemotherapy* **2011,** *55* (9), 4469-4474.

31. Singh, V.; Arora, V.; Alam, M. J.; Garey, K. W., Inhibition of biofilm formation by esomeprazole in Pseudomonas aeruginosa and Staphylococcus aureus. *Antimicrobial agents and chemotherapy* **2012,** *56* (8), 4360-4364.

32. Hall-Stoodley, L.; Costerton, J. W.; Stoodley, P., Bacterial biofilms: from the natural environment to infectious diseases. *Nature reviews microbiology* **2004,** *2* (2), 95-108.

33. Drenkard, E., Antimicrobial resistance of Pseudomonas aeruginosa biofilms. *Microbes and infection* **2003,** *5* (13), 1213-1219.

34. Nicas, T.; Hancock, R., Pseudomonas aeruginosa outer membrane permeability: isolation of a porin protein F-deficient mutant. *Journal of bacteriology* **1983,** *153* (1), 281-285.

35. Davies, D., Understanding biofilm resistance to antibacterial agents. *Nature reviews Drug discovery* **2003,** *2* (2), 114-122.

36. Costerton, J. W.; Lewandowski, Z.; Caldwell, D. E.; Korber, D. R.; Lappin-Scott, H. M., Microbial biofilms. *Annual Reviews in Microbiology* **1995,** *49* (1), 711-745.

37. Donlan, R. M., Biofilms: microbial life on surfaces. *Emerging infectious diseases* **2002,** *8* (9), 881.

38. O'Toole, G.; Kaplan, H. B.; Kolter, R., Biofilm formation as microbial development. *Annual Reviews in Microbiology* **2000,** *54* (1), 49-79.

39. Davies, J.; Spiegelman, G. B.; Yim, G., The world of subinhibitory antibiotic concentrations. *Current opinion in microbiology* **2006,** *9* (5), 445-453.

40. Mah, T.-F. C.; O'toole, G. A., Mechanisms of biofilm resistance to antimicrobial agents. *Trends in microbiology* **2001,** *9* (1), 34-39.

41. Watnick, P.; Kolter, R., Biofilm, city of microbes. *Journal of bacteriology* **2000,** *182* (10), 2675-2679.

42. Hoffman, L. R.; D'argenio, D. A.; MacCoss, M. J.; Zhang, Z.; Jones, R. A.; Miller, S. I., Aminoglycoside antibiotics induce bacterial biofilm formation. *Nature* **2005,** *436* (7054), 1171.

43. Rashid, M. H.; Kornberg, A., Inorganic polyphosphate is needed for swimming, swarming, and twitching motilities of Pseudomonas aeruginosa. *Proceedings of the National Academy of Sciences* **2000,** *97* (9), 4885-4890.

44. Butler, M. T.; Wang, Q.; Harshey, R. M., Cell density and mobility protect swarming bacteria against antibiotics. *Proceedings of the National Academy of Sciences* **2010,** *107* (8), 3776-3781.

45. Déziel, E.; Comeau, Y.; Villemur, R., Initiation of biofilm formation byPseudomonas aeruginosa 57RP correlates with emergence of hyperpiliated and highly adherent phenotypic variants deficient in swimming, swarming, and twitching motilities. *Journal of Bacteriology* **2001,** *183* (4), 1195-1204.

46. Köhler, T.; Curty, L. K.; Barja, F.; Van Delden, C.; Pechère, J.-C., Swarming of Pseudomonas aeruginosa is dependent on cell-to-cell signaling and requires flagella and pili. *Journal of bacteriology* **2000,** *182* (21), 5990-5996.

47. Caiazza, N. C.; Merritt, J. H.; Brothers, K. M.; O'Toole, G. A., Inverse regulation of biofilm formation and swarming motility by Pseudomonas aeruginosa PA14. *Journal of bacteriology* **2007,** *189* (9), 3603-3612.

48. Verstraeten, N.; Braeken, K.; Debkumari, B.; Fauvart, M.; Fransaer, J.; Vermant, J.; Michiels, J., Living on a surface: swarming and biofilm formation. *Trends in microbiology* **2008,** *16* (10), 496-506.

49. Harshey, R. M., Bacterial motility on a surface: many ways to a common goal. *Annual Reviews in Microbiology* **2003,** *57* (1), 249-273.

50. McCarter, L. L., Dual flagellar systems enable motility under different circumstances. *Journal of molecular microbiology and biotechnology* **2004,** *7* (1-2), 18-29.

51. Deziel, E.; Lepine, F.; Milot, S.; Villemur, R., rhlA is required for the production of a novel biosurfactant promoting swarming motility in Pseudomonas aeruginosa: 3-(3-hydroxyalkanoyloxy) alkanoic acids (HAAs), the precursors of rhamnolipids. *Microbiology* **2003,** *149* (8), 2005-2013.

52. Ochsner, U. A.; Fiechter, A.; Reiser, J., Isolation, characterization, and expression in Escherichia coli of the Pseudomonas aeruginosa rhlAB genes encoding a rhamnosyltransferase involved in rhamnolipid biosurfactant synthesis. *Journal of Biological Chemistry* **1994,** *269* (31), 19787-19795.

53. Ochsner, U. A.; Koch, A. K.; Fiechter, A.; Reiser, J., Isolation and characterization of a regulatory gene affecting rhamnolipid biosurfactant synthesis in Pseudomonas aeruginosa. *Journal of bacteriology* **1994,** *176* (7), 2044-2054.

54. Tremblay, J.; Déziel, E., Improving the reproducibility of Pseudomonas aeruginosa swarming motility assays. *Journal of basic microbiology* **2008,** *48* (6), 509-515.

55. Henrichsen, J., Twitching motility. *Annual Reviews in Microbiology* **1983,** *37* (1), 81-93.

56. LAUTROP, H., Bacterium anitratum transferred to the genus Cytophaga. *International Journal of Systematic and Evolutionary Microbiology* **1961,** *11* (3), 107-108.

57. Henrichsen, J., Bacterial surface translocation: a survey and a classification. *Bacteriological reviews* **1972,** *36* (4), 478.

58. Bradley, D. E., A function of Pseudomonas aeruginosa PAO polar pili: twitching motility. *Canadian journal of microbiology* **1980,** *26* (2), 146-154.

59. Darzins, A., Characterization of a Pseudomonas aeruginosa gene cluster involved in pilus biosynthesis and twitching motility: sequence similarity to the chemotaxis proteins of enterics and the gliding bacterium Myxococcus xanthus. *Molecular microbiology* **1994,** *11* (1), 137-153.

60. Whitchurch, C. B.; Hobbs, M.; Livingston, S. P.; Krishnapillai, V.; Mattick, J. S., Characterisation of a Pseudomonas aeruginosa twitching motility gene and evidence for a specialised protein export system widespread in eubacteria. *Gene* **1991,** *101* (1), 33-44.

61. Levy, S. B., The challenge of antibiotic resistance. *Scientific American* **1998,** *278* (3), 46-53.

62. Fleming, A., On the antibacterial action of cultures of a penicillium, with special reference to their use in the isolation of B. influenzae. *British journal of experimental pathology* **1929,** *10* (3), 226.

63. Schatz, A.; Bugle, E.; Waksman, S. A., Streptomycin, a Substance Exhibiting Antibiotic Activity Against Gram-Positive and Gram-Negative Bacteria.∗. *Proceedings of the Society for Experimental Biology and Medicine* **1944,** *55* (1), 66-69.

64. Calderón, C. B.; Sabundayo, B. P., 2 Antimicrobial Classifications. *Antimicrobial Susceptibility Testing Protocols* **2007**, 7.

65. Van Hoek, A. H.; Mevius, D.; Guerra, B.; Mullany, P.; Roberts, A. P.; Aarts, H. J., Acquired antibiotic resistance genes: an overview. *Frontiers in microbiology* **2011,** *2*, 203.

66. Paterson, D. L., "Collateral damage" from cephalosporin or quinolone antibiotic therapy. *Clinical Infectious Diseases* **2004,** *38* (Supplement_4), S341-S345.

67. Walsh, C., *Antibiotics: actions, origins, resistance*. American Society for Microbiology (ASM): 2003.

68. Levy, S. B.; Marshall, B., Antibacterial resistance worldwide: causes, challenges and responses. *Nature medicine* **2004,** *10* (12s), S122.

69. Martínez, J. L.; Rojo, F., Metabolic regulation of antibiotic resistance. *FEMS microbiology reviews* **2011,** *35* (5), 768-789.

70. Tille, P., *Bailey & Scott's Diagnostic Microbiology-E-Book*. Elsevier Health Sciences: 2015.

71. Brown, D., Antibiotic resistance breakers: can repurposed drugs fill the antibiotic discovery void? *Nature Reviews Drug Discovery* **2015,** *14* (12), 821.

72. Wright, G. D.; Poinar, H., Antibiotic resistance is ancient: implications for drug discovery. *Trends in microbiology* **2012,** *20* (4), 157-159.

73. Aminov, R. I., The role of antibiotics and antibiotic resistance in nature. *Environmental microbiology* **2009,** *11* (12), 2970-2988.

74. Davies, J., Are antibiotics naturally antibiotics? *Journal of Industrial Microbiology and Biotechnology* **2006,** *33* (7), 496-499.

75. Yim, G.; Wang, H. H.; Davies, J., The truth about antibiotics. *International Journal of Medical Microbiology* **2006,** *296* (2-3), 163-170.

76. Goh, E.-B.; Yim, G.; Tsui, W.; McClure, J.; Surette, M. G.; Davies, J., Transcriptional modulation of bacterial gene expression by subinhibitory concentrations of antibiotics. *Proceedings of the National Academy of Sciences* **2002,** *99* (26), 17025-17030.

77. Sengupta, S.; Chattopadhyay, M. K.; Grossart, H.-P., The multifaceted roles of antibiotics and antibiotic resistance in nature. *Frontiers in microbiology* **2013,** *4*, 47.

78. Ohnishi, M.; Golparian, D.; Shimuta, K.; Saika, T.; Hoshina, S.; Iwasaku, K.; Nakayama, S.-i.; Kitawaki, J.; Unemo, M., Is Neisseria gonorrhoeae initiating a future era of untreatable gonorrhea?: detailed characterization of the first strain with high-level resistance to ceftriaxone. *Antimicrobial agents and chemotherapy* **2011,** *55* (7), 3538-3545.

79. Carmeli, Y.; Troillet, N.; Eliopoulos, G. M.; Samore, M. H., Emergence of antibiotic-resistant Pseudomonas aeruginosa: comparison of risks associated with different antipseudomonal agents. *Antimicrobial agents and chemotherapy* **1999,** *43* (6), 1379-1382.

80. Foster, T. J., The Staphylococcus aureus "superbug". *The Journal of clinical investigation* **2004,** *114* (12), 1693-1696.

81. Bernal, P.; Molina‐Santiago, C.; Daddaoua, A.; Llamas, M. A., Antibiotic adjuvants: identification and clinical use. *Microbial biotechnology* **2013,** *6* (5), 445-449.

82. Gill, E. E.; Franco, O. L.; Hancock, R., Antibiotic adjuvants: diverse strategies for controlling drug‐resistant pathogens. *Chemical biology & drug design* **2015,** *85* (1), 56-78.

83. Kalan, L.; Wright, G. D., Antibiotic adjuvants: multicomponent anti-infective strategies. *Expert reviews in molecular medicine* **2011,** *13*.

84. Drusano, G.; Hope, W.; MacGowan, A.; Louie, A., Suppression of emergence of resistance in pathogenic bacteria: keeping our powder dry, part 2. *Antimicrobial agents and chemotherapy* **2016,** *60* (3), 1194-1201.

85. Drusano, G.; Louie, A.; MacGowan, A.; Hope, W., Suppression of emergence of resistance in pathogenic bacteria: keeping our powder dry, part 1. *Antimicrobial agents and chemotherapy* **2016,** *60* (3), 1183-1193.

86. Worthington, R. J.; Melander, C., Combination approaches to combat multidrug-resistant bacteria. *Trends in biotechnology* **2013,** *31* (3), 177-184.

87. Eliopoulos, G.; Eliopoulos, C., Antibiotic combinations: should they be tested? *Clinical Microbiology Reviews* **1988,** *1* (2), 139-156.

88. Wright, G. D., Antibiotic adjuvants: rescuing antibiotics from resistance. *Trends in microbiology* **2016,** *24* (11), 862-871.

89. Page, M. G., b-Lactamase inhibitors. *Drug Resistance Updates* **2000,** *3* (2), 109-125.

90. Wildenhain, J.; Spitzer, M.; Dolma, S.; Jarvik, N.; White, R.; Roy, M.; Griffiths, E.; Bellows, D. S.; Wright, G. D.; Tyers, M., Prediction of synergism from chemical-genetic interactions by machine learning. *Cell systems* **2015,** *1* (6), 383-395.

91. Davies, J.; Davies, D., Origins and evolution of antibiotic resistance. *Microbiology and molecular biology reviews* **2010,** *74* (3), 417-433.

92. Brauner, A.; Fridman, O.; Gefen, O.; Balaban, N. Q., Distinguishing between resistance, tolerance and persistence to antibiotic treatment. *Nature Reviews Microbiology* **2016,** *14* (5), 320-330.

93. Cohen, N. R.; Lobritz, M. A.; Collins, J. J., Microbial Persistence and the Road to Drug Resistance. *Cell Host Microbe* **2013,** *13* (6), 632-642.

94. Levin-Reisman, I.; Ronin, I.; Gefen, O.; Braniss, I.; Shoresh, N.; Balaban, N. Q., Antibiotic tolerance facilitates the evolution of resistance. *Science (Washington, DC, U. S.)* **2017,** *355* (6327), 826-830.

95. Fisher, R. A.; Gollan, B.; Helaine, S., Persistent bacterial infections and persister cells. *Nature Reviews Microbiology* **2017,** *15* (8), 453-464.

96. Rowe, S. E.; Conlon, B. P.; Keren, I.; Lewis, K., Persisters: Methods for Isolation and Identifying Contributing Factors-A Review. *Methods in Molecular Biology (New York, NY, United States)* **2016,** *1333* (Bacterial Persistence), 17-28.

97. Wood, T. K.; Knabel, S. J.; Kwan, B. W., Bacterial persister cell formation and dormancy. *Applied and Environmental Microbiology* **2013,** *79* (23), 7116-7121.

98. Shetye, G. S.; Singh, N.; Jia, C.; Nguyen, C. D. K.; Wang, G.; Luk, Y.-Y., Specific Maltose Derivatives Modulate the Swarming Motility of Nonswarming Mutant

and Inhibit Bacterial Adhesion and Biofilm Formation by Pseudomonas aeruginosa. *ChemBioChem* **2014,** *15* (10), 1514-1523.

99. Singh, N.; Shetye, G. S.; Zheng, H.; Sun, J.; Luk, Y.-Y., Chemical Signals of Synthetic Disaccharide Derivatives Dominate Rhamnolipids at Controlling Multiple Bacterial Activities. *ChemBioChem* **2016,** *17* (1), 102-111.

100. Hoffman, L. R.; D'Argenio, D. A.; MacCoss, M. J.; Zhang, Z.; Jones, R. A.; Miller, S. I., Aminoglycoside antibiotics induce bacterial biofilm formation. *Nature (London, U. K.)* **2005,** *436* (7054), 1171-1175.

101. Titz, A., Carbohydrate-Based Anti-Virulence Compounds Against Chronic Pseudomonas aeruginosa Infections with a Focus on Small Molecules. *Top. Med. Chem.* **2014,** *12* (Carbohydrates as Drugs), 169-186.

102. Grishin, A. V.; Krivozubov, M. S.; Gintsburg, A. L.; Karyagina, A. S., Pseudomonas Aeruginosa Lectins As Targets for Novel Antibacterials. *Acta Naturae* **2015,** *7* (2), 29-41.

103. Bishop, J. R.; Schuksz, M.; Esko, J. D., Heparan sulphate proteoglycans fine-tune mammalian physiology. *Nature* **2007,** *446* (7139), 1030.

104. Davies, D. G.; Parsek, M. R.; Pearson, J. P.; Iglewski, B. H.; Costerton, J. W.; Greenberg, E. P., The involvement of cell-to-cell signals in the development of a bacterial biofilm. *Science* **1998,** *280* (5361), 295-298.

105. Aitken, E.; Cheema, A.; Elliott, S.; Khan, S., Different compositions of biofilm extracellular polymeric substance reveals contrasting antibiotic resistance profiles in Pseudomonas aeruginosa. *J. Exp. Microbiol. Immunol* **2011,** *15*, 79-83.

106. Song, J.-M.; Im, J.-H.; Kang, J.-H.; Kang, D.-J., A simple method for hyaluronic acid quantification in culture broth. *Carbohydrate polymers* **2009,** *78* (3), 633-634.

107. Awad, H.; Aboul-Enein, H. Y., A validated HPLC assay method for the determination of sodium alginate in pharmaceutical formulations. *Journal of chromatographic science* **2012,** *51* (3), 208-214.

108. Correa, E.; Sletta, H.; Ellis, D. I.; Hoel, S.; Ertesvåg, H.; Ellingsen, T. E.; Valla, S.; Goodacre, R., Rapid reagentless quantification of alginate biosynthesis in Pseudomonas fluorescens bacteria mutants using FT-IR spectroscopy coupled to multivariate partial least squares regression. *Analytical and bioanalytical chemistry* **2012,** *403* (9), 2591-2599.

109. Gurin, S.; Hood, D. B., The identification and estimation of pentose in nucleic acids and nucleoproteins. *Journal of Biological Chemistry* **1941,** *139* (2), 775-785.

110. Bitter, T., A modified uronic acid carbazole reaction. *Anal. Biochem.* **1962,** *4*, 330-334.

111. Radhakrishnamurthy, B.; Berenson, G., Effect of Temperature and Time of Heating on the Carbazole Reaction of Uronic Acids and Acid Mucopolysaccharides. *Analytical Chemistry* **1963,** *35* (9), 1316-1318.

112. Dische, Z., A modification of the carbazole reaction of hexuronic acids for the study of polyuronides. *J Biol Chem* **1950,** *183*, 489-494.

113. Frazier, S. B.; Roodhouse, K. A.; Hourcade, D. E.; Zhang, L., The quantification of glycosaminoglycans: a comparison of HPLC, carbazole, and alcian blue methods. *Open glycoscience* **2008,** *1*, 31.

114. Kerem, B.-s.; Rommens, J. M.; Buchanan, J. A.; Markiewicz, D.; Cox, T. K.; Chakravarti, A.; Buchwald, M.; Tsui, L.-C., Identification of the cystic fibrosis gene: genetic analysis. *Science* **1989,** *245* (4922), 1073-1080.

115. Wiens, J. R.; Vasil, A. I.; Schurr, M. J.; Vasil, M. L., Iron-regulated expression of alginate production, mucoid phenotype, and biofilm formation by Pseudomonas aeruginosa. *MBio* **2014,** *5* (1), e01010-13.

116. Ryan Withers, T.; Heath Damron, F.; Yin, Y.; Yu, H. D., Truncation of type IV pilin induces mucoidy in P seudomonas aeruginosa strain PAO579. *Microbiologyopen* **2013,** *2* (3), 459-470.

117. Brownlee, I.; Allen, A.; Pearson, J.; Dettmar, P.; Havler, M.; Atherton, M.; Onsøyen, E., Alginate as a source of dietary fiber. *Critical reviews in food science and nutrition* **2005,** *45* (6), 497-510.

118. Govan, J.; Fyfe, J. A., Mucoid Pseudomonas aeruginosa and cystic fibrosis: resistance of the mucoid form to carbenicillin, flucloxacillin and tobramycin and the isolation of mucoid variants in vitro. *Journal of Antimicrobial Chemotherapy* **1978,** *4* (3), 233-240.

119. Schneider, G.; Decher, G.; Nerambourg, N.; Praho, R.; Werts, M. H.; Blanchard-Desce, M., Distance-dependent fluorescence quenching on gold nanoparticles ensheathed with layer-by-layer assembled polyelectrolytes. *Nano letters* **2006,** *6* (3), 530-536.

120. Lu, L.-Q.; Zheng, Y.; Qu, W.-G.; Xu, A.-W., Convenient and sensitive synchronous fluorescence detection of trace TNT based on FRET using FITC–PAH as a probe. *Analytical Methods* **2013,** *5* (3), 603-607.

121. Reibetanz, U.; Chen, M. H. A.; Mutukumaraswamy, S.; Liaw, Z. Y.; Oh, B. H. L.; Venkatraman, S.; Donath, E.; Neu, B. r., Colloidal DNA carriers for direct localization in cell compartments by pH sensoring. *Biomacromolecules* **2010,** *11* (7), 1779-1784.

122. Page, W.; Sadoff, H., Relationship between calcium and uroinic acids in the encystment of Azotobacter vinelandii. *Journal of bacteriology* **1975,** *122* (1), 145-151.

123. Adak, A.; Bandyopadhyay, M.; Pal, A., Removal of crystal violet dye from wastewater by surfactant-modified alumina. *Separation and Purification Technology* **2005,** *44* (2), 139-144.

124. Hanna, S. L.; Sherman, N. E.; Kinter, M. T.; Goldberg, J. B., Comparison of proteins expressed by Pseudomonas aeruginosa strains representing initial and chronic isolates from a cystic fibrosis patient: an analysis by 2-D gel electrophoresis and capillary column liquid chromatography–tandem mass spectrometry. *Microbiology* **2000,** *146* (10), 2495-2508.

125. Vázquez, E.; Dewitt, D. M.; Hammond, P. T.; Lynn, D. M., Construction of hydrolytically-degradable thin films via layer-by-layer deposition of degradable polyelectrolytes. *Journal of the American Chemical Society* **2002,** *124* (47), 13992-13993.

126. Maeda, H., SMANCS and polymer-conjugated macromolecular drugs: advantages in cancer chemotherapy. *Advanced drug delivery reviews* **2001,** *46* (1-3), 169-185.

127. Bodey, G. P.; Bolivar, R.; Fainstein, V.; Jadeja, L., Infections caused by Pseudomonas aeruginosa. *Review of Infectious Diseases* **1983,** *5* (2), 279-313.

128. Costerton, J. W.; Stewart, P. S.; Greenberg, E. P., Bacterial biofilms: a common cause of persistent infections. *Science* **1999,** *284* (5418), 1318-1322.

129. Davies, D. G.; Parsek, M. R.; Pearson, J. P.; Iglewski, B. H.; Costerton, J. t.; Greenberg, E., The involvement of cell-to-cell signals in the development of a bacterial biofilm. *Science* **1998,** *280* (5361), 295-298.

130. Donlan, R. M.; Costerton, J. W., Biofilms: survival mechanisms of clinically relevant microorganisms. *Clin. Microbiol. Rev.* **2002,** *15* (2), 167-193.

131. Klausen, M.; Aaes‐Jørgensen, A.; Molin, S.; Tolker‐Nielsen, T., Involvement of bacterial migration in the development of complex multicellular structures in Pseudomonas aeruginosa biofilms. *Mol. Microbiol.* **2003,** *50* (1), 61-68.

132. Lawrence, J.; Korber, D.; Hoyle, B.; Costerton, J.; Caldwell, D., Optical sectioning of microbial biofilms. *J. Bacteriol.* **1991,** *173* (20), 6558-6567.

133. Klausen, M.; Heydorn, A.; Ragas, P.; Lambertsen, L.; Aaes‐Jørgensen, A.; Molin, S.; Tolker‐Nielsen, T., Biofilm formation by Pseudomonas aeruginosa wild type, flagella and type IV pili mutants. *Mol. Microbiol.* **2003,** *48* (6), 1511-1524.

134. Davey, M. E.; Caiazza, N. C.; O'Toole, G. A., Rhamnolipid surfactant production affects biofilm architecture in Pseudomonas aeruginosa PAO1. *J. Bacteriol.* **2003,** *185* (3), 1027-1036.

135. Espinosa-Urgel, M., Resident parking only: rhamnolipids maintain fluid channels in biofilms. *J. Bacteriol.* **2003,** *185* (3), 699-700.

136. Lequette, Y.; Greenberg, E., Timing and localization of rhamnolipid synthesis gene expression in Pseudomonas aeruginosa biofilms. *J. Bacteriol.* **2005,** *187* (1), 37-44.

137. Purevdorj, B.; Costerton, J.; Stoodley, P., Influence of hydrodynamics and cell signaling on the structure and behavior of Pseudomonas aeruginosa biofilms. *Appl. Environ. Microbiol.* **2002,** *68* (9), 4457-4464.

138. Boles, B. R.; Thoendel, M.; Singh, P. K., Rhamnolipids mediate detachment of Pseudomonas aeruginosa from biofilms. *Mol. Microbiol.* **2005,** *57* (5), 1210-1223.

139. Nickzad, A.; Déziel, E., The involvement of rhamnolipids in microbial cell adhesion and biofilm development–an approach for control? *Lett. Appl. Microbiol.* **2014,** *58* (5), 447-453.

140. Schooling, S.; Charaf, U.; Allison, D.; Gilbert, P., A role for rhamnolipid in biofilm dispersion. *Biofilms* **2004,** *1* (02), 91-99.

141. Caiazza, N. C.; Shanks, R. M.; O'Toole, G., Rhamnolipids modulate swarming motility patterns of Pseudomonas aeruginosa. *J. Bacteriol.* **2005,** *187* (21), 7351-7361.

142. Tremblay, J.; Richardson, A. P.; Lépine, F.; Déziel, E., Self‐produced extracellular stimuli modulate the Pseudomonas aeruginosa swarming motility behaviour. *Environ. Microbiol.* **2007,** *9* (10), 2622-2630.

143. Hauser, G.; Karnovsky, M. L., Studies on the production of glycolipide by Pseudomonas aeruginosa. *J. Bacteriol.* **1954,** *68* (6), 645.

144. Hauser, G.; Karnovsky, M. L., Rhamnose and rhamnolipide biosynthesis by Pseudomonas aeruginosa. *J. Biol. Chem.* **1957,** *224* (1), 91-105.

145. Hauser, G.; Karnovsky, M. L., Studies on the biosynthesis of L-rhamnose. *J. Biol. Chem.* **1958,** *233* (2), 287-291.

146. Ochsner, U. A.; Reiser, J., Autoinducer-mediated regulation of rhamnolipid biosurfactant synthesis in Pseudomonas aeruginosa. *Proceedings of the National Academy of Sciences* **1995,** *92* (14), 6424-6428.

147. Welsh, M. A.; Eibergen, N. R.; Moore, J. D.; Blackwell, H. E., Small molecule disruption of quorum sensing cross-regulation in Pseudomonas aeruginosa causes major

and unexpected alterations to virulence phenotypes. *J. Am. Chem. Soc.* **2015,** *137* (4), 1510-1519.

148. Shetye, G. S.; Singh, N.; Jia, C.; Nguyen, C. D.; Wang, G.; Luk, Y. Y., Specific maltose derivatives modulate the swarming motility of nonswarming mutant and inhibit bacterial adhesion and biofilm formation by Pseudomonas aeruginosa. *ChemBioChem* **2014,** *15* (10), 1514-1523.

149. Singh, N.; Shetye, G. S.; Zheng, H.; Sun, J.; Luk, Y. Y., Chemical Signals of Synthetic Disaccharide Derivatives Dominate Rhamnolipids at Controlling Multiple Bacterial Activities. *ChemBioChem* **2016,** *17* (1), 102-111.

150. Eberhard, A.; Burlingame, A.; Eberhard, C.; Kenyon, G.; Nealson, K.; Oppenheimer, N., Structural identification of autoinducer of Photobacterium fischeri luciferase. *Biochemistry* **1981,** *20* (9), 2444-2449.

151. Lenz, P.; Søgaard-Andersen, L., Temporal and spatial oscillations in bacteria. *Nature Reviews Microbiology* **2011,** *9* (8), 565.

152. Tremblay, J.; Déziel, E., Gene expression in Pseudomonas aeruginosa swarming motility. *BMC Genomics* **2010,** *11* (1), 1.

153. Bloemberg, G. V.; O'Toole, G. A.; Lugtenberg, B.; Kolter, R., Green fluorescent protein as a marker for Pseudomonas spp. *Appl. Environ. Microbiol.* **1997,** *63* (11), 4543-4551.

154. Geske, G. D.; Wezeman, R. J.; Siegel, A. P.; Blackwell, H. E., Small molecule inhibitors of bacterial quorum sensing and biofilm formation. *J. Am. Chem. Soc.* **2005,** *127* (37), 12762-12763.

155. Miller, M. B.; Bassler, B. L., Quorum sensing in bacteria. *Annual Reviews in Microbiology* **2001,** *55* (1), 165-199.

156. Shrout, J. D.; Chopp, D. L.; Just, C. L.; Hentzer, M.; Givskov, M.; Parsek, M. R., The impact of quorum sensing and swarming motility on Pseudomonas aeruginosa biofilm formation is nutritionally conditional. *Mol. Microbiol.* **2006,** *62* (5), 1264-1277.

157. Jennings, M. C.; Ator, L. E.; Paniak, T. J.; Minbiole, K. P.; Wuest, W. M., Biofilm‐Eradicating Properties of Quaternary Ammonium Amphiphiles: Simple Mimics of Antimicrobial Peptides. *ChemBioChem* **2014,** *15* (15), 2211-2215.

158. Lee, K. K.; Yu, L.; Macdonald, D. L.; Paranchych, W.; Hodges, R. S.; Irvin, R. T., Anti-adhesin antibodies that recognize a receptor-binding motif (adhesintope) inhibit pilus/fimbrial-mediated adherence of Pseudomonas aeruginosa and Candida albicans to asialo-GM1 receptors and human buccal epithelial cell surface receptors. *Can. J. Microbiol.* **1996,** *42* (5), 479-486.

159. Huigens, R. W.; Richards, J. J.; Parise, G.; Ballard, T. E.; Zeng, W.; Deora, R.; Melander, C., Inhibition of Pseudomonas aeruginosa biofilm formation with bromoageliferin analogues. *J. Am. Chem. Soc.* **2007,** *129* (22), 6966-6967.

160. Lushniak, B. D., Antibiotic resistance: a public health crisis. *Public Health Reports* **2014,** *129* (4), 314-316.

161. Scholar, E. M.; Pratt, W. B., *The antimicrobial drugs*. Oxford University Press, USA: 2000.

162. Blair, J. M.; Webber, M. A.; Baylay, A. J.; Ogbolu, D. O.; Piddock, L. J., Molecular mechanisms of antibiotic resistance. *Nature Reviews Microbiology* **2015,** *13* (1), 42.

163. Cox, G.; Wright, G. D., Intrinsic antibiotic resistance: mechanisms, origins, challenges and solutions. *International Journal of Medical Microbiology* **2013,** *303* (6-7), 287-292.

164. Lewis, K., Multidrug tolerance of biofilms and persister cells. In *Bacterial Biofilms*, Springer: 2008; pp 107-131.

165. Poole, K., Efflux pumps as antimicrobial resistance mechanisms. *Annals of medicine* **2007,** *39* (3), 162-176.

166. Jennings, L. K.; Storek, K. M.; Ledvina, H. E.; Coulon, C.; Marmont, L. S.; Sadovskaya, I.; Secor, P. R.; Tseng, B. S.; Scian, M.; Filloux, A., Pel is a cationic exopolysaccharide that cross-links extracellular DNA in the Pseudomonas aeruginosa biofilm matrix. *Proceedings of the National Academy of Sciences* **2015,** *112* (36), 11353-11358.

167. Mah, T.-F.; Pitts, B.; Pellock, B.; Walker, G. C.; Stewart, P. S.; O'toole, G. A., A genetic basis for Pseudomonas aeruginosa biofilm antibiotic resistance. *Nature* **2003,** *426* (6964), 306.

168. Anderl, J. N.; Franklin, M. J.; Stewart, P. S., Role of antibiotic penetration limitation in Klebsiella pneumoniae biofilm resistance to ampicillin and ciprofloxacin. *Antimicrobial agents and chemotherapy* **2000,** *44* (7), 1818-1824.

169. Kester, J. C.; Fortune, S. M., Persisters and beyond: mechanisms of phenotypic drug resistance and drug tolerance in bacteria. *Critical reviews in biochemistry and molecular biology* **2014,** *49* (2), 91-101.

170. Handwerger, S.; Tomasz, A., Antibiotic tolerance among clinical isolates of bacteria. *Annual review of pharmacology and toxicology* **1985,** *25* (1), 349-380.

171. Levin, B. R.; Rozen, D. E., Non-inherited antibiotic resistance. *Nature Reviews Microbiology* **2006,** *4* (7), 556.

172. Tomasz, A.; de Vegvar, M.-L., Construction of a penicillin-tolerant laboratory mutant ofStaphylococcus aureus. *European journal of clinical microbiology* **1986,** *5* (6), 710.

173. Tuomanen, E.; Durack, D.; Tomasz, A., Antibiotic tolerance among clinical isolates of bacteria. *Antimicrobial agents and chemotherapy* **1986,** *30* (4), 521.

174. Tuomanen, E., Phenotypic tolerance: the search for β-lactam antibiotics that kill nongrowing bacteria. *Reviews of infectious diseases* **1986,** *8* (Supplement_3), S279-S291.

175. Tuomanen, E.; Tomasz, A., Mechanism of phenotypic tolerance of nongrowing pneumococci to beta-lactam antibiotics. *Scand. J. Infect. Dis. Suppl* **1990,** *74*, 102-112.

176. Lee, H. H.; Molla, M. N.; Cantor, C. R.; Collins, J. J., Bacterial charity work leads to population-wide resistance. *Nature* **2010,** *467* (7311), 82.

177. Tuomanen, E.; Cozens, R.; Tosch, W.; Zak, O.; Tomasz, A., The rate of killing of Escherichia coli byβ-lactam antibiotics is strictly proportional to the rate of bacterial growth. *Microbiology* **1986,** *132* (5), 1297-1304.

178. Zheng, Z.; Stewart, P. S., Growth limitation of Staphylococcus epidermidis in biofilms contributes to rifampin tolerance. *Biofilms* **2004,** *1* (1), 31-35.

179. Ryder, V. J.; Chopra, I.; O'Neill, A. J., Increased mutability of Staphylococci in biofilms as a consequence of oxidative stress. *PLoS One* **2012,** *7* (10), e47695.

180. Brooun, A.; Liu, S.; Lewis, K., A dose-response study of antibiotic resistance inPseudomonas aeruginosa biofilms. *Antimicrobial agents and chemotherapy* **2000,** *44* (3), 640-646.

181. Gefen, O.; Balaban, N. Q., The importance of being persistent: heterogeneity of bacterial populations under antibiotic stress. *FEMS microbiology reviews* **2009,** *33* (4), 704-717.

182. Bigger, J., Treatment of Staphyloeoeeal Infections with Penicillin by Intermittent Sterilisation. *Lancet* **1944**, 497-500.

183. Lewis, K., Programmed death in bacteria. *Microbiology and Molecular Biology Reviews* **2000,** *64* (3), 503-514.

184. Lewis, K., Riddle of biofilm resistance. *Antimicrobial agents and chemotherapy* **2001,** *45* (4), 999-1007.

185. Black, D. S.; Kelly, A. J.; Mardis, M.; Moyed, H., Structure and organization of hip, an operon that affects lethality due to inhibition of peptidoglycan or DNA synthesis. *Journal of bacteriology* **1991,** *173* (18), 5732-5739.

186. Moyed, H. S.; Bertrand, K. P., hipA, a newly recognized gene of Escherichia coli K-12 that affects frequency of persistence after inhibition of murein synthesis. *Journal of bacteriology* **1983,** *155* (2), 768-775.

187. Moyed, H. S.; Broderick, S. H., Molecular cloning and expression of hipA, a gene of Escherichia coli K-12 that affects frequency of persistence after inhibition of murein synthesis. *Journal of bacteriology* **1986,** *166* (2), 399-403.

188. Scherrer, R.; Moyed, H. S., Conditional impairment of cell division and altered lethality in hipA mutants of Escherichia coli K-12. *Journal of bacteriology* **1988,** *170* (8), 3321-3326.

189. Spoering, A. L.; Lewis, K., Biofilms and planktonic cells of Pseudomonas aeruginosa have similar resistance to killing by antimicrobials. *Journal of bacteriology* **2001,** *183* (23), 6746-6751.

190. Kussell, E., Evolution in microbes. **2013**.

191. Levin-Reisman, I.; Ronin, I.; Gefen, O.; Braniss, I.; Shoresh, N.; Balaban, N. Q., Antibiotic tolerance facilitates the evolution of resistance. *Science* **2017**, eaaj2191.

192. Van den Bergh, B.; Michiels, J. E.; Wenseleers, T.; Windels, E. M.; Boer, P. V.; Kestemont, D.; De Meester, L.; Verstrepen, K. J.; Verstraeten, N.; Fauvart, M., Frequency of antibiotic application drives rapid evolutionary adaptation of Escherichia coli persistence. *Nature microbiology* **2016,** *1* (5), 16020.

193. Kussell, E.; Kishony, R.; Balaban, N. Q.; Leibler, S., Bacterial persistence: a model of survival in changing environments. *Genetics* **2005,** *169* (4), 1807-1814.

194. Gardner, A.; West, S. A.; Griffin, A. S., Is bacterial persistence a social trait? *PLoS One* **2007,** *2* (8), e752.

195. Patra, P.; Klumpp, S., Population dynamics of bacterial persistence. *PLoS One* **2013,** *8* (5), e62814.

196. Philippi, T.; Seger, J., Hedging one's evolutionary bets, revisited. *Trends in Ecology & Evolution* **1989,** *4* (2), 41-44.

197. Beaumont, H. J.; Gallie, J.; Kost, C.; Ferguson, G. C.; Rainey, P. B., Experimental evolution of bet hedging. *Nature* **2009,** *462* (7269), 90.

198. Barbosa, C.; Trebosc, V.; Kemmer, C.; Rosenstiel, P.; Beardmore, R.; Schulenburg, H.; Jansen, G., Alternative evolutionary paths to bacterial antibiotic

resistance cause distinct collateral effects. *Molecular biology and evolution* **2017,** *34* (9), 2229-2244.

199. Talbot, G. H.; Bradley, J.; Edwards Jr, J. E.; Gilbert, D.; Scheld, M.; Bartlett, J. G., Bad bugs need drugs: an update on the development pipeline from the Antimicrobial Availability Task Force of the Infectious Diseases Society of America. *Clinical infectious diseases* **2006,** *42* (5), 657-668.

200. Ichimiya, T.; Takeoka, K.; Hiramatsu, K.; Hirai, K.; Yamasaki, T.; Nasu, M., The influence of azithromycin on the biofilm formation of Pseudomonas aeruginosa in vitro. *Chemotherapy* **1996,** *42* (3), 186-191.

201. Wagner, T.; Soong, G.; Sokol, S.; Saiman, L.; Prince, A., Effects of azithromycin on clinical isolates of Pseudomonas aeruginosa from cystic fibrosis patients. *Chest* **2005,** *128* (2), 912-919.

202. Høiby, N., Antibiotic therapy for chronic infection of Pseudomonas in the lung. *Annual review of medicine* **1993,** *44* (1), 1-10.

203. Clement, A.; Tamalet, A.; Leroux, E.; Ravilly, S.; Fauroux, B.; Jais, J.-P., Long term effects of azithromycin in patients with cystic fibrosis: a double blind, placebo controlled trial. *Thorax* **2006,** *61* (10), 895-902.

204. Saiman, L.; Marshall, B. C.; Mayer-Hamblett, N.; Burns, J. L.; Quittner, A. L.; Cibene, D. A.; Coquillette, S.; Fieberg, A. Y.; Accurso, F. J.; Campbell III, P. W., Azithromycin in patients with cystic fibrosis chronically infected with Pseudomonas aeruginosa: a randomized controlled trial. *Jama* **2003,** *290* (13), 1749-1756.

205. Favre-Bonté, S.; Köhler, T.; Van Delden, C., Biofilm formation by Pseudomonas aeruginosa: role of the C4-HSL cell-to-cell signal and inhibition by azithromycin. *Journal of antimicrobial chemotherapy* **2003,** *52* (4), 598-604.

206. Nagino, K.; Kobayashi, H., Influence of macrolides on mucoid alginate biosynthetic enzyme from Pseudomonas aeruginosa. *Clinical Microbiology and infection* **1997,** *3* (4), 432-439.

207. Tateda, K.; Comte, R.; Pechere, J.-C.; Köhler, T.; Yamaguchi, K.; Van Delden, C., Azithromycin inhibits quorum sensing in Pseudomonas aeruginosa. *Antimicrobial agents and chemotherapy* **2001,** *45* (6), 1930-1933.

208. Ceri, H.; Olson, M.; Stremick, C.; Read, R.; Morck, D.; Buret, A., The Calgary Biofilm Device: new technology for rapid determination of antibiotic susceptibilities of bacterial biofilms. *Journal of clinical microbiology* **1999,** *37* (6), 1771-1776.

209. Fernández-Olmos, A.; García-Castillo, M.; Maiz, L.; Lamas, A.; Baquero, F.; Cantón, R., In vitro prevention of Pseudomonas aeruginosa early biofilm formation with antibiotics used in cystic fibrosis patients. *International journal of antimicrobial agents* **2012,** *40* (2), 173-176.

210. Kim, K. P.; Kim, Y.-G.; Choi, C.-H.; Kim, H.-E.; Lee, S.-H.; Chang, W.-S.; Lee, C.-S., In situ monitoring of antibiotic susceptibility of bacterial biofilms in a microfluidic device. *Lab on a Chip* **2010,** *10* (23), 3296-3299.

211. De Kievit, T. R.; Parkins, M. D.; Gillis, R. J.; Srikumar, R.; Ceri, H.; Poole, K.; Iglewski, B. H.; Storey, D. G., Multidrug efflux pumps: expression patterns and contribution to antibiotic resistance in Pseudomonas aeruginosa biofilms. *Antimicrobial agents and chemotherapy* **2001,** *45* (6), 1761-1770.

212. Wang, H.; Wu, H.; Song, Z.; Høiby, N., Ciprofloxacin shows concentration-dependent killing of Pseudomonas aeruginosa biofilm in vitro. *Journal of Cystic Fibrosis* **2010,** *9*, S41.

213. Agarwal, G.; Kapil, A.; Kabra, S.; Das, B. K.; Dwivedi, S., In vitro efficacy of ciprofloxacin and gentamicin against a biofilm of Pseudomonas aeruginosa and its free-living forms. *National Medical Journal of India* **2005,** *18* (4), 184.

214. Hengzhuang, W.; Wu, H.; Ciofu, O.; Song, Z.; Høiby, N., Pharmacokinetics/Pharmacodynamics of Colistin and Imipenem on mucoid and non-mucoid Pseudomonas aeruginosa biofilm. *Antimicrobial agents and chemotherapy* **2011**, AAC. 00126-11.

215. Shawar, R. M.; MacLeod, D. L.; Garber, R. L.; Burns, J. L.; Stapp, J. R.; Clausen, C. R.; Tanaka, S., Activities of tobramycin and six other antibiotics against Pseudomonas aeruginosa isolates from patients with cystic fibrosis. *Antimicrobial agents and chemotherapy* **1999,** *43* (12), 2877-2880.

216. Garey, K. W.; Vo, Q. P.; Lewis, R. E.; Saengcharoen, W.; LaRocco, M. T.; Tam, V. H., Increased bacterial adherence and biomass in Pseudomonas aeruginosa bacteria exposed to clarithromycin. *Diagnostic microbiology and infectious disease* **2009,** *63* (1), 81-86.

217. Linares, J. F.; Gustafsson, I.; Baquero, F.; Martinez, J., Antibiotics as intermicrobial signaling agents instead of weapons. *Proceedings of the National Academy of Sciences* **2006,** *103* (51), 19484-19489.

218. Bagge, N.; Schuster, M.; Hentzer, M.; Ciofu, O.; Givskov, M.; Greenberg, E. P.; Høiby, N., Pseudomonas aeruginosa biofilms exposed to imipenem exhibit changes in

global gene expression and β-lactamase and alginate production. *Antimicrobial agents and chemotherapy* **2004,** *48* (4), 1175-1187.

219. Kohler, T.; Curty, L. K.; Barja, F.; Van, D. C.; Pechere, J.-C., Swarming of Pseudomonas aeruginosa is dependent on cell-to-cell signaling and requires flagella and pili. *Journal of Bacteriology* **2000,** *182* (Copyright (C) 2013 American Chemical Society (ACS). All Rights Reserved.), 5990-5996.

220. Jarrell, K. F.; McBride, M. J., The surprisingly diverse ways that prokaryotes move. *Nature Reviews Microbiology* **2008,** *6* (6), 466-476.

221. Caiazza, N. C.; Merritt, J. H.; Brothers, K. M.; O'Toole, G. A., Inverse regulation of biofilm formation and swarming motility by Pseudomonas aeruginosa PA14. *J. Bacteriol.* **2007,** *189* (Copyright (C) 2013 American Chemical Society (ACS). All Rights Reserved.), 3603-3612.

222. Stoodley, P.; Sauer, K.; Davies, D. G.; Costerton, J. W., Biofilms as complex differentiated communities. *Annual Review of Microbiology* **2002,** *56* (Copyright (C) 2013 American Chemical Society (ACS). All Rights Reserved.), 187-209.

223. Sauer, K.; Camper, A. K.; Ehrlich, G. D.; Costerton, J. W.; Davies, D. G., Pseudomonas aeruginosa displays multiple phenotypes during development as a biofilm. *Journal of Bacteriology* **2002,** *184* (Copyright (C) 2013 American Chemical Society (ACS). All Rights Reserved.), 1140-1154.

224. MBEC™ Assay plates : http://www.innovotech.ca/products_mbec.php.

225. Chen, J. L.; Stuckey, D. C.; Chen, J. L.; Steele, T. W. J.; Stuckey, D. C., Metabolic reduction of resazurin; location within the cell for cytotoxicity assays. *Biotechnol Bioeng* **2017**.

226. Vidal-Aroca, F.; Meng, A.; Minz, T.; Page, M. G. P.; Dreier, J., Use of resazurin to detect mefloquine as an efflux-pump inhibitor in Pseudomonas aeruginosa and Escherichia coli. *J. Microbiol. Methods* **2009,** *79* (2), 232-237.

227. Owicki, J. C., Fluorescence polarization and anisotropy in high throughput screening: perspectives and primer. *Journal of biomolecular screening* **2000,** *5* (5), 297-306.

228. Allen, M.; Reeves, J.; Mellor, G., High throughput fluorescence polarization: a homogeneous alternative to radioligand binding for cell surface receptors. *Journal of biomolecular screening* **2000,** *5* (2), 63-69.

229. Perrin, F., Polarization of light of fluorescence, average life of molecules in the excited state. *J. Phys. Radium* **1926,** *7*, 390-401.

230. Weber, G., Polarization of the fluorescence of macromolecules. 1. Theory and experimental method. *Biochemical Journal* **1952,** *51* (2), 145.

231. Weber, G., Polarization of the fluorescence of macromolecules. 2. Fluorescent conjugates of ovalbumin and bovine serum albumin. *Biochemical Journal* **1952,** *51* (2), 155.

232. Weber, G., Photoelectric method for the measurement of the polarization of the fluorescence of solutions. *JOSA* **1956,** *46* (11), 962-970.

233. Baughman, B. M.; Jake Slavish, P.; DuBois, R. M.; Boyd, V. A.; White, S. W.; Webb, T. R., Identification of influenza endonuclease inhibitors using a novel fluorescence polarization assay. *ACS Chem Biol* **2012,** *7* (3), 526-34.

234. Jolley, M. E., Fluorescence polarization assays for the detection of proteases and their inhibitors. *Journal of Biomolecular Screening* **1996,** *1* (1), 33-38.

235. Rohe, A.; Henze, C.; Erdmann, F.; Sippl, W.; Schmidt, M., A fluorescence anisotropy-based Myt1 kinase binding assay. *Assay Drug Dev Technol* **2014,** *12* (2), 136-44.

236. Vickers, C. J.; González‐Páez, G. E.; Umotoy, J. C.; Cayanan‐Garrett, C.; Brown, S. J.; Wolan, D. W., Small‐Molecule Procaspase Activators Identified Using Fluorescence Polarization. *ChemBioChem* **2013,** *14* (12), 1419-1422.

237. Jameson, D. M.; Ross, J. A., Fluorescence polarization/anisotropy in diagnostics and imaging. *Chemical reviews* **2010,** *110* (5), 2685-2708.

238. Buchli, R.; VanGundy, R. S.; Hickman-Miller, H. D.; Giberson, C. F.; Bardet, W.; Hildebrand, W. H., Development and Validation of a Fluorescence Polarization-Based Competitive Peptide-Binding Assay for HLA-A* 0201 A New Tool for Epitope Discovery. *Biochemistry* **2005,** *44* (37), 12491-12507.

239. Lakowicz, J., Principles of Fluorescence Spectroscopy, 3edrd edSpringer. *New York* **2006**.

240. Mueller, S. O.; Simon, S.; Chae, K.; Metzler, M.; Korach, K. S., Phytoestrogens and their human metabolites show distinct agonistic and antagonistic properties on estrogen receptor alpha (ERalpha) and ERbeta in human cells. *Toxicol Sci* **2004,** *80* (1), 14-25.

241. Wang, S.; Zhang, C.; Nordeen, S. K.; Shapiro, D. J., In vitro fluorescence anisotropy analysis of the interaction of full-length SRC1a with estrogen receptors alpha and beta supports an active displacement model for coregulator utilization. *J Biol Chem* **2007,** *282* (5), 2765-75.

242. Harris, D. W.; Kenrick, M. K.; Pither, R. J.; Anson, J. G.; Jones, D. A., Development of a High-Volumein SitumRNA Hybridization Assay for the Quantification of Gene Expression Utilizing Scintillating Microplates. *Analytical biochemistry* **1996,** *243* (2), 249-256.

243. Zhang, J. H.; Chung, T. D.; Oldenburg, K. R., A Simple Statistical Parameter for Use in Evaluation and Validation of High Throughput Screening Assays. *J Biomol Screen* **1999,** *4* (2), 67-73.

244. Lis, H.; Sharon, N., Lectins: carbohydrate-specific proteins that mediate cellular recognition. *Chemical reviews* **1998,** *98* (2), 637-674.

245. Sharon, N., Bacterial lectins, cell-cell recognition and infectious disease. *FEBS letters* **1987,** *217* (2), 145-157.

246. Chemani, C.; Imberty, A.; de Bentzmann, S.; Pierre, M.; Wimmerova, M.; Guery, B. P.; Faure, K., Role of LecA and LecB lectins in Pseudomonas aeruginosa-induced lung injury and effect of carbohydrate ligands. *Infect Immun* **2009,** *77* (5), 2065-75.

247. Petri Jr, W. A.; Haque, R.; Mann, B. J., The bittersweet interface of parasite and host: lectin-carbohydrate interactions during human invasion by the parasite Entamoeba histolytica. *Annual Reviews in Microbiology* **2002,** *56* (1), 39-64.

248. Rodrigues, J. A.; Acosta-Serrano, A.; Aebi, M.; Ferguson, M. A.; Routier, F. H.; Schiller, I.; Soares, S.; Spencer, D.; Titz, A.; Wilson, I. B.; Izquierdo, L., Parasite Glycobiology: A Bittersweet Symphony. *PLoS Pathog* **2015,** *11* (11), e1005169.

249. Gilboa-Garber, N., Purification and properties of hemagglutinin from Pseudomonas aeruginosa and its reaction with human blood cells. *Biochimica et Biophysica Acta (BBA)-General Subjects* **1972,** *273* (1), 165-173.

250. Gilboa-Garber, N.; Katcoff, D. J.; Garber, N. C., Identification and characterization of Pseudomonas aeruginosa PA-IIL lectin gene and protein compared to PA-IL. *FEMS Immunology & Medical Microbiology* **2000,** *29* (1), 53-57.

251. Adam, E. C.; Mitchell, B. S.; Schumacher, D. U.; Grant, G.; Schumacher, U., Pseudomonas aeruginosa II lectin stops human ciliary beating: therapeutic implications of fucose. *Am J Respir Crit Care Med* **1997,** *155* (6), 2102-4.

252. Bajolet-Laudinat, O.; Girod-de Bentzmann, S.; Tournier, J.; Madoulet, C.; Plotkowski, M.; Chippaux, C.; Puchelle, E., Cytotoxicity of Pseudomonas aeruginosa internal lectin PA-I to respiratory epithelial cells in primary culture. *Infection and immunity* **1994,** *62* (10), 4481-4487.

253. Toder, D.; Gambello, M.; Iglewski, B., Pseudomonas aeruginosa LasA: a second elastase under the transcriptional control of lasR. *Molecular microbiology* **1991,** *5* (8), 2003-2010.

254. Pal, R.; Ahmed, H.; Chatterjee, B., PSEUDOMONAS-AERUGINOSA BACTERIA HABS TYPE-2A CONTAINS 2 LECTINS OF DIFFERENT SPECIFICITY. *BIOCHEMICAL ARCHIVES* **1987,** *3* (4), 399-412.

255. Bartels, K. M.; Funken, H.; Knapp, A.; Brocker, M.; Bott, M.; Wilhelm, S.; Jaeger, K. E.; Rosenau, F., Glycosylation is required for outer membrane localization of the lectin LecB in Pseudomonas aeruginosa. *J Bacteriol* **2011,** *193* (5), 1107-13.

256. Gilboa-Garber, N.; Sudakevitz, D.; Sheffi, M.; Sela, R.; Levene, C., PA-I and PA-II lectin interactions with the ABO (H) and P blood group glycosphingolipid antigens may contribute to the broad spectrum adherence ofPseudomonas aeruginosa to human tissues in secondary infections. *Glycoconjugate journal* **1994,** *11* (5), 414-417.

257. Cioci, G.; Mitchell, E. P.; Gautier, C.; Wimmerová, M.; Sudakevitz, D.; Pérez, S.; Gilboa-Garber, N.; Imberty, A., Structural basis of calcium and galactose recognition by the lectin PA-IL ofPseudomonas aeruginosa. *FEBS Letters* **2003,** *555* (2), 297-301.

258. Loris, R.; Tielker, D.; Jaeger, K.-E.; Wyns, L., Structural Basis of Carbohydrate Recognition by the Lectin LecB from Pseudomonas aeruginosa. *Journal of Molecular Biology* **2003,** *331* (4), 861-870.

259. Joachim, I.; Rikker, S.; Hauck, D.; Ponader, D.; Boden, S.; Sommer, R.; Hartmann, L.; Titz, A., Development and optimization of a competitive binding assay for the galactophilic low affinity lectin LecA from Pseudomonas aeruginosa. *Org Biomol Chem* **2016,** *14* (33), 7933-48.

260. Novoa, A.; Eierhoff, T.; Topin, J.; Varrot, A.; Barluenga, S.; Imberty, A.; Romer, W.; Winssinger, N., A LecA ligand identified from a galactoside-conjugate array inhibits host cell invasion by Pseudomonas aeruginosa. *Angew Chem Int Ed Engl* **2014,** *53* (34), 8885-9.

261. Pertici, F.; de Mol, N. J.; Kemmink, J.; Pieters, R. J., Optimizing divalent inhibitors of Pseudomonas aeruginosa lectin LecA by using a rigid spacer. *Chemistry-A European Journal* **2013,** *19* (50), 16923-16927.

262. Craig, L.; Pique, M. E.; Tainer, J. A., Type IV pilus structure and bacterial pathogenicity. *Nature Reviews Microbiology* **2004,** *2* (5), 363-378.

263. Levine, M. M.; Nataro, J. P.; Karch, H.; Baldini, M. M.; Kaper, J. B.; Black, R. E.; Clements, M. L.; O'Brien, A. D., The diarrheal response of humans to some classic serotypes of enteropathogenic Escherichia coli is dependent on a plasmid encoding an enteroadhesiveness factor. *Journal of Infectious Diseases* **1985,** *152* (3), 550-559.

264. Craig, L.; Taylor, R. K.; Pique, M. E.; Adair, B. D.; Arvai, A. S.; Singh, M.; Lloyd, S. J.; Shin, D. S.; Getzoff, E. D.; Yeager, M., Type IV pilin structure and assembly: X-ray and EM analyses of Vibrio cholerae toxin-coregulated pilus and Pseudomonas aeruginosa PAK pilin. *Molecular cell* **2003,** *11* (5), 1139-1150.

265. Strom, M. S.; Lory, S., Structure-function and biogenesis of the type IV pili. *Annual Reviews in Microbiology* **1993,** *47* (1), 565-596.

266. Herrington, D. A.; Hall, R. H.; Losonsky, G.; Mekalanos, J. J.; Taylor, R.; Levine, M. M., Toxin, toxin-coregulated pili, and the toxR regulon are essential for Vibrio cholerae pathogenesis in humans. *Journal of Experimental Medicine* **1988,** *168* (4), 1487-1492.

267. Tacket, C. O.; Taylor, R. K.; Losonsky, G.; Lim, Y.; Nataro, J. P.; Kaper, J. B.; Levine, M. M., Investigation of the roles of toxin-coregulated pili and mannose-sensitive hemagglutinin pili in the pathogenesis of Vibrio cholerae O139 infection. *Infection and immunity* **1998,** *66* (2), 692-695.

268. Bieber, D.; Ramer, S. W.; Wu, C.-Y.; Murray, W. J.; Tobe, T.; Fernandez, R.; Schoolnik, G. K., Type IV pili, transient bacterial aggregates, and virulence of enteropathogenic Escherichia coli. *Science* **1998,** *280* (5372), 2114-2118.

269. Sheth, H.; Glasier, L.; Ellert, N.; Cachia, P.; Kohn, W.; Lee, K.; Paranchych, W.; Hodges, R.; Irvin, R., Development of an anti-adhesive vaccine for Pseudomonas aeruginosa targeting the C-terminal region of the pilin structural protein. *Biomedical peptides, proteins & nucleic acids: structure, synthesis & biological activity* **1995,** *1* (3), 141-148.

270. Lang, A. B.; Rüdeberg, A.; Schöni, M. H.; Que, J. U.; Fürer, E.; Schaad, U. B., Vaccination of cystic fibrosis patients against Pseudomonas aeruginosa reduces the proportion of patients infected and delays time to infection. *The Pediatric infectious disease journal* **2004,** *23* (6), 504-510.

271. Johansen, H. K.; Gotzsche, P. C., Vaccines for preventing infection with Pseudomonas aeruginosa in cystic fibrosis. *Cochrane Database Syst Rev* **2013,** *6*.

272. Radwan, A. A.; Alanazi, F. K., Targeting cancer using cholesterol conjugates. *Saudi pharmaceutical journal* **2014,** *22* (1), 3-16.

273. Asao, T.; Yazawa, S.; Kudo, S.; Takenoshita, S.; Nagamachi, Y., A novel ex vivo method for assaying adhesion of cancer cells to the peritoneum. *Cancer letters* **1994,** *78* (1-3), 57-62.

274. Asao, T.; Nagamachi, Y.; Morinaga, N.; Shitara, Y.; Takenoshita, S. I.; Yazawa, S., Fucosyltransferases of the peritoneum contributed to the adhesion of cancer cells to the mesothelium. *Cancer* **1995,** *75* (S6), 1539-1544.

275. Okamura, A.; Yazawa, S.; Nishimura, T.; Tanaka, S.; Takai, I.; Kudo, S.; Asao, T.; Kuwano, H.; Matta, K. L.; Akamatsu, S., A new method for assaying adhesion of cancer cells to the greater omentum and its application for evaluating anti-adhesion activities of chemically synthesized oligosaccharides. *Clinical & experimental metastasis* **2000,** *18* (1), 37-43.

276. Hahismoto, S.; Yazawa, S.; Asao, T.; Faried, A.; Nishimura, T.; Tsuboi, K.; Nakagawa, T.; Yamauchi, T.; Koyama, N.; Umehara, K., Novel sugar-cholestanols as anticancer agents against peritoneal dissemination of tumor cells. *Glycoconjugate journal* **2008,** *25* (6), 531-544.

277. Faried, A.; Faried, L. S.; Nakagawa, T.; Yamauchi, T.; Kitani, M.; Sasabe, H.; Nishimura, T.; Usman, N.; Kato, H.; Asao, T., Chemically synthesized sugar‐cholestanols possess a preferential anticancer activity involving promising therapeutic potential against human esophageal cancer. *Cancer science* **2007,** *98* (9), 1358-1367.

278. Carrico, I. S., Chemoselective modification of proteins: hitting the target. *Chemical Society Reviews* **2008,** *37* (7), 1423-1431.

279. Francis, M. B., New methods for protein bioconjugation. *Chemical Biology: From Small Molecules to Systems Biology and Drug Design, Volume 1-3* **2008**, 593-634.

280. Sletten, E. M.; Bertozzi, C. R., Bioorthogonal chemistry: fishing for selectivity in a sea of functionality. *Angewandte Chemie International Edition* **2009,** *48* (38), 6974-6998.

281. Boutureira, O.; Bernardes, G. a. J., Advances in chemical protein modification. *Chemical reviews* **2015,** *115* (5), 2174-2195.

282. Drahl, C.; Cravatt, B. F.; Sorensen, E. J., Protein‐Reactive Natural Products. *Angewandte Chemie International Edition* **2005,** *44* (36), 5788-5809.

283. Pucheault, M., Natural products: chemical instruments to apprehend biological symphony. *Organic & biomolecular chemistry* **2008,** *6* (3), 424-432.

284. Marks, K. M.; Braun, P. D.; Nolan, G. P., A general approach for chemical labeling and rapid, spatially controlled protein inactivation. *Proceedings of the National Academy of Sciences of the United States of America* **2004,** *101* (27), 9982-9987.

285. Farinas, J.; Verkman, A., Receptor-mediated targeting of fluorescent probes in living cells. *Journal of Biological Chemistry* **1999,** *274* (12), 7603-7606.

286. Chen, G.; Heim, A.; Riether, D.; Yee, D.; Milgrom, Y.; Gawinowicz, M. A.; Sames, D., Reactivity of functional groups on the protein surface: development of epoxide probes for protein labeling. *Journal of the American Chemical Society* **2003,** *125* (27), 8130-8133.

287. Williams, D. B.; Carter, C. B., The transmission electron microscope. In *Transmission electron microscopy*, Springer: 1996; pp 3-17.

288. Haguenau, F.; Hawkes, P.; Hutchison, J.; Satiat–Jeunemaître, B.; Simon, G.; Williams, D., Key events in the history of electron microscopy. *Microscopy and Microanalysis* **2003,** *9* (2), 96-138.

289. Nermut, M., General principles of virus architecture. In *Perspectives in Medical Virology*, Elsevier: 1987; Vol. 3, pp 3-18.

290. Beveridge, T. J.; Lawrence, J. R.; Murray, R. G., Sampling and staining for light microscopy. In *Methods for General and Molecular Microbiology, Third Edition*, American Society of Microbiology: 2007; pp 19-33.

291. Frasca, J. M.; Parks, V. R., A routine technique for double-staining ultrathin sections using uranyl and lead salts. *The Journal of cell biology* **1965,** *25* (1), 157.

292. McDowell, E.; Trump, B., Histologic fixatives suitable for diagnostic light and electron microscopy. *Archives of pathology & laboratory medicine* **1976,** *100* (8), 405-414.

293. Morris, J. K., A formaldehyde glutaraldehyde fixative of high osmolality for use in electron microscopy. *J. cell Biol* **1965,** *27*, 1A-149A.

294. Pembrey, R. S.; Marshall, K. C.; Schneider, R. P., Cell surface analysis techniques: what do cell preparation protocols do to cell surface properties? *Applied and Environmental Microbiology* **1999,** *65* (7), 2877-2894.

295. Zahller, J.; Stewart, P. S., Transmission electron microscopic study of antibiotic action on Klebsiella pneumoniae biofilm. *Antimicrobial agents and chemotherapy* **2002,** *46* (8), 2679-2683.

296. Karthikeyan, S.; Beveridge, T., Pseudomonas aeruginosa biofilms react with and precipitate toxic soluble gold. *Environmental Microbiology* **2002,** *4* (11), 667-675.

297. Lee, J.-U.; Beveridge, T. J., Interaction between iron and Pseudomonas aeruginosa biofilms attached to Sepharose surfaces. *Chemical Geology* **2001,** *180* (1-4), 67-80.

298. Bruzaud, J.; Tarrade, J.; Coudreuse, A.; Canette, A.; Herry, J.-M.; de Givenchy, E. T.; Darmanin, T.; Guittard, F.; Guilbaud, M.; Bellon-Fontaine, M.-N., Flagella but not type IV pili are involved in the initial adhesion of Pseudomonas aeruginosa PAO1 to hydrophobic or superhydrophobic surfaces. *Colloids and Surfaces B: Biointerfaces* **2015,** *131*, 59-66.

299. Stukalov, O.; Korenevsky, A.; Beveridge, T. J.; Dutcher, J. R., Use of atomic force microscopy and transmission electron microscopy for correlative studies of bacterial capsules. *Applied and environmental microbiology* **2008,** *74* (17), 5457-5465.

300. Hazelton, P. R.; Gelderblom, H. R., Electron microscopy for rapid diagnosis of emerging infectious agents. *Emerging infectious diseases* **2003,** *9* (3), 294.

301. Roine, E.; Wei, W.; Yuan, J.; Nurmiaho-Lassila, E.-L.; Kalkkinen, N.; Romantschuk, M.; He, S. Y., Hrp pilus: an hrp-dependent bacterial surface appendage

produced by Pseudomonas syringae pv. tomato DC3000. *Proceedings of the National Academy of Sciences* **1997,** *94* (7), 3459-3464.

302. Kubori, T.; Matsushima, Y.; Nakamura, D.; Uralil, J.; Lara-Tejero, M.; Sukhan, A.; Galán, J. E.; Aizawa, S.-I., Supramolecular structure of the Salmonella typhimurium type III protein secretion system. *Science* **1998,** *280* (5363), 602-605.

303. Koebnik, R.; Locher, K. P.; Van Gelder, P., Structure and function of bacterial outer membrane proteins: barrels in a nutshell. *Molecular microbiology* **2000,** *37* (2), 239-253.

304. Steck, T. L., The organization of proteins in the human red blood cell membrane: a review. *The Journal of cell biology* **1974,** *62* (1), 1.

305. Dirienzo, J. M.; Nakamura, K.; Inouye, M., The outer membrane proteins of Gram-negative bacteria: biosynthesis, assembly, and functions. *Annual review of biochemistry* **1978,** *47* (1), 481-532.

306. Wallin, E.; Heijne, G. V., Genome‐wide analysis of integral membrane proteins from eubacterial, archaean, and eukaryotic organisms. *Protein Science* **1998,** *7* (4), 1029-1038.

307. Paulsen, I. T.; Sliwinski, M. K.; Nelissen, B.; Goffeau, A.; Saier, M. H., Unified inventory of established and putative transporters encoded within the complete genome of Saccharomyces cerevisiae. *FEBS letters* **1998,** *430* (1-2), 116-125.

308. Seddon, A. M.; Curnow, P.; Booth, P. J., Membrane proteins, lipids and detergents: not just a soap opera. *Biochimica et Biophysica Acta (BBA)-Biomembranes* **2004,** *1666* (1), 105-117.

309. Molloy, M. P.; Herbert, B. R.; Walsh, B. J.; Tyler, M. I.; Traini, M.; Sanchez, J. C.; Hochstrasser, D. F.; Williams, K. L.; Gooley, A. A., Extraction of membrane proteins by differential solubilization for separation using two‐dimensional gel electrophoresis. *Electrophoresis* **1998,** *19* (5), 837-844.

310. Capaldi, R. A.; Vanderkooi, G., The low polarity of many membrane proteins. *Proceedings of the National Academy of Sciences* **1972,** *69* (4), 930-932.

311. Siegel, L. M.; Monty, K. J., Determination of molecular weights and frictional ratios of proteins in impure systems by use of gel filtration and density gradient centrifugation. Application to crude preparations of sulfite and hydroxylamine reductases. *Biochimica Et Biophysica Acta (BBA)-Biophysics Including Photosynthesis* **1966,** *112* (2), 346-362.

312. Fujiki, Y.; Hubbard, A. L.; Fowler, S.; Lazarow, P. B., Isolation of intracellular membranes by means of sodium carbonate treatment: application to endoplasmic reticulum. *The Journal of cell biology* **1982,** *93* (1), 97-102.

313. Hazlett, L.; Moon, M.; Singh, A.; Berk, R.; Rudner, X., Analysis of adhesion, piliation, protease production and ocular infectivity of several P. aeruginosa strains. *Current eye research* **1991,** *10* (4), 351-362.

314. Ramphal, R.; Koo, L.; Ishimoto, K. S.; Totten, P. A.; Lara, J. C.; Lory, S., Adhesion of Pseudomonas aeruginosa pilin-deficient mutants to mucin. *Infection and immunity* **1991,** *59* (4), 1307-1311.

315. Markson, J. S.; O'Shea, E. K., The molecular clockwork of a protein-based circadian oscillator. *FEBS letters* **2009,** *583* (24), 3938-3947.

316. Rothfield, L.; Taghbalout, A.; Shih, Y.-L., Spatial control of bacterial division-site placement. *Nature Reviews Microbiology* **2005,** *3* (12), 959.

317. Lutkenhaus, J., Assembly dynamics of the bacterial MinCDE system and spatial regulation of the Z ring. *Annu. Rev. Biochem.* **2007,** *76*, 539-562.

318. Jacobs, C.; Domian, I. J.; Maddock, J. R.; Shapiro, L., Cell cycle–dependent polar localization of an essential bacterial histidine kinase that controls DNA replication and cell division. *Cell* **1999,** *97* (1), 111-120.

Hewen Zheng

hezheng@syr.edu

ADDRESS: 5719 N 19th St., Philadelphia, PA, 19141. TEL: (315) 930-5847.

Education

Syracuse University

(08/2013-current)

M. Phil., Syracuse University, 2015
GPA: 3.857/4.000

Dalian University of Technology

(09/2009-06/2013)

B.Sc., Dalian University of Technology, 2013
GPA: 3.413/4.000

Professional Involvement

Research Assistant in Dr. Yan-Yeung Luk Group, Syracuse University

(05/2015 – 05/2016, 01/2018 – current)

- Established and developed assays and validated analytical methods including design of biofilm quantification assay by confocal laser scanning microscopy, swarming and twitching motility assays.
- Developed fluorescent polarization assay for studying ligand-receptor binding and TEM for characterizing bacterial surface disruption by synthetic drug molecules.
- Discovered and synthesized small molecules that modulate the multicellular behaviors and control the phenotypes of a clinical strain of Pseudomonas aeruginosa.
- Performed maintenance and calibration for the laboratory equipment and system including LCMS, HPLC, confocal microscope and UV-VIS.

Research Scientist in LifeUnit LLC, Syracuse

(05/2016 – 01/2017)

- Developed an assay to test the synergistic effect of swarming inhibitor with antibiotics on mature biofilm formed by Pseudomonas aeruginosa.
- Made considerable progress on the mechanistic understanding of how ligand-receptor binding was achieved by designing a ligand molecule that can covalently react with the receptor protein and form a covalent conjugate.

Teaching Assistant, Syracuse University

(08/2013 – 05/2015)

- Instructed laboratory classes of General Chemistry Laboratory and Organic Chemistry Laboratory for undergraduate level.
- Designed and instructed a green chemistry reaction- Vitamin C Clock Reaction, which has been included in the General Chemistry Laboratory II text book (ISBN 978-1-5249-4829-0).

Publications and Poster Presentations

- **Zheng, Hewen**, Ivan V. Korendovych, and Yan-Yeung Luk. "Quantification of alginate by aggregation induced by calcium ions and fluorescent polycations." *Analytical Biochemistry* 492 (2016): 76-81.
- **Zheng, Hewen**, Nischal Singh, Gauri S. Shetye, Yucheng Jin, Diana Li, and Yan-Yeung Luk. "Synthetic analogs of rhamnolipids modulate structured biofilms formed by a rhamnolipid-nonproducing mutant of Pseudomonas aeruginosa." *Bioorganic & Medicinal Chemistry* 25, no. 6 (2017): 1830-1838.
- Singh, Nischal, Gauri S. Shetye, **Hewen Zheng**, Jiayue Sun, and Yan-Yeung Luk. "Chemical Signals of Synthetic Disaccharide Derivatives Dominate Rhamnolipids at Controlling Multiple
  Bacterial Activities." *ChemBioChem* 17, no. 1 (2016): 102-111.
- McDonough, Richard T., **Hewen Zheng**, Mercy A. Alila, Jerry Goodisman, and Joseph Chaiken. "Optical interference probe of biofilm hydrology: label-free characterization of the dynamic hydration behavior of native biofilms." *Journal of Biomedical Optics* 22, no. 3 (2017): 035003-035003.
- Gordon research conference: Bacterial Cell Surfaces, Presenting Poster Entitled: Chemical Inhibition of Alginate Production by Mucoid Pseudomonas aeruginosa via Appendage Binding, 06/26/2016 - 07/01/2016.
- Gordon research conference: Bacterial Cell Surfaces, Presenting Poster Entitled: Pili-Mediated Chemical Signaling: Bacterial Activities and Therapeutic Potentials, 06/26/2016 - 07/01/2016.
- Chapter 3, Vitamin C Clock Reaction, General Chemistry Laboratory II, ISBN 978-1-5249-4829-0.

Skills

- Proficiency in conducting various analytical equipment including AAS, AES, UV-VIS, LCMS, GCMS, HPLC, MALDI-TOF, TEM, SEM, polarizing and phase contrast microscopy, FTIR spectroscopy, NMR spectroscopy.
- Proficiency in handling bacterial cell cultures within bio-safety level 2 (BSL-2) conditions including generating various scales of biofilms using a bioreactor or flow cell system.
- Proficiency in Korean and Chinese, and a strong ability and interest in learning foreign languages.